QA: QA

ANL-NBS-MD-000001 REV 02

March 2004

Features, Events, and Processes in UZ Flow and Transport

U0170

Prepared for:
U.S. Department of Energy
Office of Civilian Radioactive Waste Management
Office of Repository Development
1551 Hillshire Drive
Las Vegas, Nevada 89134-6321

Prepared by:
Bechtel SAIC Company, LLC
1180 Town Center Drive
Las Vegas, Nevada 89144

Under Contract Number
DE-AC28-01RW12101

DISCLAIMER

This report was prepared as an account of work sponsored by an agency of the United States Government. Neither the United States Government nor any agency thereof, nor any of their employees, nor any of their contractors, subcontractors or their employees, makes any warranty, express or implied, or assumes any legal liability or responsibility for the accuracy, completeness, or any third party's use or the results of such use of any information, apparatus, product, or process disclosed, or represents that its use would not infringe privately owned rights. Reference herein to any specific commercial product, process, or service by trade name, trademark, manufacturer, or otherwise, does not necessarily constitute or imply its endorsement, recommendation, or favoring by the United States Government or any agency thereof or its contractors or subcontractors. The views and opinions of authors expressed herein do not necessarily state or reflect those of the United States Government or any agency thereof.

Features, Events, and Processes in UZ Flow and Transport

BSC 2003 [164873]

U0170

March 2004

INTENTIONALLY LEFT BLANK

OCRWM	SCIENTIFIC ANALYSIS SIGNATURE PAGE/ CHANGE HISTORY	1. Page iii of 166

2. Scientific Analysis Title

Features, Events, and Processes in UZ Flow and Transport

3. DI (including Revision Number)

ANL-NBS-MD-000001 REV02

4. Total Appendices	5. Number of Pages in Each Appendix
2	I-16, II-4

	Printed Name	Signature	Date
6. Originator	J.E. Houseworth	James E Houseworth	3/24/04
7. Checker	P. Persoff	Pete Persoff	3/24/04
8. QER	S. Harris	Stephen Harris	3/24/04
9. Responsible Manager/Lead	J.S.Y. Wang	Joseph S.Y. Wang	3/24/04
10. Responsible Manager	P. Dixon	Paul Dixon	3/24/04

11. Remarks

Technical Error Report (TER) Log Number addressed in this report

CR-159 (Previously TER-02-0090) is addressed in Section 6.3.2.

Change History

12. Revision/ICN No.	13. Total Pages	14. Description of Change
REV 00	181	Initial Issue
REV 01	229	Revision addresses bases for assumptions, disposition descriptions, secondary FEPs, and provides more detailed exclusion arguments. Entire analysis was extensively revised such that change bars are not prudent.
REV 02	186	Entire scientific analysis documentation was revised. Changes were too extensive to use side bars (per Step 5.6c)1) of AP-SIII.9Q/Rev. 1/ICN 3). Revision addresses changes in the FEP list and updates to the include/exclude status and associated discussions based on revisions to technical inputs.

INTENTIONALLY LEFT BLANK

CONTENTS

Page

CONTENTS (Continued)

Page

CONTENTS (Continued)

Page

CONTENTS (Continued)

Page

TABLES

Page

INTENTIONALLY LEFT BLANK

ACRONYMS

CFR	Code of Federal Regulations
CRWMS M&O	Civilian Radioactive Waste Management System Management and Operating Contractor
DE	Disruptive Events
DSCPA	Drift Scale Coupled Processes Abstraction
DTN	Data Tracking Number
EBS	Engineered Barrier System
EDZ	Excavation-Disturbed Zone
ESF	Exploratory Studies Facility
FEP	Feature, Event, and Process
HLW	High-Level Waste
LA	License Application
MWCF	major water-conducting faults
NRC	Nuclear Regulatory Commission
NSP	Nevada State Plane
QA	Quality Assurance
RT	radionuclide transport
SC	Safety Category
SCM	Software Configuration Management
SNF	Spent Nuclear Fuel
SYS	System Level FEPs Report
SZ	saturated zone
TH	thermal-hydrological
THC	Thermal-Hydrological-Chemical
THM	thermal-hydrological-mechanical
THMC	thermal/hydrological/mechanical/chemical
TSPA	Total-System Performance Assessment
TSPA-LA	Total System Performance Assessment – License Application
TSPA-SR	Total-System Performance Assessment – Site Recommendation

ACRONYMS (continued)

UZ unsaturated zone

WP Work Package

YMP Yucca Mountain Project

MAJOR HYDROGEOLOGICAL UNITS

CHn Calico Hills nonwelded hydrogeological unit

PTn Paintbrush Tuff nonwelded hydrogeological unit

TSw Topopah Spring welded hydrogeological unit

1. PURPOSE

Unsaturated zone (UZ) flow and radionuclide transport is a component of the natural barriers that affects repository performance. This Analysis Report discusses all FEPs identified as associated with UZ flow and radionuclide transport. Included within the general category of UZ flow and radionuclide transport are such diverse topics as climate, surface water infiltration, drift seepage, and thermal-coupled processes. The purpose of this analysis is to give a comprehensive summary of all UZ flow and radionuclide transport FEPs and their treatment in, or exclusion from, TSPA-LA models. The scope of this analysis is to provide a summary of the FEPs associated with UZ flow and radionuclide transport and to provide a reference roadmap to other documentation where detailed discussions of these FEPs, treated explicitly in TSPA-LA models, are offered. Other FEPs are screened out from treatment in TSPA-LA by direct regulatory exclusion or through arguments concerning low probability and/or low consequence of the FEPs on repository performance. Arguments for exclusion of FEPs are presented in this analysis. In some cases, where a FEP covers multiple technical areas it may be shared with other FEP analysis reports. In these cases, this document may provide only a partial technical basis for the screening of the FEP. The full technical basis for these shared FEPs is addressed collectively by all of the sharing FEP analysis reports.

This Analysis Report has been developed in accordance with *Technical Work Plan for: Performance Assessment Unsaturated Zone* (Bechtel SAIC Company, LLC (BSC) 2004 [167969]), which includes planning documents for the technical work scope, content, and management of this Analysis Report in Section 1.12, Work Package AUZM08, "Coupled Effects on Flow and Seepage" and Section 2.4. This report has been developed using the most recent version of the *Yucca Mountain Review Plan* (YMRP; NRC 2003 [163274]) instead of the *Yucca Mountain Review Plan, Draft Report for Comment* (NRC 2002 [158449]) identified in the *Technical Work Plan for: Performance Assessment Unsaturated Zone* (BSC 2004 [167969], Section 3). The list of FEPs given in the *Technical Work Plan for: Performance Assessment Unsaturated Zone* (BSC 2004 [167969], Section 2.4) was superseded by the FEP list given in the LA FEP List (DTN: MO0307SEPFEPS4.000 [164527]). Evaluation by subject matter experts resulted in subsequent minor changes (to correct typographical or editorial errors) in the name of one FEP and in the descriptions of four other FEPs. These FEPs are identified in Section 6 in this Analysis Report. Furthermore, the UZ reports that directly support TSPA-LA have been expanded from the list identified in the *Technical Work Plan for: Performance Assessment Unsaturated Zone* (BSC 2004 [167969], Section 2.4) to also include *Analysis of Infiltration Uncertainty* (BSC 2003 [165991]) and *Radionuclide Transport Models Under Ambient Conditions* (BSC 2003 [163228]).

Because this Analysis Report is intended for use as a source of information to populate a FEPs database (an update to the database presented in BSC 2001 [154365], Appendix B), it contains self-identifying references (i.e., "in this Analysis Report" or a FEP Number) within the text of Section 6 and subsections.

INTENTIONALLY LEFT BLANK

2. QUALITY ASSURANCE

Development of this Analysis Report and the supporting modeling activities have been determined to be subject to the Yucca Mountain Project's quality assurance (QA) program, as indicated in *Technical Work Plan for: Performance Assessment Unsaturated Zone*, TWP-NBS-HS-000003 REV 02 (Bechtel SAIC Company, LLC (BSC) 2004 [167969], Section 8.2, Work Package (WP) AUZM08). Approved QA procedures identified in the TWP (BSC 2004 [167969], Section 4) have been used to conduct and document the activities described in this Analysis Report. This report deviates from the TWP (BSC 2004 [167969], Section 8.4, WP AUZM08) due to procedural changes in AP-SV.1Q REV 01 ICN 01, Control of the Electronic Management of Information, which now requires an evaluation of sensitive, unclassified electronic information. Because no sensitive, unclassified electronic information is produced from the work activities/processes/process functions in this document, further evaluation and controls are not applicable

This Scientific Analysis Report provides information pertaining to radionuclide transport through the unsaturated zone, which is a natural barrier and is classified in the *Q-List* (BSC 2003 [165179]) as SC (Safety Category) because it is important to waste isolation, as defined in AP-2.22Q, *Classification Analyses and Maintenance of the Q-List*. The results of this report are important to the demonstration of compliance with the post-closure performance objectives prescribed in 10 CFR 63.113 [156605]. The report contributes to the analysis and modeling data used to support postclosure perfomance assessment; the conclusions do not directly impact engineered features important to preclosure safety, as defined in AP-2.22Q.

INTENTIONALLY LEFT BLANK

3. USE OF SOFTWARE

No software requiring qualification in accordance with AP-SI.1Q, *Software Management* was used for the development of this Analysis Report. Standard functions of Excel (v 97-SR-1) and visual display graphics programs (Tecplot v. 7.0-4.0 for MS-WINDOWS) were used. All information required for an independent person to reproduce the work using these standard software programs, including the input, computation, and output, is included in this report. Excel calculations are documented in Appendices A and B.

INTENTIONALLY LEFT BLANK

4. INPUTS

4.1 DIRECT INPUTS

FEPs are classified as either included or excluded in this Analysis Report. Included FEPs are summarized in this report. Detailed information about how the included FEPs are treated in TSPA-LA is provided in the referenced reports. Arguments used to justify the exclusion from TSPA-LA of the excluded FEPs are presented in this Analysis Report. These arguments are based on inputs from sources external to this Analysis Report. The direct inputs used in this report are given in Table 4-1.

Table 4-1. Inputs

Section Number	Input	Type	Description
1	MO0307SEPFEPS4.000 [164527]	Data[a]	LA FEPs List
6.1.1 6.1.2 6.1.4 6.1.6 6.1.7 6.1.10 6.1.11 6.1.13 6.1.15 6.1.19 6.1.20 6.1.21 6.1.22 6.1.28 6.1.29 6.1.35 6.1.37 6.1.38 6.1.39	BSC 2004 [167972]	Data	Treatment of seepage water chemistry in TSPA-LA
6.1.2 6.1.3 6.1.4 6.1.5 6.1.6 6.1.7 6.1.10 6.1.11 6.1.13 6.1.14 6.1.15 6.1.16 6.1.18 6.1.19 6.1.20 6.1.25 6.1.30 6.1.37 6.1.41 6.1.43	BSC 2004 [166883]	Data[a]	Treatment of UZ flow in TSPA-LA

Table 4-1. Inputs (continued)

Section Number	Input	Type	Description
6.1.28 6.1.31 6.1.33 6.1.36	BSC 2003 [163228]	Data	Treatment of sorption in TSPA-LA
6.1.2 6.1.3 6.1.4 6.1.6 6.1.10 6.1.11 6.1.13 6.1.15 6.1.16 6.1.17 6.1.18 6.1.19 6.1.20 6.1.23 6.1.32 6.1.33 6.1.34 6.1.44	BSC 2004 [162730]	Data	Treatment of radionuclide transport in TSPA-LA
6.1.2 6.1.4 6.1.11 6.1.12 6.1.19 6.1.40 6.1.41 6.1.42 6.1.43	BSC 2003 [165991]	Data	Treatment of infiltration uncertainty in TSPA-LA
6.1.1 6.1.2 6.1.4 6.1.6 6.1.7 6.1.8 6.1.9 6.1.10 6.1.11 6.1.13 6.1.15 6.1.19 6.1.20 6.1.21 6.1.22 6.1.24 6.1.26 6.1.38 6.1.39	BSC 2004 [167970]	Data	Treatment of drift seepage in TSPA-LA

Table 4-1. Inputs (continued)

Section Number	Input	Type	Description
6.1.2 6.1.6 6.1.7 6.1.8 6.1.10 6.1.11 6.1.13 6.1.15 6.1.19 6.1.23 6.1.27 6.1.30	BSC 2004 [167959]	Data	Treatment of radionuclide transport near waste emplacement drifts in TSPA-LA
6.1.2 6.1.11 6.2.32 6.1.33	LA0311BR831371.003 [166515]	Data	UZ Transport Abstraction Model, transport parameters and base case simulation results
6.1.1 6.1.2 6.1.4 6.1.6 6.1.7 6.1.10 6.1.11 6.1.13 6.1.15 6.1.19 6.1.20 6.1.21 6.1.22 6.1.28 6.1.29 6.1.35 6.1.35 6.1.37 6.1.38 6.1.39	LB0302DSCPTHCS.002 [161976]	Data	Drift-Scale Coupled Processes (THC Seepage) Model: Data summary
6.1.2 6.1.8 6.1.11 6.1.13 6.1.15 6.1.19 6.1.26	LB0304SMDCREV2.002 [163687]	Data	Seepage model look-up tables for TSPA
6.1.1 6.1.2 6.1.8 6.1.11 6.1.13 6.1.15 6.1.19 6.1.21 6.1.22 6.1.26 6.1.38 6.1.39	LB0301DSCPTHSM.002 [163689]	Data[a]	TH seepage model results

Table 4-1. Inputs (continued)

Section Number	Input	Type	Description
6.1.1 6.1.2 6.1.4 6.1.6 6.1.7 6.1.10 6.1.11 6.1.13 6.1.15 6.1.19 6.1.20 6.1.22 6.1.28 6.1.29 6.1.35 6.1.37 6.1.38 6.1.39	LB0307DSTTHCR2.002 [165541]	Data	Drift-Scale Coupled Processes (DST Seepage) Model: Data summary
6.1.1 6.1.2 6.1.4 6.1.6 6.1.7 6.1.10 6.1.11 6.1.13 6.1.15 6.1.19 6.1.20 6.1.21 6.1.22 6.1.28 6.1.29 6.1.35 6.1.37 6.1.38 6.1.39	LB0311ABSTHCR2.001 [166714]	Data	Calculate summary statistics predicted aqueous species and CO_2 gas concentrations
6.1.1 6.1.2 6.1.4 6.1.6 6.1.7 6.1.10 6.1.11 6.1.13 6.1.15 6.1.19 6.1.20 6.1.21 6.1.22 6.1.28 6.1.29 6.1.35 6.1.37 6.1.38 6.1.39	LB0311ABSTHCR2.003 [166713]	Data	MS Excel 97 spreadsheets summarizing geochemical speciation at the original drift wall, and in and around the rubble zone. These data were used to generate time profiles for predicted TH parameters, aqueous species, and CO_2 gas concentrations

Table 4-1. Inputs (continued)

Section Number	Input	Type	Description
6.1.2 6.1.8 6.1.11 6.1.13 6.1.15 6.1.19, 6.1.26	LB0307SEEPDRCL.002 [164337]	Data	Seepage results for collapsed drift scenario
6.1.2 6.1.4 6.1.11, 6.1.12, 6.1.19, 6.1.40, 6.1.42, 6.1.43	SN0308T0503100.008 [165640]	Data	Frequency distributions for net infiltrations and weighting factors applied to lower, mean, and upper climates
6.1.3 6.1.4 6.1.6 6.1.7 6.1.10 6.1.11 6.1.13 6.1.14 6.1.15 6.1.18 6.1.19 6.1.20 6.1.25 6.1.41 6.1.42 6.1.43	LB0305TSPA18FF.001 [165625]	Data	Flow fields for TSPA from UZ flow model
6.1.4 6.1.6 6.1.7	LB0302PTNTSW9I.001 [162277]	Data	PTn/TSw flux maps from UZ flow model
6.1.4 6.1.6 6.1.7	LB0305PTNTSW9I.001 [163690]	Data	PTn/TSw flux maps from UZ flow model – alternative model
6.1.7	LB0104AMRU0185.012 [163906]	Data	Flow focusing distribution
6.1.24	LB0302SCMREV02.002 [162273]	Data	Seepage calibration model capillary strength parameter results
6.1.28 6.1.31 6.1.33 6.1.36	LA0302AM831341.002 [162575]	Data	Unsaturated zone distribution coefficients (Kds) for U, Np, Pu, Am, Pa, Cs, Sr, Ra, and Th
6.1.28 6.1.31 6.1.33 6.1.36	LA0311AM831341.001 [167015]	Data	Correlation matrix for sampling of sorption coefficient probability distributions
6.1.32	LA0311BR831229.001 [166924]	Data	Transfer function calculation files for UZ Transport Abstraction Model
6.1.33	SN0306T0504103.006 [164131]	Data	Colloid concentration and radionuclide sorption coefficients onto colloids
6.1.34	LL000122051021.116 [142973]	Data	Summary of analyses of glass dissolution filtrates
6.1.34	LA0303HV831352.002 [163558]	Data	Colloid retardation factors for the Saturated Zone fractured volcanics
6.2.1	BSC 2003 [168180]	Data	Borehole location relative to waste emplacement

Table 4-1. Inputs (continued)

Section Number	Input	Type	Description
6.2.1	BSC 2003 [160109]	Data	Stratigraphic sequence
6.2.1	BSC 2004 [168370]	Data[a]	Repository layout information
6.2.1	SNF40060298001.001 [107372]	Data	Stratigraphic contact depths
6.2.1	MO0010CPORGLOG.003 [155959]	Data	Borehole design information for USW UZ-7a
6.2.1	MO9906GPS98410.000 [109059]	Data	Surface borehole coordinates
6.2.1	MO0004QGFMPICK.000 [152554]	Data[a]	Stratigraphic contact depths in boreholes
6.2.1	BSC 2003 [161727]	Data	Emplacement drift end point coordinates
6.2.1, 6.3.5	Wu et al. 2000 [154918], Section 4.1	Data[a]	Episodic flow behavior in the PTn
Appendix A	LB03023DSSCP9I.001 [163044]	Data	Fracture and matrix saturation in gridblocks where perched water occurs; used to estimate potential quick release of perched water and to calculate how many years of flux this corresponds to; also to confirm that the PTN overlies the entire repository.
6.2.1	BSC 2003 [161773], Table 7 LB0205REVUZPRP.001 [159525]	Data	Fracture area per unit volume
6.2.2, 6.8.2	BSC 2004 [167970], Section 6.4.2.5 BSC 2003 [163226], Section 6.5	Data	Effects of rock bolt holes on drift seepage
6.2.2, 6.8.2	BSC 2003 [163226], Table 6-4	Data	Effects of boreholes on drift seepage
6.2.3	MO9805YMP98040.000 [164898]	Data[a]	Map of flood prone areas on the site surface
6.2.3	BSC 2002 [160857], Requirement 2.1.1.4	Data	Design requirement concerning surface water inundation of the subsurface facilities
6.2.3	Mineart 2003 [165898], Sections 5.2.3 and 5.16.3	Data[a]	Flooding at Yucca Mountain
6.2.6, 6.8.2	BSC 2003 [163226], Section 6.3.1	Data	Lateral flow near repository drifts
6.2.6	BSC 2003 [163999], Section 6.3.2.14	Data	Design for shafts relative to surface water flooding
6.2.6	Wu et al. 2000 [154918], Section 4.2	Data[a]	Episodic flow in the PTn
6.3.1	USGS 2003 [167961], Section 6.2	Data	Paleoclimate interpretation concerning permafrost at Yucca Mountain
6.3.1	USGS 2003 [167961], Section 6.6.2	Data	Mean annual temperatures for glacial-transition climate
6.3.1	Sharpe 2003 [161591], Section 6.3.2	Data[a]	Mean annual temperatures for glacial-transition climate
6.3.1	Sharpe 2003 [161591], Table 6-3	Data[a]	Mean annual temperatures for full glacial OIS6/16 climate
6.3.1	Sharpe 2003 [161591], Table 6-5	Data[a]	Timing for return of full glacial OIS6/16 climate
6.3.1, 6.4.1	YMP 1993 [100520], pp. 55–56	Data[a]	Erosion rate
6.3.2	Simmons 2004 [166960], Section 6.4	Data	Paleoclimate interpretation concerning permafrost at Yucca Mountain

Table 4-1. Inputs (continued)

Section Number	Input	Type	Description
6.3.2	Simmons 2004 [166960], Section 6.4.1.2.2	Data	Information on glaciation in the vicinity of Yucca Mountain
6.3.3	USGS 2003 [167961], Section 6.6	Data	Future climates
6.3.4	BSC 2003 [163228], Equation 6-23	Data	Stokes-Einstein Equation
6.3.4	Perry and Chilton 1973 [104946], Equation 5-215	Established Fact	Stokes' law
6.3.4	Vanoni 1977 [164901], Figure 2.51	Data[b]	Entrainment of cohesive sediments in flowing water
6.3.4	BSC 2003 [163228], Section 6.18.4	Data	Colloid transport time in the UZ
6.3.5	CRWMS M&O 1998 [100356], Section 2.4.2.8	Data[a]	Quantity of water and dissolved constituents that penetrate the PTn as a transient flow phenomenon
6.4.1	YMP 2001 [154386], Section 5.2.2.1	Data[a]	Site reclamation plan
6.4.1	YMP 1995 [102215], Sections 2.5.2 and 4.2	Data[a]	Effects of debris flows on erosion processes
6.4.2	YMP 1993 [100520], p. 55	Data[a]	Deposition rate
6.4.3	Simmons 2004 [166960], Section 3.3.2	Data	Bulk mineral composition of Yucca Mountain
6.4.4	Keller 1992 [146831], p. 142	Data[c]	Subsidence behavior in coal mines
6.4.4	BSC 2004 [167040]	Data	Drift spacing
6.4.4, 6.8.2	BSC 2003 [164101]	Data	Drift diameter
6.4.4	BSC 2003 [162711], Attachment XVIII	Data	Effects of drift collapse
6.4.4	BSC 2004 [167973], Section 8.1	Data	Effects of drift collapse
6.4.6	DOE 1998 [100282], Section 1.1.3.3.2	Data[a]	Mass wasting at Yucca Mountain
6.5.1 6.5.2 6.5.3 6.5.4	10 CFR 63.305(c) [156605]	Established Fact	Regulatory exclusion of human effects on climate.
6.5.1 6.5.2 6.5.3, 6.5.4	66 FR 55732 [156671], p. 55757	Established fact	Rationale for regulatory position excluding human influences on climate.
6.5.1	67 FR 62628 [162317]	Established fact	Rationale for regulatory position excluding human influences on climate.
6.5.5	Simmons 2004 [166960], Section 3.6	Data	Resources at Yucca Mountain valuable for human development
6.5.5	10 CFR 63.305(c) [156605]	Established fact	Rationale for regulatory position excluding human influences on soil and water
6.6.1	Richards 1931 [104252]	Established fact	Unsaturated flow mathematical approximation
6.6.2	LB0302DSCPTHCS.002 [161976]	Data	Drift-Scale Coupled Processes (THC Seepage) Model: Data summary
6.6.3	DOE 2002 [155970], Section I.7	Data[a]	Gas-phase dose for C-14
6.6.3	CRWMS M&O 2000 [153246], Figure 4.1-7	Data	Aqueous-phase dose for C-14

Table 4-1. Inputs (continued)

Section Number	Input	Type	Description
6.6.3	BSC 2004 [162730]	Data	Treatment of radionuclide transport in TSPA-LA
6.7.1, 6.7.4	Valentine et al. 1998 [119132], p. 5-74	Data[a]	Mineral alteration resulting from hydrothermal activity
6.7.1, 6.7.4	BSC 2003 [166407], Section 6.3.1	Data	Dike thicknesses
6.7.1, 6.7.4	BSC 2003 [165923], Figure 161	Data	Spatial extent of boiling near dikes
6.7.2, 6.7.4	Simmons 2004 [166960], Section 4.2.3.5	Data	Spatial extent of contact metamorphism
6.7.1, 6.7.4	BSC 2003 [163769], Table 21	Data	Probability of a volcanic event
6.7.2	BSC 2003 [163769], Figure 3	Data	Spatial relationship between Yucca Mountain and the associated caldera
6.7.2	BSC 2003 [163769], Section 6.2	Data	Silicic magmatism at Yucca Mountain
6.7.2	Simmons 2004 [166960], Section 3.6.2	Data	Evidence for hydrothermal activity
6.7.2	Wilson et al. 2003 [163589], Section 8	Data[a]	Two-phase fluid inclusions
6.7.2	BSC 2003 [163769], Section 6.2	Data	Decline in eruptive volume in the southwestern Nevada volcanic fluid
6.7.2	BSC 2003 [163769], Section 6.3	Data	Probability of intersection of a dike with the repository
6.7.3	Carrigan et al. 1991 [100967], p. 1159	Data[a]	Water table excursions due to a fault slip
6.7.3	Bruhn 1994 [118920]	Data[d]	Effects of fault slips on permeability
6.7.3	Stock et al. 1985 [101027]	Data[a]	Residual stress field at Yucca Mountain
6.7.3	Stock and Healy 1988 [101022]	Data[a]	Interpretation of stress measurements at Yucca Mountain
6.7.4	USGS 2001 [160355], Attachment IV	Data	Soil permeability
6.7.4	Zhou et al. 2003 [162133]	Data[a]	Effects of small-scale heterogeneity on flow and transport
6.7.4	BSC 2003 [166407], Section 6.4	Data	Ash deposit grain sizes
6.7.5, 6.7.6	BSC 2004 [167973], Section 6.2	Data	Effects of thermal-mechanical stress on rock matrix properties
6.7.6	CRWMS M&O 2000 [151953], Section 6	Data	Effects of changes in fault properties on flow and transport behavior
6.7.6	USGS 1998 [100354], Figure 8.3	Data[a]	Future fault movement for Solitario Canyon Fault
6.7.7	CRWMS M&O 2000 [151953], Section 6.2.2.4	Data	Effects of changes in fracture properties on flow and transport
6.7.7	BSC 2004 [166883], Section 6.7.3	Data[a]	Effects of infiltration uncertainty on transport uncertainty
6.7.8	BSC 2004 [168370]	Data[a]	Waste emplacement area
6.7.8	BSC 2003 [166262], Section 6.4.5	Data	Water table rise.
6.7.8	BSC 2004 [162730], Table 6-6	Data	Minimum average water content of rock in the UZ within 100 m of the water table.
6.7.9	BSC 2004 [166883], Sections 6.2.2.1 and 6.6.3	Data[a]	Flow and transport patterns in the UZ

Table 4-1. Inputs (continued)

Section Number	Input	Type	Description
6.7.9	BSC 2004 [166883], Sections 6.2.2.2 and 6.6.3	Data[a]	Effects of perched water on lateral diversion
6.7.9	CRWMS M&O 2000 [151953], Section 7	Data	Effects of changes in fault properties on transport in the UZ
6.7.9	BSC 2001 [158726], Sections 6.2.2 and 6.2.5	Data[e]	Alternative perched water models
6.7.9	BSC 2001 [158726], Section 6.7.2	Data[e]	Transport sensitivity to perched water models
6.8.1	BSC 2004 [167970]	Data	Treatment of drift seepage in TSPA-LA
6.8.1, 6.8.7, 6.8.13	BSC 2004 [167974], Section 6.6.2.3.1	Data	Changes in fracture permeability due to THC processes
6.8.1, 6.8.7, 6.8.13	BSC 2004 [167974], Figures 6.5-16, 6.6-4, 6.8-40b, 6.8-41b	Data	Changes in fracture permeability due to Thermal-Hydrological-Chemical (THC) processes
6.8.2	BSC 2003 [163226], Section 6.5	Data	Effects of rock bolt holes on drift seepage
6.8.2	BSC 2003 [164101], p. 1	Data	Ground support materials
6.8.2	BSC 2004 [167461], Table 6.6-4	Data	Seepage water composition
6.8.2	BSC 2004 [167461], Tables 6.6-8 through 6.6-12	Data	Seepage water composition
6.8.2	BSC 2004 [167461], Section 6.8.4.3	Data	Effects of stainless steel on water composition
6.8.2	BSC 2004 [167461], Section 6.12.4.1	Data	Effects of stainless steel on water composition
6.8.2	BSC 2004 [167461], Section 6.12.4.1.3	Data	Effects of stainless steel on water composition
6.8.2	BSC 2003 [164052], p. 1	Data	Use of cementitious materials for ground support
6.8.3, 6.8.10	BSC 2004 [167973], Section 6.7	Data	Effects of Thermal-Hydrological-Mechanical (THM) coupled processes on temperature and flow
6.8.3, 6.8.10	BSC 2004 [167970], Section 6.4.4.1	Data	Effects of temperature-induced stress changes on permeability
6.8.3, 6.8.10	BSC 2004 [167970], Section 6.5.1.4	Data	Effects of temperature-induced stress changes on permeability
6.8.3, 6.8.10	BSC 2004 [167973], Sections 6.5.5 and 6.6.2	Data	Effects of temperature-induced stress changes in permeability on the flow field
6.8.3, 6.8.10	BSC 2004 [167973]	Data	Effects of THM coupled processes on drift seepage
6.8.3, 6.8.10	BSC 2004 [167970], Section 6.4.4.1	Data	Effects of THM coupled processes on drift seepage
6.8.4	BSC 2003 [166512], Section 6.2.1.3.3	Data[a]	Effects of pre-closure dryout on thermal seepage
6.8.5, 6.8.8	BSC 2003 [166845], Section 6.3.1	Data	Source of colloids
6.8.5, 6.8.8	BSC 2003 [166845], Figure 1b	Data	Effects of solubility limits on true colloids
6.8.5, 6.8.8	BSC 2003 [166845], Section 6.3.1	Data	Formation of true colloids from waste form
6.8.6	BSC 2004 [167959]	Data	Effects of fracture aperture on fracture-matrix partitioning of radionuclides entering the UZ

Table 4-1. Inputs (continued)

Section Number	Input	Type	Description
6.8.6	BSC 2004 [167973], Sections 6.5.1 and 6.6.1	Data	Effects of stress relief
6.8.6	CRWMS M&O 2000 [153246], Figures 4.1-5 and 4.1-7	Data	Change in dose rates over 10,000 years
6.8.6	CRWMS M&O 2000 [153246], Figure 4.1	Data	Waste package failures as a function of time
6.8.7	BSC 2004 [167974]	Data	Effects of THC processes on water composition
6.8.7, 6.8.13	BSC 2004 [167974], Figures 6.5-9, 6.7-11, 6.8-13	Data	Effects of THC processes on pH
6.8.7, 6.8.13	BSC 2003 [163228], Attachment I	Data	Effects of pH on radionuclide sorption
6.8.7, 6.8.13	BSC 2004 [167974], Table 6.2-1	Data	Range of variability in pH for pore water compositions
6.8.7, 6.8.13	BSC 2004 [167974], Figure 6.8-17	Data	Effects of THC processes on water aqueous silica, Ca, Na, and Cl
6.8.7	BSC 2004 [167975], Section 6.4.3.3.2	Data	Magnitude and duration of water composition changes due to THC processes along aqueous radionuclide pathways
6.8.9	BSC 2004 [167975], Figures 6.2-10a and b, 6.3.1-18	Data	Effects of Thermal-Hydrological (TH) processes on flow
6.8.9	BSC 2003 [166512], Section 6.2.2.1	Data	Diversion of water around thermal dryout zone
6.8.9	BSC 2003 [166512], Section 6.2.2.1.1	Data	Effects of thermal dryout and drift shadow on radionuclide transport
6.8.9	CRWMS M&O 1999 [103618]	Data[a]	Thermal effects on vegetation
6.8.10	BSC 2004 [167973], Sections 6.5 and 6.6	Data	Effects of THM processes on temperature and flow
6.8.11	BSC 2004 [167973], Section 6.8.5	Data	Effects of THM coupled processes on permeability
6.8.12	BSC 2004 [167975], Section 6.5	Data	Effects of THM processes on flow away from the waste emplacement drifts
6.8.13	BSC 2003 [166845], Section 6.3.1	Data	Source of colloids
6.8.13	BSC 2003 [166845], Section 6.3.1.2	Data	Effects of temperature on colloidal stability
6.8.13	BSC 2004 [167972], Section 6.4.4.5	Data	Effects of temperature on radionuclide sorption
6.8.13	BSC 2004 [167975], Section 6.4.3.3.2	Data	Magnitude and duration of water composition changes due to THC processes along aqueous radionuclide pathways
6.8.14	BSC 2004 [167975], Sections 6.4.3.3.3 and 6.4.3.3.4	Data	Mineral alteration and hydrogeologic effects of precipitation/dissolution in the CHn
6.8.14	BSC 2003 [163228], Attachment I	Data	Effects of rock type on radionuclide sorption.
6.8.15	BSC 2004 [167975], Sections 6.4.3.3.3 and 6.4.3.3.4	Data	Mineral alteration and hydrogeologic effects of precipitation/dissolution in the TSw vitrophyre

Table 4-1. Inputs (continued)

Section Number	Input	Type	Description
6.8.15	BSC 2003 [163228], Attachment I	Data	Effects of rock type on radionuclide sorption.
6.8.16	BSC 2003 [160109], Section 5.2	Data	Location of zeolites in the UZ
6.8.16	BSC 2004 [167975], Figure 6.2-6c	Data	Peak temperatures in zeolitic units
6.8.16	BSC 2003 [160109], Figures 5 and 6	Data	Peak temperatures in zeolitic units
6.8.16	BSC 2004 [167975], Section 6.3.1	Data	Peak temperatures in zeolitic units
6.8.16	Smyth 1982 [119483], p. 201	Data[a]	Zeolitic alteration temperature

NOTES: Arguments in Sections 6.2.4, 6.2.5, 6.2.7, and 6.2.8 are based on discussions in Section 6.2.1 and 6.2.6

Documentation of the suitability of data that does not originate from OCRWM-supported research (i.e., "outside sources" in AP-SIII.9Q) for use in this analysis report is based upon the following criteria, as referred to in footnotes b-d below.

(1) reliability of source of the data
(2) qualifications of the personnel or organizations generating the data
(3) extent to which the data demonstrates the properties of interest
(4) prior uses of the data, and
(5) availability of corroborating data.

[a] TBV

[b] Based on experimental evidence concerning the behavior of entrained cohesive sediments (colloids) upon changes in water flow rates. Published in the American Society of Civil Engineers Manual and Reports on Engineering Practice series. Therefore, the employed methodology is acceptable and confidence in the results is warranted. This meets criteria (1), (2), and (3) above.

[c] This criterion (that subsidence occurs when more than half the rock is removed) is based on many years of coal-mining experience, and is published in a standard geology textbook. The amount of rock removed in Yucca Mountain drifts is planned to be much less than half. Therefore, confidence in the results is warranted. This meets all 5 criteria above.

[d] Based on observations of fault properties before and after seismic events. Published as a USGS open file report. Therefore, the employed methodology is acceptable and confidence in the results is warranted. This meets criteria (1), (2), and (3) above.

[e] This Model Report has been superseded, but the model simulations presented therein are suitable for use because they were developed using qualified software and are output from a model that was developed for Site Recommendation and validated in accordance with the Quality Assurance program. Changes in the repository footprint and rock properties for License Application do not affect the conclusions concerning perched water.

4.2 CRITERIA

The licensing criteria for postclosure performance assessment are stated in 10 CFR 63.114 [156605]. The requirements to be satisfied by TSPA-LA are identified in the Yucca Mountain *Project Requirements Document* (Canori and Leitner 2003 [166275]). The acceptance criteria that will be used by the Nuclear Regulatory Commission (NRC) to determine whether the technical requirements have been met are identified in *Yucca Mountain Review Plan, Final Report* (YMRP; NRC 2003 [163274]). The pertinent requirements and criteria for this Analysis Report are summarized in Table 4-2.

Table 4-2. Project Requirements and YMRP Acceptance Criteria Applicable to This Analysis Report

Requirement Number[a]	Requirement Title[a]	10 CFR 63 Link	YMRP Acceptance Criteria
PRD-002/T-015	Requirements for Performance Assessment	10 CFR 63.114(a-f) [156605]	Criteria 1 and 2 for Scenario Analysis and Event Probability[b]

NOTES: [a] from Canori and Leitner (2003 [166275])
[b] from NRC (2003 [163274], Section 2.2.1.2.1.3)

The acceptance criteria identified in Section 2.2.1.2.1.3 of the YMRP (NRC 2003 [163274]) are given below, followed by a short description of their applicability to this Analysis Report (Note: This report has been developed using the most recent version of the Yucca Mountain Review Plan (YMRP; NRC 2003 [163274]) instead of the *Yucca Mountain Review Plan, Draft Report for Comment* (NRC 2002 [158449]) identified in the *Technical Work Plan for: Performance Assessment Unsaturated Zone* (BSC 2004 [167969], Section 3), which has resulted in different criteria numbers compared with those cited in the *Technical Work Plan for: Performance Assessment Unsaturated Zone* (BSC 2004 [167969], Table 3-1):

- Acceptance Criterion 1, *The Identification of a List of Features, Events, and Processes Is Adequate* (also refer to Section 6 of this Analysis Report):

This Analysis Report contains a complete list of features, events, and processes, related to the UZ (outside the waste emplacement drift) that would affect the performance of the repository (BSC 2001 [154365]; BSC 2002 [158966]; Freeze 2003 [165394]; DTN: MO0307SEPFEPS4.000 [164527]). The list is consistent with the site characterization data. Moreover, the comprehensive features, events, and processes list includes, but is not limited to, hydrologic processes; radionuclide transport processes; effects of repository and site characterization construction; effects of repository heat and materials on hydrologic and transport processes; potentially disruptive events related to igneous activity (extrusive and intrusive); seismic shaking (high-frequency-low magnitude, and rare large-magnitude events); tectonic evolution (slip on existing faults and formation of new faults); and climatic change (change to pluvial conditions).

- Acceptance Criterion 2, *Screening of the List of Features, Events, and Processes Is Appropriate* (also refer to Section 6 of this Analysis Report):

This Analysis Report identifies all excluded features, events, and processes related to the UZ (outside the waste emplacement drift) affecting the performance of the repository. Furthermore,

justifications and their technical bases for exclusion are described. Acceptable justifications for excluding features, events, and processes are that either the feature, event, and process is specifically excluded by regulation; probability of the feature, event, and process (generally an event) falls below the regulatory criterion; or omission of the feature, event, and process does not significantly change the magnitude and time of the resulting radiological exposures to the reasonably maximally exposed individual, or radionuclide releases to the accessible environment.

4.2.1 The FEPs Screening Criteria

The NRC requires the consideration and evaluation of FEPs as part of the performance assessment activities. More specifically, the NRC regulations allow the exclusion of FEPs from the TSPA-LA if they can be shown to be of low probability or of low consequence. Specified criteria can be summarized in the form of two FEP screening statements as follows:

1) The event has at least one chance in 10,000 of occurring over 10,000 years (see 10 CFR 63.114(d) [156605]).

2) The magnitude and time of the resulting radiological exposure to the Reasonably Maximally Exposed Individual, or radionuclide release to the accessible environment, would be significantly changed by its omission (see 10 CFR 63.114 (e and f) [156605]).

Additionally, the Acceptance Criteria in the YMRP (NRC 2003 [163274], Section 2.2.1.2.1.3) call for evaluating the FEPs based on the regulations. This criterion can be summarized in the form of a third FEP screening statement.

3) The FEP is not excluded by regulation.

If there are affirmative conditions for all three screening criteria, the FEP is *Included* in the TSPA-LA model. Any negating condition in the three screening criteria *Excludes* the FEP from the TSPA-LA model. These criteria are described further in the following three subsections.

4.2.1.1 Low Probability

The low-probability criterion is stated in 10 CFR 63.114(d) [156605]:

> *Consider only events that have at least one chance in 10,000 of occurring over 10,000 years.*

and supported by 10 CFR 63.342 [156605]:

> *The Department of Energy's (DOE) performance assessments shall not include consideration of very unlikely features, events, or processes, i.e., those that are estimated to have less than one chance in 10,000 of occurring within 10,000 years of disposal.*

The low probability criterion for very unlikely events is stated as less than one chance in 10,000 of occurring in 10,000 years ($10^{-4}/10^{4}$ yr).

4.2.1.2 Low Consequence

The low consequence criterion is stated in 10 CFR 63.114 (e and f) [156605]:

> *(e) Provide the technical basis for either inclusion or exclusion of specific features, events, and processes in the performance assessment. Specific features, events, and processes must be evaluated in detail if the magnitude and time of the resulting radiological exposures to the reasonably maximally exposed individual, or radionuclide releases to the accessible environment, would be significantly changed by their omission.*
>
> *(f) Provide the technical basis for either inclusion or exclusion of degradation, deterioration, or alteration processes of engineered barriers in the performance assessment, including those processes that would adversely affect the performance of natural barriers. Degradation, deterioration, or alteration processes of engineered barriers must be evaluated in detail if the magnitude and time of the resulting radiological exposures to the reasonably maximally exposed individual, or radionuclide releases to the accessible environment, would be significantly changed by their omission.*

and supported by 10 CFR 63.342 [156605]:

> *DOE's performance assessments need not evaluate the impacts resulting from any features, events, and processes or sequences of events and processes with a higher chance of occurrence if the results of the performance assessments would not be changed significantly.*

Some FEPs have a beneficial effect on the TSPA, as opposed to an adverse effect. As identified in 10 CFR 63.102(j) [156605], the concept of a performance assessment includes that:

> *The features, events, and processes considered in the performance assessment should represent a wide range of both beneficial and potentially adverse effects on performance (e.g., beneficial effects of radionuclide sorption; potentially adverse effects of fracture flow or a criticality event). Those features, events, and processes expected to materially affect compliance with [10 CFR] 63.113(b) or be potentially adverse to performance are included, while events (event classes or scenario classes) that are very unlikely (less than one chance in 10,000 over 10,000 years) can be excluded from the analysis. ...*

The Yucca Mountain Review Plan, NUREG-1804 (NRC 2003 [163274], Section 2.2.1), states that:

> *In many regulatory applications, a conservative approach can be used to decrease the need to collect additional information or to justify a simplified modeling approach. Conservative estimates for the dose to the reasonably maximally exposed individual may be used to demonstrate that the proposed repository meets U.S. Nuclear Regulatory Commission regulations and provides adequate protection of*

> *public health and safety. ...The total system performance assessment is a complex analysis with many parameters, and the U.S. Department of Energy may use conservative assumptions to simplify its approaches and data collection needs. However, a technical basis ... must be provided.*

On the basis of these statements, those FEPs that are demonstrated to have only beneficial effects on the radiological exposures to the reasonably maximally exposed individual, or radionuclide releases to the accessible environment, can be excluded on the basis of low consequence because they have no adverse effects on performance.

4.2.1.3 By Regulation

The Acceptance Criteria for FEPs screening presented in NUREG-1804 echo the screening criteria of low probability and low consequence (NRC 2003 [163274], Section 2.2.1.2.1.3 Acceptance Criterion 2, *Screening of the List of Features, Events, and Processes Is Appropriate*), but also allows for exclusion of a FEP if the process is specifically excluded by the regulations. To wit:

An acceptable justification for excluding features, events, and processes is that either the feature, event, and process is specifically excluded by regulation; probability of the feature, event, and process (generally an event) falls below the regulatory criterion; or omission of the feature, event, and process does not significantly change the magnitude and time of the resulting radiological exposures to the reasonably maximally exposed individual, or radionuclide releases to the accessible environment.

4.3 CODES AND STANDARDS

This document addresses NRC regulatory arguments presented in 10 CFR Part 63 (66 FR 55732 [156671]). Portions of the NRC regulations applicable to FEP screening are identified in Section 4.1.

INTENTIONALLY LEFT BLANK

5. ASSUMPTIONS

It is assumed that regulations expressed as probability criterion can also be expressed as an annual exceedance probability, which is defined as "the probability that a specified value will be exceeded during one year". More specifically, a stated probability screening criterion for very unlikely FEPs of one chance in 10,000 in 10,000 years ($10^{-4}/10^{4}$ yr) is assumed equivalent to a 10^{-8} annual-exceedance probability or annual-exceedance frequency.

Justification: The assumption of equivalence of annual-exceedance probability is appropriate if the possibility of an event is equal for any given year. Geologic events such as earthquakes are considered as independent events with regard to size, time, and location. Consequently, assuming annual equivalence is reasonable. No further confirmation is required.

Use: This assumption is used in Sections 6.7.6 and 6.7.7 of this Analysis Report.

INTENTIONALLY LEFT BLANK

6. ANALYSIS

The development of a comprehensive list of FEPs potentially relevant to post-closure performance of the potential Yucca Mountain repository is an ongoing, iterative process based on site-specific information, design, and regulations. The approach for developing an initial list of FEPs, in support of TSPA–Site Recommendation (SR), was documented in BSC (2001 [154365]). To support TSPA-LA, the YMP FEP list was re-evaluated in accordance with BSC 2002 [158966] and Freeze 2003 [165394]. The resulting 367 TSPA-LA FEPs are identified in a preliminary TSPA-LA FEP list (DTN: MO0307SEPFEPS4.000 [164527]).

Each FEP is assigned to subject matter experts in a specific technical area for analysis and resolution. The screening decisions and supporting analysis are documented in a corresponding set of FEP analysis reports. In some cases, where a FEP covers multiple technical areas it may be shared with other FEP analysis reports. In these cases, the full technical basis for these shared FEPs is addressed collectively by all of the sharing FEP analysis reports.

There are 94 TSPA-LA FEPs identified as relevant to unsaturated zone flow and transport in the preliminary TSPA-LA FEP list (DTN: MO0307SEPFEPS4.000 [164527]); they are addressed in this FEP analysis report. These include TSPA- LA FEPs that derive from TSPA-SR FEPs that were documented in the previous version of *Features, Events, and Processes in UZ Flow and Transport* (BSC 2001 [154826]) and some that were previously documented in *Features, Events, and Processes in Thermal Hydrology and Coupled Processes* (CRWMS M&O 2001 [153935]). Evaluation of these FEPs by subject matter experts resulted in subsequent minor changes (to correct typographical or editorial errors) in the name of one FEP (1.2.10.01.0A) and in the descriptions of four other FEPs (1.3.07.01.0A, 1.3.07.02.0B, 2.2.06.01.0A, and 2.2.07.01.0A). Table 6-1 lists these 94 TSPA-LA FEPs, identifies associated TSPA-SR FEPs, and identifies those FEPs that are shared with other FEP analysis reports. Note that this cross-walk is not reversible (SR to LA), because some listed SR FEPs were split among areas other than UZ.

Table 6-1. Cross-Walk between LA and SR FEPs

LA FEP Number	LA FEP Name	SR FEP Number	SR FEP Name	Other FEP reports that address shared FEP
1.1.01.01.0A	Open site investigation boreholes	1.1.01.01.00 1.1.01.02.00 1.4.04.02.00	Open site investigation boreholes Loss of integrity of borehole seals Abandoned and undetected boreholes	
1.1.01.01.0B	Influx through holes drilled in drift wall or crown	1.1.01.01.00	Open site investigation boreholes	
1.1.02.01.0A	Site flooding (during construction and operation)	1.1.02.01.00	Site flooding (during construction and operation)	
1.1.02.02.0A	Pre-closure ventilation	1.1.02.02.00	Effects of pre-closure ventilation	Engineered Barrier System (EBS)
1.1.04.01.0A	Incomplete closure	1.1.04.01.00	Incomplete closure	
1.1.11.00.0A	Monitoring of repository	1.1.11.00.00	Monitoring of repository	System Level FEPs Report (SYS)
1.2.02.01.0A	Fractures	1.2.02.01.00	Fractures	Saturated Zone (SZ)
1.2.02.02.0A	Faults	1.2.02.02.00	Faulting	SZ
1.2.04.02.0A	Igneous activity causes changes to rock properties	1.2.04.02.00	Igneous activity causes changes to rock properties	Disruptive Events (DE) SZ
1.2.06.00.0A	Hydrothermal activity	1.2.06.00.00	Hydrothermal activity	SZ
1.2.07.01.0A	Erosion/denudation	1.2.07.01.00	Erosion/Denudation	
1.2.07.02.0A	Deposition	1.2.07.02.00	Deposition	
1.2.09.02.0A	Large-scale dissolution	1.2.09.02.00	Large-scale dissolution	SZ
1.2.10.01.0A	Hydrologic response to seismic activity	1.2.10.01.00	Hydrological response to seismic activity	DE SZ
1.2.10.02.0A	Hydrologic response to igneous activity	1.2.10.02.00	Hydrologic response to igneous activity	DE SZ
1.3.01.00.0A	Climate change	1.3.01.00.00	Climate change, global	Bio
1.3.04.00.0A	Periglacial effects	1.3.04.00.00	Periglacial effects	Bio
1.3.05.00.0A	Glacial and ice sheet effect	1.3.05.00.00	Glacial and ice sheet effects, Local	Bio
1.3.07.01.0A	Water table decline	1.3.07.01.00	Drought / water table decline	SZ
1.3.07.02.0B	Water table rise affects UZ	1.3.07.02.00	Water table rise	
1.4.01.00.0A	Human influences on climate	1.4.01.00.00	Human influences on climate	Bio
1.4.01.01.0A	Climate modification increases recharge	1.4.01.01.00	Climate modification increases recharge	
1.4.01.02.0A	Greenhouse gas effects	1.4.01.02.00	Greenhouse gas effects	Bio
1.4.01.03.0A	Acid rain	1.4.01.03.00	Acid rain	Bio
1.4.01.04.0A	Ozone layer failure	1.4.01.04.00	Ozone layer failure	Bio
1.4.06.01.0A	Altered soil or surface water chemistry	1.4.06.01.00	Altered soil or surface water chemistry	
2.1.05.01.0A	Flow through seals (access ramps and ventilation shafts)	2.1.05.01.00	Seal physical properties	
2.1.05.02.0A	Radionuclide transport through seals	2.1.05.02.00	Groundwater flow and radionuclide transport in seals	
2.1.05.03.0A	Degradation of seals	2.1.05.03.00 2.1.05.01.00	Seal degradation Seal physical properties	
2.1.08.01.0A	Water influx at the repository	2.1.08.01.00	Increased unsaturated water flux at the repository	
2.1.08.02.0A	Enhanced influx at the repository	2.1.08.02.00	Enhanced influx (Philip's drip)	
2.1.09.12.0A	Rind (chemically altered zone) forms in the near-field	2.1.09.12.00	Rind (altered zone) formation in waste, EBS, and adjacent rock	

Table 6-1. Cross-Walk between LA and SR FEPs (continued)

LA FEP Number	LA FEP Name	SR FEP Number	SR FEP Name	Other FEP reports that address shared FEP
2.1.09.21.0C	Transport of particles larger than colloids in the UZ	2.1.09.21.00	Transport of particles larger than colloids in EBS*	
2.2.01.01.0A	Mechanical effects of excavation/construction in the near field	2.2.01.01.00	Excavation and construction-related changes in the adjacent host rock	
2.2.01.01.0B	Chemical effects of excavation/construction in the near-field	2.2.01.01.00	Excavation and Construction-Related Changes in the Adjacent Host Rock	
2.2.01.02.0A	Thermally-induced stress changes in the near-field	2.2.01.02.00	Thermal and Other Waste and EBS-Related Changes in the Adjacent Host Rock	EBS
2.2.01.03.0A	Changes in fluid saturations in the excavation disturbed zone	2.2.01.03.00	Changes in fluid saturations in the excavation disturbed zone (EDZ)	
2.2.01.04.0A	Radionuclide solubility in the excavation disturbed zone	2.2.01.04.00	Radionuclide solubility in the excavation disturbed zone*	
2.2.01.05.0A	Radionuclide transport in the excavation disturbed zone	2.2.01.05.00	Radionuclide transport in excavation disturbed zone	
2.2.03.01.0A	Stratigraphy	2.2.03.01.00	Stratigraphy	SZ
2.2.03.02.0A	Rock properties of host rock and other units	2.2.03.02.00	Rock properties of host rock and other units	SZ
2.2.06.01.0A	Seismic activity changes porosity and permeability of rock	2.2.06.01.00 1.2.02.02.00 1.2.03.01.00	Changes in stress (due to thermal, seismic, or tectonic effects) change porosity and permeability of rock Faulting Seismic activity	DE SZ
2.2.06.02.0A	Seismic activity changes porosity and permeability of faults	2.2.06.02.00 1.2.03.01.00	Changes in stress (due to thermal, seismic, or tectonic effects) produce change in permeability of faults Seismic activity	DE SZ
2.2.06.02.0B	Seismic activity changes porosity and permeability of fractures	1.2.02.01.00 2.2.06.02.00 1.2.03.01.00	Fractures Changes in stress (due to thermal, seismic, or tectonic effects) produce change in permeability of faults Seismic activity	DE SZ
2.2.06.03.0A	Seismic activity alters perched water zones	2.2.06.03.00 1.2.03.01.00	Changes in stress (due to seismic or tectonic effects) alter perched water zones Seismic activity	DE
2.2.06.04.0A	Effects of subsidence	2.2.06.04.00	Effects of subsidence	
2.2.07.01.0A	Locally saturated flow at bedrock/alluvium contact	2.2.07.01.00	Locally saturated flow at bedrock/alluvium contact	
2.2.07.02.0A	Unsaturated groundwater flow in the geosphere	2.2.07.02.00	Unsaturated groundwater flow in geosphere	
2.2.07.03.0A	Capillary rise in the UZ	2.2.07.03.00	Capillary rise	
2.2.07.04.0A	Focusing of unsaturated flow (fingers, weeps)	2.2.07.04.00	Focusing of unsaturated flow (fingers, weeps)	
2.2.07.05.0A	Flow in the UZ from episodic infiltration	2.2.07.05.00	Flow and transport in the UZ from episodic infiltration	
2.2.07.06.0A	Episodic / pulse release from repository	2.2.07.06.00	Episodic/pulse release from repository	EBS

Table 6-1. Cross-Walk between LA and SR FEPs (continued)

LA FEP Number	LA FEP Name	SR FEP Number	SR FEP Name	Other FEP reports that address shared FEP
2.2.07.06.0B	Long-term release of radionuclides from the repository	2.2.07.06.00	Episodic / pulse release from repository	EBS
2.2.07.07.0A	Perched water develops	2.2.07.07.00	Perched water develops	
2.2.07.08.0A	Fracture flow in the UZ	2.2.07.08.00	Fracture flow in the unsaturated zone	
2.2.07.09.0A	Matrix imbibition in the UZ	2.2.07.09.00	Matrix imbibition in the unsaturated zone	
2.2.07.10.0A	Condensation zone forms around drifts	2.2.07.10.00	Condensation zone forms around drifts	
2.2.07.11.0A	Resaturation of geosphere dry-out zone	2.2.07.11.00	Return flow from condensation cap / resaturation of dry-out zone	
2.2.07.15.0B	Advection and dispersion in the UZ	2.2.07.15.00	Advection and dispersion in the SZ*	
2.2.07.18.0A	Film flow into the repository	2.2.07.18.00	Film flow into drifts	
2.2.07.19.0A	Lateral flow from Solitario Canyon Fault enters drifts	2.2.07.19.00	Lateral flow from Solitario Canyon Fault enters potential waste emplacement drifts	
2.2.07.20.0A	Flow diversion around repository drifts		New FEP for LA No corresponding SR FEP	
2.2.07.21.0A	Drift shadow forms below repository		New FEP for LA No corresponding SR FEP	
2.2.08.01.0B	Chemical characteristics of groundwater in the UZ	2.2.08.01.00 2.2.08.03.00	Groundwater chemistry / composition in UZ and SZ Geochemical interactions in geosphere (dissolution, precipitation, weathering) and effects on radionuclide transport	
2.2.08.03.0B	Geochemical interactions and evolution in the UZ	2.2.08.03.00 2.2.08.01.00 2.2.08.02.00	Geochemical interactions in geosphere (dissolution, precipitation, weathering) and effects on radionuclide transport Groundwater chemistry / composition in UZ and SZ Radionuclide transport occurs in a carrier plume in geosphere	
2.2.08.04.0A	Redissolution of precipitates directs more corrosive fluids to containers	2.2.08.04.00	Redissolution of precipitates directs more corrosive fluids to containers	EBS
2.2.08.05.0A	Diffusion in the UZ	2.2.08.05.00	Osmotic processes	
2.2.08.06.0B	Complexation in the UZ	2.2.08.06.00	Complexation in geosphere	
2.2.08.07.0B	Radionuclide solubility limits in the UZ	2.2.08.07.00	Radionuclide solubility limits in the geosphere	
2.2.08.08.0B	Matrix diffusion in the UZ	2.2.08.08.00 2.2.08.05.00	Matrix diffusion in geosphere Osmotic processes	
2.2.08.09.0B	Sorption in the UZ	2.2.08.09.00	Sorption in UZ and SZ	
2.2.08.10.0B	Colloidal transport in the UZ	2.2.08.10.00	Colloidal transport in geosphere	
2.2.08.12.0A	Chemistry of water flowing into the drift	2.2.08.12.00	Chemistry of water flowing into the EBS*	
2.2.09.01.0B	Microbial activity in the UZ	2.2.09.01.00	Microbial activity in geosphere	
2.2.10.01.0A	Repository-induced thermal effects on flow in the UZ	2.2.10.01.00	Repository-induced thermal effects in geosphere	
2.2.10.03.0B	Natural geothermal effects on flow in the UZ	2.2.10.03.00 2.2.10.13.00	Natural geothermal effects Density driven groundwater flow (thermal)	
2.2.10.04.0A	Thermo-mechanical stresses alter characteristics of fractures near repository	2.2.10.04.00 2.2.06.02.00 1.2.02.01.00	Thermo-mechanical alteration of fractures near repository Changes in stress (due to thermal, seismic, or tectonic effects) produce change in permeability of faults Fractures	SZ

Table 6-1. Cross-Walk between LA and SR FEPs (continued)

LA FEP Number	LA FEP Name	SR FEP Number	SR FEP Name	Other FEP reports that address shared FEP[a]
2.2.10.04.0B	Thermo-mechanical stresses alter characteristics of faults near repository	2.2.10.04.00 2.2.06.02.00 1.2.02.02.00	Thermo-mechanical alteration of fractures near repository Changes in stress (due to thermal, seismic, or tectonic effects) produce change in permeability of faults Faults	SZ
2.2.10.05.0A	Thermo-mechanical stresses alter characteristics of rocks above and below the repository	2.2.10.05.00 2.2.06.03.00 2.2.06.01.00	Thermo-mechanical alteration of rocks above and below the repository Changes in stress (due to thermal, seismic, or tectonic effects) produce change in permeability of faults Changes in stress (due to thermal, seismic, or tectonic effects) change porosity and permeability of rock*	SZ
2.2.10.06.0A	Thermo-chemical alteration in the UZ (solubility, speciation, phase changes, precipitation/dissolution)	2.2.10.06.00	Thermo-chemical alteration (solubility, speciation, phase changes, precipitation/dissolution)	
2.2.10.07.0A	Thermo-chemical alteration of the Calico Hills unit	2.2.10.07.00	Thermo-chemical alteration of the calico hills unit	
2.2.10.09.0A	Thermo-chemical alteration of the Topopah Spring basal vitrophyre	2.2.10.09.00	Thermo-chemical alteration of the Topopah Spring basal vitrophyre	
2.2.10.10.0A	Two-phase buoyant flow / heat pipes	2.2.10.10.00	Two-phase buoyant flow / heat pipes	
2.2.10.11.0A	Natural air flow in the UZ	2.2.10.11.00	Natural air flow in unsaturated zone	
2.2.10.12.0A	Geosphere dry-out due to waste heat	2.2.10.12.00	Geosphere dry-out due to waste heat	
2.2.10.14.0A	Mineralogic dehydration reactions	2.2.10.14.00	Mineralogic dehydration reactions	
2.2.11.02.0A	Gas effects in the UZ	2.2.11.02.00 2.2.11.01.00 2.2.12.01.00	Gas pressure effects Naturally-occurring gases in geosphere Gas generation	
2.2.11.03.0A	Gas transport in geosphere	2.2.11.03.00	Gas transport in geosphere	
2.2.12.00.0A	Undetected features in the UZ	2.2.12.00.00	Undetected features (in geosphere)	
2.3.01.00.0A	Topography and morphology	2.3.01.00.00	Topography and morphology	
2.3.11.01.0A	Precipitation	2.3.11.01.00	Precipitation	Bio
2.3.11.02.0A	Surface runoff and flooding	2.3.11.02.00	Surface runoff and flooding	
2.3.11.03.0A	Infiltration and recharge	2.3.11.03.00	Infiltration and recharge (hydrologic and chemical effects)	
3.1.01.01.0A	Radioactive decay and ingrowth	3.1.01.01.00	Radioactive decay and ingrowth	WFMisc SZ Bio

NOTE: * SR FEPs not treated in *Features, Events, and Processes in UZ Flow and Transport* (BSC 2001 [154826]) or *Features, Events, and Processes in Thermal Hydrology and Coupled Processes* (CRWMS M&O 2001 [153935])

[a] Bio: BSC 2003 [165843]
DE: BSC 2004 [167720]
EBS: BSC 2004 [167253]
SYS: BSC 2003 [163574]
SZ: BSC 2003 [163128]
WFMisc: BSC 2003 [163925]

For the purposes of this report, the FEPs are divided into two broad categories: included and excluded FEPs. There are 44 included FEPs and 50 excluded FEPs. Included FEPs are those directly (or, in some cases, implicitly) represented in TSPA-LA models. Included FEPs are identified and the method for inclusion is summarized, with reference to the reports that provide additional detailed information.

Excluded FEPs are those excluded due to low probability, low consequence, or by regulation, and therefore not modeled in TSPA-LA. In particular, low-probability means that the occurrence of a FEP has a probability lower than 10^{-4} in 10^{4} years. Low-consequence arguments in this analysis are based on the UZ subsystem performance. UZ subsystem performance is defined by the release of radionuclides at the water table and water seepage into waste emplacement drifts. A subsystem consequence argument for exclusion is always conservative with respect to a total system argument, because the other components of the total system that contribute to performance are not amplified by changes in UZ performance. Waste package and engineered barrier performance over 10,000 years are not strong functions of drift seepage (BSC 2003 [161317], Sections 6.7.1.1 and 6.7.1.2), and the rate of radionuclide transport in the saturated zone is independent of the source-term strength. Therefore, some FEPs may have a significant effect on radionuclide transport or drift seepage in the UZ and yet have an insignificant effect on total system performance, because of the contributions of the other system components to total system performance. Thus, if a FEP can be shown to have minimal consequence on the UZ subsystem performance, then it will also have a minimal consequence on total system performance in terms of the time or magnitude of the resulting radiological exposures to the reasonably maximally exposed individual, or radionuclide releases to the accessible environment.

The rationale for exclusion of a FEP is given in the screening argument presented for each excluded FEP. Section 6.1 discusses FEPs that are included in TSPA-LA. Sections 6.2 through 6.8 discuss FEPs that are excluded from TSPA-LA.

The following standardized format is used to present the status of each FEP as presented in the third-order subsections of this chapter.

Third-Order Subsection Heading: FEP Name (FEP Number)

FEP Description: Descriptions of FEPs are as presented in the LA FEP list (DTN: MO0307SEPFEPS4.000 [164527]). Note that subsequent changes have been made to the Names and/or Descriptions for the following FEPs: 1.2.10.01.0A, 1.3.07.01.0A, 1.3.07.02.0B, 2.2.06.01.0A and 2.2.07.01.0A. These changes were minor in nature (e.g., to correct typographical errors) and did not change the meaning or scope of any FEP.

Descriptor Phrases: Additional detail/key phrases summarizing the FEP.

Screening Decision: Identifies the YMP screening decision as either “Included” or “Excluded.” For excluded FEPs this also indicates whether FEPs are excluded on the basis of low consequence, low probability, or by regulation.

Screening Argument: This field provides the argument for why a FEP has been excluded from TSPA-LA, including the specific regulation if the exclusion is based on a regulation. If the screening decision is "included", the screening argument field is not used.

TSPA Disposition: This field describes how the included FEP is treated in TSPA-LA and provides referencing to more detailed documentation, as applicable. If the screening decision is "excluded", the TSPA disposition field is not used.

Supporting Reports: This field is only used for included FEPs. It lists reports BSC 2004 [166883], BSC 2004 [162730], BSC 2004 [167970], BSC 2004 [167959], BSC 2003 [163228], BSC 2003 [165991], and BSC 2004 [167972], which provide inputs to TSPA-LA. Other reports, which do not provide inputs to TSPA-LA, are not listed.

For included FEPs, uncertainty is captured in the treatment of the processes as implemented in TSPA-LA. Therefore, uncertainty from the standpoint of the FEPs evaluation is concerned only with uncertainty in the exclusion of FEPs. Because there is no mechanism to capture uncertainty in the FEPs analysis in TSPA-LA, uncertainty leads to conservatism in the FEPs exclusion analyses, i.e., exclusions are based on conservative arguments that are unlikely to change with more detailed or accurate input information. The only restrictions for subsequent use that result from this approach is that worst-case or conservative analyses may overemphasize the importance of FEPs included on that basis. This overemphasis should be weighted appropriately when prioritizing future work to reduce uncertainties.

6.1 INCLUDED FEPS

Table 6-2 gives the section numbers, FEP numbers, and names of Included FEPs.

Table 6-2. Included UZ FEPs

Section Number	FEP Number	FEP Name
6.1.1	1.1.02.02.0A	Pre-closure ventilation
6.1.2	1.2.02.01.0A	Fractures
6.1.3	1.2.02.02.0A	Faults
6.1.4	1.3.01.00.0A	Climate change
6.1.5	1.3.07.02.0B	Water table rise affects UZ
6.1.6	1.4.01.01.0A	Climate modification increases recharge
6.1.7	2.1.08.01.0A	Water influx at the repository
6.1.8	2.1.08.02.0A	Enhanced influx at the repository
6.1.9	2.2.01.01.0A	Mechanical effects of excavation/construction in the near field
6.1.10	2.2.03.01.0A	Stratigraphy
6.1.11	2.2.03.02.0A	Rock properties of host rock and other units
6.1.12	2.2.07.01.0A	Locally saturated flow at bedrock/alluvium contact
6.1.13	2.2.07.02.0A	Unsaturated groundwater flow in the geosphere
6.1.14	2.2.07.03.0A	Capillary rise in the UZ
6.1.15	2.2.07.04.0A	Focusing of unsaturated flow (fingers, weeps)
6.1.16	2.2.07.06.0A	Episodic / pulse release from repository
6.1.17	2.2.07.06.0B	Long-term release of radionuclides from the repository

Table 6-2. Included FEPs (Continued)

Section Number	FEP Number	FEP Name
6.1.18	2.2.07.07.0A	Perched water develops
6.1.19	2.2.07.08.0A	Fracture flow in the UZ
6.1.20	2.2.07.09.0A	Matrix imbibition in the UZ
6.1.21	2.2.07.10.0A	Condensation zone forms around drifts
6.1.22	2.2.07.11.0A	Resaturation of geosphere dry-out zone
6.1.23	2.2.07.15.0B	Advection and dispersion in the UZ
6.1.24	2.2.07.18.0A	Film flow into the Repository
6.1.25	2.2.07.19.0A	Lateral flow from Solitario Canyon Fault Enters Drifts
6.1.26	2.2.07.20.0A	Flow diversion around repository drifts
6.1.27	2.2.07.21.0A	Drift shadow forms below repository
6.1.28	2.2.08.01.0B	Chemical characteristics of groundwater in the UZ
6.1.29	2.2.08.04.0A	Redissolution of precipitates directs more corrosive fluids to containers
6.1.30	2.2.08.05.0A	Diffusion in the UZ
6.1.31	2.2.08.06.0B	Complexation in the UZ
6.1.32	2.2.08.08.0B	Matrix diffusion in the UZ
6.1.33	2.2.08.09.0B	Sorption in the UZ
6.1.34	2.2.08.10.0B	Colloidal transport in the UZ
6.1.35	2.2.08.12.0A	Chemistry of water flowing into the drift
6.1.36	2.2.09.01.0B	Microbial activity in the UZ
6.1.37	2.2.10.03.0B	Natural geothermal effects on flow in the UZ
6.1.38	2.2.10.10.0A	Two-phase buoyant flow / heat pipes
6.1.39	2.2.10.12.0A	Geosphere dry-out due to waste heat
6.1.40	2.3.01.00.0A	Topography and morphology
6.1.41	2.3.11.01.0A	Precipitation
6.1.42	2.3.11.02.0A	Surface runoff and flooding
6.1.43	2.3.11.03.0A	Infiltration and Recharge
6.1.44	3.1.01.01.0A	Radioactive decay and ingrowth

Source: LA FEP List (DTN: MO0307SEPFEPS4.000 [164527])

6.1.1 Pre-Closure Ventilation (1.1.02.02.0A)

FEP Description: The duration of pre-closure ventilation acts together with waste package spacing (as per design) to control the extent of the boiling front (zone of reduced water content).

Descriptor Phrases: Pre-closure ventilation

Screening Decision: Included

Screening Argument: None

TSPA Disposition: Preclosure ventilation in drifts will remove a considerable amount of the heat output from the waste canisters. The ventilation period following emplacement is 50 years, during which a large fraction of the heat energy supplied to the rock by the waste is removed from the drifts by ventilation (BSC 2004 [167657], Table 8-3). This effect of preclosure ventilation on the thermal load provided to the rock is explicitly simulated with the Thermal-

Hydrological (TH) Seepage Model (BSC 2003 [166512], Section 4.1.1.3) that feeds into seepage abstraction, by using time-dependent boundary conditions for the thermal load (BSC 2004 [167970], Section 6.4.3.1). These boundary conditions reflect the current emplacement design (waste package spacing, average heat output of waste canisters, etc.), as provided in design drawings 800-IED-MGR0-00201-000-00A (BSC 2004 [167040]). Thus, the TH modeling results from the TH Seepage Model (DTN: LB0301DSCPTHSM.002 [163689]) directly account for the impact of preclosure ventilation and waste package spacing on two-phase flow and the TH conditions in the near-drift rock. As discussed in BSC (2004 [167970], Section 6.5.2.1), the abstraction of thermal seepage utilizes these modeling results to develop an appropriate thermal seepage abstraction methodology. Note that preclosure ventilation also causes initial rock drying in the drift vicinity as a result of evaporation effects. The reduced relative humidity in the emplacement drifts leads to evaporation of water at the drift surfaces and the development of a small zone of reduced saturation in the drift vicinity. This early dryout as a result of evaporation is neglected in the TH Seepage Model, because seepage into ventilated drifts is highly unlikely (BSC 2004 [167970], Section 6.5.2.1).

The effect of preclosure ventilation on the thermal load provided to the rock is also explicitly simulated with the THC Seepage Model that feeds into the Drift Scale Coupled Processes Abstraction (DSCPA) model, by using time-dependent boundary conditions for the thermal load (BSC 2004 [167974], Section 4.1.7). These boundary conditions reflect the current emplacement design (waste package spacing, average heat output of waste canisters, etc.), as provided in design drawings 800-IED-MGR0-00201-000-00A (BSC 2004 [167040]).

Thus, the results from the THC Seepage Model and their abstraction (BSC 2004 [167972], Section 6.2; summary tables of concentrations through time submitted under DTNs: LB0302DSCPTHCS.002 [161976], LB0307DSTTHCR2.002 [165541], and LB0311ABSTHCR2.003 [166713]; and tables of concentrations and summary statistics through time submitted under DTN: LB0311ABSTHCR2.001 [166714]) explicitly account for the impact of preclosure ventilation and waste package spacing on the THC conditions in the near-drift rock. DTNs: LB0302DSCPTHCS.002 [161976] and LB0311ABSTHCR2.001 [166714] are used to feed and/or provide technical basis for another model (BSC 2004 [167461]) that generates lookup tables that are used in the TSPA-LA Model.

Note that pre-closure ventilation also causes initial rock drying in the drift vicinity as a result of evaporation effects. The reduced relative humidity in the emplacement drifts leads to evaporation of water at the drift surfaces and the development of a small zone of reduced saturation in the drift vicinity. This early dryout as a result of evaporation is neglected in the THC Seepage Model, because seepage into ventilated drifts is highly unlikely (BSC 2004 [167970], Section 6.5.2.1).

Supporting Reports: BSC 2004 [167970], BSC 2004 [167972].

6.1.2 Fractures (1.2.02.01.0A)

FEP Description: Groundwater flow in the Yucca Mountain region and transport of any released radionuclides may take place along fractures. The rate of flow and the extent of

transport in fractures are influenced by characteristics such as orientation, aperture, asperity, fracture length, connectivity, and the nature of any linings or infills.

Descriptor Phrases: Fractures in the UZ, Fractures (characteristics), Fractures (infills)

Screening Decision: Included

Screening Argument: None

TSPA Disposition: This FEP on "Fractures" is included in process models for UZ flow and transport. The UZ Flow Model is based on a dual-permeability concept, with fractures represented by a continuum (BSC 2004 [166883], Section 6.1.2). The fracture continuum represents the spatially averaged flow through discrete fractures. The fracture continuum interacts with the matrix continuum, which represents matrix blocks separated by fractures.

Fracture continuum properties include permeability, porosity, interface area per unit volume, van Genuchten α and m parameters for the saturation-capillary pressure and relative permeability functions, and an active fracture parameter. These parameters and associated range of values are presented in BSC (2004 [166883], Section 4.1) for each UZ Model layer (DTN: LB0205REVUZPRP.001 [159525]).

Fracture permeability is based on field measurements, which integrate the discrete fracture characteristics such as orientation, aperture, asperity, fracture length, connectivity, and the nature of any linings or infills. Permeabilities and other properties are further calibrated as described in the Model Reports *Calibrated Properties Model* (BSC 2003 [166509]) and *Analysis of Hydrologic Properties Data* (BSC 2003 [161773]). The fracture continuum properties are used as inputs to the UZ Flow Model, and their effects are incorporated into the output flow fields developed for use in TSPA-LA (output flow fields are in DTN: LB0305TSPA18FF.001 [165625]).

The influence of fractures on radionuclide transport through UZ is investigated through the dual permeability model (BSC 2004 [162730], Section 6.4.3). The influences of fracture characteristics on UZ flow are included through the pre-generated flow fields (BSC 2004 [162730], Section 6.5.1; DTN: LB0305TSPA18FF.001 [165625]). Fracture aperture, porosity, and frequency (DTNs: LB0205REVUZPRP.001 [159525] and LB0207REVUZPRP.001 [159526]) affecting UZ radionuclide transport are summarized in BSC (2004 [162730], Section 6.5.7). Fracture porosity and frequency data will be statistically sampled during TSPA-LA multi-realization runs using the distribution given in DTN: LA0311BR831371.003 [166515].

Flow processes in fractures or other channels are important for seepage abstraction because the amount of seepage is determined by the diversion capacity of the fracture flow in the drift vicinity (BSC 2004 [167970], Section 6.3.1). These flow processes are influenced by fracture characteristics such as orientation, aperture, asperity, length, connectivity, and fillings. All seepage process models that feed into seepage abstraction explicitly simulate the flow processes in fractures, using appropriate continuum properties that represent these characteristics (BSC 2004 [167970], Section 6.4).

For ambient seepage, the relevant continuum properties are the continuum permeability and the effective fracture capillary-strength in the drift vicinity. For seepage abstraction, probability distributions describing the spatial variability and uncertainty of these parameters have been developed in BSC (2004 [167970], Section 6.8.1), based on air-permeability measurements and liquid-release tests combined with inverse modeling (BSC 2004 [167970], Sections 6.6 and 6.4.1). Ambient seepage calculations will be conducted within the TSPA-LA by sampling from these probability distributions and interpolating seepage rates from the look-up tables given in DTNs: LB0304SMDCREV2.002 [163687] and LB0307SEEPDRCL.002 [164337]. During the thermal period, the ambient seepage rates will be adjusted based on the TH modeling results from TH Seepage Model, which explicitly simulates the thermally perturbed fracture flow conditions. Results are given in DTN: LB0301DSCPTHSM.002 [163689]. The abstraction methodology for thermal seepage is developed in BSC (2004 [167970], Section 6.5.2.1). THM and THC effects on fracture characteristics are evaluated with process models that explicitly account for fracture flow affected by THM and THC parameter alterations (BSC 2004 [167970], Sections 6.4.4.1 and 6.4.4.2) (see Sections 6.8.1 (FEP 2.1.09.12.0A) and 6.8.10 (FEP 2.2.10.04.0A)). It was demonstrated that these potential alterations can be neglected in the TSPA-LA, because the expected changes would lead to less seepage (BSC 2004 [167970], Section 6.5.1.4).

Flow processes in fractures or other channels affect modeled THC coupled processes because of 1) their strong effect on TH behavior (BSC 2004 [167970], Sections 6.4.4.1 and 6.4.4.2), and 2) their strong effect on water and gas chemistry (BSC 2004 [167974], Section 6.2.1). The latter is primarily due to volatilization of steam and CO_2 from the rock matrix-water and subsequent transport and condensation in fractures. The amount of mobilized CO_2 with steam directly affects the pH of the condensate, which in turn affects the degree of water-rock interaction and water chemistry. These THC processes are influenced by the fracture characteristics, such as orientation, aperture, asperity, length, connectivity, and fillings. The THC Seepage Model that feeds into the DSPCA model explicitly simulates the flow processes in fractures using appropriate continuum properties that represent these characteristics (BSC 2004 [167974], Sections 6.4.3, 6.4.4, and 6.4.7).

Thus, the results from the THC Seepage Model and their abstraction (BSC 2004 [167972], Section 6.2; summary tables of concentrations through time submitted under DTNs: LB0302DSCPTHCS.002 [161976], LB0307DSTTHCR2.002 [165541], and LB0311ABSTHCR2.003 [166713]; and tables of concentrations and summary statistics through time submitted under DTN: LB0311ABSTHCR2.001 [166714]) explicitly account for the effect of fractures on predicted water and gas chemistry. DTNs: LB0302DSCPTHCS.002 [161976] and LB0311ABSTHCR2.001 [166714] are used to feed and/or provide technical basis for another model (BSC 2004 [167461]) that generates lookup tables that are used in the TSPA-LA Model.

This FEP is also included in TSPA-LA through the treatment of drift-scale radionuclide transport (BSC 2004 [167959]). This is captured through the fracture-matrix partitioning model for the fraction of releases from a waste emplacement drift without seepage to the fractures of the underlying rock mass (BSC 2004 [167959], Tables 6.4-6 and 6.4-7). The fraction of the releases from a drift without seepage to the fractures is represented as an uncertain parameter, caused in

part by uncertainty in fracture characteristics (parameters f, m, and ϕ_f in BSC 2004 [167959], Table 6.4-5). Distributions that represent the effects of this uncertainty in the fraction released to fractures are developed for use in TSPA-LA as a probabilistic parameter applied to the total radionuclide flux entering the rock from waste emplacement drifts.

The effects of fractures are also included in the treatment of infiltration uncertainty for TSPA-LA (BSC 2003 [165991]). Infiltration uncertainty is represented through three discrete infiltration scenarios (lower, mean, and upper), which are sampled in TSPA-LA according to weighting factors BSC (2003 [165991], Section 7.1). Fractures are included in the infiltration uncertainty analysis by incorporation of the fracture parameters for bedrock permeability (BRPERM) and bedrock porosity (BRPOROS) that are included implicitly in the determination of the weighting factors. The uncertainties for these parameters are described in BSC (2003 [165991], Tables 6-2 and 6-3). These uncertainties are propagated through the infiltration numerical model and so are implicitly included in the output (weighting factors) that is passed to TSPA-LA (BSC 2003 [165991]; DTN: SN0308T0503100.008 [165640]).

Supporting Reports: BSC 2004 [166883], BSC 2004 [162730], BSC 2004 [167970], BSC 2004 [167972], BSC 2004 [167959], BSC 2003 [165991], BSC 2003 [163228].

6.1.3 Faults (1.2.02.02.0A)

FEP Description: Numerous faults of various sizes have been noted in the Yucca Mountain Region and in the repository area in specific. Faults may represent an alteration of the rock permeability and continuity of the rock mass, alteration or short-circuiting of the flow paths and flow distributions close to the repository, and represent unexpected pathways through the repository.

Descriptor Phrases: Faults (displacement), Faults (dip-slip), Faults (strike-slip), Faults (detachment), Faults in the UZ

Screening Decision: Included

Screening Argument: None

TSPA Disposition: Major displacement, dip-slip, strike-slip, and detachment faults within the model domain are explicitly discretized in the mountain-scale UZ flow and transport models described in BSC (2004 [166883], Sections 6.1.5, 6.2.2, 6.2.5, 6.6.2, 6.6.3, 6.7.3) and BSC (2003 [160109], Sections 6.4 and 6.6.1). These faults are represented in the UZ Model Grid as vertical or inclined discrete zones 30 m wide, and include existing displacements that affect the relative geometry of the hydrogeologic model units. Specific hydrogeological properties are assigned to the fault zones. Fault properties (matrix and fracture parameters) are in DTN: LB02092DSSCFPR.002 [162128] as listed in BSC (2004 [166883], Table 4.1-1). These properties have been calibrated as described in the Model Reports *Calibrated Properties Model* (BSC 2003 [166509]) and *Analysis of Hydrologic Properties Data* (BSC 2003 [161773]). The fault properties are used as inputs to the UZ Flow Model, and their effects are incorporated into the output flow fields developed for use in TSPA-LA (output flow fields are in DTN: LB0305TSPA18FF.001 [165625]).

The influence of faults on radionuclide transport is implicitly included through the use of dual permeability model, the use of pre-generated flow fields that includes the faults in the 3-D model (BSC 2004 [162730], Section 6.5.1; DTN: LB0305TSPA18FF.001 [165625]), and the characteristics of fractures within the faults (BSC 2004 [162730], Section 6.5.7). In TSPA-LA runs, the influence of faults is included through the use of fault properties and the pre-generated flow fields under different climate conditions as described in BSC (2004 [162730], Sections 6.5.1 and 6.5.7). However, BSC (2004 [162730]) does not generate a direct data feed.

Supporting Reports: BSC 2004 [166883], BSC 2004 [162730], BSC 2003 [163228].

6.1.4 Climate Change (1.3.01.00.0A)

FEP Description: Climate change may affect the long-term performance of the repository. This includes the effects of long-term change in global climate (e.g., glacial/interglacial cycles) and shorter-term change in regional and local climate. Climate is typically characterized by temporal variations in precipitation and temperature.

Descriptor Phrase: Climate change

Screening Decision: Included

Screening Argument: None

TSPA Disposition: Global climate change is addressed in TSPA-LA, using a climate model based on paleoclimate information. That is, the record of climate changes in the past is used to predict the expected changes in climate for the future. Future climates are described in terms of discrete climate states that are used to approximate continuous variations in climate. The effects of seasonality are included in the climate model through the use of climate analogs with specific seasonal meteorological records. More specific information about the methods used to predict future climate change and the findings for the climate model are given in USGS (2003 [167961], Section 6). Climate modeling is incorporated into TSPA-LA through the UZ flow fields that have different surface water infiltration as a result of different climates corresponding to three distinct different climates (climate change timing in parentheses): present day (from 0 to 600 years after present), monsoon (from 600 to 2000 years after present), and glacial transition (2000 to 30,000 years after present) (BSC 2004 [166883], Section 6.9). The nine infiltration rates are summarized in Table 6-3 for average values over the model domain.

Table 6-3. Infiltration Rates (mm/year) Averaged over the UZ Model Domain

Scenario	Lower-Bound Infiltration	Mean Infiltration	Upper-Bound Infiltration
Present-Day/Modern	1.25	4.43	10.74
Monsoon	4.43	11.83	19.23
Glacial Transition	2.35	17.02	31.69

NOTE: Values averaged from DTN: GS000308311221.005 [147613]

Future climate conditions are addressed in the infiltration model USGS (2003 [166518], Sections 6.3 and 6.9) through the selection of analogs at other locations with present day climates that are representative of the range of future climate conditions at Yucca Mountain (USGS 2003

[167961], Section 6.6). The meteorological data from these analogs are then used for modeling infiltration under future climate conditions at Yucca Mountain. A description of the modeling methods used for infiltration, and of how infiltration is affected by climate, is given in USGS (2003 [166518], Sections 6.3 and 6.9). The results of the infiltration model are then used for computing UZ flow throughout the UZ flow-model domain, which includes the repository waste emplacement zone. The UZ flow model uses the infiltration results as upper-boundary conditions for UZ flow calculations (BSC 2004 [166883], Section 6.1.4). The UZ flow fields are used directly in TSPA-LA (BSC 2004 [166883], Section 6.2.5). The output flow fields are in DTN: LB0305TSPA18FF.001 [165625], developed for use in Performance Assessment (BSC 2003 [166296]; BSC 2004 [166883], Attachment IV).

Climate change is implicitly included in the treatment of radionuclide transport for TSPA-LA as discussed in BSC (2004 [162730], Section 6.4.9). The effect of climate change on repository performance was studied by using pre-generated flow fields under different climates (DTN: LB0305TSPA18FF.001 [165625]). For TSPA-LA, the pre-generated flow fields are used by the FEHM model as described in BSC (2004 [162730], Section 6.4.9). However, BSC (2004 [162730]) does not generate a direct data feed.

Potential effects of climate change on the amount of infiltration and percolation at Yucca Mountain are taken implicitly into account in the THC Seepage Model by considering different climate stages and climate scenarios when setting infiltration rates at the top model boundary (BSC 2004 [167974], Sections 6.2.1.3 and 6.8.2). Thus, the results from the THC Seepage Model and their abstraction (BSC 2004 [167972], Section 6.2; summary tables of concentrations through time submitted under DTNs: LB0302DSCPTHCS.002 [161976], LB0307DSTTHCR2.002 [165541], and LB0311ABSTHCR2.003 [166713]; and tables of concentrations and summary statistics through time submitted under DTN: LB0311ABSTHCR2.001 [166714]) implicitly account for the effect of climate change on THC processes. DTNs: LB0302DSCPTHCS.002 [161976] and LB0311ABSTHCR2.001 [166714] are used to feed and/or provide technical basis for another model (BSC 2004 [167461]) that generates lookup tables that are used in the TSPA-LA Model. Note that seepage is calculated in the TSPA-LA using percolation flux distributions based on results from the UZ Flow and Transport Model (BSC 2004 [167970], Section 6.6.4.1), given in DTNs: LB0302PTNTSW9I.001 [162277] and LB0305PTNTSW9I.001 [163690]. These flux distributions are based on the same varying climate stages and scenarios as identified and used in the THC Seepage Model.

Potential effects of climate change on the amount of infiltration and percolation at Yucca Mountain are taken into account in the seepage abstraction by considering different climate stages and climate scenarios (BSC 2004 [167970], Section 6.6.4). Seepage is calculated in the TSPA-LA using percolation flux distributions based on results from the UZ Flow and Transport Model (BSC 2004 [167970], Section 6.6.4.1), given in DTNs: LB0302PTNTSW9I.001 [162277] and LB0305PTNTSW9I.001 [163690]. These flux distributions include different climate stages and scenarios.

The effects of climate change are also included in the treatment of infiltration uncertainty for TSPA-LA (BSC 2003 [165991]). Infiltration uncertainty is represented through three discrete infiltration scenarios (lower, mean, and upper), which are sampled in TSPA-LA according to

weighting factors BSC (2003 [165991], Section 7.1). Climate change is incorporated through the use of the analog climate (lower-bound, mean, and upper-bound) infiltration rate maps (see BSC 2003 [165991], Table 6-7; DTN: GS000308311221.005 [147613]) developed by the USGS in the report *Simulation of Net Infiltration for Modern and Potential Future Climates* (USGS 2003 [166518]) by using the climate analog data as direct input. It is incorporated implicitly by inclusion of the spatial average analog net infiltration rate maps in the calculation of the weighting factors which are passed to TSPA-LA (BSC 2003 [165991]; DTN: SN0308T0503100.008 [165640).

Supporting Reports: BSC 2004 [166883], BSC 2004 [167972], BSC 2004 [167970], BSC 2004 [162730], BSC 2003 [165991], BSC 2003 [163228], BSC 2004 [167959].

6.1.5 Water Table Rise Affects UZ (1.3.07.02.0B)

FEP Description: Climate change could produce increased infiltration, leading to a rise in the regional water table, possibly affecting the release and exposure from the repository by altering flow and transport pathways in the UZ. A regionally higher water table and change in UZ flow patterns might flood the repository.

Descriptor Phrases: Climate change (wetter), Time-dependent infiltration (increase), Water table elevation, Unsaturated flow and pathways in the UZ

Screening Decision: Included

Screening Argument: None

TSPA Disposition: The potential for water table rise caused by climate change is included in TSPA-LA calculations using a water table rise model based on paleoclimate data. The paleoclimate data indicates that the historical water table has never risen to the level of the repository (Forester et al. 1999 [109425], pp. 46, 56). Water table changes are implemented in the TSPA-LA by allowing the water table to change elevation instantaneously upon change in climate, concurrent with changes in infiltration (implemented by the postprocessor software WTRISE (LBNL 2003 [163453]) for radionuclide transport), thus affecting the unsaturated flow and pathways in the UZ. WTRISE allows the user to specify a water table location and removes all the particles in the gridblocks below the specified water table instantaneously by setting full saturation to the submerged gridblocks (BSC 2004 [166883], Section 6.6.3). The particles removed from the UZ gridblocks enter the SZ transport model. WTRISE is implemented in the TSPA-LA model. The water table for future climates is specified in BSC (2004 [162730], Section 6.4.9). Future climate flow fields have been generated using WTRISE for three monsoon and three glacial-transition climate flow fields, which are given in DTN: LB0312TSPA06FF.001 [166671].

Supporting Reports: BSC 2004 [166883], This FEP was also addressed in BSC 2004 [162730] but was not explicitly listed as an included FEP in that report.

6.1.6 Climate Modification Increases Recharge (1.4.01.01.0A)

FEP Description: Climate modification causes an increase in recharge in the Yucca Mountain region. Increased recharge might lead to increased flux through the repository, perched water, or water table rise.

Descriptor Phrase: Climate change (effects on infiltration)

Screening Decision: Included

Screening Argument: None

TSPA Disposition: The effects of climate changes (BSC 2003 [166296], Section 4.1) on UZ flux through the repository are incorporated through the explicit simulations of UZ flow fields corresponding to the upper-bound, mean, and lower-bound infiltrations of three distinct different climates: present-day, monsoon, and glacial transition. The nine base-case flow fields and nine alternative flow fields are presented in BSC (2004 [166883], Section 6.6). The output flow fields are in DTN: LB0305TSPA18FF.001 [165625], developed for use in Performance Assessment (BSC 2003 [166296]; BSC 2004 [166883], Attachment IV).

Above the repository, perched water bodies were neither observed in the field nor predicted by the UZ Flow Model. The potential effect of perched water above the repository is indirectly related to lateral diversion of percolation flux in the PTn above the repository. PTn effects on the flow field are discussed in (BSC 2004 [166883], Section 6.6). The potential for water table rise caused by climate change is included in TSPA-LA calculations, using the water table rise model (implemented by software WTRISE (LBNL 2003 [163453]), also see Section 6.1.5 (FEP 1.3.07.02.0B)) based on paleoclimate data (USGS 2003 [167961], Section 6.2).

The effect of climate changes in the form of increased recharge is implicitly included in the transport model for TSPA-LA through the use of pre-generated flow fields (BSC 2004 [162730], Section 6.5.1 and DTN: LB0305TSPA18FF.001 [165625]). In multi-realization TSPA-LA runs, different climate patterns are applied and the effect of climate change is included through FEHM's use of pre-generated flow fields for the corresponding climates as described in BSC (2004 [162730], Section 6.5.1). However, BSC (2004 [162730]) does not generate a direct data feed.

Potential effects of climate change on the amount of infiltration and percolation at Yucca Mountain are taken into account in the THC Seepage Model by implicitly considering different climate stages and climate scenarios when setting infiltration rates at the top model boundary (BSC 2004 [167974], Sections 6.2.1.3 and 6.8.2). Thus, the results from the THC Seepage Model and their abstraction (BSC 2004 [167972], Section 6.2; summary tables of concentrations through time submitted under DTNs: LB0302DSCPTHCS.002 [161976], LB0307DSTTHCR2.002 [165541], and LB0311ABSTHCR2.003 [166713]; and tables of concentrations and summary statistics through time submitted under DTN: LB0311ABSTHCR2.001 [166714]) implicitly account for the effect of climate change on predicted water and gas chemistry. DTNs: LB0302DSCPTHCS.002 [161976] and LB0311ABSTHCR2.001 [166714] are used to feed and/or provide technical basis for another model (BSC 2004 [167461]) that generates lookup tables that are used in the TSPA-LA Model.

Note that seepage is calculated in the TSPA-LA using percolation flux distributions based on results from the UZ Flow and Transport Model (BSC 2004 [167970], Section 6.6.4.1), given in DTNs: LB0302PTNTSW9I.001 [162277] and LB0305PTNTSW9I.001 [163690]. These flux distributions are based on the same varying climate stages and scenarios as identified and used in the THC Seepage Model.

Potential effects of climate change on the amount of flux through the repository are taken into account in the seepage abstraction by considering different climate stages and climate scenarios (BSC 2004 [167970], Section 6.6.4). Seepage is calculated in the TSPA-LA using percolation flux distributions based on results from the UZ Flow and Transport Model (BSC 2004 [167970], Section 6.6.4.1), given in DTNs: LB0302PTNTSW9I.001 [162277] and LB0305PTNTSW9I.001 [163690]. These flux distributions include different climate stages and scenarios.

This FEP is also included in TSPA-LA through the treatment of drift-scale radionuclide transport (BSC 2004 [167959]). This is captured through the fracture-matrix partitioning model for the fraction of releases from a waste emplacement drift without seepage to the fractures of the underlying rock mass (BSC 2004 [167959], Tables 6.4-6 and 6.4-7). Unsaturated flow in the vicinity of the repository is treated for the case of the glacial transition climate, based on flow fields as computed in the UZ flow model (BSC 2004 [166883], Section 6.1.4), is included as part of the model for radionuclide transport from the waste emplacement drift to the rock (parameters q_m and q_f in BSC (2004 [167959], Table 6.4-5). The fraction of the releases from a drift without seepage to the fractures is represented as an uncertain parameter, caused in part by uncertainty in unsaturated flow under the glacial transition climate. The effects of this uncertainty in the fraction released to fractures are developed for use in TSPA-LA as independent parameter distributions for the total radionuclide flux entering the rock from waste emplacement drifts under lower-mean and upper infiltration conditions.

Supporting Reports: BSC 2004 [166883], BSC 2004 [162730], BSC 2004 [167972], BSC 2004 [167970], BSC 2004 [167959], BSC 2003 [163228].

6.1.7 Water Influx at the Repository (2.1.08.01.0A)

FEP Description: An increase in the unsaturated water flux at the repository affects thermal, hydrologic, chemical, and mechanical behavior of the system. Increases in flux could result from climate change, but the cause of the increase is not an essential part of the FEP.

Descriptor Phrases: Time-dependent seepage, Climate (effects on seepage), Thermal effects on seepage

Screening Decision: Included

Screening Argument: None

TSPA Disposition: This FEP is considered to be included implicitly in the TSPA-LA. Changes in UZ flow in response to climate changes are incorporated in the output flow fields developed for use in the TSPA-LA (output flow fields are in DTN: LB0305TSPA18FF.001 [165625]). Furthermore, the outputs from BSC 2004 [166883] are also used by other models and evaluations that are intermediate between this model and the TSPA-LA model.

The influence of water influx at the repository on radionuclide transport is implicitly included through the use of pre-generated flow fields under different climates (DTN: LB0305TSPA18FF.001 [165625]). In TSPA-LA multi-realization runs, climate changes and the change of water influx at the repository on radionuclide transport are addressed through the use of corresponding pre-generated flow fields.

The thermal model output from BSC (2004 [166883]) is used for setting initial conditions for the downstream mountain-scale coupled process evaluation. The effects of changes in UZ flow caused by climate change are also included in the calculations for the thermal-hydrological behavior of the repository system (BSC 2003 [163056], Section 6). The effects of transient flow driven by thermal-hydrological (TH) processes are also included in TSPA-LA calculations for drift seepage in the Model Report *Abstraction of Drift Seepage,* (BSC 2004 [167970]). The effects of THC and THM on seepage are also addressed in the seepage abstraction report.

The potential increase in the magnitude of percolation flux at the repository, as a result of climate changes or flow focusing effects, is accounted for in the seepage abstraction by considering different climate stages, climate scenarios, and introducing flow focusing factors (BSC 2004 [167970], Section 6.6.4). Seepage is calculated in the TSPA-LA using percolation flux distributions based on results from the UZ Flow and Transport Model (BSC 2004 [167970], Section 6.6.4.1), given in DTNs: LB0302PTNTSW9I.001 [162277] and LB0305PTNTSW9I.001 [163690]. These flux distributions include different climate stages and scenarios. The potential focusing of flow towards individual drift sections is accounted for by a distribution of flow focusing factors, as discussed in BSC (2004 [167970], Section 6.6.4.2). This distribution is given in DTN: LB0104AMRU0185.012 [163906]. The local percolation flux distribution used for the seepage calculations in the TSPA-LA is derived by multiplying the percolation flux values from the site-scale model with the randomly sampled flow focusing factors (BSC 2004 [167970], Section 6.8.1).

The potential increase in the magnitude of percolation flux at the repository, as a result of climate changes is accounted for in the THC Seepage Model by implicitly considering different climate stages, and climate scenarios when setting infiltration rates at the top model boundary (BSC 2004 [167974], Sections 6.2.1.3 and 6.8.2). Also, flux increases caused by reflux of water upon boiling are explicitly accounted for by the modeling of coupled THC processes (BSC 2004 [167974], Sections 6.2.1 and 6.8.5.2). Therefore, these effects are directly accounted for in results from the THC Seepage Model and their abstraction (BSC 2004 [167972], Section 6.2; summary tables of concentrations through time submitted under DTNs: LB0302DSCPTHCS.002 [161976], LB0307DSTTHCR2.002 [165541], and LB0311ABSTHCR2.003 [166713]; and tables of concentrations and summary statistics through time submitted under DTN: LB0311ABSTHCR2.001 [166714]). DTNs: LB0302DSCPTHCS.002 [161976] and LB0311ABSTHCR2.001 [166714] are used to feed and/or provide technical basis for another model (BSC 2004 [167461]) that generates lookup tables that are used in the TSPA-LA Model. Note that seepage is calculated in the TSPA-LA using percolation flux distributions that are based on results from the UZ Flow and Transport Model (BSC 2004 [167970], Section 6.6.4.1), given in DTNs: LB0302PTNTSW9I.001 [162277] and LB0305PTNTSW9I.001 [163690]. These flux distributions include the same different climate stages and scenarios as used in the THC Seepage Model.

This FEP is also included in TSPA-LA through the treatment of drift-scale radionuclide transport (BSC 2004 [167959]). This is captured through the fracture-matrix partitioning model for the fraction of releases from a waste emplacement drift without seepage to the fractures of the underlying rock mass (BSC 2004 [167959], Tables 6.4-6 and 6.4-7). Water influx through both the fractures and porous rock matrix is included as part of the model for radionuclide transport from the waste emplacement drift to the rock (parameters q_m and q_f in BSC 2004 [167959], Table 6.4-5). The fraction of the releases from a drift without seepage to the fractures is represented as an uncertain parameter, caused in part by uncertainty in water flux in the fractures and matrix. Distributions that represent the effects of this uncertainty in the fraction released to fractures are developed for use in TSPA-LA as a probabilistic parameter applied to the total radionuclide flux entering the rock from waste emplacement drifts.

Supporting Reports: BSC 2004 [166883], BSC 2004 [167970], BSC 2004 [167972], BSC 2004 [167959], BSC 2003 [163228].

6.1.8 Enhanced Influx at the Repository (2.1.08.02.0A)

FEP Description: An opening in unsaturated rock alters the hydraulic potential, affecting local saturation around the opening and redirecting flow. Some of the flow is directed to the opening where it is available to seep into the opening.

Descriptor Phrase: Flow focusing (Philip's drip)

Screening Decision: Included

Screening Argument: None

TSPA Disposition: The impact of an underground opening on the unsaturated flow field (including capillary barrier effect and flow diversion around the drifts) and its relevance for seepage is explicitly captured in the seepage process models used for the seepage abstraction (BSC 2004 [167970], Sections 6.4.1, 6.4.2, and 6.4.3; BSC 2003 [163226], Section 6.3). From these model simulations, seepage predictions are available in the form of look-up tables in DTNs: LB0304SMDCREV2.002 [163687] and LB0307SEEPDRCL.002 [164337]. These will be used in the TSPA-LA to calculate ambient seepage, by sampling parameter cases of seepage-relevant parameters from the probability distributions that are defined in BSC (2004 [167970], Section 6.8.1). These seepage-relevant parameters are the effective capillary-strength parameter, the permeability, and the local percolation flux. The percolation flux distributions include flow focusing effects, as discussed in BSC (2004 [167970], Section 6.6.4.2). During the thermal period, the ambient seepage rates will be adjusted based on the TH modeling results from DTN: LB0301DSCPTHSM.002 [163689], using the abstraction methodology developed in BSC (2004 [167970], Section 6.5.2.1).

This FEP is also included in TSPA-LA through the treatment of drift-scale radionuclide transport (BSC 2004 [167959]). This is captured through the fracture-matrix partitioning model for the fraction of releases from a waste emplacement drift without seepage to the fractures of the underlying rock mass (BSC 2004 [167959], Tables 6.4-6 and 6.4-7). Local flow focusing in fractures is included as part of the model for radionuclide transport from the waste emplacement drift to the rock (parameter F in BSC 2004 [167959], Table 6.4-5). The fraction of the releases

from a drift without seepage to the fractures is represented as an uncertain parameter, caused in part by uncertainty in flow focusing. Distributions that represent the effects of this uncertainty in the fraction released to fractures are developed for use in TSPA-LA as a probabilistic parameter applied to the total radionuclide flux entering the rock from waste emplacement drifts.

Supporting Reports: BSC 2004 [167970], BSC 2004 [167959].

6.1.9 Mechanical Effects of Excavation/Construction in the Near Field (2.2.01.01.0A)

FEP Description: Excavation will produce some disturbance of the rocks surrounding the drifts due to stress relief. Stresses associated directly with excavation (e.g. boring and blasting operations) may also cause some changes in rock properties. Properties that may be affected include rock strength, fracture spacing, and block size and hydrologic properties such as permeability.

Descriptor Phrases: Mechanical effects of excavation on EDZ fractures, Mechanical effects of excavation on near-field fractures, Mechanical effects of excavation on seepage

Screening Decision: Included

Screening Argument: None

TSPA Disposition: Excavation effects, including mechanical effects of excavation on EDZ fractures, near-field fractures, and seepage, are taken into account in the seepage abstraction through the use of post-excavation air-permeability data (BSC 2004 [167970], Table 6.6-3) and the estimation of a capillary-strength parameter determined from seepage tests (BSC 2004 [167970], Table 6.6-1). These data reflect the impact of excavation around a large opening (niche or drift). The measured post-excavation air-permeability data are supported by THM modeling results (BSC 2004 [167970], Section 6.6.2.1). The probability distributions for permeability and capillary strength given in BSC (2004 [167970], Section 6.8.1) are based on the values given in BSC (2004 [167970], Tables 6.6-3 and 6.6-1), respectively, and thus account for such excavation effects. These distributions will be used in the TSPA-LA to calculate seepage from the seepage look-up tables, using the methodology defined in BSC (2004 [167970], Section 6.8.1). The Seepage Abstraction Model also captures the effects of drift collapse (BSC 2004 [167970], Sections 6.4.2.4 and 6.7.1.2) in terms of the larger drift profile that results.

Supporting Reports: BSC 2004 [167970].

6.1.10 Stratigraphy (2.2.03.01.0A)

FEP Description: Stratigraphic information is necessary information for the performance assessment. This information should include identification of the relevant rock units, soils and alluvium, and their thickness, lateral extents, and relationships to each other. Major discontinuities should be identified.

Descriptor Phrases: Rock properties in the UZ, Hydrologic properties in the UZ

Screening Decision: Included

Screening Argument: None

TSPA Disposition: This FEP is included in the UZ Flow Model (BSC 2004 [166883], Sections 6.1.1 and 6.1.2) by use of the grids developed with the information contained in the Geological Framework Model (GFM2000; MO0012MWDGFM02.002 [153777]). The stratigraphic unit and layers are developed into a model grid in the Model Report *Development of Numerical Grids for UZ Flow and Transport Modeling* (BSC 2003 [160109]). Since the assignment of hydrological properties is associated with the grid used for the UZ flow model, the stratigraphy information is implicitly embedded in the TSPA-LA through the output flow fields. Aspects that affect hydrogeologic properties for flow are further discussed in BSC (2003 [160109], Section 6 and BSC 2003 [166509], Section 6). See also Section 6.1.11 (FEP 2.2.03.02.0A).

This FEP is also implicitly included for UZ transport through the use of pre-generated flow fields (DTN: LB0305TSPA18FF.001 [165625]) as used by FEHM in TSPA-LA UZ multi-realization runs as described in BSC (2004 [162730], Section 6.5.1). However, BSC (2004 [162730]) does not generate a direct data feed.

Ambient seepage as a result of flow diversion around drifts is a local process simulated by drift-scale seepage process models (BSC 2004 [167970], Sections 6.4.1.1 and 6.4.2.1). In these models, the stratigraphy below and above the repository unit can be neglected. In contrast, the UZ Flow and Transport Model (BSC 2004 [166883], Sections 6.1.1 and 6.1.2) (which provides the percolation flux distributions used for seepage calculations) explicitly accounts for the various geological units and major faults in the UZ. This is because the overall distribution of percolation flux at the repository horizon is influenced by stratigraphic layering and by major discontinuities. For example, the PTn unit overlying the Topopah Spring welded tuff units can divert a fraction of percolating water to intercepting faults and fault zones, thereby changing the spatial distribution of fluxes (BSC 2004 [167970], Section 6.4.1.1). The drift-scale process models addressing TH, THM, and THC processes (BSC 2004 [167970], Sections 6.4.3.1, 6.4.4.1, and 6.4.4.2) also represent the stratigraphy in the UZ at Yucca Mountain in an explicit manner. This is needed because the thermal perturbation of the unsaturated rock extends far into the overlying and underlying geological units. Thus, the stratigraphy information is inherently embedded in the respective model results from the UZ Flow and Transport Model and the TH, THM, and THC drift-scale models.

The overall distribution of percolation flux at the repository horizon is influenced by stratigraphic layering and by major discontinuities. For example, the PTn- unit overlying the Topopah Spring welded tuff units can divert a fraction of percolating water to intercepting faults and fault zones, thereby changing the spatial distribution of fluxes (BSC 2004 [167970], Section 6.4.1.1), which could affect water-rock interaction and seepage water chemistry. Also, the mineralogy of stratigraphic intervals affects seepage water chemistry. For example, the presence of fluorite in the Tptpll hydrogeologic unit may affect fluoride concentrations in pore waters in this unit (BSC 2004 [167974], Section 6.7.5.2). Finally, the thermal perturbation of the unsaturated rock extends far into the geologic units overlying and underlying the emplacement drifts. For these reasons, the THC seepage model includes explicitly the Yucca Mountain stratigraphy (BSC 2004 [167974], Sections 4.1.2, 6.5.1, 6.7.1, and 6.8.1), using stratigraphic information from DTN: LB990501233129.004 [111475] and mineralogical information from DTNs: LA9908JC831321.001 [113495], LA9912SL831151.001 [146447],

LA9912SL831151.002 [146449], and LA0009SL831151.001 [153485]. Therefore, the results from the THC Seepage Model and their abstraction (BSC 2004 [167972], Section 6.2; summary tables of concentrations through time submitted under DTNs: LB0302DSCPTHCS.002 [161976], LB0307DSTTHCR2.002 [165541], and LB0311ABSTHCR2.003 [166713]; and tables of concentrations and summary statistics through time submitted under DTN: LB0311ABSTHCR2.001 [166714]) explicitly account for the effect of stratigraphy on predicted water and gas chemistry. DTNs: LB0302DSCPTHCS.002 [161976] and LB0311ABSTHCR2.001 [166714] are used to feed and/or provide technical basis for another model (BSC 2004 [167461]) that generates lookup tables that are used in the TSPA-LA Model.

This FEP is also included in TSPA-LA through the treatment of drift-scale radionuclide transport (BSC 2004 [167959]). This is captured through the fracture-matrix partitioning model for the fraction of releases from a waste emplacement drift without seepage to the fractures of the underlying rock mass (BSC 2004 [167959], Tables 6.4-6 and 6.4-7). The fraction of the releases from a drift without seepage to the fractures is represented as an uncertain parameter, caused in part by uncertainty in rock characteristics based on stratigraphy (BSC 2004 [167959], Table 4.1-2h). Note that the variability represented by the hydrogeologic units is treated as uncertainty because the fracture-matrix partitioning distributions were not developed on a unit-by-unit basis. Distributions that represent the effects of this uncertainty in the fraction released to fractures are developed for use in TSPA-LA as a probabilistic parameter applied to the total radionuclide flux entering the rock from waste emplacement drifts.

Note that the basis for the UZ and SZ stratigraphic models are different. The UZ uses the Geological Framework Model (GFM2000; MO0012MWDGFM02.002 [153777]) and the SZ uses the Hydrogeologic Framework Model (HFM–USGS 2003 [165176]). These different models for stratigraphy are used as a result of the different domains treated by the UZ and SZ models. The UZ model encompasses rock above the water table over a region around the repository that is roughly 2 km × 9 km (BSC 2004 [166883], Figure 6.1-1). The SZ model encompasses rock below the water table over an area that is roughly 30 km × 50 km (BSC 2003 [166262], Figure 1).

Supporting Reports: BSC 2004 [166883], BSC 2004 [162730], BSC 2004 [167970], BSC 2004 [167972], BSC 2004 [167959], BSC 2003 [163228].

6.1.11 Rock Properties of Host Rock and Other Units (2.2.03.02.0A)

FEP Description: Physical properties such as porosity and permeability of the relevant rock units, soils, and alluvium are necessary for the performance assessment. Possible heterogeneities in these properties should be considered. Questions concerning events and processes that may cause these physical properties to change over time are considered in other FEPs.

Descriptor Phrases: Rock properties in the UZ, Hydrologic properties in the UZ

Screening Decision: Included

Screening Argument: None

TSPA Disposition: This FEP is similar to FEP 2.2.03.01.0A on stratigraphy. Rock properties used are defined for each of the stratigraphic units/layers classified in the Geological Framework Model (GFM2000; MO0012MWDGFM02.002 [153777]), which is further developed into model grid in the Model Report *Development of Numerical Grids for UZ Flow and Transport Modeling* (BSC 2003 [160109]). For the UZ Flow Model (BSC 2004 [166883], Sections 6.1.5, 6.2.3, and 6.4.2), heterogeneity is modeled in terms of the sequence of hydrogeologic units and discrete faults (BSC 2004 [166883], Section 6.1). Therefore, rock properties are implicitly embedded in the TSPA-LA through the output flow fields, with site-scale layering and faults explicitly taken into account. On the drift scale, the effects of rock heterogeneity on seepage are discussed in the Model Report *Abstraction of Drift Seepage,* (BSC 2004 [167970]).

Rock properties of host rock and other units are included and used in the simulations of radionuclide transport through the UZ. BSC (2004 [162730], Sections 6.5.3 and 6.5.7) documents the matrix porosity, rock density, fracture porosity, fracture spacing, and aperture data (DTNs: LB0305TSPA18FF.001 [165625], LB0210THRMLPRP.001 [160799], LB0205REVUZPRP.001 [159525], and LB0207REVUZPRP.001 [159526]). The generated distributions of fracture porosity and fracture frequency are given in (DTN: LA0311BR831371.003 [166515]) and will be used by TSPA-LA in multi-realization runs as described in BSC (2004 [162730], Sections 6.5.3 and 6.5.7).

All the seepage process models that feed into seepage abstraction explicitly represent the physical properties of the unsaturated rock and their heterogeneity (BSC 2004 [167970], Section 6.4). Small-scale heterogeneity is accounted for by a stochastic continuum representation of fracture permeability. Thus, heterogeneity on this scale is implicitly embedded in the model output from the Seepage Calibration Model (BSC 2004 [167976]), the Seepage Model for PA (BSC 2003 [163226]), and the TH Seepage Model (BSC 2003 [166512]) (provided in DTNs: LB0304SMDCREV2.002 [163687]; LB0307SEEPDRCL.002 [164337]; and LB0301DSCPTHSM.002 [163689]). The intermediate-scale spatial variability and uncertainty of seepage-relevant rock properties are accounted for by appropriate probability distributions that were developed in this abstraction (BSC 2004 [167970], Sections 6.6.1 and 6.6.2). Potential alterations of these properties, as a result of THM or THC processes, have been assessed using drift-scale process models (BSC 2004 [167970], Sections 6.4.4.1 and 6.4.4.2). It was demonstrated that these potential alterations can be neglected in the TSPA-LA, because the expected changes would lead to less seepage (BSC 2004 [167970], Section 6.5.1.4) (see Sections 6.8.1 (FEP 2.1.09.12.0A) and 6.8.10 (FEP 2.2.10.04.0A). Percolation flux distributions are provided by the UZ Flow and Transport Model (BSC 2004 [167970], Section 6.6.4.1), which accounts for rock properties and their variation on a larger scale, e.g., stemming from stratigraphy effects.

The THC Seepage Model feeding into the Drift Scale Coupled Process Abstraction (DSCPA) model explicitly represents the physical properties of the unsaturated rock (BSC 2004 [167974], Section 6.4.7). Therefore, these effects are explicitly accounted for in results from the THC Seepage Model and their abstraction (BSC 2004 [167972], Section 6.2; summary tables of concentrations through time submitted under DTNs: LB0302DSCPTHCS.002 [161976], LB0307DSTTHCR2.002 [165541], and LB0311ABSTHCR2.003 [166713]; and tables of concentrations and summary statistics through time submitted under DTN: LB0311ABSTHCR2.001 [166714]). DTNs: LB0302DSCPTHCS.002 [161976] and

LB0311ABSTHCR2.001 [166714] are used to feed and/or provide technical basis for another model (BSC 2004 [167461]) that generates lookup tables that are used in the TSPA-LA Model. Small-scale fracture permeability heterogeneity was also investigated and deemed not to significantly affect seepage water chemistry (BSC 2004 [167974], Section 6.6.2.3). The THC Seepage Model includes rock properties from DTNs: LB991091233129.006 [111480], LB0205REVUZPRP.001 [159525], LB0208UZDSCPMI.002 [161243], LB0207REVUZPRP.002 [159672] and LB0210THRMLPRP.001 [160799]). Potential alterations of these properties as a result of THC processes are explicitly accounted for by the modeling of coupled THC processes, and result in reducing fracture permeability (BSC 2004 [167974], Section 6.8.5.4).

This FEP is also included in TSPA-LA through the treatment of drift-scale radionuclide transport (BSC 2004 [167959]). This is captured through the fracture-matrix partitioning model for the fraction of releases from a waste emplacement drift without seepage to the fractures of the underlying rock mass (BSC 2004 [167959], Tables 6.4-6 and 6.4-7). The fraction of the releases from a drift without seepage to the fractures is represented as an uncertain parameter, caused in part by uncertainty in rock host characteristics (parameters f, m, ϕ_f, ϕ_m, k_m in BSC 2004 [167959], Table 6.4-5). Distributions that represent the effects of this uncertainty in the fraction released to fractures are developed for use in TSPA-LA as a probabilistic parameter applied to the total radionuclide flux entering the rock from waste emplacement drifts.

The effects of rock properties are also included in the treatment of infiltration uncertainty for TSPA-LA (BSC 2003 [165991]). Infiltration uncertainty is represented through three discrete infiltration scenarios (lower, mean, and upper), which are sampled in TSPA-LA according to weighting factors BSC (2003 [165991], Section 7.1). Rock properties are included through the fracture parameters bedrock permeability (BRPERM) and bedrock porosity (BRPOROS). The uncertainties for these parameters are described in (BSC 2003 [165991], Tables 6-2 and 6-3). These uncertainties are propagated through the infiltration numerical model and so are implicitly included in the output (weighting factors) that is passed to TSPA-LA (BSC 2003 [165991]; DTN: SN0308T0503100.008 [165640]). Heterogeneities in these properties are included in the input used in the analysis reported in *Simulation of Net Infiltration for Modern and Potential Future Climates* (USGS 2003 [166518]).

Supporting Reports: BSC 2004 [166883], BSC 2004 [167970], BSC 2004 [162730], BSC 2004 [167972], BSC 2004 [167959], BSC 2003 [165991], BSC 2003 [163228].

6.1.12 Locally Saturated Flow at Bedrock/Alluvium Contact (2.2.07.01.0A)

FEP Description: In washes in arid areas, infiltration can descend to the alluvium/bedrock interface and then proceed down the wash at that interface as a saturated flow system distinct from the surface and distinct from the local water table.

Descriptor Phrases: Locally saturated flow in the UZ (bedrock/alluvium contact), Preferential flow/percolation in the UZ

Screening Decision: Included

Screening Argument: None

TSPA Disposition: The phenomenon of infiltration resulting in a saturated condition at the bedrock/alluvium contact, with subsequent lateral drainage of this water, is indirectly included in the infiltration model. Although not explicitly modeled, runoff at the bedrock/alluvium contact is accounted for in the overall model water balance through the calibration process (using runoff measurements). The details concerning how this calibration is performed are given in USGS (2003 [166518], Section 6.8). The impacts of runoff processes on preferential flow/percolation in the UZ is incorporated into the TSPA-LA through the UZ flow fields that use the infiltration model results (DTN: GS000308311221.005 [147613]) as upper boundary conditions BSC (2004 [166883], Section 6.1.4). The incorporation of UZ flow fields into the TSPA-LA is described in BSC (2004 [166883], Section 6.2.5).

The effects of rock properties are also included in the treatment of infiltration uncertainty for TSPA-LA (BSC 2003 [165991]). Infiltration uncertainty is represented through three discrete infiltration scenarios (lower, mean, and upper), which are sampled in TSPA-LA according to weighting factors BSC (2003 [165991], Section 7.1). Flow through the alluvium/bedrock interface is incorporated into the uncertainty analysis using the uncertain parameters such as soil depth (SOILDEPM), the soil permeability (SOILPERM), and the effective bedrock permeability (BRPERM). It is incorporated implicitly by inclusion of uncertainty in the soil depth, the soil permeability, and the effective bedrock permeability in the calculation of the weighting factors which are passed to TSPA-LA (BSC 2003 [165991]; DTN: SN0308T0503100.008 [165640]).

Supporting Reports: BSC 2003 [165991]

6.1.13 Unsaturated Groundwater Flow in the Geosphere (2.2.07.02.0A)

FEP Description: Groundwater flow occurs in unsaturated rocks in most locations above the water table at Yucca Mountain, including at the location of the repository. See related FEPs for discussions of specific issues related to unsaturated flow.

Descriptor Phrase: Unsaturated flow and pathways in the UZ

Screening Decision: Included

Screening Argument: None

TSPA Disposition: This FEP is included in the UZ process models for mountain-scale flow, drift seepage, mountain-scale radionuclide transport, drift-scale radionuclide transport, and seepage chemistry. The flow model is for three-dimensional, steady flow in a heterogeneous dual-permeability system that includes discrete fault zones (BSC 2004 [166883], Sections 6.2, 6.6, and 6.7) that allows for a realistic description of flow pathways in the UZ. The flow fields (DTN: LB0305TSPA18FF.001 [165625]) generated by the UZ Flow Model are used directly by the TSPA-LA and are also implicitly included in the TSPA-LA via the abstractions for drift seepage (BSC 2004 [167970], Section 6.6.4.1) and radionuclide transport simulations (BSC 2004 [162730], Section 6.5.1). These models and abstractions use a quasi-steady flow-field approximation for climate change (BSC 2004 [166883], Section 6.1.4). The effects of soil depth

on UZ flow at Yucca Mountain are included in the infiltration model (USGS 2003 [166518], Section 6).

Unsaturated groundwater flow in the UZ is the driving force for radionuclide transport through the UZ. This FEP is implicitly addressed through the use of pre-generated flow fields (BSC 2004 [162730], Section 6.5.1; DTN: LB0305TSPA18FF.001 [165625]) in TSPA-LA multi-realization runs. The pre-generated flow fields are directly used by FEHM as described in BSC (2004 [162730], Section 6.5.1). However, BSC (2004 [162730]) does not generate a direct data feed.

Unsaturated flow processes are accounted for in the seepage abstraction by using results from process models that explicitly account for various relevant aspects of unsaturated groundwater flow. All the seepage process models that feed into seepage abstraction simulate groundwater flow processes in unsaturated rock (BSC 2004 [167970], Section 6.4). For ambient seepage, the fracture flow processes in the drift vicinity and the resulting seepage rates are predicted by model simulations from the Seepage Model for PA (BSC 2003 [163226]; BSC 2004 [167970], Section 6.4.2). Results are available as look-up tables in DTNs: LB0304SMDCREV2.002 [163687] and LB0307SEEPDRCL.002 [164337]. These will be used in the TSPA-LA to calculate ambient seepage, by sampling parameter cases of seepage-relevant parameters from the probability distributions defined in BSC (2004 [167970], Section 6.8.1). During the thermal period, the ambient seepage rates will be adjusted based on the TH modeling results from TH Seepage Model, which explicitly simulates thermally perturbed groundwater flow processes. Results are given in DTN: LB0301DSCPTHSM.002 [163689]. The abstraction methodology for thermal seepage is developed in BSC (2004 [167970], Section 6.5.2.1). THM and THC effects on fracture flow processes are evaluated with process models that explicitly account for groundwater flow processes affected by THM and THC parameter alterations (BSC 2004 [167970], Sections 6.4.4.1 and 6.4.4.2). It was demonstrated that these potential alterations can be neglected in the TSPA-LA, as the expected changes would lead to less seepage (BSC 2004 [167970], Section 6.5.1.4) (see Sections 6.8.1 (FEP 2.1.09.12.0A) and 6.8.10 (FEP 2.2.10.04.0A). Percolation flux distributions are provided by the UZ Flow and Transport Model (see BSC 2004 [167970], Section 6.6.4.1), which accounts for groundwater flow on a larger scale, influenced by climate changes, infiltration variability, and stratigraphy effects.

The THC Seepage Model that feeds into the DSCPA Model simulates groundwater flow and water-gas-rock interactions in unsaturated rock and explicitly accounts for various relevant aspects of unsaturated groundwater flow (BSC 2004 [167974], Section 6.2.1). Therefore, the results from the THC Seepage Model and their abstraction (BSC 2004 [167972], Section 6.2; summary tables of concentrations through time submitted under DTNs: LB0302DSCPTHCS.002 [161976], LB0307DSTTHCR2.002 [165541], and LB0311ABSTHCR2.003 [166713]; and tables of concentrations and summary statistics through time submitted under DTN: LB0311ABSTHCR2.001 [166714]) explicitly account for the effect of unsaturated groundwater flow on predicted water and gas chemistry. DTNs: LB0302DSCPTHCS.002 [161976] and LB0311ABSTHCR2.001 [166714] are used to feed and/or provide technical basis for another model (BSC 2004 [167461]) that generates lookup tables that are used in the TSPA-LA Model.

This FEP is also included in TSPA-LA through the treatment of drift-scale radionuclide transport (BSC 2004 [167959]). This is captured through the fracture-matrix partitioning model for the fraction of releases from a waste emplacement drift without seepage to the fractures of the

underlying rock mass (BSC 2004 [167959], Tables 6.4-6 and 6.4-7). Unsaturated flow in the geosphere, based on unsaturated flow as computed in the UZ flow model (BSC 2004 [166883], Sections 6.2, 6.6, and 6.7), is included as part of the model for radionuclide transport from the waste emplacement drift to the rock (parameters q_m and q_f; BSC 2004 [167959], Table 6.4-5). The fraction of the releases from a drift without seepage to the fractures is represented as an uncertain parameter, caused in part by uncertainty in unsaturated flow. Distributions that represent the effects of this uncertainty in the fraction released to fractures are developed for use in TSPA-LA as a probabilistic parameter applied to the total radionuclide flux entering the rock from waste emplacement drifts.

Supporting Reports: BSC 2004 [166883], BSC 2004 [162730], BSC 2004 [167972], BSC 2004 [167970], BSC 2004 [167959], BSC 2003 [163228].

6.1.14 Capillary Rise in the UZ (2.2.07.03.0A)

FEP Description: Capillary rise involves the drawing up of water, above the water table or above locally saturated zones, in continuous pores of the unsaturated zone until the suction gradient is balanced by the gravitational pull downward.

Descriptor Phrase: Capillary effects (wicking) in the UZ

Screening Decision: Included

Screening Argument: None

TSPA Disposition: Capillary forces are included in the UZ Flow Model. These forces affect the distribution of water in the UZ through capillary effects on water flow, also known as capillary wicking. Parameters used for capillarity modeling are incorporated within the matrix properties (DTN: LB02091DSSCP3I.002 [161433]) and fracture properties (DTN: LB0205REVUZPRP.001 [159525]) as described in BSC (2004 [166883], Section 4.1 and Table 4.1-1). These parameters are used as direct input to the UZ Flow Model and are incorporated into the output flow fields used in the TSPA-LA (output flow fields are in DTN: LB0305TSPA18FF.001 [165625]).

Supporting Reports: BSC 2004 [166883].

6.1.15 Focusing of Unsaturated Flow (Fingers, Weeps) (2.2.07.04.0A)

FEP Description: Unsaturated flow can differentiate into zones of greater and lower saturation (fingers) that may persist as preferential flow paths. Heterogeneities in rock properties, including fractures and faults, may contribute to focusing. Focused flow may become locally saturated.

Descriptor Phrases: Flow focusing in the UZ, Flow focusing effects on seepage, Locally saturated flow in the UZ

Screening Decision: Included

Screening Argument: None

TSPA Disposition: The UZ flow fields represent the redistribution of infiltration through UZ layers, with faults explicitly taken into account (BSC 2004 [166883], Sections 6.1.2, 6.2.5, 6.6.3, 6.7.3). The flux redistribution is based on tuff layer properties including fracture and matrix interaction (BSC 2004 [166883], Sections 6.6). Faults are included in the UZ Flow Model as discrete features; therefore, flow in faults is also included in the UZ Flow Model (BSC 2004 [166883]). Flow model results indicate that as flow moves downward through the UZ, the flow tends to focus into fault zones, with the fraction of flow in the faults increasing from about 30–40% at the repository to about 60% at the water table (BSC 2004 [166883], Section 6.6.3).

For radionuclide transport, the effect of focusing unsaturated flow is implicitly included through the use of pre-generated flow fields (BSC 2004 [162730], Section 6.5.1; DTN: LB0305TSPA18FF.001 [165625]) in simulations (BSC 2004 [162730], Section 6.6.2). In TSPA-LA runs, pre-generated flow fields are used directly by the transport model FEHM. However, BSC (2004 [162730]) does not generate a direct data feed.

Intermediate-scale focusing of flow from the site scale to the drift scale is accounted for in the seepage abstraction by using appropriate flow focusing factors (BSC 2004 [167970], Section 6.6.4.2). Small-scale preferential flow is explicitly simulated in the seepage process models that feed into the abstraction, by use of heterogeneous fracture permeability fields (BSC 2004 [167970], Sections 6.4.1.1, 6.4.2.1, and 6.4.3.1). Thus, preferential flow is inherently embedded in the seepage look-up tables for ambient seepage given in DTNs: LB0304SMDCREV2.002 [163687] and LB0307SEEPDRCL.002 [164337], and in the thermal seepage results provided in DTN: LB0301DSCPTHSM.002 [163689]. The abstraction methodology for both ambient and thermal seepage is described in BSC (2004 [167970], Section 6.8.1). The possibility of episodic finger flow is accounted for with an alternative conceptual model analyzed in the thermal seepage model report. Results from this alternative conceptual model are consistent with results from the TH Seepage Model used for this abstraction (BSC 2004 [167970], Section 6.4.3.2).

Intermediate-scale focusing of flow from the site scale to the drift scale is implicitly accounted for in the TH seepage abstraction by using appropriate flow focusing factors (BSC 2004 [167970], Section 6.6.4.2). Such flow focusing is not taken into account in the THC Seepage Model results and their abstraction (BSC 2004 [167972], Section 6.2; summary tables of concentrations through time submitted under DTNs: LB0302DSCPTHCS.002 [161976], LB0307DSTTHCR2.002 [165541], and LB0311ABSTHCR2.003 [166713]; and tables of concentrations and summary statistics through time submitted under DTN: LB0311ABSTHCR2.001 [166714]). This is because fracture permeability heterogeneity was deemed not to significantly affect seepage water chemistry (BSC 2004 [167974], Section 6.6.2.3). DTNs: LB0302DSCPTHCS.002 [161976] and LB0311ABSTHCR2.001 [166714] are used to feed and/or provide technical basis for another model (BSC 2004 [167461]) that generates lookup tables that are used in the TSPA-LA Model.

This FEP is also included in TSPA-LA through the treatment of drift-scale radionuclide transport (BSC 2004 [167959]). This is captured through the fracture-matrix partitioning model for the fraction of releases from a waste emplacement drift without seepage to the fractures of the underlying rock mass (BSC 2004 [167959], Tables 6.4-6 and 6.4-7). Local flow focusing in

fractures is included as part of the model for radionuclide transport from the waste emplacement drift to the rock (parameter *F* in BSC 2004 [167959], Table 6.4-5). The fraction of the releases from a drift without seepage to the fractures is represented as an uncertain parameter, caused in part by uncertainty in flow focusing. Distributions that represent the effects of this uncertainty in the fraction released to fractures are developed for use in TSPA-LA as a probabilistic parameter applied to the total radionuclide flux entering the rock from waste emplacement drifts.

Supporting Reports: BSC 2004 [166883], BSC 2004 [167970], BSC 2004 [167959], BSC 2004 [162730], BSC 2004 [167972], BSC 2003 [163228].

6.1.16 Episodic / Pulse Release from Repository (2.2.07.06.0A)

FEP Description: Episodic or pulse release of radionuclides from the repository and radionuclide transport in the UZ may occur both because of episodic flow into the repository, and because of pulse releases from failed waste packages.

Descriptor Phrases: Pulse release from repository (episodic flow)

Screening Decision: Included

Screening Argument: None

TSPA Disposition: The effects of intermittent waste package failures over a long period of time are included in the source term model for TSPA-LA (BSC 2003 [166296], Section 5.1). This is done by modeling the environmental conditions of the waste packages in different parts of the repository and by modeling corrosion processes under these environmental conditions that lead to waste package failure. Other factors such as drift seepage, seepage water chemistry, rate of waste form dissolution, and rate of radionuclide transport inside the waste emplacement drift also influence the rate of release of radionuclides from the repository and are included in the models (BSC 2003 [166296], Section 5.1). Releases from the waste package and engineered barrier system serve as a time-dependent boundary condition to the mountain-scale radionuclide transport model, which allows for a general time-dependent radionuclide source term, including episodic or pulse releases (BSC 2004 [162730], Section 6.4.7). UZ model components for flow, drift seepage, drift seepage chemistry, and radionuclide transport include step-change transients resulting from climate change at 600 and 2000 years (FEP 1.3.01.00.0A). The step-change transients lead to pulse-release from the unsaturated zone due to the step change in water table elevation with climate change (FEP 1.3.07.02.0B). The effects of short-term episodic flow at the mountain scale are discussed in Section 6.3.5 (FEP 2.2.07.05.0A).

This FEP is implicitly included through the radionuclide transport abstraction for TSPA-LA. The implementation of episodic/pulse release from repository is discussed in BSC (2004 [162730], Sections 6.4.6 through 6.4.9). In TSPA-LA simulation runs, episodic/pulse release from repository is implemented by passing radionuclide mass release from GoldSim to FEHM through the GoldSim-FEHM interface (BSC 2004 [162730], Sections 6.4.6 and 6.4.7). In TSPA-LA, episodic/pulse release caused by climate change is addressed in BSC (2004 [162730], Sections 6.4.8 and 6.4.9) through switching from one flow field to a new flow field at time of climate change. However, BSC (2004 [162730]) does not generate a direct data feed.

Supporting Reports: BSC 2004 [162730], BSC 2004 [166883].

6.1.17 Long-Term Release of Radionuclides from the Repository (2.2.07.06.0B)

FEP Description: The release of radionuclides from the repository may occur over a long period of time, as a result of the timing and magnitude of the waste packages and drip shield failures, waste form degradation, and radionuclide transport through the invert.

Descriptor Phrase: Time-dependent release from the repository

Screening Decision: Included

Screening Argument: None

TSPA Disposition: The effects of long-term waste package failures over a long period of time are included in the source term model for TSPA-LA (BSC 2003 [166296], Section 5.1). This is done by modeling the environmental conditions of the waste packages in different parts of the repository and by modeling corrosion processes under these environmental conditions that lead to waste package failure. Releases from the waste package and engineered barrier system serve as a time-dependent boundary condition to the mountain-scale radionuclide transport model, which allows for a general time-dependent radionuclide source term that accounts for long-term releases (BSC 2004 [162730], Section 6.4.7). For each GoldSim-FEHM run, GoldSim passes radionuclide mass releases to FEHM and FEHM simulates the transport process through the UZ. Long-term radionuclide release due to the failure of waste packages in the repository is implicitly included in BSC (2004 [162730], Sections 6.4.6 and 6.4.7). However, BSC (2004 [162730]) does not generate a direct data feed.

Supporting Reports: BSC 2004 [162730], BSC 2004 [163228]

6.1.18 Perched Water Develops (2.2.07.07.0A)

FEP Description: Zones of perched water may develop above the water table. If these zones occur above the repository, they may affect UZ flow between the surface and the waste packages. If they develop below the repository, for example at the base of the Topopah Spring welded unit, they may affect flow pathways and radionuclide transport between the waste packages and the saturated zone.

Descriptor Phrases: Effects of perched water above the repository on flow/percolation, Effects of perched water below the repository on flow/percolation

Screening Decision: Included

Screening Argument: None

TSPA Disposition: The seepage abstraction model contains a wide range of seepage possibilities, including flow focusing and variability (BSC 2004 [167970], Section 6). Therefore, the potential for effects of perched water above the repository are indirectly captured in the seepage abstraction model through cases with high percolation flux (DTN:

LB0305TSPA18FF.001 [165625]), as described in the Model Report *Abstraction of Drift Seepage* (BSC 2004 [167970]). However, above the repository, no perched water bodies were observed in the fields predicted by the UZ Flow Model. The effects of existing perched water zones below the repository are also included, and potential changes in these perched-water zones caused by climate changes are also included in the mountain-scale UZ flow model (BSC 2004 [166883], Sections 6.2.2, 6.2.3, 6.2.5, 6.6.2, and 6.6.3). The potential for this effect is captured in the output flow fields developed for use in TSPA-LA (output flow fields are in DTN: LB0305TSPA18FF.001 [165625]).

This FEP is also implicitly included through the use of pre-generated flow fields (DTN: LB0305TSPA18FF.001 [165625]) for radionuclide transport in the UZ. In TSPA-LA runs, pre-generated flow fields are used by FEHM and used in UZ transport simulations as described in BSC (2004 [162730], Section 6.5.1). However, BSC (2004 [162730]) does not generate a direct data feed.

Supporting Reports: BSC 2004 [166883], BSC 2004 [162730], BSC 2003 [163228].

6.1.19 Fracture Flow in the UZ (2.2.07.08.0A)

FEP Description: Fractures or other analogous channels act as conduits for fluids to move into the subsurface to interact with the repository and as conduits for fluids to leave the vicinity of the repository and be conducted to the SZ. Water may flow through only a portion of the fracture network, including flow through a restricted portion of a given fracture plane.

Descriptor Phrases: Fracture flow in the UZ, Channeling in the UZ

Screening Decision: Included

Screening Argument: None

TSPA Disposition: The UZ Flow Model is based on the dual-permeability concept, with the fractures represented by a continuum (BSC 2004 [166883], Section 6.1.2). The fracture continuum represents the spatially averaged flow through discrete fractures. The fracture continuum interacts with the matrix continuum, which represents matrix blocks separated by fractures. Fracture continuum properties including permeability, porosity, interface area per unit volume, van Genuchten α and m parameters for the saturation-capillary pressure and relative permeability functions, and active fracture parameter are presented in BSC (2004 [166883], Section 4.1) for each UZ Model layer (DTN: LB0205REVUZPRP.001 [159525] listed in BSC (2004 [166883], Table 4.1-1). Channeling in the UZ is captured as discussed in FEP 2.2.07.04.0A. Permeabilities and other properties are further calibrated as described in the Model Reports *Calibrated Properties Model* (BSC 2003 [166509]) and *Analysis of Hydrologic Properties Data* (BSC 2003 [161773]). The fracture-continuum properties are used as inputs to the UZ Flow Model, and their effects are incorporated into the output flow fields developed for use in TSPA-LA (output flow fields are in DTN: LB0305TSPA18FF.001 [165625]).

In the unsaturated zone, fracture flow plays an important role in the transport of radionuclides. In TSPA-LA runs, direct effect of fracture flow on radionuclide transport (advection) is implicitly included through FEHM's use of pre-generated flow fields (DTN: LB0305TSPA18FF.001

[165625]) in UZ transport simulations as described in BSC (2004 [162730], Section 6.5.1). However, BSC (2004 [162730]) does not generate a direct data feed.

Flow processes in fractures or other channels are important for seepage abstraction, because the amount of seepage is determined by the diversion capacity of the fracture flow in the drift vicinity (BSC 2004 [167970], Section 6.3.1). All the seepage process models that feed into seepage abstraction simulate flow processes in fractured rock (BSC 2004 [167970], Section 6.4). Spatial variability in the fracture flow, potentially leading to water flow through only a portion of the fracture network, is accounted for by using a stochastic continuum representation. For ambient seepage, the fracture flow processes in the drift vicinity and the resulting seepage rates are predicted by model simulations from the Seepage Model for PA (BSC 2003 [163226]; BSC 2004 [167970], Section 6.4.2). Results are available as look-up tables in DTNs: LB0304SMDCREV2.002 [163687] and LB0307SEEPDRCL.002 [164337]. These will be used in the TSPA-LA to calculate ambient seepage, by sampling parameter cases of seepage-relevant parameters from the probability distributions defined in BSC (2004 [167970], Section 6.8.1). During the thermal period, the ambient seepage rates will be adjusted based on the TH modeling results from the TH Seepage Model, which explicitly simulates thermally perturbed fracture flow conditions. Results are given in DTN: LB0301DSCPTHSM.002 [163689]. The abstraction methodology for thermal seepage is developed in BSC (2004 [167970], Section 6.5.2.1). THM and THC effects on fracture flow processes are evaluated with process models that explicitly account for fracture flow affected by THM and THC parameter alterations (BSC 2004 [167970], Sections 6.4.4.1 and 6.4.4.2). It was demonstrated that these potential alterations can be neglected in the TSPA-LA, because the expected changes would lead to less seepage (BSC 2004 [167970], Section 6.5.1.4) (see Sections 6.8.1 (FEP 2.1.09.12.0A) and 6.8.10 (FEP 2.2.10.04.0A). Percolation flux distributions are provided by the UZ Flow and Transport Model (BSC 2004 [167970], Section 6.6.4.1), which accounts for fracture flow on a larger scale (influenced by climate changes), infiltration variability, and stratigraphy effects. Flow focusing effects (channeling) are included as discussed in BSC (2004 [167970], Section 6.6.4.2).

Flow processes in fractures or other channels affect modeled THC coupled processes because of 1) their strong effect on TH behavior (BSC 2004 [167970], Sections 6.4.4.1, 6.4.4.2, and 2) their strong effect on water and gas chemistry (BSC 2004 [167974], Section 6.2.1). The latter is primarily due to volatilization of steam and CO_2 from the rock matrix-water and subsequent transport and condensation in fractures. The amount of mobilized CO_2 with steam directly affects the pH of the condensate, which in turn affects the degree of water-rock interaction and water chemistry. These THC processes are influenced by the fracture characteristics, such as orientation, aperture, asperity, length, connectivity, and fillings. The THC Seepage Model that feeds into the DSPCA model explicitly simulate the flow processes in fractures using appropriate continuum properties that represent these characteristics (BSC 2004 [167974], Sections 6.4.3, 6.4.4, and 6.4.7). Thus, the results from the THC Seepage Model and their abstraction (BSC 2004 [167972], Section 6.2; summary tables of concentrations through time submitted under DTNs: LB0302DSCPTHCS.002 [161976], LB0307DSTTHCR2.002 [165541], and LB0311ABSTHCR2.003 [166713]; and tables of concentrations and summary statistics through time submitted under DTN: LB0311ABSTHCR2.001 [166714]) explicitly account for the effect of fractures on predicted water and gas chemistry. DTNs: LB0302DSCPTHCS.002 [161976] and LB0311ABSTHCR2.001 [166714] are used to feed and/or provide technical basis for another model (BSC 2004 [167461]) that generates lookup tables that are used in the TSPA-LA Model.

This FEP is also included in TSPA-LA through the treatment of drift-scale radionuclide transport (BSC 2004 [167959]). This is captured through the fracture-matrix partitioning model for the fraction of releases from a waste emplacement drift without seepage to the fractures of the underlying rock mass (BSC 2004 [167959], Tables 6.4-6 and 6.4-7). Advective transport in fractures, based on fracture flow (parameter q_f in BSC 2004 [167959], Table 6.4-5) as computed in the UZ Flow Model (BSC 2004 [166883], Sections 6.2, 6.6, and 6.7), is included through the fracture-matrix partitioning model for the fraction of radionuclide releases from a waste emplacement drift without seepage to the fractures of the underlying rock mass (BSC 2004 [167959], Tables 6.4-6 and 6.4-7). The fraction of the releases from a drift without seepage to the fractures is represented as an uncertain parameter, caused in part by uncertainty in fracture flow. Distributions that represent the effects of this uncertainty in the fraction released to fractures are developed for use in TSPA-LA as a probabilistic parameter applied to the total radionuclide flux entering the rock from waste emplacement drifts.

The effects of fracture flow are also included in the treatment of infiltration uncertainty for TSPA-LA (BSC 2003 [165991]). Infiltration uncertainty is represented through three discrete infiltration scenarios (lower, mean, and upper), which are sampled in TSPA-LA according to weighting factors BSC (2003 [165991], Section 7.1). This FEP is implicitly included in the determination of the weighing factors fed to TSPA-LA (BSC 2003 [165991]; DTN: SN0308T0503100.008 [165640]). This FEP is incorporated in the uncertain parameters describing the bedrock permeability multiplier (BRPERM) and bedrock porosity (BRPOROS).

Supporting Reports: BSC 2004 [166883], BSC 2004 [162730], BSC 2004 [167970], BSC 2004 [167972], BSC 2004 [167959], BSC 2003 [165991], BSC 2003 [163228].

6.1.20 Matrix Imbibition in the UZ (2.2.07.09.0A)

FEP Description: Water flowing in fractures or other channels in the unsaturated zone is imbibed into the surrounding rock matrix. This may occur during steady flow, episodic flow, or into matrix pores that have been dried out during the thermal period.

Descriptor Phrase: Matrix imbibition in the UZ

Screening Decision: Included

Screening Argument: None

TSPA Disposition: Matrix imbibition is included in the process model for UZ flow at the mountain scale (BSC 2004 [166883], Section 6.1.2). Matrix imbibition refers to the movement of water into the matrix as a result of capillary forces. This process affects the distribution of flow between fractures and matrix in a dual-permeability flow model for fractured rock. The influence of matrix imbibition on episodic flow is discussed in BSC (2004 [166883], Section 6.1.2). Imbibition is captured in the UZ Flow Model through capillarity modeling, which uses matrix and fracture properties as model input. Therefore, the effect of imbibition is implicitly incorporated in the output flow fields (DTN: LB0305TSPA18FF.001 [165625]) used in the TSPA-LA.

For TSPA-LA runs, the pre-generated flow fields (DTN: LB0305TSPA18FF.001 [165625]) are used by FEHM in UZ transport simulations as described in BSC (2004 [162730], Section 6.5.1). Therefore, the effects of matrix imbibition are implicitly included in the treatment of UZ radionuclide transport. However, BSC (2004 [162730]) does not generate a direct data feed.

The THC Seepage Model explicitly accounts for matrix imbibition using appropriate dual-permeability modeling concepts (BSC 2004 [167974], Section 6.2.1). This is needed because the thermal perturbation of the unsaturated rock results in significant transfer of liquid and gas from the matrix into the fractures and vice versa (e.g., BSC 2004 [167974], Figure 6.2-2). Therefore, these effects are directly accounted for in results from the THC Seepage Model and their abstraction (BSC 2004 [167972], Section 6.2; summary tables of concentrations through time submitted under DTNs: LB0302DSCPTHCS.002 [161976], LB0307DSTTHCR2.002 [165541], and LB0311ABSTHCR2.003 [166713]; and tables of concentrations and summary statistics through time submitted under DTN: LB0311ABSTHCR2.001 [166714]). DTNs: LB0302DSCPTHCS.002 [161976] and LB0311ABSTHCR2.001 [166714] are used to feed and/or provide technical basis for another model (BSC 2004 [167461]) that generates lookup tables that are used in the TSPA-LA Model.

Ambient seepage is mainly governed by flow in the fractures, as discussed in BSC (2004 [167970], Sections 6.4.1.1 and 6.4.2.1). Thus, in the predictive model for ambient seepage, i.e., the Seepage Calibration Model (BSC 2004 [167976]) and the Seepage Model for PA (BSC 2003 [163226]), matrix imbibition is neglected. In contrast, the drift-scale process models addressing TH, THM, and THC processes (BSC 2004 [167970], Sections 6.4.3.1, 6.4.4.1, and 6.4.4.2) explicitly account for matrix imbibition using appropriate dual-permeability modeling concepts. This is needed because the thermal perturbation of the unsaturated rock results in significant transfer of liquid and gas from the matrix into the fractures and vice versa. The UZ Flow and Transport Model (which provides the percolation flux distributions used for seepage calculations) also accounts for the impact of matrix imbibition in an explicit manner (BSC 2004 [167970], Section 6.6.4.1). Thus, matrix imbibition effects are inherently embedded in the respective model results used for this abstraction.

Supporting Reports: BSC 2004 [166883], BSC 2004 [167970], BSC 2004 [167972], BSC 2004 [162730], BSC 2003 [163228].

6.1.21 Condensation Zone Forms around Drifts (2.2.07.10.0A)

FEP Description: Condensation of the two-phase flow generated by repository heat forms in the rock where the temperature drops below the local vaporization temperature. Waste package emplacement geometry and thermal loading will affect the scale at which condensation caps form (over waste packages, over panels, or over the entire repository), and to the extent to which "shedding" will occur as water flows from the region above one drift to the region above another drift or into the rock between drifts.

Descriptor Phrases: Condensation zone in UZ above repository, Condensation zone in UZ effects on seepage

Screening Decision: Included

Screening Argument: None

TSPA Disposition: The coupled processes of vapor condensation forming a condensation cap in the fractured rock above the drifts are explicitly simulated with the TH Seepage Model (BSC 2003 [166512], Sections 6.2 and 7.4) that feeds into the seepage abstraction. The coupled processes of vapor condensation forming a condensation cap above the drifts and occurrence of "shedding" between drifts (BSC 2004 [167970], Section 6.3.2) are explicitly simulated with the TH Seepage Model that feeds into the seepage abstraction. Using this model, the impact of condensation and shedding on seepage is assessed for various simulation cases (BSC 2004 [167970], Section 6.4.3.3). Thus, the TH modeling results from DTN: LB0301DSCPTHSM.002 [163689] inherently include these effects. As discussed in BSC (2004 [167970], Section 6.5.2.1), the abstraction of thermal seepage utilizes these modeling results to develop an appropriate thermal-seepage abstraction methodology.

The coupled processes of vapor condensation forming a condensation cap above the drifts and occurrence of "shedding" between drifts are explicitly simulated with the THC Seepage Model (BSC 2004 [167974], Sections 6.2.1, 6.5.5.1, 6.6.2.1 and 6.8.5.4). Using this model, the impact of condensation and drainage on seepage water chemistry is assessed for various simulation cases (BSC 2004 [167974], Sections 6.3, 6.5, 6.6, 6.7, and 6.8). Therefore, the results from the THC Seepage Model and their abstraction (BSC 2004 [167972], Section 6.2; summary tables of concentrations through time submitted under DTNs: LB0302DSCPTHCS.002 [161976], LB0307DSTTHCR2.002 [165541], and LB0311ABSTHCR2.003 [166713]; and tables of concentrations and summary statistics through time submitted under DTN: LB0311ABSTHCR2.001 [166714]) explicitly include these effects. DTNs: LB0302DSCPTHCS.002 [161976] and LB0311ABSTHCR2.001 [166714] are used to feed and/or provide technical basis for another model (BSC 2004 [167461]) that generates lookup tables that are used in the TSPA-LA Model.

Supporting Reports: BSC 2004 [167970], BSC 2004 [167972].

6.1.22 Resaturation of Geosphere Dry-Out Zone (2.2.07.11.0A)

FEP Description: Following the peak thermal period, water in the condensation cap may flow downward into the drifts. Influx of cooler water from above, such as might occur from episodic flow, may accelerate return flow from the condensation cap by lowering temperatures below the condensation point. Percolating groundwater will also contribute to resaturation of the dry out zone. Vapor flow, as distinct from liquid flow by capillary processes, may also contribute.

Descriptor Phrases: Saturation increase in near-field, Condensation zone in UZ above repository, Flow/percolation in the UZ

Screening Decision: Included

Screening Argument: None

TSPA Disposition: Resaturation of the dryout zone around drifts, and the potential of return flow from the condensation zone back to the drifts, are explicitly simulated with the TH Seepage Model (BSC 2003 [166512]) that feeds into seepage abstraction. Using this model, the impact of

resaturation and reflux (on) seepage is assessed for various simulation cases (BSC 2004 [167970], Section 6.4.3.3). Thus, the TH modeling results from DTN: LB0301DSCPTHSM.002 [163689] inherently include these effects. As discussed in BSC (2004 [167970], Section 6.5.2.1), the abstraction of thermal seepage utilizes these modeling results to develop an appropriate thermal-seepage abstraction methodology. The impact of potential episodic flow was addressed with an alternative conceptual model for thermal seepage, as discussed in BSC (2004 [167970], Section 6.4.3.2). It was shown that results from this alternative conceptual model are consistent with the process model results from the TH Seepage Model used for this abstraction.

Resaturation of the dryout zone around drifts, and the potential of return flow from the condensation zone back to the drifts, are explicitly simulated with the THC Seepage Model (BSC 2004 [167974], Sections 6.2.1, 6.5.5, 6.6.2, 6.7.5, 6.8.5). Using this model, the impact of resaturation on reflux chemistry is assessed as part of the abstraction methodology (i.e., the compositions of abstracted "FRONT" waters reflect concentration increases due to the dissolution of salts precipitated during dryout; see BSC 2004 [167972], Section 6.2.4.1.2). Therefore, the results from the THC Seepage Model and their abstraction (BSC 2004 [167972], Section 6.2; summary tables of concentrations through time submitted under DTNs: LB0302DSCPTHCS.002 [161976], LB0307DSTTHCR2.002 [165541], and LB0311ABSTHCR2.003 [166713]; and tables of concentrations and summary statistics through time submitted under DTN: LB0311ABSTHCR2.001 [166714]) explicitly include these effects. DTNs: LB0302DSCPTHCS.002 [161976] and LB0311ABSTHCR2.001 [166714] are used to feed and/or provide technical basis for another model (BSC 2004 [167461]) that generates lookup tables that are used in the TSPA-LA Model.

Supporting Reports: BSC 2004 [167970], BSC 2004 [167972].

6.1.23 Advection and Dispersion in the UZ (2.2.07.15.0B)

FEP Description: Advection and dispersion processes may affect contaminant transport in the UZ.

Descriptor Phrases: Advection of dissolved radionuclides in the UZ, Dispersion of dissolved radionuclides in the UZ

Screening Decision: Included

Screening Argument: None

TSPA Disposition: Radionuclide transport through the UZ by advection is simulated using the RTTF (Residence Time Transfer Function) method documented in BSC (2004 [162730], Section 6.4.1). Dispersion is incorporated into the RTTF algorithm through the use of a transfer function based on an analytical solution to the advection-dispersion equation (BSC 2004 [162730], Section 6.4.2). In TSPA–LA runs, advection and dispersion are implicitly included through the use of FEHM RTTF model and the pre-generated flow fields as described in BSC (2004 [162730], Sections 6.4.1 and 6.4.2). However, BSC (2004 [162730]) does not generate a direct data feed.

This FEP is also included in TSPA-LA through the treatment of drift-scale radionuclide transport (BSC 2004 [167959]). This is captured through the fracture-matrix partitioning model for the fraction of releases from a waste emplacement drift without seepage to the fractures of the underlying rock mass (BSC 2004 [167959], Tables 6.4-6 and 6.4-7). Advective transport in fractures and matrix, based on flow as computed in the UZ Flow Model (BSC 2004 [166883], Sections 6.2, 6.6, and 6.7), is included as part of the model for radionuclide transport from the waste emplacement drift to the rock (parameters q_m and q_f in BSC 2004 [167959], Table 6.4-5). Diffusive transport in fractures is also included (parameter D_m in BSC 2004 [167959], Table 6.4-5), but hydrodynamic dispersion is not considered. The fraction of the releases from a drift without seepage to the fractures is represented as an uncertain parameter, caused in part by uncertainty in fracture and matrix flow. Distributions that represent the effects of this uncertainty in the fraction released to fractures are developed for use in TSPA-LA as a probabilistic parameter applied to the total radionuclide flux entering the rock from waste emplacement drifts.

Supporting Reports: BSC 2004 [162730], BSC 2004 [167959], BSC 2003 [163228].

6.1.24 Film Flow into the Repository (2.2.07.18.0A)

FEP Description: Water entering waste emplacement drifts may occur by a film flow process. This differs from the traditional view of flow in a capillary network, where the wetting phase exclusively occupies capillaries with apertures smaller than some level defined by the capillary pressure. As a result, a film flow process could allow water to enter a waste emplacement drift at non-zero capillary pressure. Dripping into the drifts could also occur through collection of the film flow on the local minima of surface roughness features along the crown of the drift.

Descriptor Phrase: Film flow effects on seepage

Screening Decision: Included

Screening Argument: None

TSPA Disposition: The potential impact of film flow is represented in the Seepage Calibration Model (BSC 2004 [167976]) results that are used for the seepage abstraction; i.e., in the calibrated values of the capillary-strength parameter given in BSC (2004 [167970], Table 6.6-1) (DTN: LB0302SCMREV02.002 [162273]). If water originating from film flow seeps into the opening during a liquid-release test, it is reflected in the corresponding seepage data point used for model calibration. That is, film flow is inherently accounted for in the estimated seepage-related capillary-strength parameter from the Seepage Calibration Model (BSC 2004 [167976]), and thus in the prediction of seepage into waste emplacement drifts (BSC 2004 [167970], Section 6.4.1.1). Note that in theory, film-flow behavior may be influenced by the elevated temperatures in the drift vicinity during the first several thousand years after emplacement. This effect is not included in the ambient liquid-release tests. However, the potential changes in film flow as a result of temperature increase are not expected to be significant for drift seepage.

Supporting Reports: BSC 2004 [167970].

6.1.25 Lateral Flow from Solitario Canyon Fault Enters Drifts (2.2.07.19.0A)

FEP Description: Water movement down Solitario Canyon Fault could enter waste emplacement drifts through lateral flow mechanisms in the Topopah Spring welded hydrogeologic unit. This percolation pathway is more likely to transmit episodic transient flow to waste emplacement locations due to the major fault pathway through the overlying units.

Descriptor Phrases: Locally saturated flow in the UZ (Solitario Canyon Fault), Preferential flow/percolation in the UZ (faults)

Screening Decision: Included

Screening Argument: None

TSPA Disposition: The UZ Flow Model contains potential hydrogeological connections between the Solitario Canyon Fault and the waste emplacement horizon. The potential connection is captured using a property set of the PTn unit (BSC 2004 [166883], Sections 6.2.2.1, 6.2.3 and 6.6) with calibrated fracture-matrix properties that favor lateral flow. Therefore, flow from this fault to waste emplacement locations is addressed. This water may seep into waste emplacement drifts if the flux is sufficient to overcome the capillary barrier represented in the drift seepage model (BSC 2004 [167970]). The lateral flow effect is implicitly incorporated in the output flow fields (DTN: LB0305TSPA18FF.001 [165625]) used in the TSPA-LA. Other aspects of flow focusing in faults (preferential flow in faults) are discussed in Section 6.1.15; FEP 2.2.07.04.0A. Locally saturated flow (otherwise known as perched water) is discussed in Section 6.1.8, FEP 2.2.07.07.0A.

Supporting Reports: BSC 2004 [166883]

6.1.26 Flow Diversion around Repository Drifts (2.2.07.20.0A)

FEP Description: Flow in unsaturated rock tends to be diverted by openings such as waste emplacement drifts due to the effects of capillary forces. The resulting diversion of flow could have an effect on seepage into the repository. Flow diversion around the drift openings could also lead to the development of a zone of lower flow rates and low saturation beneath the drift, known as the drift shadow.

Descriptor Phrases: Flow diversion around drifts, Flow diversion effects on seepage

Screening Decision: Included

Screening Argument: None

TSPA Disposition: The impact of flow diversion around the drifts and its relevance for seepage is explicitly captured in the seepage process models used for the seepage abstraction (BSC 2004 [167970], Sections 6.4.1, 6.4.2, and 6.4.3). From these model simulations, seepage predictions are available in the form of look-up tables in DTNs: LB0304SMDCREV2.002 [163687] and LB0307SEEPDRCL.002 [164337]. These will be used in the TSPA-LA to calculate ambient seepage, by sampling parameter cases of seepage-relevant parameters from the probability

distributions defined in BSC (2004 [167970], Section 6.8.1). These seepage-relevant parameters are the effective capillary-strength parameter permeability and local percolation flux. During the thermal period, the ambient rates will be adjusted based on the TH modeling results from DTN: LB0301DSCPTHSM.002 [163689], using the abstraction methodology developed in BSC (2004 [167970], Section 6.5.2.1). The Drift Seepage Model also captures the effects of drift collapse (BSC 2004 [167970], Sections 6.4.2.4 and 6.7.1.2) in terms of the larger drift profile that results.

Supporting Reports: BSC 2004 [167970], BSC 2004 [167959], BSC 2004 [167972].

6.1.27 Drift Shadow Forms below Repository (2.2.07.21.0A)

FEP Description: Flow in unsaturated rock tends to be diverted by openings such as waste emplacement drifts due to the effects of capillary forces. Flow diversion around the drift openings could lead to the development of a zone of lower flow rates and low saturation beneath the drift, known as the drift shadow. Radionuclide transport rates through the unsaturated rock may be dependent on whether or not radionuclide releases occur from drifts that are underlain by a drift shadow.

Descriptor Phrases: Flow diversion around drifts, Drift shadow effects on transport

Screening Decision: Included

Screening Argument: None

TSPA Disposition: The drift shadow effect is a result of flow diversion around drifts (see Section 6.1.26; FEP 2.2.07.20.0A). This FEP is included in TSPA-LA through the treatment of drift-scale radionuclide transport (BSC 2004 [167959]). The drift shadow effect on radionuclide transport is included through the fracture-matrix partitioning model for the fraction of releases from a waste emplacement drift without seepage to the fractures of the underlying rock mass (BSC 2004 [167959], Tables 6.4-6 and 6.4-7). This boundary condition (initiation of geosphere transport in the rock matrix or fractures) is found to control, in large part, the general behavior of radionuclide transport through the drift shadow zone. Based on these results, the additional effects of the drift shadow on radionuclide transport are not further considered in TSPA-LA. In particular, the reduction in flow over a region beneath the waste emplacement drift scaled by the size of the drift is not further considered. The fraction of the releases from a drift without seepage to the fractures is represented as an uncertain parameter, caused by uncertainty in rock fracture and matrix properties, invert properties, diffusion characteristics in the rock and invert, and hydrological conditions beneath the drift. Distributions that represent the effects of this uncertainty in the fraction released to fractures are developed for use in TSPA-LA as a probabilistic parameter applied to the total radionuclide flux entering the rock from waste emplacement drifts.

Supporting Reports: BSC 2004 [167959].

6.1.28 Chemical Characteristics of Groundwater in the UZ (2.2.08.01.0B)

FEP Description: Chemistry and other characteristics of groundwater in the unsaturated zone may affect groundwater flow and radionuclide transport of dissolved and colloidal species.

Groundwater chemistry and other characteristics, including temperature, pH, Eh, ionic strength, and major ionic concentrations, may vary spatially throughout the system as a result of different rock mineralogy.

Descriptor Phrases: Initial THC characteristics in the UZ (temperature, pH, Eh, water conc., gas conc., ionic strength), Spatially-dependent chemical effects on sorption in the UZ

Screening Decision: Included

Screening Argument: None

TSPA Disposition: THC Seepage Model simulations (BSC 2004 [167974]) feeding the drift scale coupled processes abstraction were run explicitly using five different input water compositions spanning the range of compositions at Yucca Mountain (Attachment III) (see also BSC 2004 [167974], Sections 6.2.2 and 6.8.5). This variability of pore-water compositions in repository host units implicitly reflects spatial variations in rock mineralogy and infiltration rates. Therefore, the results of the THC Seepage Model and their abstraction (BSC 2004 [167972], Section 6.2; summary tables of concentrations through time submitted under DTNs: LB0302DSCPTHCS.002 [161976], LB0307DSTTHCR2.002 [165541], and LB0311ABSTHCR2.003 [166713]; and tables of concentrations and summary statistics through time submitted under DTN: LB0311ABSTHCR2.001 [166714]) explicitly reflect the natural variability of pore-water compositions and implicitly reflect the natural variability of rock mineralogy. DTNs: LB0302DSCPTHCS.002 [161976] and LB0311ABSTHCR2.001 [166714] are used to feed and/or provide technical basis for another model (BSC 2004 [167461]) that generates lookup tables that are used in the TSPA-LA Model.

The effects of groundwater chemical characteristics are included in the radionuclide sorption coefficients under ambient conditions. The sorption coefficient data on which the distributions are based are obtained in laboratory experiments in which crushed rock samples from the Yucca Mountain site are contacted with groundwaters (or simulated groundwaters) representative of the site, spiked with one or more of the elements of interest (BSC 2003 [163228], Section I.5). The chemistry of pore waters and perched waters in the UZ along potential flowpaths to the accessible environment is discussed in BSC (2002 [160247]). In the UZ, two distinct water types exist in the ambient system. One is perched water and the other is pore water. Perched water is generally more dilute than pore water. The J-13 and UE p#1 waters were used in sorption experiments as end-member compositions intended to bracket the impact of water composition on sorption coefficients (BSC 2003 [163228], Section I.4). Some spatial trends in water composition through the TSw and CHn geologic units have been noted (BSC 2002 [160247], Section 6.5.3.1). However, the uncertainty in these spatial variations (BSC 2004 [167974], Section 6.2.2.1) and the uncertainty with respect to the effects of the bounding water compositions on sorption (BSC 2003 [163228], Sections I.8.C, I.8.D, and I.8.I) have led to the treatment of natural variability in water composition as uncertainty. Sorption experiments have been carried out as a function of time, element concentration, atmospheric composition, particle size, and temperature. In some cases, the solids remaining from sorption experiments were contacted with unspiked groundwater in desorption experiments. The experimental data used to determine the sorption K_ds are provided in the following DTNs: LA0305AM831341.001 [163789], LA0309AM831341.002 [165523], LA0309AM831341.003 [165524],

LA0309AM831341.004 [165525], LA0309AM831341.005 [165526], LA0309AM831341.006 [165527], LA0309AM831341.007 [165528], and LA0310AM831341.001 [165865]. The sorption and desorption experiments together provide information on the equilibration rates of the forward and backward sorption reactions. For elements that sorb primarily through surface complexation reactions, the experimental data are augmented with the results of modeling calculations using PHREEQC V2.3 (BSC 2001 [155323]). The inputs for the modeling calculations include groundwater compositions, surface areas, binding constants for the elements of interest, and thermodynamic data for solution species. These modeling calculations provide a basis for interpolation and extrapolation of the experimentally derived sorption coefficient dataset. The effects of nonlinear sorption are approximated by capturing the effective K_d range (BSC 2003 [163228], Section I.8).

The effects of groundwater composition with respect to sorption coefficients are provided in terms of probability distributions for the sorption coefficient of each element of interest among the three major rock types (devitrified, zeolitic, and vitric) found in the UZ. The influence of expected variations in water chemistry, radionuclide concentrations, and variations in rock surface properties within one of the major rock types are incorporated into these probability distributions. These distributions are specified for each radionuclide/rock type combination (BSC 2003 [163228], Section I.8) and are sampled in the TSPA-LA to account for the effects of natural variations in pore water chemistry and mineral surfaces on sorption. Correlations for sampling sorption coefficient probability distributions have been derived for the elements investigated (BSC 2003 [163228], Section II). To derive the correlations, a rating system was first developed to rate the impact of six different variables on the sorption coefficient for a given element in each of the three major rock types. The six variables are pH, Eh, water chemistry, rock composition, rock surface area, and radionuclide concentration. Water chemistry refers to the major ion concentrations and silica. Rock composition refers to both the mineralogic composition of the rocks and the chemical composition of the minerals (e.g., zeolite compositions). The output DTNs for the sorption K_ds and correlations are LA0302AM831341.002 [162575] and LA0311AM831341.001 [167015].

Supporting Reports: BSC 2004 [167972], BSC 2003 [163228].

6.1.29 Redissolution of Precipitates Directs More Corrosive Fluids to Containers (2.2.08.04.0A)

FEP Description: Redissolution of precipitates which have plugged pores as a result of evaporation of groundwater in the dry-out zone, produces a pulse of fluid reaching the waste packages when gravity-driven flow resumes, which is more corrosive than the original fluid in the rock.

Descriptor Phrases: Effects of resaturation of dry-out zone (seepage of corrosive fluids), Thermal effects on seepage (inflowing water composition)

Screening Decision: Included

Screening Argument: None

TSPA Disposition: The THC Seepage Model simulations feeding BSC (2004 [167972]) explicitly consider the formation of salt precipitates upon dryout (BSC 2004 [167974], Section 6.4.5) and their dissolution during re-wetting around drifts (BSC 2004 [167974], Section 6.8.5.3) and the resulting effect on percolation water chemistry (BSC 2004 [167972], Section 6.2.4.1.2) (see also BSC 2004 [167974], Section 6.8.5.4, p. 240). Therefore, the results of the THC Seepage Model and their abstraction (BSC 2004 [167972], Section 6.2; summary tables of concentrations through time submitted under DTNs: LB0302DSCPTHCS.002 [161976], LB0307DSTTHCR2.002 [165541], and LB0311ABSTHCR2.003 [166713]; and tables of concentrations and summary statistics through time submitted under DTN: LB0311ABSTHCR2.001 [166714]) explicitly reflect the effect of salt redissolution upon rewetting. The effect results in an increase in both salinity and variability (BSC 2004 [167972], Section 6.2.4.1.2). DTNs: LB0302DSCPTHCS.002 [161976] and LB0311ABSTHCR2.001 [166714] are used to feed and/or provide technical basis for another model (BSC 2004 [167461]) that generates lookup tables that are used in the TSPA-LA Model.

Supporting Reports: BSC 2004 [167972].

6.1.30 Diffusion in the UZ (2.2.08.05.0A)

FEP Description: Molecular diffusion processes may affect radionuclide transport in the UZ. This includes osmotic processes in response to chemical gradients.

Descriptor Phrases: Diffusion of dissolved radionuclides in the UZ, Osmosis of dissolved radionuclides in the UZ

Screening Decision: Included

Screening Argument: None

TSPA Disposition: This FEP is included in TSPA-LA through the treatment of drift-scale radionuclide transport (BSC 2004 [167959]). This is captured through the fracture-matrix partitioning model for the fraction of releases from a waste emplacement drift without seepage to the fractures of the underlying rock mass (BSC 2004 [167959], Tables 6.4-6 and 6.4-7). Diffusive transport in fractures is included as part of the model for radionuclide transport from the waste emplacement drift to the rock (parameter Dm in BSC 2004 [167959], Table 6.4-5). For drifts without seepage, the fracture flow pattern is abstracted as a zone beneath the drifts where fracture flow does not occur that interfaces with a zone of undisturbed fracture flow as predicted in the mountain-scale UZ flow model. Diffusion is the transport mechanism for radionuclides to migrate through fractures between the base of the drift and flowing fractures. The fraction of the releases from a drift without seepage to the fractures is represented as an uncertain parameter, caused in part by uncertainty in diffusion in fractures. Distributions that represent the effects of this uncertainty in the fraction released to fractures are developed for use in TSPA-LA as a probabilistic parameter applied to the total radionuclide flux entering the rock from waste emplacement drifts.

For mountain-scale UZ transport, the effects of molecular diffusion on larger-scale dispersion are primarily due to dispersion processes explicitly represented in the dual-permeability model as a result of differential advection in the fracture and matrix continua and diffusive exchange

between these continua (see Section 6.1.32, FEP 2.2.08.08.0B concerning the treatment of matrix diffusion).

Osmosis is addressed in Section 6.1.32 (FEP 2.2.08.08B).

Supporting Reports: BSC 2004 [167959], BSC 2004 [166883], BSC 2003 [163228]

6.1.31 Complexation in the UZ (2.2.08.06.0B)

FEP Description: Complexing agents such as humic and fulvic acids present in natural groundwaters could affect radionuclide transport in the UZ.

Descriptor Phrase: Complexation in the UZ

Screening Decision: Included

Screening Argument: None

TSPA Disposition: The effects of complexation are implicitly included in the radionuclide sorption coefficients under ambient conditions. The sorption coefficient data on which the distributions are based are obtained in laboratory experiments in which crushed rock samples from the Yucca Mountain site are contacted with groundwaters (or simulated groundwaters) representative of the site, spiked with one or more of the elements of interest (BSC 2003 [163228], Section I.5). As such, the sorption experiments contain representative ligands responsible for complex formation, such as carbonates (Triay et al. 1997 [100422], p. 85). Sorption experiments have been carried out as a function of time, element concentration, atmospheric composition, particle size, and temperature. In some cases, the solids remaining from sorption experiments were contacted with unspiked groundwater in desorption experiments. The experimental data used to determine the sorption K_ds are provided in the following DTNs: LA0305AM831341.001 [163789], LA0309AM831341.002 [165523], LA0309AM831341.003 [165524], LA0309AM831341.004 [165525], LA0309AM831341.005 [165526], LA0309AM831341.006 [165527], LA0309AM831341.007 [165528], and LA0310AM831341.001 [165865]. The sorption and desorption experiments together provide information on the equilibration rates of the forward and backward sorption reactions. For elements that sorb primarily through surface complexation reactions, the experimental data are augmented with the results of modeling calculations using PHREEQC V2.3 (BSC 2001 [155323]). The inputs for the modeling calculations include groundwater compositions, surface areas, binding constants for the elements of interest, and thermodynamic data for solution species. These modeling calculations provide a basis for interpolation and extrapolation of the experimentally derived sorption coefficient dataset. The effects of nonlinear sorption are approximated by capturing the effective K_d range (BSC 2003 [163228], Section I.8).

The effects of organics on sorption were also investigated by Triay et al. (1997 [100422], Section IV.B). Their experiments tested the effects of organic materials (DOPA (dihydroxyphenylalanine) and NAFA (Nordic Aquatic Fulvic Acid)) on the sorption of Pu and Np on tuff materials. The results of these tests showed very little effect of the organic materials for sorption of these radionuclides in tuffs. The effects of complexation with respect to sorption coefficients are provided in terms of probability distributions for the sorption coefficient of each

element of interest among the three major rock types (devitrified, zeolitic, and vitric) found in the UZ. The influence of expected variations in water chemistry, radionuclide concentrations, and variations in rock surface properties within one of the major rock types are incorporated into these probability distributions. These distributions are specified for each radionuclide/rock type combination (BSC 2003 [163228], Section I.8) and are sampled in the TSPA-LA to account for the effects of natural variations in pore water chemistry and mineral surfaces on sorption. Correlations for sampling sorption coefficient probability distributions have been derived for the elements investigated (BSC 2003 [163228], Section II). To derive the correlations, a rating system was first developed to rate the impact of six different variables on the sorption coefficient for a given element in each of the three major rock types. The six variables are pH, Eh, water chemistry, rock composition, rock surface area, and radionuclide concentration. Water chemistry refers to the major ion concentrations and silica. Rock composition refers to both the mineralogic composition of the rocks and the chemical composition of the minerals (e.g., zeolite compositions). The output DTNs from BSC (2003 [163228]) for the sorption K_ds and correlations are LA0302AM831341.002 [162575] and LA0311AM831341.001 [167015].

Supporting Reports: BSC 2003 [163228].

6.1.32 Matrix Diffusion in the UZ (2.2.08.08.0B)

FEP Description: Matrix diffusion is the process by which radionuclides and other species transported in the UZ by advective flow in fractures or other pathways move into the matrix of the porous rock by diffusion. This includes osmotic process in response to chemical gradients. Matrix diffusion can be a very efficient retarding mechanism, especially for strongly sorbed radionuclides due to the increase in rock surface accessible to sorption.

Descriptor Phrase: Matrix diffusion in the UZ, Osmosis of dissolved radionuclides in the UZ

Screening Decision: Included

Screening Argument: None

TSPA Disposition: Migration of radionuclides from fast flow fracture into surrounding slow flow matrix blocks by diffusion could play an important role in delaying the transport process of radionuclides in fractures. The role of matrix diffusion is included through the development of the particle tracking approach as described in BSC (2004 [162730], Section 6.4.3). Transfer function curves (DTN: LA0311BR831229.001 [166924]) generated are a direct feed to TSPA-LA and will be used by FEHM in simulating the effect of matrix diffusion on radionuclide transport in TSPA-LA runs as described in BSC (2004 [162730], Section 6.4.3 and Attachment III). This particle tracking approach was used to simulate matrix diffusion of dissolved radionuclides. This treatment of matrix diffusion includes the effects of partial saturation of the matrix, radionuclide sorption in the matrix, and finite spacing of fractures. Osmosis would tend to cause water from fractures to flow into the matrix, if the matrix presents a suitable barrier to the migration of dissolved salts. Matrix diffusion of colloids was assumed not to occur because its effects would be small and would only retard transport (BSC 2004 [162730], Section 6.5.5). One important factor affecting the strength of matrix diffusion is matrix diffusion coefficient. Matrix diffusion coefficient is related to matrix water content and matrix effective permeability

through the relationship developed by Reimus et al. (2002 [163008]). The distributions of matrix water content and matrix effective permeability are an output of (BSC 2004 [162730], Section 6.5.5; DTN: LA0311BR831371.003 [166515]) and are used by TSPA-LA in multiple realization runs for randomly generating matrix diffusion coefficients.

Supporting Reports: BSC 2004 [162730], BSC 2003 [163228], BSC 2004 [167959].

6.1.33 Sorption in the UZ (2.2.08.09.0B)

FEP Description: Sorption of dissolved and colloidal radionuclides in the UZ can occur on the surfaces of both fractures and matrix in rock or soil along the transport path. Sorption may be reversible or irreversible, and it may occur as a linear or nonlinear process. Sorption kinetics and the availability of sites for sorption should be considered. Sorption is a function of the radioelement type, mineral type, and groundwater composition.

Descriptor Phrases: Sorption of dissolved radionuclides in the UZ, Sorption of colloids in the UZ

Screening Decision: Included

Screening Argument: None

TSPA Disposition: Sorption is included in the TSPA-LA model for mountain-scale unsaturated zone radionuclide transport as a linear equilibrium sorption (K_d) model (BSC 2003 [163228], Attachment I). Sorption is only accounted for in the matrix continuum; there is no sorption modeled in the fracture continuum. Sorption characteristics of the rock minerals are assumed to be static in time. Sorption K_ds have been derived for the elements Am, Cs, Np, Pa, Pu, Ra, Sr, Th, and U as dissolved radionuclides. Other dissolved radionuclide elements treated by TSPA-LA (e.g. Tc) are modeled as non-sorbing.

The sorption coefficient data on which the distributions are based are obtained in laboratory experiments in which crushed rock samples from the Yucca Mountain site are contacted with groundwaters (or simulated groundwaters) representative of the site, spiked with one or more of the elements of interest (BSC 2003 [163228], Section I.5). Sorption experiments have been carried out as a function of time, element concentration, atmospheric composition, particle size, and temperature. In some cases, the solids remaining from sorption experiments were contacted with unspiked groundwater in desorption experiments. The experimental data used to determine the sorption K_ds are provided in the following DTNs: LA0305AM831341.001 [163789], LA0309AM83341.002 [165523], LA0309AM83341.003 [165524], LA0309AM83341.004 [165525], LA0309AM83341.005 [165526], LA0309AM83341.006 [165527], LA0309AM83341.007 [165528], and LA0310AM831341.001 [165865]. The sorption and desorption experiments together provide information on the equilibration rates of the forward and backward sorption reactions. For elements that sorb primarily through surface complexation reactions, the experimental data are augmented with the results of modeling calculations using PHREEQC V2.3 (BSC 2001 [155323]). The inputs for the modeling calculations include groundwater compositions, surface areas, binding constants for the elements of interest, and thermodynamic data for solution species. These modeling calculations provide a basis for interpolation and extrapolation of the experimentally derived sorption coefficient dataset. The

effects of nonlinear sorption are approximated by capturing the effective K_d range (BSC 2003 [163228], Section I.8).

Sorption coefficients are provided in terms of probability distributions for the sorption coefficient of each element of interest among the three major rock types (devitrified, zeolitic, and vitric) found in the UZ. The influence of expected variations in water chemistry, radionuclide concentrations, and variations in rock surface properties within one of the major rock types are incorporated into these probability distributions. These distributions are specified for each radionuclide/rock type combination (BSC 2003 [163228], Section I.8) and are sampled in the TSPA-LA to account for the effects of natural variations in pore water chemistry and mineral surfaces on sorption. Correlations for sampling sorption coefficient probability distributions have been derived for the elements investigated (BSC 2003 [163228], Section II). To derive the correlations, a rating system was first developed to rate the impact of six different variables on the sorption coefficient for a given element in each of the three major rock types. The six variables are pH, Eh, water chemistry, rock composition, rock surface area, and radionuclide concentration. Water chemistry refers to the major ion concentrations and silica. Rock composition refers to both the mineralogic composition of the rocks and the chemical composition of the minerals (e.g., zeolite compositions). The output DTNs for the sorption K_ds and correlations are LA0302AM831341.002 [162575] and LA0311AM831341.001 [167015].

Sorption in the UZ is treated as a linear process in the radionuclide transport abstraction model (BSC 2004 [162730], Section 5, assumption 4). In the matrix, sorption is incorporated in the generation of transfer function curves and expressed as part of the defined dimensionless parameters (BSC 2004 [162730], Section 6.4.3). For colloid facilitated radionuclide transport, radionuclide sorption onto colloids and its effect on transport is simulated through the colloid K_c factor (BSC 2004 [162730], Section 6.4.5). The K_c factor is the product of the radionuclide sorption coefficient onto colloids and the colloid concentration (BSC 2004 [162730], Section 6.5.12). Radionuclide sorption coefficients used in the simulation of radionuclide transport in UZ are documented in BSC (2004 [162730], Section 6.5.4; DTN: LA0302AM831341.002 [162575]). Colloid concentration and radionuclide sorption coefficients onto colloids are documented in BSC (2004 [162730], Section 6.5.12; DTNs: SN0306T0504103.005 [164132] and SN0306T0504103.006 [164131]). In TSPA-LA runs, sorption coefficients are sampled and fed into FEHM. Sorption onto fracture surfaces is neglected because of few data available in supporting such a retardation mechanism in the UZ. Thus, a fracture surface retardation factor of 1 is set for use in TSPA-LA runs (BSC 2004 [162730], Section 6.5.8; DTN: LA0311BR831371.003 [166515]).

Supporting Reports: BSC 2003 [163228], BSC 2004 [162730], BSC 2004 [167959].

6.1.34 Colloidal Transport in the UZ (2.2.08.10.0B)

FEP Description: Radionuclides may be transported in groundwater in the UZ as colloidal species. Types of colloids include true colloids, pseudo colloids, and microbial colloids.

Descriptor Phrases: Advection of colloids in the UZ, Diffusion of colloids in the UZ, Sorption of colloids in the UZ

Screening Decision: Included

Screening Argument: None

TSPA Disposition: The influence of colloid transport on radionuclide migration through the UZ is implicitly included and discussed in BSC (2004 [162730], Section 6.4.5). However, BSC (2004 [162730]) does not generate a direct data feed. Parameters that can impact colloid transport in the UZ include colloid size (DTN: LL000122051021.116 [142973]), colloid concentration (DTN: SN0306T0504103.005 [164132]), radionuclide sorption coefficient onto colloid (DTN: SN0306T0504103.006 [164131]), and colloid retardation factors (DTN: LA0303HV831352.002 [163558]), and are documented in BSC (2004 [162730], Sections 6.5.9 through 6.5.13). Colloid transport processes include advection and dispersion. Sorption of colloids is addressed in FEP 2.2.08.09.0B. Colloid matrix diffusion was assumed not to occur because its effect would be small and would only retard transport (BSC 2004 [162730], Section 6.5.5). In TSPA-LA runs, colloid facilitated radionuclide transport is investigated through the FEHM colloid transport model and variations of colloid transport parameters.

Supporting Reports: BSC 2004 [162730], BSC 2003 [163228].

6.1.35 Chemistry of Water Flowing into the Drift (2.2.08.12.0A)

FEP Description: Inflowing water chemistry may be used in analysis or modeling that requires initial water chemistry in the drift. Chemistry of water flowing into the drift is affected by initial water chemistry in the rock, mineral and gas composition in the rock, and thermal-hydrological-chemical processes in the rock.

Descriptor Phrase: Inflowing water composition (into drift)

Screening Decision: Included

Screening Argument: None

TSPA Disposition: The THC Seepage Model was designed specifically to investigate the effect of thermal-hydrological-chemical processes in the host rock (BSC 2004 [167974], Section 6.2.1.2), including the effects of initial water chemistry (BSC 2004 [167974], Section 6.2.2.1), and mineral and gas compositions in the rock (BSC 2004 [167974], Section 6.2.2.2). Therefore, these effects are explicitly taken into account in the results of the THC Seepage Model and their abstraction (BSC 2004 [167972], Section 6.2; summary tables of concentrations through time submitted under DTNs: LB0302DSCPTHCS.002 [161976], LB0307DSTTHCR2.002 [165541], and LB0311ABSTHCR2.003 [166713]; and tables of concentrations and summary statistics through time submitted under DTN: LB0311ABSTHCR2.001 [166714]). DTNs: LB0302DSCPTHCS.002 [161976] and LB0311ABSTHCR2.001 [166714] are used to feed and/or provide technical basis for another model (BSC 2004 [167461]) that generates lookup tables that are used in the TSPA-LA Model. Because no water is predicted to actually seep into the modeled drift, the abstraction method was specifically designed to consider waters deemed most representative of potential in-drift seepage (BSC 2004 [167972], Section 6.2.1, Figures 6.2-2 and 6.2-3; DTN: LB0311ABSTHCR2.001 [166714]).

Supporting Reports: BSC 2004 [167972].

6.1.36 Microbial Activity in the UZ (2.2.09.01.0B)

FEP Description: Microbial activity in the UZ may affect radionuclide mobility in rock and soil through colloidal processes, by influencing the availability of complexing agents, or by influencing groundwater chemistry. Changes in microbial activity could be caused by the response of the soil zone to changes in climate.

Descriptor Phrase: Microbial effects on sorption in the UZ

Screening Decision: Included

Screening Argument: None

TSPA Disposition: The effects of microbes on sorption are included in the distributions for sorption coefficients used in TSPA-LA. The sorption coefficient data on which the distributions are based are obtained in laboratory experiments in which crushed rock samples from the Yucca Mountain site are contacted with groundwaters (or simulated groundwaters) representative of the site, spiked with one or more of the elements of interest (BSC 2003 [163228], Section I.5). The basic technique for the laboratory determination of sorption coefficients involved the contact of a groundwater sample, spiked with the radionuclide of interest, with a crushed sample of tuff or alluvium. The rock sample was generally obtained as a core sample. The rock and water samples were not sterilized and therefore contain representative microbial biota from the UZ. Sorption experiments have been carried out as a function of time, element concentration, atmospheric composition, particle size, and temperature. In some cases, the solids remaining from sorption experiments were contacted with unspiked groundwater in desorption experiments. The experimental data used to determine the sorption K_ds are provided in the following DTNs: LA0305AM831341.001 [163789], LA0309AM831341.002 [165523], LA0309AM831341.003 [165524], LA0309AM831341.004 [165525], LA0309AM831341.005 [165526], LA0309AM831341.006 [165527], LA0309AM831341.007 [165528], and LA0310AM831341.001 [165865]. The sorption and desorption experiments together provide information on the equilibration rates of the forward and backward sorption reactions. For elements that sorb primarily through surface complexation reactions, the experimental data are augmented with the results of modeling calculations using PHREEQC V2.3 (BSC 2001 [155323]). The inputs for the modeling calculations include groundwater compositions, surface areas, binding constants for the elements of interest, and thermodynamic data for solution species. These modeling calculations provide a basis for interpolation and extrapolation of the experimentally derived sorption coefficient dataset. The effects of nonlinear sorption are approximated by capturing the effective K_d range (BSC 2003 [163228], Section I.8). The effects of microbial activity with respect to sorption coefficients are provided in terms of probability distributions for the sorption coefficient of each element of interest among the three major rock types (devitrified, zeolitic, and vitric) found in the UZ. The influence of expected variations in water chemistry, radionuclide concentrations, and variations in rock surface properties within one of the major rock types are incorporated into these probability distributions. These distributions are specified for each radionuclide/rock type combination (BSC 2003 [163228], Section I.8) and are sampled in the TSPA-LA to account for the effects of natural variations in

pore water chemistry and mineral surfaces on sorption. Correlations for sampling sorption coefficient probability distributions have been derived for the elements BSC 2003 [163228], Section II). To derive the correlations, a rating system was first developed to rate the impact of six different variables on the sorption coefficient for a given element in each of the three major rock types. The six variables are pH, Eh, water chemistry, rock composition, rock surface area, and radionuclide concentration. Water chemistry refers to the major ion concentrations and silica. Rock composition refers to both the mineralogic composition of the rocks and the chemical composition of the minerals (e.g., zeolite compositions). The output DTNs for the sorption K_ds and correlations are LA0302AM831341.002 [162575] and LA0311AM831341.001 [167015].

Supporting Reports: BSC 2003 [163228].

6.1.37 Natural Geothermal Effects on Flow in the UZ (2.2.10.03.0B)

FEP Description: The existing geothermal gradient, and spatial or temporal variability in that gradient, may affect groundwater flow in the UZ.

Descriptor Phrase: Natural geothermal effects on flow in the UZ

Screening Decision: Included

Screening Argument: None

TSPA Disposition: Natural geothermal effects are included in the models of thermal-hydrological processes used to describe the effects of waste heat in the repository (BSC 2003 [163056], Sections 6.3.3, 6.4.3, 6.5.3) The thermal-hydrological models contain the natural geothermal gradient in its initialization. This gradient is primarily determined by the ground surface temperature, the water table temperature, water flux through the UZ, and the thermal conductivity from layer to layer.

The natural geothermal gradient at Yucca Mountain is explicitly included in starting conditions of the THC Seepage Model by setting the ground surface temperature (top model boundary) and the temperature at the water table (bottom boundary) to measured values (BSC 2004 [167974], Section 6.8.2). The effect of this temperature gradient on flow is explicitly accounted for by the coupled heat/flow transport algorithms implemented into the THC simulator (TOUGHREACT V3.0 LBNL 2002 [161256]). Therefore, this effect is explicitly taken into account in the results of the THC Seepage Model and their abstraction (BSC 2004 [167972], Section 6.2; summary tables of concentrations through time submitted under DTNs: LB0302DSCPTHCS.002 [161976], LB0307DSTTHCR2.002 [165541], and LB0311ABSTHCR2.003 [166713]; and tables of concentrations and summary statistics through time submitted under DTN: LB0311ABSTHCR2.001 [166714]). DTNs: LB0302DSCPTHCS.002 [161976] and LB0311ABSTHCR2.001 [166714] are used to feed and/or provide technical basis for another model (BSC 2004 [167461]) that generates lookup tables that are used in the TSPA-LA Model.

Natural geothermal effects on unsaturated flow in the absence of repository thermal effects have been investigated in the models of natural thermal processes in the UZ (BSC 2004 [166883], Section 6.3). The natural temperature gradient is determined by the ground surface temperature,

the water table temperature, and the thermal conductivity from layer to layer. The results of these models have found that the effects of the natural temperature gradient on UZ flow are insignificant.

Supporting Reports: BSC 2004 [167972], BSC 2004 [166883]

6.1.38 Two-Phase Buoyant Flow/Heat Pipes (2.2.10.10.0A)

FEP Description: Heat from waste generates two-phase buoyant flow. The vapor phase (water vapor) escapes from the mountain. A heat pipe consists of a system for transferring energy between a hot and a cold region (source and sink respectively) using the heat of vaporization and movement of the vapor as the transfer mechanism. Two-phase circulation continues until the heat source is too weak to provide the thermal gradients required to drive it. Alteration of the rock adjacent to the drift may include dissolution, which maintains the permeability necessary to support the circulation (as inferred for some geothermal systems).

Descriptor Phrases: Two-phase flow in the UZ, Thermally-driven flow (heat pipes, convection) in the UZ

Screening Decision: Included

Screening Argument: None

TSPA Disposition: The coupled processes causing heat-pipe behavior (BSC 2004 [167970], Section 6.3.2) are explicitly simulated with the TH Seepage Model (BSC 2003 [166512]) that feeds into the seepage abstraction. Using this model, the impact of heat-pipe behavior on seepage is assessed for various simulation cases (BSC 2004 [167970], Section 6.4.3.3). Thus, the TH modeling results from DTN: LB0301DSCPTHSM.002 [163689] inherently include the effect of heat pipes. As discussed in BSC (2004 [167970], Section 6.5.2.1), the abstraction of thermal seepage utilizes these modeling results to develop an appropriate thermal-seepage abstraction methodology.

The coupled processes causing heat-pipe behavior are explicitly simulated with the THC Seepage Model (BSC 2004 [167974], Section 6.2.1.1). The continuous boiling and refluxing of water in this zone affects water-rock interactions (BSC 2004 [167974], Section 6.2.1.2). The resulting water chemistry in the heat pipe is captured by the HISAT waters (BSC 2004 [167972], Section 6.2.4.1.1) (see also BSC 2004 [167974], Section 6.8.5.3.2). Therefore, the effect of heat pipes on predicted water and gas chemistries is explicitly taken into account in the results of the THC Seepage Model and their abstraction (BSC 2004 [167972], Section 6.2; summary tables of concentrations through time submitted under DTNs: LB0302DSCPTHCS.002 [161976], LB0307DSTTHCR2.002 [165541], and LB0311ABSTHCR2.003 [166713]; and tables of concentrations and summary statistics through time submitted under DTN: LB0311ABSTHCR2.001 [166714]). DTNs: LB0302DSCPTHCS.002 [161976] and LB0311ABSTHCR2.001 [166714] are used to feed and/or provide technical basis for another model (BSC 2004 [167461]) that generates lookup tables that are used in the TSPA-LA Model.

Supporting Reports: BSC 2004 [167970], BSC 2004 [167972].

6.1.39 Geosphere Dry-Out due to Waste Heat (2.2.10.12.0A)

FEP Description: Repository heat evaporates water from the UZ rocks near the drifts as the temperature exceeds the vaporization temperature. This zone of reduced water content (reduced saturation) migrates outward during the heating phase (about the first 1000 years) and then migrates back to the containers as heat diffuses throughout the mountain and the radioactive sources decay. This FEP addresses the effects of dry-out within the rocks.

Descriptor Phrase: Saturation decrease in near-field

Screening Decision: Included

Screening Argument: None

TSPA Disposition: The coupled processes of vaporization, dryout, and resaturation are explicitly simulated with the TH Seepage Model (BSC 2003 [166512]) that feeds into the seepage abstraction. Using this model, the impact of such coupled processes on seepage is assessed for various simulation cases (BSC 2004 [167970], Section 6.4.3.3). Thus, the TH modeling results from DTN: LB0301DSCPTHSM.002 [163689] inherently include these effects. As discussed in BSC (2004 [167970], Section 6.5.2.1), the abstraction of thermal seepage utilizes these modeling results to develop an appropriate thermal-seepage abstraction methodology.

The coupled processes of vaporization, dryout, and resaturation are explicitly simulated with the THC Seepage Model, including the formation of a dry (or nearly dry) zone around drifts, expanding and then receding through time following the pulse of heat released from the waste packages (BSC 2004 [167974], Sections 6.2.1 and 6.8.5.2). Therefore, these effects are explicitly taken into account in the results of the THC Seepage Model and their abstraction (BSC 2004 [167972], Section 6.2; summary tables of concentrations through time submitted under DTNs: LB0302DSCPTHCS.002 [161976], LB0307DSTTHCR2.002 [165541], and LB0311ABSTHCR2.003 [166713]; and tables of concentrations and summary statistics through time submitted under DTN: LB0311ABSTHCR2.001 [166714]). DTNs: LB0302DSCPTHCS.002 [161976] and LB0311ABSTHCR2.001 [166714] are used to feed and/or provide technical basis for another model (BSC 2004 [167461]) that generates lookup tables that are used in the TSPA-LA Model.

The effects of dryout on surface infiltration are discussed in Section 6.8.9 (FEP 2.2.10.01.0A).

Supporting Reports: BSC 2004 [167970], BSC 2004 [167972].

6.1.40 Topography and Morphology (2.3.01.00.0A)

FEP Description: This FEP is related to the topography and surface morphology of the disposal region. Topographical features include outcrops and hills, water-filled depressions, wetlands, recharge areas, and discharge areas. Topography, precipitation, and surficial permeability distribution in the system will determine the flow boundary conditions, i.e. location and amount of recharge and discharge in the system.

Descriptor Phrase: Topography (effects on infiltration)

Screening Decision: Included

Screening Argument: None

TSPA Disposition: Topographical features, precipitation, and surficial permeability distribution are incorporated into the INFIL V2.0 (USGS 2001 [139422]; USGS 2003 [166518]) model, while precipitation and surficial permeability distribution are also incorporated into the uncertainty analysis (BSC 2003 [165991]). Topographical features are captured in the INFIL V2.0 (USGS 2001 [139422]; USGS 2003 [166518]) model using data from the Digital Elevation Model (DEM). The impacts of topography and morphology on preferential flow/percolation in the UZ is incorporated into the TSPA-LA through the UZ flow fields that use the infiltration model results (DTN: GS000308311221.005 [147613]) as upper boundary conditions BSC (2004 [166883], Section 6.1.4). The incorporation of UZ flow fields into the TSPA-LA is described in BSC (2004 [166883], Section 6.2.5).

The effects of rock properties are also included in the treatment of infiltration uncertainty for TSPA-LA (BSC 2003 [165991]). Infiltration uncertainty is represented through three discrete infiltration scenarios (lower, mean, and upper), which are sampled in TSPA-LA according to weighting factors BSC (2003 [165991], Section 7.1). Precipitation and the surficial permeability distributions are captured in the uncertainty analysis using the precipitation multiplier (PRECIPM), the soil permeability multiplier (SOILPERM), and the effective bedrock permeability multiplier (BRPERM). They are incorporated implicitly by inclusion of uncertainty in the precipitation multiplier, soil permeability multiplier, and effective bedrock permeability multiplier in the calculation of the weighting factors, which are passed to TSPA-LA (BSC 2003 [165991], DTN: SN0308T0503100.008 [165640]).

Supporting Reports: BSC 2003 [165991].

6.1.41 Precipitation (2.3.11.01.0A)

FEP Description: Precipitation is an important control on the amount of recharge. It transports solutes with it as it flows downward through the subsurface or escapes as runoff. Precipitation influences agricultural practices of the receptor. The amount of precipitation depends on climate.

Descriptor Phrases: Precipitation (effects on infiltration)

Screening Decision: Included

Screening Argument: None

TSPA Disposition: Precipitation affects the net infiltration, as discussed in *Simulation of Net Infiltration for Modern and Potential Future Climates* (USGS 2003 [166518]). The net infiltration map outputs (DTN: GS000308311221.005 [147613]) are used as a boundary condition for the UZ Flow Model (BSC 2004 [166883], Sections 6.1.3 and 6.1.4). Flow fields developed for use in TSPA-LA (DTN: LB0305TSPA18FF.001 [165625]) using the UZ Flow Model therefore include the effects of precipitation and changes of precipitation under future climate conditions, including low, mean, and upper bounds of infiltrations in glacial, monsoon, and present-day (or modern) climatic scenarios.

The effects of precipitation are also included in the treatment of infiltration uncertainty for TSPA-LA (BSC 2003 [165991]). Infiltration uncertainty is represented through three discrete infiltration scenarios (lower, mean, and upper), which are sampled in TSPA-LA according to weighting factors BSC (2003 [165991], Section 7.1). Precipitation is incorporated in the infiltration uncertainty analysis through the precipitation-rate multiplier (PRECIPM) (BSC 2003 [165991], Table 6-3 and Section 6.1.2). The precipitation-rate multiplier operates on the precipitation rate, as prescribed in the input file TULELAKE.INP, which contains the precipitation record for the selected "mean glacial transition-climate" analog site, within the infiltration model software, INFIL VA_2.a1 (SNL 2001 [147608]) (and also INFIL V2.0; USGS 2001 [139422]).

Supporting Reports: BSC 2003 [165991], BSC 2004 [166883].

6.1.42 Surface Runoff and Flooding (2.3.11.02.0A)

FEP Description: Surface runoff and evapotranspiration are components in the water balance, together with precipitation and infiltration. Surface runoff produces erosion, and can feed washes, arroyos, and impoundments, where flooding may lead to increased recharge.

Descriptor Phrase: Runoff (effects on infiltration)

Screening Decision: Included

Screening Argument: None

TSPA Disposition: Evapotranspiration and surface runoff affect the net infiltration, as discussed in *Simulation of Net Infiltration for Modern and Potential Future Climates* (USGS 2003 [166518]). The net infiltration map outputs (DTN: GS000308311221.005 [147613]) are used as a boundary condition for the UZ Flow Model (BSC 2004 [166883], Sections 6.1.3 and 6.1.4). Flow fields developed for use in TSPA-LA (DTN: LB0305TSPA18FF.001 [165625]) using the UZ Flow Model therefore include the effects of precipitation and changes of precipitation under future climate conditions, including low, mean, and upper bounds of infiltrations in glacial, monsoon, and present-day (or modern) climatic scenarios.

The effects of evapotranspiration are included in the treatment of infiltration uncertainty for TSPA-LA (BSC 2003 [165991]). Infiltration uncertainty is represented through three discrete infiltration scenarios (lower, mean, and upper), which are sampled in TSPA-LA according to weighting factors BSC (2003 [165991], Section 7.1). Evapotranspiration is incorporated in the infiltration uncertainty analysis through the two evapotranspiration coefficient-rate multipliers (BSC 2003 [165991], Table 6-3 and Section 6.1.2.). The evapotranspiration-rate multiplier operates on the evapotranspiration rate, as calculated within the infiltration model software, INFIL VA_2.a1 (SNL 2001 [147608]) (and also INFIL V2.0; USGS 2001 [139422]). Surface runoff is incorporated through the inclusion of a parameter that defines the fraction of each grid cell in the infiltration model that is affected by overland flow and channel flow during the routing of runoff (FLAREA). It is incorporated implicitly by inclusion of uncertainty in the fraction of each grid cell in the infiltration model that is affected by overland flow and channel flow during the routing of runoff (FLAREA) in the calculation of the weighting factors which are passed to TSPA-LA (BSC 2003 [165991]; DTN: SN0308T0503100.008 [165640]).

Supporting Reports: BSC 2003 [165991].

6.1.43 Infiltration and Recharge (2.3.11.03.0A)

FEP Description: Infiltration into the subsurface provides a boundary condition for groundwater flow. The amount and location of the infiltration influences the hydraulic gradient and the height of the water table. Different sources of recharge water could change the composition of groundwater passing through the repository. Mixing of these waters with other groundwaters could result in precipitation, dissolution, and altered chemical gradients.

Descriptor Phrases: Infiltration water composition, Climate (effects on infiltration), Time-dependent infiltration, Flow/percolation in the UZ

Screening Decision: Included

Screening Argument: None

TSPA Disposition: The hydrological effects of infiltration and recharge are included in the infiltration model (see Section 6.1.4, FEP 1.3.01.00.0A). This model includes the effects of seasonal and climate variations, climate change, surface-water runoff, and site topology such as hillslopes and washes (USGS 2003 [166518], Sections 6.4 and 6.5). The time dependence of infiltration results is linked to the timing of climate change as discussed in Section 6.1.4; FEP 1.3.01.00.0A. This is incorporated into the TSPA-LA through the UZ flow fields that use the infiltration model results (DTN: GS000308311221.005 [147613]) as upper boundary conditions BSC (2004 [166883], Section 6.1.4). Flow fields for TSPA-LA are in DTN: LB0305TSPA18FF.001 [165625]. The effects caused by the present-day water composition infiltrating from the ground surface are accounted for in the analysis of seepage-water chemistry by using the measured pore-water chemistry in the UZ (BSC 2004 [167974], Table 6.2-1).

Infiltration uncertainty, as it applies to the determination of weighting factors used in TSPA-LA (BSC 2003 [165991]; DTN: SN0308T0503100.008 [165640]), is documented in BSC 2003 [165991]. The way it is handled is summarized in BSC (2003 [165991], Section 1.1, paragraph 3). "TSPA-LA License Application (LA) has included three distinct climate regimes in the comprehensive repository performance analysis for Yucca Mountain: present-day, monsoon, and glacial transition. Each climate regime was characterized using three infiltration-rate maps, including a lower- and upper-bound and a mean value (equal to the average of the two boundary values). For each of these maps, which were obtained based on analog site climate data, a spatially averaged value was also calculated by the USGS. For a more detailed discussion of these infiltration-rate maps, see *Simulation of Net Infiltration for Modern and Potential Future Climates* (USGS 2003 [166518]). For this Scientific Analysis report, spatially averaged values were calculated for the lower-bound, mean, and upper-bound climate analogs only for the glacial transition climate regime, within the simulated multi-rectangular region approximating the repository footprint, shown in BSC (2003 [165991], Figure 1-1)".

Supporting Reports: BSC 2003 [165991], BSC 2004 [166883].

6.1.44 Radioactive Decay and Ingrowth (3.1.01.01.0A)

FEP Description: Radioactivity is the spontaneous disintegration of an unstable atomic nucleus that results in the emission of subatomic particles. Radioactive isotopes are known as radionuclides. Radioactive decay of the fuel in the repository changes the radionuclide content in the fuel with time and generates heat. Radionuclide quantities in the system at any time are the result of the radioactive decay and the growth of daughter products as a consequence of that decay (i.e., ingrowth). Over a 10,000-year performance period, these processes will produce daughter products that need to be considered in order to adequately evaluate the release and transport of radionuclides to the accessible environment.

Descriptor Phrases: Radioactive decay and ingrowth (in the UZ)

Screening Decision: Included

Screening Argument: None

TSPA Disposition: Decay and ingrowth are implicitly included through the development of an effective integration algorithm (BSC 2004 [162730], Section 6.4.4). This algorithm can handle multiple species decay and ingrowth processes. Radionuclide half lives and daughter products considered in the UZ transport abstraction model are documented in BSC (2004 [162730], Section 6.5.14). In TSPA-LA runs, 36 species of radionuclides are simulated through the UZ using the FEHM (V2.21; LANL 2003 [165741]) decay/ingrowth model over a specified time period as described in the above mentioned sections of BSC (2004 [162730]). However, BSC (2004 [162730]) does not generate a direct data feed. The output of the UZ radionuclide transport model is a boundary condition for the SZ radionuclide transport model, which accounts for decay and ingrowth during radionuclide transport as described in BSC (2003 [164870], Section 6.3).

Supporting Reports: BSC 2004 [162730], BSC [163228].

6.2 BOREHOLES AND REPOSITORY SEALS

These FEPs concern the effects of boreholes and repository drifts as pathways for fluid and radionuclide migration. The implicit treatment of boreholes in the TSPA-LA is that boreholes are sealed so that the borehole region is indistinguishable from the natural rock in terms of fluid flow and radionuclide transport. Although boreholes will be sealed, the specific properties of the seals and their evolution over time are not accounted for in the flow and transport modeling. Similarly, repository drifts will be assumed to be sealed such that liquids or gases cannot migrate between emplacement drifts (other than through geosphere pathways). Arguments are presented here to demonstrate that the potential effects of borehole or repository-seal leakage have a negligible effect on the potential performance of the repository. Therefore, these FEPs are excluded from the TSPA-LA calculation, based on low consequence.

Table 6-4 gives the FEP numbers and names categorized under boreholes and repository seals.

Table 6-4. Excluded FEPs: Repository and Borehole Seals

Section Number	FEP Number	FEP Name
6.2.1	1.1.01.01.0A	Open site investigation boreholes
6.2.2	1.1.01.01.0B	Influx through holes drilled in drift wall or crown
6.2.3	1.1.02.01.0A	Site flooding (during construction and operation)
6.2.4	1.1.04.01.0A	Incomplete closure
6.2.5	1.1.11.00.0A	Monitoring of repository
6.2.6	2.1.05.01.0A	Flow through seals (access ramps and ventilation shafts)
6.2.7	2.1.05.02.0A	Radionuclide transport through seals
6.2.8	2.1.05.03.0A	Degradation of seals

Source: LA FEP List (DTN: MO0307SEPFEPS4.000 [164527])

6.2.1 Open Site Investigation Boreholes (1.1.01.01.0A)

FEP Description: Site investigation boreholes that have been left open, degraded, improperly sealed, or reopened for some reason, could modify flow and transport properties and produce enhanced pathways between the surface and the repository.

Descriptor Phrases: Open boreholes (effects on flow/percolation in the UZ), Open boreholes (preferential pathway to/from surface)

Screening Decision: Excluded – Low Consequence

Screening Argument: The implicit treatment of boreholes in the TSPA-LA is that boreholes are sealed so that the borehole region is indistinguishable from the natural rock in terms of fluid flow and radionuclide transport. Although boreholes will be sealed, the specific properties of the seals and their evolution over time are not accounted for in the flow and transport modeling. Similarly, repository drifts will be assumed to be sealed such that liquids or gases cannot migrate between emplacement drifts (other than through geosphere pathways).

The consequence of site-investigation boreholes depends on several factors, such as location and depth of the boreholes. The following arguments demonstrate that, based on a number of factors and considerations, the existing test boreholes will not have a significant impact on either radionuclide transport or the performance of the repository.

Table 6-5. Deep Boreholes in or Close to the Repository Block

Borehole Identifier	Elevation (feet)	Lowest Stratigraphic Contact Depth (feet)[16] (except as noted)	Tptpv3‡ Depth (feet)[16] (except as noted)	Nominal Borehole Diameter (inches)†	Easting (feet)	Northing (feet)
UE-25 WT #18**	4384	1620	1501	8.75[1]	564854	771167
USW G-1*	4350	3558	1287	3.875[2]	561001	770502
USW G-4**	4166	2950	1317	12.25[3]	563082	765808
USW H-1*	4274	3661	1410	13.25[4]	562388	770255
USW H-5*	4851	3422	1582	14.75[5]	558908	766634
USW NRG-7a**	4207	1498	1415	5.5[6]	562984	768880
USW SD-7*	4472	2612	1182	8.75[7]	561240	758950
USW SD-9*	4273	2016	1358	8.5[8]	561818	767998
USW SD-12*	4343	2138	1278	12.25[9]	561606	761957
USW UZ-1*	4425	1145	979[17]	17.5[10]	560222	771277
USW UZ-6**	4925	1829	1333	17.5[11]	558325	759730
USW UZ-7a**	4228	759[18]	629[17]	12.25[12]	562270	760693
USW UZ-14*	4425	2072	1279	12.25[13]	560142	771310
USW WT-2**	4268	1794	1179	8.75[14]	561924	760662
USW SD-6**	4905[20]	2506[19]	1456[19]	12.25[15]	558608[20]	762421[20]

NOTE: DTN: MO9906GPS98410.000 [109059] except where other source noted; easting, northing, and elevation values have been rounded to the nearest foot. *In repository block; ** lose to repository block; †based on drill bit size used to create borehole in the repository host rock; ‡Top contact of Tptpv3, or lower contact of Tptpln (BSC 2003 [160109], page 46). Tptpln is the lowest stratigraphic unit identified for waste emplacement (see BSC (2004 [168370])); [1]Fenix & Scisson (1986 [101238], p. 63); [2]Fenix & Scisson (1987 [103102], p. 3); [3]Fenix & Scisson (1987 [103102], p. 109); [4]Fenix & Scisson (1987 [126415], p. 3); [5]Fenix & Scisson (1987 [126415], p. 51); [6]DTN: TMUSWNRG7A0096.002 ([166424], Attachment VII); [7]CRWMS M&O (1996 [129957], p. 13); [8]CRWMS M&O (1996 [114799], p. 11); [9]DTN: TM000000SD12RS.012 ([105627], p. 9); [10]Fenix & Scisson (1987 [165939], p. 3); [11]Fenix & Scisson (1987 [165939], p. 35); [12]CRWMS M&O (1996 [130425], p. 2); [13]CRWMS M&O (1996 [130429], p. 9); [14]Fenix & Scisson (1986 [101238], p. 75); [15]YMP (1999 [166080], Attachment 8).[16]DTN: MO0004QGFMPICK.000 [152554], note that borehole UE-25 WT#18 is designated as USW WT#18 in this DTN; [17]nearest repository waste emplacement depth, also uses information from BSC (2004 [164519]) and 800-IED-WIS0-00104-000-00Ab (BSC 2003 [168180]); [18]maximum depth of borehole data, DTN: MO0010CPORGLOG.003 [155959]; [19]DTN: SNF40060298001.001 [107372]; [20]DTN: MO9912GSC99492.000 [165922].

Only boreholes within or close to the repository block are important to the performance of the UZ. Boreholes well outside the footprint of the repository block will not influence water movement to the waste emplacement drifts or radionuclide transport from the waste emplacement drifts to the water table. Table 6-5 lists 8 deep boreholes in the repository block and 7 deep boreholes near the repository block. The definition for deep borehole in the repository block is a borehole that penetrates the TSw. The definition for deep borehole near the repository block is a borehole that penetrates below the elevation of waste emplacement. (DTNs: MO9906GPS98410.000 [109059]; MO0004QGFMPICK.000 [152554]; BSC 2003 [161727]). Boreholes that terminate in or above the PTn will have a negligible effect on percolation flux at the repository because flow through these boreholes will tend to be

homogenized by matrix flow in the underlying Paintbrush nonwelded hydrogeologic unit (CRWMS M&O 1998 [100356], Section 2.4.2.8; Wu et al. 2000 [154918], Section 4.1). The locations of the boreholes listed in Table 6-5 relative to waste emplacement locations are shown in BSC (2003 [168180]).

Many of the boreholes penetrate the UZ entirely and terminate at or below the water table. Based on the design layout (BSC 2003 [161727]) and borehole locations in Table 6-5, none of the existing boreholes will intersect with a waste emplacement drift. Therefore, water entering these boreholes would continue to flow through these boreholes to the water table, bypassing waste emplacement locations. One of the deep boreholes within the waste emplacement footprint, USW UZ-1, only partially penetrates the UZ. USW UZ-1 has a total depth of 1,270 feet but terminates near the TSw vitrophyre beneath waste emplacement locations. Therefore, none of the deep boreholes in the repository block terminates above potential waste emplacement locations. In the event that a drift unexpectedly encounters a borehole during repository construction, such boreholes will either be sealed and/or waste packages will have a stand-off distance from the location of the borehole penetration into the waste emplacement drift.

The other aspect of this problem is the movement of dissolved radionuclides and radionuclides associated with mobile colloids between the repository and the water table. Fractures and faults represent continuous rapid-transport pathways from the repository to the water table. Any significant lateral flow beneath the repository eventually finds one of these high-permeability pathways to the water table. The principle difference between these high-permeability pathways and boreholes is that the cross-sectional area of the boreholes available to intercept lateral flow is much smaller than the area associated with fractures and faults. The 15 boreholes in Table 6-5 with depths greater than 1000 ft present a total cross-sectional area per unit depth that may be calculated by the product of the borehole diameter times the number of boreholes. The average borehole size may be bounded by a value of 1 m (see Table 6-5), given that borehole diameters can exceed the size of the drill bit. This gives a borehole area per unit depth of 15 m^2/m. The fractured rock between the repository and the water table has a fracture area per unit volume of 0.1 m^{-1} or more (BSC 2003 [161773], Table 7). Multiplying this by the 5×10^6 m^2 footprint of the repository (BSC 2004 [168370]) gives a minimum fracture area per unit depth of about 5×10^5 m^2/m. Therefore, the contribution of boreholes to the steady state flow and transport pattern between the repository and the water table is negligible. A potential scenario that could lead to greater radionuclide releases is the migration of perched water through the borehole pathways if a borehole seal should fail.

A bounding calculation was performed that assessed the potential for radionuclides in the perched water to be suddenly released to the water table (see Appendix A in this Analysis Report for details; also see FEP 2.2.06.03.0A). The calculation considers the volume of perched water contained in the fractures to be available for rapid release. This volume is restricted to fractures with permeability greater than 1 millidarcy. In no case (of the nine UZ flow scenarios) does this volume represent more than three months of percolation flux. Therefore, the potential effects of these boreholes on flow/percolation in the UZ or as preferential pathways for radionuclide transport, even if the borehole seals should fail completely, are negligible. It follows that any effects on repository performance are negligible, given that these are the factors associated with boreholes that could affect repository performance.

Test boreholes drilled in the underground facility are all relatively short (they remain within the TSw hydrogeologic unit) and are only present in access and observation drifts, not in the waste emplacement drifts. See also Section 6.2.2 (FEP 1.1.01.01.0B). Therefore, these boreholes will not have any significant effect on radionuclide transport between the repository and the water table. See Section 6 in this Analysis Report for a discussion explaining why low consequence for specific elements of the UZ system leads to low consequence for total system performance.

TSPA Disposition: None

6.2.2 Influx through Holes Drilled in Drift Wall or Crown (1.1.01.01.0B)

FEP Description: Holes may be drilled through the drift walls or crown for a variety of reasons including, but not limited to, rock bolt and ground support, monitoring and testing, or construction related activities. These openings may promote flow or seepage into the drifts and onto the waste packages.

Descriptor Phrase: Influx through holes drilled in drift wall

Screening Decision: Excluded—Low Consequence

Screening Argument: Detailed simulations were made using the predictive Seepage Model for PA (BSC 2003 [163226], Section 6.5) to study the effect of rock bolts in the drift crown. In a sensitivity analysis, several combinations of capillarity and permeability were examined, including cases representing both grouted and ungrouted rock bolts and an open hole. These features were found to have only a minor effect on seepage (less than 2% (BSC 2003 [163226], Table 6-4)) due to the small area for water to enter the boreholes from the surrounding formation (BSC 2004 [167970], Section 6.4.2.5). These conclusions are not dependent on the activity that creates a hole in the drift wall or crown (i.e. ground support, monitoring, testing, or construction activities). From these results, the presence of holes drilled in drift wall or crown is not considered significant for seepage into drifts. See Section 6 in this Analysis Report for a discussion explaining why low consequence for specific elements of the UZ system leads to low consequence for total system performance.

TSPA Disposition: None

6.2.3 Site Flooding (During Construction and Operation) (1.1.02.01.0A)

FEP Description: Flooding of the site during construction and operation could introduce water into the underground tunnels, which could affect the long-term performance of the repository.

Descriptor Phrase: Repository flooding (during construction and operation)

Screening Decision: Excluded—Low Consequence

Screening Argument: This FEP describes an issue related to preclosure operations. Flooding is not expected to reach the main portals of the Exploratory Studies Facility (ESF) (Mineart 2003 [165898], Sections 5.2.3 and 5.10.3) or the intake and exhaust shafts (Mineart 2003 [165898], Section 5.11). Design requirements also address the issue of surface water inundation of

subsurface facilities (BSC 2002 [160857], Requirement 2.1.1.4). Very little of the flood zone overlies waste emplacement zones. A small region of the expected flood zone overlies the repository footprint in the upper part of Drill Hole Wash (DTN: MO9805YMP98040.000 [164898]). Boreholes USW NRG-7a, USW G-1, and USW H-1 lie close to or within the potential flood zone of Drill Hole Wash that overlies the repository footprint. As discussed for FEP 1.1.01.01.0A (Section 6.2.1), if water should enter these boreholes, it is not expected to enter waste emplacement locations. Flooding, in general, during storm events is not unusual and leads to infiltration and runoff. The effects of flooding are addressed in the infiltration model (see FEP 2.3.11.02.0A). See Section 6 in this Analysis Report for a discussion explaining why low consequence for specific elements of the UZ system leads to low consequence for total system performance.

TSPA Disposition: None

6.2.4 Incomplete Closure (1.1.04.01.0A)

FEP Description: Disintegration of society could result in incomplete closure, sealing and decommissioning of the disposal vault.

Descriptor Phrases: Open boreholes (preferential pathway to/from surface), Incomplete closure

Screening Decision: Excluded – Low Consequence and By Regulation

Screening Argument: This FEP is similar in content to the ones discussed in Sections 6.2.1 (FEP 1.1.01.01.0A) and 6.2.6 (FEP 2.1.05.01.0A). In these FEPs, the effects of boreholes on water movement between the surface and the repository and transport of radionuclides between the repository and the water table were argued to be negligible. Also, the effects of short test boreholes drilled in the underground test facility were found (see FEP 1.1.01.01.0A) to be negligible with respect to repository performance. The effects of drift seals on water or gas movement through the drifts were also assessed (FEP 2.1.05.01.0A) to have a negligible effect on repository performance under nominal case performance modeling. With regard to sealing of the access portals, FEP 1.1.02.01.0A indicates that the maximum probable flood would not result in water entry into the portals, even if not sealed. Therefore, this FEP is excluded on the basis of low consequence. See Section 6 in this Analysis Report for a discussion explaining why low consequence for specific elements of the UZ system leads to low consequence for total system performance. Per 10 CFR 63.305 [156605], the NRC specifies that "DOE should not project changes to society..." This FEP is predicated on an assumption of a disintegration of society (i.e., a projected change) and the FEP is, therefore, also excluded by regulation.

TSPA Disposition: None

6.2.5 Monitoring of Repository (1.1.11.00.0A)

FEP Description: This FEP addresses the potential for monitoring that is carried out during or after operations, for either operational safety or verification of long-term performance, to detrimentally affect long-term performance. For instance, monitoring boreholes could provide enhanced pathways between the surface and the repository.

Descriptor Phrase: Monitoring (performance confirmation)

Screening Decision: Excluded – Low Consequence

Screening Argument: This FEP is similar to the ones discussed in Sections 6.2.1 (FEP 1.1.01.01.0A) and 6.2.6 (FEP 2.1.05.01.0A). The effects of boreholes on water movement between the surface and the repository and transport of radionuclides between the repository and the water table were found to be negligible. Also, the effects of short test boreholes drilled in the underground test facility were found (see FEP 1.1.01.01.0A) to be negligible with respect to repository performance. The effects of drift seals on water or gas movement through the drifts were also assessed (FEP 2.1.05.01.0A) to have a negligible effect on repository performance. Therefore, this FEP is excluded on the basis of low consequence. These conclusions are not dependent on the activity that creates a hole in the drift wall or crown (i.e. ground support, monitoring, testing, or construction activities).

Other activities associated with performance confirmation are given in Snell et al. (2003 [166219], Section 5). These include air permeability and gas and liquid tracer tests prior to waste emplacement and monitoring, sampling, and laboratory testing of condensation water quantities, composition, and ionic characteristics, including microbial effects, from a thermally accelerated emplacement drift. These activities do not present any disturbance greater than the creation of test boreholes or other similar activities conducted during site characterization.

See Section 6 in this Analysis Report for a discussion explaining why low consequence for specific elements of the UZ system leads to low consequence for total system performance.

TSPA Disposition: None

6.2.6 Flow through Seals (Access Ramps and Ventilation Shafts) (2.1.05.01.0A)

FEP Description: The conceptual model for the shafts and shaft seals used in performance assessment should be chosen to provide a reasonable and realistic basis for simulating long-term fluid flow through the shaft seal system and to allow evaluation of the effect that uncertainty about long-term properties of the shaft seal system may have on cumulative radionuclide releases from the disposal system.

Descriptor Phrases: Water flow and pathways through seals, Gas flow through seals

Screening Decision: Excluded—Low Consequence

Screening Argument: The host rock in the repository is highly fractured; hence seals for repository access drifts are of little consequence for water movement in the repository environment. There is only a small driving force for water to move along the relatively horizontal access drifts or emplacement drifts. Water is expected to move in a general vertical flow pattern through the waste emplacement horizon relative to the length scale of these drifts, with some flow diversion around the drifts caused by the capillary barrier effect. This flow pattern is consistent with the drift-scale seepage model having no-flow lateral boundary conditions (BSC 2003 [163226], Section 6.3.1). The ventilation shafts connect to access drifts at the waste emplacement level, and therefore represent pathways for water to enter the waste

emplacement drifts. For postclosure, the ventilation shafts will be backfilled. The hydrogeologic effects of ventilation shafts provide high-permeability pathways similar to smaller fault features with respect to flow from the surface to the repository. The design for the shafts will account for the effects of flooding (BSC 2003 [163999], Section 6.3.2.14). Therefore, the quantity of water available to flow through the ventilation shafts is limited to rainfall and should not exceed infiltration that occurs in smaller fault features. Although fault features are suspected pathways for rapid migration of water from the surface to the repository (as observed from ^{36}Cl measurements), the amount of water that can bypass matrix flow in the Paintbrush nonwelded hydrogeologic unit is a only a small fraction (generally less than 5% in fault zones) of the total infiltration (CRWMS M&O 1997 [124052], Section 6.12.4). This result is also supported by transport calculations between the ground surface and the PTn-TSw boundary, which show 5% breakthrough at several hundred years (Wu et al. 2000 [154918], Section 4.2, Figure 4.2-6). Similarly, flow through the backfilled ventilation shafts is expected to have a large component of matrix flow, greatly reducing the amount of transient water pulses penetrating from the surface to the waste emplacement drifts, regardless of the specific characteristics or evolution of the backfill over time. Therefore, the effect of the ventilation shafts on flow from the surface to the repository is negligible. Gas flow could potentially move through the drifts, so drift seals could affect the nature of this flow. However, the fractured nature of the host rock ensures that gas will be able to move between drifts if there is a driving force for this flow pattern. Given these conditions, the seals in the repository access drifts and ventilation shafts are expected to have very little effect on the movement of gas or water in the repository environment and therefore have little effect on repository performance. The effects of borehole seal failure properties can be excluded on the basis of low consequence, as discussed in Section 6.2.1 (FEP 1.1.01.01.0A). See Section 6 in this Analysis Report for a discussion explaining why low consequence for specific elements of the UZ system leads to low consequence for total system performance.

TSPA Disposition: None

6.2.7 Radionuclide Transport through Seals (2.1.05.02.0A)

FEP Description: Groundwater flow through seals in the access ramps, ventilation shafts, and exploratory boreholes could affect long-term performance of the disposal system. Radionuclide transport through seals should be considered.

Descriptor Phrase: Radionuclide transport through seals

Screening Decision: Excluded—Low Consequence

Screening Argument: This FEP is similar in content to the ones discussed in Sections 6.2.1 (FEP 1.1.01.01.0A) and 6.2.6 (FEP 2.1.05.01.0A). The effects of water movement between the surface and the repository, the movement of radionuclides between the repository and the water table, and the effects of short test boreholes drilled in the underground facility were all found (see FEP 1.1.01.01.0A) to be negligible with respect to repository performance under nominal case performance modeling. The effects of drift seals on water or gas movement through the drifts were also assessed (Section 6.2.6; FEP 2.1.05.01.0A) to have a negligible effect on repository performance. Therefore, this FEP is excluded on the basis of low consequence. See

Section 6 in this Analysis Report for a discussion explaining why low consequence for specific elements of the UZ system leads to low consequence for total system performance.

TSPA Disposition: None

6.2.8 Degradation of Seals (2.1.05.03.0A)

FEP Description: Degradation of seals in the access ramps, ventilation shafts, and exploratory boreholes could modify flow and transport properties. Physical properties of the seals emplaced in the access ramps, and ventilation shafts, and exploratory boreholes may affect the long-term performance of the disposal system. These properties include the location of the seals (and the openings they seal), and the physical and chemical characteristics of the sealing materials. Possible mechanisms for seal degradation include: chemical alteration from water interactions, wetting associated with condensation, and thermally induced stress-strain changes.

Descriptor Phrases: Mechanical degradation of seals, Chemical degradation of seals (water interactions), Thermal effects on seals (stress changes), Wetting of seals from condensation, Improper sealing

Screening Decision: Excluded—Low Consequence

Screening Argument: A detailed analysis of different seal-failure mechanisms is unnecessary because the effects of borehole seal failure, discussed in Section 6.2.1 (FEP 1.1.01.01.0A), and drift seal failure, discussed in Section 6.2.6 (FEP 2.1.05.01.0A), are found to have negligible effects on repository performance under nominal case performance modeling. Borehole and drift seals are not relied upon for repository performance. Therefore, this FEP is excluded on the basis of low consequence. See Section 6 in this Analysis Report for a discussion explaining why low consequence for specific elements of the UZ system leads to low consequence for total system performance.

TSPA Disposition: None

6.3 EXTREME CLIMATE/ALTERNATIVE FLOW PROCESSES

These FEPs concern the effects of climate and alternative flow processes on hydrological conditions, flow, and radionuclide transport in the UZ. Episodic (or short duration) transient flows are found to have a negligible effect and an average steady flow is used to represent the effects of flow. The rationale for this approximation is discussed below. Longer-term changes in climate are addressed in TSPA-LA using a quasi-steady flow approximation, i.e., the flow fields instantaneously adjust to steady conditions for a given climate (infiltration). However, certain aspects of climate discussed in this section are excluded based on low probability and others on low consequence.

Table 6-6 gives the FEP numbers and names categorized under extreme climate/alternative flow processes.

Table 6-6. Excluded FEPs: Climate and Episodic Transient Flow

Section Number	FEP Number	FEP Name
6.3.1	1.3.04.00.0A	Periglacial effects
6.3.2	1.3.05.00.0A	Glacial and ice sheet effect
6.3.3	1.3.07.01.0A	Water table decline
6.3.4	2.1.09.21.0C	Transport of particles larger than colloids in the UZ
6.3.5	2.2.07.05.0A	Flow in the UZ from episodic infiltration.

Source: LA FEP List (DTN: MO0307SEPFEPS4.000 [164527])

6.3.1 Periglacial Effects (1.3.04.00.0A)

FEP Description: This FEP addresses the physical processes and associated landforms in cold but ice-sheet-free environments. Permafrost and seasonal freeze/thaw cycles are characteristic of periglacial environments. These effects could include erosion and deposition.

Descriptor Phrases: Climate change (glaciation), Permafrost, Soil erosion (from glaciation), Soil deposition (from glaciation)

Screening Decision: Excluded—Low Consequence and Low Probability

Screening Argument: This FEP refers to climate conditions that could produce a cold, but glacier-free environment. Results of such a climate could include permafrost (permanently frozen ground). Paleoclimate records indicate that the climate conditions necessary to form permafrost are not expected at Yucca Mountain over the next 10,000 years (USGS 2003 [167961], Section 6.2). The glacial-transition climate (identified as "intermediate" in Sharpe 2001 [161591], Table 6-6) has the lowest predicted mean annual temperatures for the 10,000-year period (USGS 2003 [167961], Section 6.6.2; Sharpe 2003 [161591], Section 6.3.2). For the glacial-transition climate, the estimated range of mean annual temperatures is 8.3°C to 10.1°C (Sharpe 2003 [161591], Table 6-3), which is too warm to sustain permafrost. Only the coldest scenario for the full glacial climate (Oxygen Isotope Stage 6/16) is expected to have a mean annual temperature of 0°C (Sharpe 2003 [161591], Table 6-3). The expected return for such a climate is 200,000 years after present (Sharpe 2003 [161591], Table 6-5). Therefore, soil erosion and deposition at Yucca Mountain as a result of permafrost is not credible. Freeze/thaw mechanical erosion will likely increase as the climate cools. However, the magnitude of erosion will not likely be significant even during the cooler climate condition. The maximum erosion over a 10,000-year period is expected to be less than 10 cm (YMP 1993 [100520], pp. 55-56), which is within the range of existing surface irregularities. This is based on estimates for erosion rates that have occurred at Yucca Mountain over the last 12 million years (YMP 1993 [100520], pp. 55-56), and therefore includes the effects of cooler climates. Therefore, this FEP is excluded from TSPA-LA on the basis of low consequence and low probability. See Section 6 in this Analysis Report for a discussion explaining why low consequence for specific elements of the UZ system leads to low consequence for total system performance.

TSPA Disposition: None

6.3.2 Glacial and Ice Sheet Effect (1.3.05.00.0A)

FEP Description: This FEP addresses the effects of glaciers and ice sheets occurring within the region of the repository, including direct geomorphologic effects and hydrologic effects. These effects include changes in topography (due to glaciation and melt water), changes in flow fields, and isostatic depression and rebound. These effects could include erosion and deposition.

Descriptor Phrases: Climate change (glaciation), Permafrost, Soil erosion (from glaciation), Soil deposition (from glaciation)

Screening Decision: Excluded—Low Probability

Screening Argument: This FEP refers to the local effects of glaciers and ice sheets. Paleoclimate records indicate that glaciers and ice sheets have not occurred at Yucca Mountain at any time in the past (Simmons 2004 [166960], Section 6.4). The closest alpine glaciers to Yucca Mountain during the Pleistocene were in the Sierra Nevada of California (Simmons 2004 [166960], Section 6.4.1.2.2), too far from Yucca Mountain to have any effect on site geomorphology or hydrology. Given the relatively low elevation of Yucca Mountain, there is no credible mechanism by which a glacier could form at the site over the next 10,000 years. The geomorphologic and hydrological effects associated with glaciers, such as changes in topography resulting from erosion, deposition, and glacial transport, changes in flow fields, and isostatic depression and rebound, are not credible processes at Yucca Mountain. Therefore, this FEP is excluded from TSPA-LA on the basis of low probability. Note, however, that the regional climatic effects of ice sheets that might form further north are addressed in the TSPA-LA (see FEP 1.3.01.00.0A).

TSPA Disposition: None

6.3.3 Water Table Decline (1.3.07.01.0A)

FEP Description: Climate change could produce decreased infiltration (e.g., an extended drought), leading to a decline in the water table in the saturated zone, which would affect the release and exposure pathways from the repository.

Descriptor Phrases: Climate change (drier), Time-dependent infiltration (decrease), Water table elevation

Screening Decision: Excluded—Low Consequence

Screening Argument: This FEP refers to the effects of a climate change that leads to much drier climate conditions. Some of the consequences of this type of climate change are a decrease in infiltration rate over time, water table decline, and desertification of the surface environment. However, the Yucca Mountain region is already a desert environment, and future climates are only expected to have increased precipitation (USGS 2003 [167961], Section 6.6). In any case, a decline in the water table and lower infiltration rates would only enhance the UZ as a barrier to radionuclide movement. Therefore, this FEP is excluded on the basis of low consequence because it has no adverse effects on performance. See Section 6 in this Analysis Report for a

discussion explaining why low consequence for specific elements of the UZ system leads to low consequence for total system performance.

TSPA Disposition: None

6.3.4 Transport of Particles Larger Than Colloids in the UZ (2.1.09.21.0C)

FEP Description: Particles of radionuclide-bearing material larger than colloids could be entrained in suspension and then be transported in water flowing through the UZ.

Descriptor Phrases: Groundwater rinse in the UZ, Gravitational settling of colloids in the UZ

Screening Decision: Excluded – Low Consequence

Screening Argument: Particles larger than colloids are not expected to show much mobility in the UZ because of the large gravitational settling that occurs relative to diffusive movement for such particles. A relevant velocity scale for particle diffusion is the particle diffusion coefficient divided by the particle diameter. The colloid diffusion coefficient is given by the Stokes-Einstein equation (BSC 2003 [163228], Equation 6-23). The gravitational settling velocity for a colloid may be computed from Stokes law (Perry and Chilton 1973 [104946], Equation 5-215). The particle diameter, d_p, at which these velocities are equal is given by

$$d_p = \left[\frac{6kT}{\pi g (\rho_c - \rho_w)} \right]^{\frac{1}{4}}$$

where k is the Boltzmann constant (1.38×10^{-23} J/K), T is the temperature in Kelvins (300 K), g is the gravitational acceleration (9.81 m/s^2), ρ_c is the colloid grain density (2650 kg/m^3), and ρ_w is the density of water (1,000 kg/m^3). This equation indicates that for a value of d_p equal to 0.836 microns, gravitational settling and diffusion will be roughly in balance. For particles larger than colloids (greater than 100 microns) gravitational settling will dominate particle movement. Therefore, particles larger than colloids are not mobile.

The effects of perturbed TH conditions or other perturbed flow conditions (e.g. "groundwater rinse") on colloid movement (or movement of particles larger than colloids) are expected to be negligible because of the limited entrainment expected. Tests with fine, cohesive sediments presented in Vanoni (1977 [164901], Figure 2.51) show that although entrainment does occur, for a wide variety of conditions this appears to be a very limited transient response. Entrainment is observed for a few days, and then the system stabilizes with no further initiation of motion, as compared with unretarded colloid transport, which has a 10 percent breakthrough in about 5 years (BSC 2003 [163228], Section 6.18.4). The limited time frame for enhanced colloid movement is negligible with respect to the time frames for waste release and transport. Therefore, this FEP may be excluded based on low consequence. See Section 6 in this Analysis Report for a discussion explaining why low consequence for specific elements of the UZ system leads to low consequence for total system performance.

TSPA Disposition: None

6.3.5 Flow in the UZ from Episodic Infiltration (2.2.07.05.0A)

FEP Description: Episodic flow occurs in the UZ as a result of episodic infiltration. Episodic flow may affect transport.

Descriptor Phrase: Episodic flow/percolation in the UZ

Screening Decision: Excluded—Low Consequence

Screening Argument: The process that drives infiltration in the UZ is precipitation, which is clearly episodic in nature. Studies of episodic infiltration and percolation have found, however, that matrix-dominated flow in the PTn damps out the transient nature of the percolation such that UZ flow below the PTn is essentially steady (CRWMS M&O 1998 [100356], Section 2.4.2.8; Wu et al. 2000 [154918], Section 4.1). Furthermore, the PTn overlies the entire repository block (see Appendix B in this Analysis Report). This damping of transient flow is due to capillary forces and high matrix permeability in the PTn that lead to matrix imbibition of water from fractures to the matrix. Therefore, this FEP is excluded on the basis that the UZ flow is steady at the repository and along radionuclide transport pathways. Very small amounts of fracture flow do appear to penetrate as fast pathways through fault zones between the ground surface and the repository elevation as evidenced by high ^{36}Cl concentrations in samples taken from the ESF. Higher concentrations of this isotope found in the ESF can only be explained through surface deposition of ^{36}Cl from nuclear weapons testing and subsequent aqueous transport to certain ESF sampling locations in a period of approximately 50 years. The flow responsible for rapid transport could occur either as steady flow or as episodic transient flow. In either case the key to fast transport through the PTn is for solute to move through fractures and bypass transport through the rock matrix. However, the flow and transport models indicate that the quantity of water and dissolved constituents that do penetrate the PTn as a result of fast pathways (generally less than 1% of the total infiltration (CRWMS M&O 1997 [124052], Section 6.12.4)) is negligible with respect to repository performance (CRWMS M&O 1998 [100356], Section 2.4.2.8). Additional validation studies are being carried out concerning the measurement and interpretation of "bomb pulse" ^{36}Cl at the repository level. However, the conclusions of these studies are not yet available (BSC 2003 [166104], Section 6.14.2.1.1). See Section 6 in this Analysis Report for a discussion explaining why low consequence for specific elements of the UZ system leads to low consequence for total system performance.

TSPA Disposition: None

6.4 EROSION/DISSOLUTION/SUBSIDENCE

These FEPs concern the effects of surface erosion, mineral dissolution, and subsidence on hydrological conditions, flow, and radionuclide transport in the UZ. All of these processes are expected to occur at Yucca Mountain at low rates. These FEPs are all excluded on the basis of low consequence given conservative bounds on the extent that these processes can affect the hydrogeologic system at Yucca Mountain in a 10,000-year period.

Table 6-7 gives the FEP numbers and names categorized under Erosion/Dissolution/Subsidence.

Table 6-7. Excluded FEPs: Erosion/Dissolution/Subsidence

Section Number	FEP Number	FEP Name
6.4.1	1.2.07.01.0A	Erosion/denudation
6.4.2	1.2.07.02.0A	Deposition
6.4.3	1.2.09.02.0A	Large-scale dissolution
6.4.4	2.2.06.04.0A	Effects of subsidence

Source: LA FEP List (DTN: MO0307SEPFEPS4.000 [164527])

6.4.1 Erosion/Denudation (1.2.07.01.0A)

FEP Description: Erosion and denudation are processes that cause significant changes in the present-day topography and thus affect local and regional hydrology. Erosion of surficial materials can occur by a variety of means, including physical weathering (including glacial and fluvial erosion), chemical weathering, erosion by wind (aeolian erosion), and mass wasting (e.g., landslide) processes. The extent of erosion depends to a large extent on climate and uplift.

Descriptor Phrase: Soil erosion (effects on infiltration)

Screening Decision: Excluded—Low Consequence

Screening Argument: Erosion is a process that will be ongoing at Yucca Mountain over the 10,000-year performance period. The maximum erosion due to various processes (e.g. fluvial erosion, aeolian erosion, chemical weathering) over a 10,000-year period is expected to be less than 10 cm (YMP 1993 [100520], pp. 55-56), which is within the range of existing surface irregularities. DOE (1988 [100282], Section 1.1.3.3.2) indicates that mass wasting, such as landslides, does not play a significant role in the present erosional regime at Yucca Mountain.

Debris flows are the primary mechanism for hillslope erosion of unconsolidated deposits in the Yucca Mountain region (YMP 1995 [102215], Section 2.5.2). However, the effects of debris flows are generally restricted to channelized areas (YMP 1995 [102215], Section 4.2) and are not an effective erosion mechanism for unweathered bedrock. Therefore, debris flows have a limited influence on the evolution of surficial materials at Yucca Mountain. The effects of debris flows, over a 10,000-year period, are captured within the maximum expected erosion of 10 cm or less and are, therefore, insignificant.

The effects of surface construction and characterization activities at the ground surface on future erosion will also be negligible because of the planned reclamation of the site ground surface. As stated in YMP (2001 [154386], Section 5.2.2.1), "Recontouring and erosion control practices include backfilling spoil material and grading disturbed sites, so that a stable land form is created that blends with the surrounding topography. Following site decommissioning, disturbed areas will be graded such that the natural drainage pattern (predisturbance drainage) is restored. The sites will be stabilized and recontoured to blend into the natural topography of the area." Therefore, the effects of surface erosion are negligible due to low consequence. See Section 6 in this Analysis Report for a discussion explaining why low consequence for specific elements of the UZ system leads to low consequence for total system performance.

TSPA Disposition: None

6.4.2 Deposition (1.2.07.02.0A)

FEP Description: Deposition is a process that causes significant changes in the present-day topography and thus affects local and regional hydrology. Deposition of surficial materials can occur by a variety of means, including fluvial, aeolian, and lacustrine deposition and redistribution of soil through weathering and mass wasting processes.

Descriptor Phrase: Soil deposition (effects on infiltration)

Screening Decision: Excluded—Low Consequence

Screening Argument: Like erosion, deposition is a process that will be ongoing at Yucca Mountain over the 10,000-year performance period. However, given the topographic relief of Yucca Mountain, erosion is expected to dominate over deposition. Deposition is believed to be a dominant process in Fortymile Wash (YMP 1993 [100520], p. 55). However, this drainage channel has no effect on UZ flow and transport at Yucca Mountain due to its lateral offset. Therefore deposition is excluded from TSPA-LA on the basis of low consequence. The effects of igneous disruptive events and possible ash deposition are addressed in Section 6.7.4 (FEP 1.2.10.02.0A). See Section 6 in this Analysis Report for a discussion explaining why low consequence for specific elements of the UZ system leads to low consequence for total system performance.

TSPA Disposition: None

6.4.3 Large-Scale Dissolution (1.2.09.02.0A)

FEP Description: Dissolution can occur when any soluble mineral is removed by flowing water, and large-scale dissolution is a potentially important process in rocks that are composed predominantly of water-soluble evaporite minerals, such as salt.

Descriptor Phrases: Large scale dissolution in the UZ

Screening Decision: Excluded—Low Consequence

Screening Argument: This FEP is principally concerned with the dissolution of highly soluble evaporite rocks such as halite or carbonates. Evaporitic minerals are present, but the UZ at Yucca Mountain is primarily composed of vitric high-silica rhyolite and quartz latite (or trachyte) (Simmons 2004 [166960], Section 3.3.2). Solubilities of these minerals are too low to produce large dissolution cavities, breccia pipes, or solution chimneys over the time scales of interest and expected water flow rates. Local dissolution processes that affect, for example, fracture filling minerals are discussed in Section 6.8.7 (FEP 2.2.08.03.0B). Therefore, large-scale dissolution plays a very minor role at Yucca Mountain and this FEP can be excluded on the basis of low consequence. See Section 6 in this Analysis Report for a discussion explaining why low consequence for specific elements of the UZ system leads to low consequence for total system performance.

TSPA Disposition: None

6.4.4 Effects of Subsidence (2.2.06.04.0A)

FEP Description: Subsidence above the mined underground facility or other openings affects the properties of the overlying rocks and surface topography. Changes in rock properties, such as enhanced permeability, may alter flow paths from the surface to the repository. Changes in surface topography may alter run-off and infiltration, and may perhaps create impoundments.

Descriptor Phrases: Subsidence (fractures in the UZ), Subsidence (drift collapse)

Screening Decision: Excluded—Low Consequence

Screening Argument: Subsidence can occur as a result of underground excavations. In coal mining, subsidence has been found to occur when more than 50% of the coal bed was removed (Keller 1992 [146831], p. 142). In the case of Yucca Mountain, the percent of earth removal is very small. The emplacement drift diameter is less than 10% of the drift spacing (BSC 2004 [167040]; BSC 2003 [164101]). Furthermore, drift collapse has been modeled (BSC 2003 [162711], Attachment XVIII), and the collapse is found to extend only about 7 m above the initial drift crown elevation and does not propagate further upward. Therefore, drift collapse will not result in the formation of surface depressions. The effects of changes to fracture characteristics around emplacement drifts caused by stress relief have been found to be small to moderate and to have no adverse effects on seepage (BSC 2004 [167973], Section 8.1). Therefore, subsidence is expected to have a negligible impact on large-scale UZ flow or surface topography, and is excluded from TSPA-LA modeling. See Section 6 in this Analysis Report for a discussion explaining why low consequence for specific elements of the UZ system leads to low consequence for total system performance.

TSPA Disposition: None

6.5 HUMAN INFLUENCES ON CLIMATE/SOIL

This group of FEPs is excluded from the TSPA-LA calculation because they postulate a human influence on climatic effects. The licensing rule and preamble (66 FR 55732 [156671]) indicate that only natural evolution of the reference biosphere is to be included in the performance assessment. Naturally occurring climate change effects are addressed in the TSPA-LA through climate modeling and ranges of parameters used to characterize UZ water chemistry.

Table 6-8 gives the FEP numbers and names categorized under Human Influences on Climate/Soil.

Table 6-8. Excluded FEPs: Human Influences on Climate/Soil

Section Number	FEP Number	FEP Name
6.5.1	1.4.01.00.0A	Human influences on climate
6.5.2	1.4.01.02.0A	Greenhouse gas effects
6.5.3	1.4.01.03.0A	Acid rain
6.5.4	1.4.01.04.0A	Ozone layer failure
6.5.5	1.4.06.01.0A	Altered soil or surface water chemistry

Source: LA FEP List (DTN: MO0307SEPFEPS4.000 [164527])

6.5.1 Human Influences on Climate (1.4.01.00.0A)

FEP Description: This FEP addresses future human actions that could influence global, regional, or local climate. Human actions may be intentional or accidental.

Descriptor Phrase: Climate change (anthropogenic)

Screening Decision: Excluded—By Regulation

Screening Argument: Human influences on climate are excluded on the basis of requirements of 10 CFR 63.305(c) [156605]. The licensing rule and the preamble (66 FR 55732 [156671]) indicate that only natural evolution of the reference biosphere is to be included in the performance assessment and that the changes caused by the future human behaviors are not to be included. In response to comments on climate change (66 FR 55732 [156671], p. 55757), the NRC emphasized the importance of including "climate change in both the geosphere and biosphere performance assessment calculations to ensure that the conceptual model of the environment is consistent with our scientific understanding of reasonably anticipated natural events." Similarly, in the background discussion of the 2002 amendment to the rule the NRC stated "DOE's performance assessments are required to consider the naturally occurring features, events and processes that could affect the performance of a geologic repository…" (67 FR 62628 [162317]). As the part of the response to the comments the NRC also stated that considering future economic growth trends and human behaviors would add inappropriate speculation into the requirements and would lead to problems deciding which alternative futures are credible and which are unrealistic (66 FR 55732 [156671], p. 55757). The NRC stated further that the natural systems of the biosphere should be allowed to vary consistent with the geologic records, which provide basis for predicting future biosphere changes (66 FR 55732 [156671], p. 55757). Because human behavior cannot be similarly predicted, such an approach cannot be used for the RMEI (66 FR 55732 [156671], p. 55757) and, extending this reasoning, for the human-induced changes to the environment. Prediction of the human-induced climate changes, would not only involve speculations about the local population but also introduce inherently large uncertainties in prediction of the global population behaviors and their consequences. In their discussion of consideration of future economic growth trends the NRC concluded that inclusion of such future predictions would not only add inappropriate speculation but also would not enhance public safety and be likely inconsistent with the Environmental Protection Agency (EPA) standards. Based on these statements, the FEPs associated with the characteristics of the reference biosphere and their change are limited to naturally occurring FEPs and exclude FEPs related to human activities. Likewise, the geological, hydrological and climatological factors that the DOE must vary under 10 CFR 63.305(c) [156605], are also limited to naturally occurring FEPs.

TSPA Disposition: None

6.5.2 Greenhouse Gas Effects (1.4.01.02.0A)

FEP Description: The greenhouse effect refers to the presence of carbon dioxide and other gases in the atmosphere that tend to allow solar radiation through to the earth's surface and reflect heat back to it. Thus, these gases act much as the glass of a greenhouse, with the earth as the greenhouse. Human activities such as burning of fossil fuels, forest clearance, and industrial

processes produce these greenhouse gases. The greenhouse effect could increase concentrations of carbon dioxide and other gases in the atmosphere, and lead to changes in climate such as global warming.

Descriptor Phrase: Climate change (greenhouse gasses)

Screening Decision: Excluded—By Regulation

Screening Argument: Human influences on climate are excluded on the basis of requirements of 10 CFR 63.305(c) [156605]. The licensing rule and the preamble (66 FR 55732 [156671]) indicate that only natural evolution of the reference biosphere is to be included in the performance assessment and that the changes caused by the future human behaviors are not to be included. See Section 6.5.1; FEP 1.4.01.00.0A.

TSPA Disposition: None

6.5.3 Acid Rain (1.4.01.03.0A)

FEP Description: Human actions may result in acid rain on a local to regional scale. Acid rain can detrimentally affect aquatic and terrestrial life by interfering with the growth, reproduction and survival of organisms. It can influence the behavior and transport of contaminants in the biosphere, particularly by affecting surface water and soil chemistry.

Descriptor Phrases: Climate change (acid rain), Surface water (chemistry)

Screening Decision: Excluded—By Regulation

Screening Argument: Human influences on climate are excluded on the basis of requirements of 10 CFR 63.305(c) [156605]. The licensing rule and the preamble (66 FR 55732 [156671]) indicate that only natural evolution of the reference biosphere is to be included in the performance assessment and that the changes caused by the future human behaviors are not to be included. See Section 6.5.1; FEP 1.4.01.00.0A.

TSPA Disposition: None

6.5.4 Ozone Layer Failure (1.4.01.04.0A)

FEP Description: Human actions (i.e., the use of certain industrial chemicals) may lead to destruction or damage to the earth's ozone layer. This may lead to significant changes to the climate, affecting properties of the geosphere such as groundwater flow patterns.

Descriptor Phrase: Climate change (ozone failure)

Screening Decision: Excluded—By Regulation

Screening Argument: Human influences on climate are excluded on the basis of requirements of 10 CFR 63.305(c) [156605]. The licensing rule and the preamble (66 FR 55732 [156671]) indicate that only natural evolution of the reference biosphere is to be included in the

performance assessment and that the changes caused by the future human behaviors are not to be included. See Section 6.5.1; FEP 1.4.01.00.0A.

TSPA Disposition: None

6.5.5 Altered Soil or Surface Water Chemistry (1.4.06.01.0A)

FEP Description: Human activities (e.g., industrial pollution, agricultural chemicals) may produce local changes to the soil chemistry or to the chemistry of water infiltrating Yucca Mountain and could provide a plume of unspecified nature to interact with the repository and possibly with waste packages.

Descriptor Phrases: Surface water (chemistry), Surface activities (industrial)

Screening Decision: Excluded—By Regulation

Screening Argument: Human activities may affect soil and surface water chemistry because of agricultural activities or pollution from industrial activities. Current land use at Yucca Mountain does not include activities such as these that may lead to large-scale changes in soil or water chemistry. There is no expectation that such activities would occur at Yucca Mountain, because the site does not offer known mineral resources (Simmons 2004 [166960], Section 3.6), commercial or industrial land uses (CRWMS M&O 2000 [151945], Section 3.2), or land that is suitable for agricultural development due to the rough terrain, thin soils, low rainfall, and deep water table. Furthermore, 10 CFR 63.305(b) [156605] states that "DOE should not project changes in society, the biosphere (other than climate), human biology, or increases or decreases in human knowledge or technology. In all analyses done to demonstrate compliance with this part, the DOE must assume that all of those factors remain constant as they are at the time of submission of the license application." Therefore, human activities (changes in the social and institutional attributes of society, lifestyle, land use, and water use) that would alter soil or surface water chemistry are excluded on the basis of the regulatory requirements (10 CFR 63.305(b) [156605]).

TSPA Disposition: None

6.6 GAS PHASE EFFECTS

This group of FEPs is excluded from the TSPA-LA calculation. These FEPs concern the effects of gas generation caused by chemical reactions in the repository, the intrusion of naturally occurring gases such as methane, gas-phase radionuclide transport, and natural air flow. These FEPs are all excluded on the basis of low consequence to performance.

Table 6-9 gives the FEP numbers and names categorized under Natural Gas/Gas Generation Effects.

Table 6-9. Excluded FEPs: Natural Gas/Gas Generation Effects

Section Number	FEP Number	FEP Name
6.6.1	2.2.10.11.0A	Natural air flow in the UZ
6.6.2	2.2.11.02.0A	Gas effects in the UZ
6.6.3	2.2.11.03.0A	Gas transport in geosphere

Source: LA FEP List (DTN: MO0307SEPFEPS4.000 [164527])

6.6.1 Natural Air Flow in the UZ (2.2.10.11.0A)

FEP Description: Natural convective air circulation has been observed at a borehole at the top of the mountain. Repository heat is expected to increase this flow.

Descriptor Phrase: Air flow in the UZ

Screening Decision: Excluded—Low Consequence

Screening Argument: Natural air flow is expected to have a negligible impact on TH processes, owing to the large volume of thermally generated flow, including water vapor. The effects of repository heat on air flow are discussed in Section 6.1.38; FEP 2.2.10.10.0A. The effects of natural air flow have little consequence on water movement in the UZ because of the high mobility of the gas phase, hence little dynamic interaction occurs between the phases. It is standard practice when modeling unsaturated liquid flow is to neglect the effects resulting from flow in the gas phase (Richards 1931 [104252]). See Section 6 in this Analysis Report for a discussion explaining why low consequence for specific elements of the UZ system leads to low consequence for total system performance.

TSPA Disposition: None

6.6.2 Gas Effects in the UZ (2.2.11.02.0A)

FEP Description: Pressure variations due to gas generation may affect flow patterns and contaminant transport in the UZ or may intrude into the repository. Degassing could affect flow and transport of gaseous contaminants. Gases could also affect other contaminants if water flow is driven by large gas bubbles forming in the repository. Potential gas sources include degradation of repository components and naturally occurring gases from clathrates, microbial degradation of organic material or deep gases in general.

Descriptor Phrases: Gas pressure effects on flow/percolation in the UZ, Naturally-occurring gases in the UZ

Screening Decision: Excluded—Low Consequence

Screening Argument: In the Yucca Mountain UZ, the build-up of any significant gas pressure is unlikely, because of the permeable fracture pathways. Furthermore, sealing of fractures due to precipitation in the thermally perturbed repository environment has a negligible effect on hydrogeologic properties of the fractures relative to gas pressure effects. This can be seen by comparing the gas-phase pressures in fractures for TH calculations (no mineral precipitation)

with those for THC calculations (mineral precipitation included) (DTN: LB0302DSCPTHCS.002 [161976]; BSC 2004 [167974]). This FEP also addresses the effects of gas bubbles. Because the repository at Yucca Mountain is located in the UZ with high aqueous to gas-phase contact, bubbles would quickly be absorbed into the gas phase and could not drive substantial water flow. Therefore, the bubble-release mechanism is negligible. This argument is valid regardless of the specific potential sources of gas generation (e.g. degradation of repository components or microbial degradation of organic matter). Therefore, the FEP is excluded on the basis of low consequence. See Section 6 in this Analysis Report for a discussion explaining why low consequence for specific elements of the UZ system leads to low consequence for total system performance.

TSPA Disposition: None

6.6.3 Gas Transport in Geosphere (2.2.11.03.0A)

FEP Description: Gas released from the drifts and gas generated in the near-field rock will flow through fracture systems in the near-field rock and in the geosphere. Certain gaseous or volatile radionuclides may be able to migrate through the far-field faster than the groundwater advection rate.

Descriptor Phrases: Gas transport in the UZ, Gas transport in the SZ

Screening Decision: Excluded—Low Consequence

Screening Argument: All radionuclides in TSPA-LA are released into the aqueous phase (DOE 2002 [155970], Section I.7). This is expected to bound any dose effects of gas-phase releases. The only radionuclides that would have a potential for gas transport are carbon-14 and radon-222. Iodine-129 can exist in a gas phase, but it is highly soluble and, therefore, would be more likely to dissolve in groundwater rather than migrate as a gas. Other gas-phase isotopes have been eliminated in a screening analysis (DOE 2002 [155970], Section I.3.3), usually because they have short half-lives and are not decay products of long-lived isotopes.

An analysis of the potential dose from gas-phase release of carbon-14 shows that the maximum dose was found to be 1.8×10^{-10} mrem per year (DOE 2002 [155970], Section I.7). This may be compared with doses from carbon-14 in TSPA-SR, which found peak doses from aqueous C-14 release to be in excess of 10^{-4} mrem/yr (CRWMS M&O 2000 [153246], Figure 4.1-7). Because gas-phase releases compose approximately 2% of the carbon-14 inventory (DOE 2002 [155970], Section I.7), these releases should result in a maximum dose of about 10^{-6} mrem/yr, given aqueous release. Therefore, the dose from aqueous release of carbon-14 bounds the gaseous release dose.

Radon is a decay product of uranium and would be generated for as long as any uranium remained in the repository. Based on gas flow studies, radon is expected to decay before it reaching the ground surface (DOE 2002 [155970], Section I.7.3). Therefore, aqueous release will also bound the dose from radon-222, primarily through aqueous transport of the parent uranium radionuclide and generation of radon-222 as a decay product at the accessible environment.

In summary, all radionuclides are transported in the aqueous phase. The effects of gas phase transport on radiological exposures and radionuclide releases are bounded by aqueous phase transport and can therefore be excluded on the basis of low consequence. See Section 6 in this Analysis Report for a discussion of why low consequence for specific elements of the UZ system leads to low consequence for total system performance.

TSPA Disposition: None

Supporting Reports: BSC 2004 [162730]. (This FEP was listed as an Included FEP in BSC 2004 [162730]. Subsequent evaluation in this UZ FEP AR has determined that it is excluded.)

6.7 SEISMIC/IGNEOUS/ROCK CHARACTERISTICS

This group of FEPs is excluded from the TSPA-LA calculation. These FEPs concern the potential effects of seismic and igneous events and processes on existing rock properties and characteristics.

Table 6-10 gives the FEP numbers and names categorized under Seismic/ Igneous/Rock Characteristics.

Table 6-10. Excluded FEPs: Seismic/Igneous/Rock Characteristics

Section Number	FEP Number	FEP Name
6.7.1	1.2.04.02.0A	Igneous activity changes rock properties
6.7.2	1.2.06.00.0A	Hydrothermal activity
6.7.3	1.2.10.01.0A	Hydrologic response to seismic activity
6.7.4	1.2.10.02.0A	Hydrologic response to igneous activity
6.7.5	2.2.06.01.0A	Seismic activity changes porosity and permeability of rock
6.7.6	2.2.06.02.0A	Seismic activity changes porosity and permeability of faults
6.7.7	2.2.06.02.0B	Seismic activity changes porosity and permeability of fractures
6.7.8	2.2.06.03.0A	Seismic activity alters perched-water zones
6.7.9	2.2.12.00.0A	Undetected features in the UZ

Source: LA FEP List (DTN: MO0307SEPFEPS4.000 [164527]). The FEP Name for FEP 1.2.10.01.0A has been changed slightly subsequent to DTN: MO0307SEPFEPS4.000 [164527].

6.7.1 Igneous Activity Changes Rock Properties (1.2.04.02.0A)

FEP Description: Igneous activity near the underground facility causes extreme changes in rock stress and the thermal regime, and may lead to rock deformation, including activation, creation, and sealing of faults and fractures. This may cause changes in the rock hydrologic and mineralogic properties. Permeabilities of dikes and sills and the heated regions immediately around them can differ from those of country rock. Mineral alterations can also change the chemical response of the host rock to contaminants.

Descriptor Phrases: Igneous activity (rock properties in the UZ)

Screening Decision: Excluded—Low Consequence

Screening Argument: Basaltic igneous activity typically has minimal physical and mineralogical effects on local rock properties. Basalt magma chills rapidly against country rock, forming a nonvesicular aphanitic border facies having low thermal conductivity and low chemical reactivity. The country rock itself may be baked to form a thin rind or hornfels. It is unlikely that contact mineral alterations would change the chemical response to contaminants, because alteration usually results in only a dense screen of aphanitic anhydrous silicate minerals. Any such alteration in the welded tuff units would be minimal, owing to the dearth of hydrous minerals and the large component of high-temperature feldspars in the tuff. Furthermore, studies of analog sites suggest that the consequences of hydrothermal activity in terms of the amount and extent of mineral alteration are small (Valentine et al. 1998 [119132], p. 5-74; CRWMS M&O 1998 [105347]; Carter-Krogh and Valentine 1996 [160928], pp. 7–8).

Dikes are expected to range between about 0.5 m to 4.5 m in thickness, with an average of 1.5 m (BSC 2003 [166407], Section 6.3.1). A simple conduction-only, dike-cooling model indicates that a dike of 5.5 m thickness will cool to sub-boiling in less than 60 years, with boiling temperatures no more than 20 m from the dike (BSC 2003 [165923], Figure 161). Contact metamorphism resulting from dikes appears to be confined to distances of 5 to 10 m from the dike (Valentine et al. 1998 [119132], p. 5-74). With significant thermal perturbations limited to less than 100 years and alteration limited to zones of a few meters around the dike, the effects of basaltic magmatism on UZ processes is negligible.

On the basis of these confined and short-duration features and processes, this FEP is excluded on basis of low consequence. Furthermore, the probability for the occurrence of a volcanic event at Yucca Mountain is 1.7×10^{-8} per year (BSC 2003 [163769], Table 22), which results in a greatly reduced expected consequence from a probability-weighted perspective. See Section 6 in this Analysis Report for a discussion explaining why low consequence for specific elements of the UZ system leads to low consequence for total system performance.

TSPA Disposition: None

6.7.2 Hydrothermal Activity (1.2.06.00.0A)

FEP Description: Naturally-occurring high-temperature groundwater may induce hydrothermal alteration of minerals in the rocks through which the high-temperature groundwater flows.

Descriptor Phrases: Hydrothermal alteration of the UZ

Screening Decision: Excluded—Low Consequence

Screening Argument: The earliest volcanism in the Yucca Mountain region was dominated by a major episode of caldera-forming, silicic volcanism that occurred primarily between ~15 and 11 million years, forming the southwestern Nevada volcanic field (Sawyer et al. 1994 [100075]). Silicic volcanism was approximately coincident with a major period of extension, which occurred primarily between 13 and 9 million years ago (Sawyer et al. 1994 [100075], Figure 4). Based on eruption volume, the southwestern Nevada volcanic field is considered to have virtually ceased eruptive activity since about 7.5 million years ago (BSC 2003 [163769], Section 6.2). The commencement of basaltic volcanism occurred during the latter part of the caldera-forming phase, as extension rates waned, and small-volume basaltic volcanism has continued

into the Quaternary (BSC 2003 [163769], Section 6.2). The focus of igneous-related FEPs is on the potential for small scale basaltic volcanism and the mean probability of a basaltic dike intersecting the repository footprint has been calculated to be 1.7×10^{-8} per year (BSC 2003 [163769], Table 22)

Yucca Mountain is an uplifted, erosional remnant of voluminous ash-flow tuff deposits formed during the early phase of silicic volcanism (BSC 2003 [163769], Section 6.2). Hydrothermal alteration and mineralization that followed the deposition of the Paintbrush Group are present within a few kilometers of the Yucca Mountain site in the Calico Hills and in Claim Canyon. However, no clear evidence for hydrothermal activity exists in the repository area (Simmons 2004 [166960], Section 3.6.2). Yucca Mountain is located outside the caldera margin, hence it was never near a hydrothermal source (BSC 2003 [163769], Figure 3). Studies of two-phase fluid inclusions at Yucca Mountain using petrography, microthermometry, and U-Pb dating indicate that temperatures have remained close to the current ambient values over the past 2 to 5 million years (Wilson et al. 2003 [163589], Section 8).

Based on the geologic history and setting, the recurrence of silicic volcanism is not further considered and concern is focused on basaltic intrusion (BSC 2003 [163769], Section 6.2; Reamer 1999 [119693], p. 5). Although basaltic magmatism could occur during the regulatory period, the effects of any related hydrothermal system would be of limited scale as described in Section 6.7.1 (FEP 1.2.04.02.0A) where the effects of basaltic magmatism are addressed. Due to the limited scale of effects from basaltic dikes, the potential effects of hydrothermal alteration are excluded based on low consequence. See Section 6 in this Analysis Report for a discussion of why low consequence for specific elements of the UZ system leads to low consequence for total system performance.

TSPA Disposition: None

6.7.3 Hydrologic Response To Seismic Activity (1.2.10.01.0A)

FEP Description: Seismic activity, associated with fault movement, may create new or enhanced flow pathways and/or connections between stratigraphic units, or it may change the stress (and therefore fluid pressure) within the rock. These responses have the potential to significantly change the surface- and groundwater-flow directions, water level, water chemistry, and temperature.

Descriptor Phrases: Water table elevation, Unsaturated flow and pathways in the UZ

Screening Decision: Excluded—Low Consequence and Low Probability

Screening Argument: This FEP addresses the effects of seismic activity on UZ flow and transport at the mountain scale and for drift seepage. It also addresses the possible water table rise in response to seismic activity. The aspects of this FEP related to flow and transport are addressed in Sections 6.7.5 (FEP 2.2.06.01.0A), 6.7.6 (FEP 2.2.06.02.0A), and 6.7.7 (FEP 2.2.06.02.0B). Here we assess the effects of seismically induced water table rise caused by seismic pumping and changes in the large hydraulic gradient.

Seismic pumping (Szymanski 1989 [106963], pp. 3–22) is the temporary increase in height of the water table caused by fault movement. This movement of the water table is caused by the opening and closing of fractures during an earthquake cycle. Longer-term changes result from complex strain adjustments, but these changes are dissipated under the influence of regional stress field, which brings the state of the SZ fracture network back to an ambient, preseismic state as postseismic relaxation occurs. Numerical simulations by Carrigan et al. (1991 [100967]) of tectonohydrological coupling involving earthquakes typical of the Basin and Range province (~ 1 m slip) produced 2 to 3 m excursions of a water table 500 m below ground surface. Extrapolation to an event of about 4 m slip would result in a transient rise of 17 m near the fault (Carrigan et al. 1991 [100967], p. 1159). Changes in the water table along faults is a different story, because permeability along the fault plane is drastically altered by seismic slip (Bruhn 1994 [118920]). This phenomenon results in seismic pumping. Carrigan et al. (1991 [100967]) modeled a 100 m wide fracture zone centered on a vertical fault, such that vertical permeability was increased by 10^3. Water level excursions in the fracture zone were twice as great as in the adjacent block. For a fault-fracture zone with 1 m slip, transient excursions of about 12 m can occur.

The very complex structure of the Paleozoic aquifer beneath Yucca Mountain makes any generalization of water table behavior impossible; local rise is as likely as local fall. The significance of a rise in the water table is that it reduces the barrier capability of the UZ by shortening the flow path from the repository to the SZ. Regardless, data and modeling results indicate that changes in water table elevation at Yucca Mountain are not likely to exceed several meters and are likely to be transient. What seems most reasonable is that the water table excursions caused by earthquakes do not cause sufficient water table level fluctuations to threaten, even temporarily, the repository horizon, which in the current design is approximately 300 m above the water table. Given this limited water table movement, changes to surface- and groundwater-flow directions, water level, water chemistry, and temperature would also be negligible. Therefore, the seismic effects on water table rise resulting from seismic pumping are excluded from TSPA-LA on the basis of low consequence.

Another aspect of the water-table rise issue concerns the large hydraulic gradient that exists north of the repository. North of the repository, the water table elevation decreases by about 250 m as one moves from north to south towards the repository. If this gradient were to migrate southward, the resulting water table below the repository could be much higher than present-day conditions.

The work of Davies and Archambeau (1997 [103180], p. 28) presents a hypothesis that the gradient is a result of stress variations in the rock that are residual stress effects induced by the Timber Mountain caldera. Furthermore, they suggest that moderate earthquakes in this area could induce a sufficient change in geomechanical strain downstream of the current large hydraulic gradient to induce a similar gradient downstream of the repository. This would result in a large (150 m to 250 m) rise in the water table beneath the repository. However, the hypothesis regarding the residual stress effects of the 10 million-year (Ma) Timber Mountain caldera contradicts extensive previous experience in the region of the Nevada Test Site (Stock et al. 1985 [101027]). This composite experience is compiled from 14 sources reporting results from diverse methods, including hydraulic fracturing, overcoring stress measurements, earthquake focal mechanisms, borehole breakouts, orientations of explosion-produced fractures,

and study of Quaternary faults and cinder-cone alignments. These studies show a reasonably uniform direction of extension between northwest and west, with a mixed potential-slip regime of normal faulting (mainly for shallow indicators) and strike-slip faulting (mainly for deep indicators). The Davies and Archambeau discussion is also inconsistent with actual stress measurements in G-2 as reported by Stock and Healy (1988 [101022]), which is cited, though erroneously, as a source of "slug-test" data. Stock and Healy (1988 [101022]) characterize G-2 as being within the same ("combined normal and strike-slip") faulting regime as that indicated by the results from the three holes that they tested south of the large gradient. Based on the stress measurements in the four holes, the tendency for strike-slip faulting is greatest in the southeastern hole, UE-25p#1, not in the northern Yucca Mountain area where G-2 is located, as Davies and Archambeau propose.

The available data do not support a residual stress effect from the Timber Mountain caldera, do not support a modern stress field changing from strike-slip in northern Yucca Mountain to normal south of the hydraulic gradient, and do not support a southward decrease of the least principal stress. Although it is reasonable that the area of the large hydraulic gradient is less transmissive than the area to the south-southeast, a more reasonable explanation for this lower transmissivity is that durable differences of lithology, alteration history, and structural deformation have affected this region, rather than a transient state of stress. Given that this mechanism is inconsistent with the existing data, any associated changes to surface- and groundwater-flow directions, water level, water chemistry, and temperature due to the hypothesized mechanism are not expected. Therefore, the seismic effects on water table rise caused by migration of the large hydraulic gradient are excluded from TSPA-LA on the basis of low probability.

TSPA Disposition: None

6.7.4 Hydrologic Response to Igneous Activity (1.2.10.02.0A)

FEP Description: Igneous activity includes magmatic intrusions, which may alter groundwater flow pathways, and thermal effects which may heat up groundwater and rock. Igneous activity may change the groundwater flow directions, water level, water chemistry, and temperature. Eruptive and extrusive phases may change the topography, surface drainage patterns, and surface soil conditions. This may affect infiltration rates and locations.

Descriptor Phrases: Water table elevation, Unsaturated flow and pathways in the UZ

Screening Decision: Excluded—Low Consequence

Screening Argument: Intrusion of a basalt dike at or near the repository block could present a radical contrast in hydrological properties to the native rock. However, analog studies show that alteration is quite limited, typically only found within 5–10 meters of intrusions (Valentine et al. 1998 [119132], p. 5-74). The effects of local-scale heterogeneity on unsaturated flow and transport at Yucca Mountain were investigated by Zhou et al. (2003 [162133]). The conclusions reached in this study were that local heterogeneity in fracture permeability had a negligible effect on flow. Effects on transport were found to be more significant, but the uncertainty in transport behavior caused by local heterogeneity was less than that caused by uncertainty in matrix

diffusion. Therefore, local variations in properties caused by dike intrusions would result in only minor changes to the flow patterns. Other aspects related to the effects of igneous intrusions, such as mineral alteration, are discussed in Sections 6.7.1 (FEP 1.2.04.02.0A) and 6.7.2 (FEP 1.2.06.00.0A). These aspects were also found to be limited in extent and duration.

Dikes are expected to range between about 0.5 m to 4.5 m in thickness, with an average of 1.5 m (BSC 2003 [166407], Section 6.3.1). A simple conduction-only dike-cooling model indicates that a dike of 5.5 m thickness will cool to sub-boiling in less than 60 years, with boiling temperatures no more than 20 m from the dike (BSC 2003 [165923], Figure 161). Contact metamorphism caused by dikes appears to be confined to distances of less than 5 m from the dike (Simmons 2004 [166960], Section 4.2.3.5). With significant thermal perturbations limited to less than 100 years and alteration limited to zones of a few meters around the dike, the thermal and chemical effects of basaltic magmatism on UZ processes is negligible. The effects on water level are discussed in Section 6.7.3 (FEP 1.2.10.01.0A).

Igneous activity could also affect the ground surface of the repository through eruptions of lava or ash. If lava were to dam one or more washes that drain the repository block the dam would not produce a large surface-water impoundment relative to the repository emplacement area. Such lava dams would probably not be effective in any case, as the lava would consist of clinker or aa (aa is a lava flow with a surface typified by angular, jagged blocks). Another potential effect would be the deposition of an ash cover on the repository block. Ash deposits investigated at the Lathrop Wells cone indicate that grain sizes are typically on the order of 0.2 to 2 mm (BSC 2003 [166407], Section 6.4). This grain size is characteristic of a medium to coarse sand which has a typical porosity range of 0.35 to 0.4 (Bear 1972 [156269], pp. 40 and 46). Using this porosity and grain size range and the modified Kozeny-Carmen equation for permeability (Bear 1972 [156269], p. 166), the estimated permeability range of the ash deposit is 2×10^{-11} to 4×10^{-9} m^2. Bedrock permeability in the infiltration model ranges from 2×10^{-17} to 6×10^{-13} m^2 and soil permeability ranges from 6×10^{-13} to 4×10^{-12} m^2 (USGS 2003 [166518], Attachment IV). Therefore, an ash deposit is expected to be orders of magnitude more permeable than the underlying bedrock and soil. Rainfall will tend to infiltrate and runoff along the ash-bedrock or ash-soil interface resulting in minimal effects of the ash on runoff or infiltration.

As an additional consideration, the mean probability for the occurrence of a volcanic intrusion at Yucca Mountain is 1.7×10^{-8} per year (BSC 2003 [163769], Table 22). This results in a greatly reduced expected consequence from a probability-weighted perspective. Therefore, this FEP is excluded on the basis of low consequence. See Section 6 in this Analysis Report for a discussion explaining why low consequence for specific elements of the UZ system leads to low consequence for total system performance.

TSPA Disposition: None

6.7.5 Seismic Activity Changes Porosity and Permeability of Rock (2.2.06.01.0A)

FEP Description: Seismic activity (fault displacement or vibratory ground motion) has a potential to change rock stresses and result in strains that affect flow properties in rock outside the excavation-disturbed zone. It could result in strains that alter the permeability in the rock matrix. These effects may decrease the transport times for potentially released radionuclides.

Descriptor Phrases: Seismic activity (rock properties in the UZ)

Screening Decision: Excluded—Low Consequence

Screening Argument: This argument is directed towards the effects of seismic activity on the rock matrix. For effects of seismic activity on the rock fractures, see Sections 6.7.6 (FEP 2.2.06.02.0A) and 6.7.7 (FEP 2.2.06.02.0B). The effects of stress changes on flow in the UZ have been investigated by BSC (2004 [167973]). In this model, the effects of thermal stress are evaluated in terms of changes to rock fracture properties but not rock matrix (BSC 2004 [167973], Section 6.2). This modeling approach is based on the approximation that the effects of changes to the rock matrix porosity and permeability caused by changes in rock stress are negligible compared with changes to the fracture porosity and permeability. The basis for this approximation is that the fracture aperture is sensitive to mechanical strain due to the small porosity of the fracture continuum. The matrix, on the other hand, has much greater porosity than the fractures in general, and its properties are not expected to be as sensitive to mechanical strain. This approximation is reasonable given the fact that fracture porosity is much less than matrix porosity at Yucca Mountain. This should be true for other sources of mechanical stress, such as seismic activity. Therefore, changes to the rock matrix characteristics due to seismic activity are excluded from TSPA-LA on the basis of low consequence. See Section 6 in this Analysis Report for a discussion explaining why low consequence for specific elements of the UZ system leads to low consequence for total system performance.

TSPA Disposition: None

6.7.6 Seismic Activity Changes Porosity and Permeability of Faults (2.2.06.02.0A)

FEP Description: Seismic activity (fault displacement or vibratory ground motion) has a potential to produce jointed-rock motion and change stress and strains that alter the permeability along faults. This could result in reactivation of preexisting faults or generate new faults and significantly change the flow and transport paths, alter or short-circuit the flow paths and flow distributions close to the repository, and create new pathways through the repository. These effects may decrease the transport times for potentially released radionuclides.

Descriptor Phrases: Seismic activity (faults in the UZ)

Screening Decision: Excluded—Low Consequence

Screening Argument: This FEP is similar in content to the one discussed in Section 6.7.7 (FEP 2.2.06.02.0B). Like fractures, faulting is a characteristic feature of Yucca Mountain geology. The present-day faults are addressed in the flow and transport models of the UZ (see Section 6.1.3; FEP 1.2.02.02.0A). Fault movements can affect the fracture properties through changes in rock stress. This aspect of the problem is discussed in Section 6.7.7 (FEP 2.2.06.02.0B). Fault movements can also change the properties of the faults themselves, and this aspect has been investigated with a sensitivity study (CRWMS M&O 2000 [151953], Section 6).

Movements produced by a fault displacement will result in changes in the rock stress in the vicinity of the fault. The change in rock stress will decrease with distance from any given fault that does move. However, the magnitude of the changes in rock stress as a function of distance

from the fault depends on the specific details of the fault displacement (e.g., magnitude of fault motion, direction of fault movement, extent of the fault that participates in the movement) and the mechanical properties of the surrounding rock (e.g., fracture spacing, fracture stiffness, geomechanical properties of the rock matrix). Given some change in rock stress, the fractured rock mass will respond to the change in stress through deformation, or strain, in the rock. Note that this induced strain can affect the geometry of fractures in the rock. The effects of stress changes on flow in the UZ have been investigated by BSC (2004 [167973]). In this model, the effects of thermal stress are evaluated in terms of changes to rock fracture properties but not rock matrix (BSC 2004 [167973], Section 6.2; see also Section 6.7.5, FEP 2.2.06.01.0A). This modeling approach is used because the effects of changes to the rock matrix porosity and permeability caused by changes in rock stress are negligible compared with changes to the fracture porosity and permeability. It is reasonable to expect that this should be true for other sources of mechanical stress, such as seismic activity. In theory, the effects of a given fault displacement could be evaluated using process-level calculations for the effects of the induced stress and strain on fracture geometry. However, this direct approach was not further used to specifically evaluate seismic effects because of the large uncertainty in the specification of the seismic event and complexity of translating seismic motion along faults into imposed stresses. An alternative bounding approach was used to assess the potential effects of fault displacement on repository performance (CRWMS M&O 2000 [151953], Section 6.2).

The approach used to investigate the effects of fault displacements was to evaluate the sensitivity of radionuclide transport in the UZ to changes in fracture apertures (CRWMS M&O 2000 [151953], Section 6.2.1.5). This is investigated over a wide enough range to bound the potential changes in fracture aperture that could result from any fault displacement at Yucca Mountain, with an annual exceedance probability of greater than 10^{-8} (see Section 5 in this Analysis Report). The largest fault movement close to the repository is likely to be along the Solitario Canyon fault (CRWMS M&O 2000 [151953], Section 6.1.1). The general topic of seismic hazard at Yucca Mountain has been investigated in detail in the report *Probabilistic Seismic Hazard Analyses for Fault Displacement and Vibratory Ground Motion at Yucca Mountain, Nevada* (USGS 1998 [100354]). For the Solitario Canyon fault, the hazard analysis shows fault displacement 10 m (USGS 1998 [100354], Figure 8.3) at an annual exceedance probability of 10^{-8} (see Section 5 in this Analysis Report). An approximately 10 m fault movement was used as the fault displacement for these analyses. The results of geomechanical models suggest that a factor of 10 change in aperture would bound the effects of tensile strain from such a fault movement (CRWMS M&O 2000 [151953], Section 6.2.1.5). Based on the cubic law for fracture permeability, a factor of 10 change in aperture leads to a factor of 1,000 change in permeability. Fracture permeabilities reduced by a factor of 1,000 were found to be inconsistent with infiltration rates. Therefore, reductions in aperture were limited to factors of 0.2, and in the case of a wetter climate, the lowest value that could be used was a factor of 0.5, leading to permeability reductions of 125 and 8, respectively.

The sensitivity study considered the effects of changes in fracture aperture on porosity, permeability, and capillary pressure (CRWMS M&O 2000 [151953], Section 6.2.1.6). Calculations were then performed for unsaturated flow and transport using the modified fracture properties (CRWMS M&O 2000 [151953], Sections 6.2.2.1 to 6.2.2.4). A subset of these sensitivity calculations considered changes to these hydrological properties restricted to major faults (Solitario Canyon, Ghost Dance, Dune Wash, Bow Ridge, and Sundance faults) for

present-day and glacial transition climates (CRWMS M&O 2000 [151953], Section 6.2.2.4, Figures 17 and 18). The results showed almost no change in transport behavior between the repository and the water table for a range in fracture apertures affected by factors of 0.2 to 10 when only fault fractures are altered.

The conclusions study found that radionuclide transport in the UZ is highly insensitive to the fault properties. Therefore, changes to fault properties due to seismic activity are excluded from TSPA-LA on the basis of low consequence. See Section 6 in this Analysis Report for a discussion explaining why low consequence for specific elements of the UZ system leads to low consequence for total system performance.

TSPA Disposition: None

6.7.7 Seismic Activity Changes Porosity and Permeability of Fractures (2.2.06.02.0B)

FEP Description: Seismic activity (fault displacement or vibratory ground motion) has a potential to change stress and strains that alter the permeability along fractures. This could result in reactivation of preexisting fractures or generation of new fractures. Generation of new fractures and reactivation of preexisting fractures may significantly change the flow and transport paths, alter or short-circuit the flow paths and flow distributions close to the repository and create new pathways through the repository. These effects may decrease the transport times for potentially released radionuclides.

Descriptor Phrases: Seismic activity (fractures in the UZ)

Screening Decision: Excluded—Low Consequence

Screening Argument: Movements produced by a fault displacement will result in changes in the rock stress in the vicinity of the fault. The change in rock stress will decrease with distance from any given fault that does move. However, the magnitude of the changes in rock stress as a function of distance from the fault depends on the specific details of the fault displacement (e.g., magnitude of fault motion, direction of fault movement, extent of the fault that participates in the movement) and the mechanical properties of the surrounding rock (e.g., fracture spacing, fracture stiffness, geomechanical properties of the rock matrix). Given some change in rock stress, the fractured rock mass will respond to the change in stress through deformation, or strain, in the rock. Note that this induced strain can affect the geometry of fractures in the rock. The effects of stress changes on flow in the UZ have been investigated by BSC (2004 [167973]). In this model, the effects of thermal stress are evaluated in terms of changes to rock fracture properties but not rock matrix (BSC 2004 [167973], Section 6.2; see also Section 6.7.5, FEP 2.2.06.01.0A). This modeling approach is used because the effects of changes to the rock matrix porosity and permeability caused by changes in rock stress are negligible compared with changes to the fracture porosity and permeability. It is reasonable to expect that this should be true for other sources of mechanical stress, such as seismic activity. In theory, the effects of a given fault displacement could be evaluated using process-level calculations for the effects of the induced stress and strain on fracture geometry. However, this direct approach was not further used to specifically evaluate seismic effects because of the large uncertainty in the specification of the seismic event and complexity of translating seismic motion along faults into imposed stresses.

An alternative bounding approach was used to assess the potential effects of fault displacement on repository performance (CRWMS M&O 2000 [151953], Section 6.2).

The approach used to investigate the effects of fault displacements was to evaluate the sensitivity of radionuclide transport in the UZ to changes in fracture apertures (CRWMS M&O 2000 [151953], Section 6.2.1.5). This is investigated over a wide enough range to bound the potential changes in fracture aperture that could result from any fault displacement at Yucca Mountain, with an annual exceedance probability of greater than 10^{-8} (see Section 5 in this Analysis Report). The largest fault movement close to the repository is likely to be along the Solitario Canyon fault (CRWMS M&O 2000 [151953], Section 6.1.1). The general topic of seismic hazard at Yucca Mountain has been investigated in detail in the report *Probabilistic Seismic Hazard Analyses for Fault Displacement and Vibratory Ground Motion at Yucca Mountain, Nevada* (USGS 1998 [100354]). For the Solitario Canyon fault, the hazard analysis shows fault displacement 10 m (USGS 1998 [100354], Figure 8.3) at an annual exceedance probability of 10^{-8} (see Section 5 in this Analysis Report). A 10 m fault movement was used as the fault displacement for these analyses. The results of geomechanical models suggest that a factor of 10 change in aperture would bound the effects of tensile strain from a 10 m fault movement (CRWMS M&O 2000 [151953], Section 6.2.1.5). Based on the cubic law for fracture permeability, a factor of 10 change in aperture leads to a factor of 1,000 change in permeability. Fracture permeabilities reduced by a factor of 1,000 were found to be inconsistent with infiltration rates. Therefore, reductions in aperture were limited to factors of 0.2, and in the case of a wetter climate, the lowest value that could be used was a factor of 0.5, leading to permeability reductions of 125 and 8, respectively.

The sensitivity study considered the effects of changes in fracture aperture on porosity, permeability, and capillary pressure (CRWMS M&O 2000 [151953], Section 6.2.1.6). Calculations were then performed for unsaturated flow and transport using the modified fracture properties (CRWMS M&O 2000 [151953], Sections 6.2.2.1 to 6.2.2.4). Fracture permeabilities reduced by a factor of 1,000 were found to be inconsistent with infiltration rates under wetter climate conditions; therefore, rather than reducing infiltration rates, aperture reduction was limited to a factor of 2, leading to a permeability reduction of a factor of 8.

The combined effects of seismic and thermal stresses also have the potential to produce fracture changes. The general effects of thermal stresses on fracture permeability due to repository heating are evaluated in BSC (2003 [167975], Section 6.5.12). This analysis indicates that in the zones near the repository and below the repository, the fracture permeability is either reduced or unaffected. However, radionuclide transport is slower when the fracture permeability is reduced (CRWMS M&O 2000 [151953], Section 6.2.2.4). Therefore, no additional adverse effects result from the combination of seismic-induced and thermally-induced stress changes.

In the context of the TSPA-SR 3-D UZ flow and transport model, sensitivity studies for UZ flow and transport presented in this analysis suggest that transport between the repository and the water table is only weakly coupled to changes in fracture aperture. Overall, insignificant changes in transport behavior are found for large changes in fracture aperture. Breakthrough at some points is found to be at most only about one order of magnitude earlier than the base case (under the present-day or the glacial transition climate), for an extremely conservative ten-fold increase in fracture aperture applied over the entire UZ domain. Effects of such magnitude on travel time

are less significant than those caused by some of the other uncertainties. For example, infiltration uncertainties (BSC 2004 [166883], Section 6.7.3) result in breakthrough curve uncertainties with more than 3 orders of magnitude variation. Therefore, changes to fracture properties due to seismic activity are excluded from TSPA-LA on the basis of low consequence. See Section 6 in this Analysis Report for a discussion explaining why low consequence for specific elements of the UZ system leads to low consequence for total system performance.

TSPA Disposition: None

6.7.8 Seismic Activity Alters Perched Water Zones (2.2.06.03.0A)

FEP Description: Strain caused by stress changes from tectonic or seismic events alters the rock permeabilities that allow formation and persistence of perched-water zones.

Descriptor Phrase: Seismic activity (alters perched water)

Screening Decision: Excluded—Low Consequence

Screening Argument: Perched water zones below the elevation of the repository have been found in site characterization boreholes. The potential to release perched water as a result of stress changes and fracture openings driven by seismic activity should be considered. In that regard, the major bounding scenario identified for TSPA-LA is the sudden release of perched water, with resulting mobilization of radionuclides in the perched water. Although this may only have a small effect on the ultimate cumulative releases of radionuclides to the SZ, it could focus the radionuclide releases in a relatively sharp "pulse" when the perched water is allowed to drain. This possibility has been investigated by considering the volume of perched water in the fracture domain below the repository. The perched water in high-permeability fracture domains is the relevant feature because it is this volume that could potentially be quickly released to the saturated zone. Perched water in the matrix or low-permeability fractures would also ultimately desaturate, but this would be a much slower process and unlikely to cause any temporal pulses of radionuclide flux at the water table. The UZ flow model shows that the volume of perched water in the high-permeability fracture domain below the repository ranges from about 466 m^3 to 1,190 m^3 (see Appendix A in this Analysis Report). This volume may be compared with the water flux entering the repository footprint (i.e., the average infiltration rate times the area of the repository footprint), which ranges from 2,000 m^3/yr to 192,000 m^3/yr (Appendix A in this Analysis Report). As shown in Appendix A in this Analysis Report, the perched-water volume is seen to represent about 0.006 to 0.2 years of water flux. Thus, the perched-water volume in high-permeability fractures is small compared to the water flux through the repository horizon for one year. The radionuclides that could be contained in this water volume is not expected to cause a significant "pulse" in radionuclide mass flux at the water table. Therefore, the effects of changes in perched water due to seismic or tectonic effects are excluded from TSPA-LA due to low consequence. For comparison, note that water table rise caused by climate change in the nominal performance assessment calculations instantly releases radionuclides from a much larger quantity of water in the UZ – on the order of 10^8 m^3 of water (see discussion in Section 6.1.5, FEP 1.3.07.02.0B). (This is an order of magnitude estimate based on the following data: Repository footprint ≈ 10^7 m^2 (5×10^6 m^2) (BSC 2004 [168370]); Water table rise ≈ 100 m (BSC 2003 [166262], Section 6.4.5); Water content of rock ≈ 0.1 (range from 0.1 to 0.3 BSC 2004

[162730], Table 6-6). See Section 6 in this Analysis Report for a discussion explaining why low consequence for specific elements of the UZ system leads to low consequence for total system performance.

TSPA Disposition: None

6.7.9 Undetected Features in the UZ (2.2.12.00.0A)

FEP Description: This FEP is related to undetected features in the UZ portion of the geosphere that can affect long-term performance of the disposal system. Undetected but important features may be present, and may have significant impacts. These features include unknown active fracture zones, inhomogeneities, faults and features connecting different zones of rock, different geometries for fracture zones, and induced fractures due to the construction or presence of the repository.

Descriptor Phrases: Undetected features (flow and pathways in the UZ), Undetected features (fractures in the UZ), Undetected features (faults in the UZ)

Screening Decision: Excluded—Low Consequence

Screening Argument: Two kinds of undetected features are of concern: (1) features which, on the basis of previous investigations, could be thought to be present, (2) features totally unexpected. Features that could be present include buried Plio-Pleistocene basaltic intrusions: such features may be the cause of unresolved anomalies in existing geophysical mapping and investigations of such anomalies are ongoing. As discussed in Section 6.7.4, FEP 1.2.10.02.0A, the effects of small intrusions, or more generally, any heterogeneous features approximating meter scale intrusions (or smaller) are expected to have a negligible effect on flow and transport behavior in the UZ. The scenario that a major, critical feature in the vicinity of Yucca Mountain, such as a large seismogenic fault zone, has been overlooked is not expected, given the extensive site characterization conducted at Yucca Mountain (DOE 1998 [100548], p. 1-1).

Unexpected features encountered in waste emplacement drifts will be assessed in terms of potential standoffs for waste package emplacement. The design criterion for standoff between Type I faults and repository openings is 60 m (Minwalla 2003 [161362], Section 4.11.2). By way of corroboration and clarification, the following standoff requirements have been identified in BSC (2003 [165572], Sections 7.1.3 and 7.3.1):

"It is conservatively estimated that a 60-meter (197 foot) standoff from the trace of any Type I fault is adequate to reduce the impact of potential fault movement. This standoff considers potential fractured ground in proximity of the Type I fault and uncertainty as to where the fault is located at depth. The use of a 60-meter (197-foot) standoff for a LA design is conservatively applied.

In the event that the standoff from repository openings to a Type I fault is waived following a site impact analysis, a standoff must be maintained between Type I faults and any waste package. A standoff must be maintained between splays associated with Type I faults and any waste package. Areas that contain Type I faults should be avoided but, if unavoidable, they must be allowed for in engineering design. It is conservatively estimated that a standoff from the edge

of the Type I fault or fault zone by 15 meters (49-feet) is adequate to reduce the impact of potential fault movement. Using a 15-meter (49-foot) standoff to establish useable drift length for the LA design is conservatively applied."

The major effect of fault features on flow and transport patterns below the repository is to allow downward pathways for flow that has been diverted laterally (BSC 2004 [166883], Sections 6.2.2.1 and 6.6.3). The effects of the fault properties have been found to be much less important (CRWMS M&O 2000 [151953], Section 7). Lateral diversion beneath the repository is affected significantly by the presence of perched water bodies, which are postulated to exist as a result of permeability barriers (BSC 2004 [166883], Sections 6.2.2.2 and 6.6.3). The effects of flow path diversion on transport may be evaluated based on the alternative perched water models presented in BSC (2001 ([158726], Section 6.2.2). Perched water models #1 and #2 are named the "flow through" perched water model and "by-passing" perched water model, respectively (BSC 2001 [158726], Section 6.2.2). For model #1, the minimum permeability barriers are introduced to produce the known perched water bodies. For model #2, all zeolitic units are modeled as unfractured and result in more extensive perched water. As the names imply, there is less lateral diversion in model #1 as compared with model #2 (BSC 2001 [158726], Section 6.2.5). An extreme case is "no perched water" model #3, which does not introduce any permeability barrier, leading to minimal lateral flow. However, this model is not supported by the data because it does not predict perched water where such features are known to exist.

Comparisons for transport between the repository and the water table for the three perched water models were performed using sorbing and nonsorbing radionuclides (BSC 2001 [158726], Section 6.7.2). The transport results for perched water models #1 and #2 have only minor differences (BSC 2001 [158726], Figures 6-54 through 6-56). Although early breakthroughs are more substantial for model #3, transport times are about the same or longer after 1,000 years for both sorbing and nonsorbing radionuclides. Furthermore, the effect of a finite number of undetected fault features that could potentially act as pathways to the water table necessarily has less impact on flow pathways than model #3, as evidenced by the existence of large perched water bodies. Therefore, this FEP is excluded based on low consequence. See Section 6 in this Analysis Report for a discussion explaining why low consequence for specific elements of the UZ system leads to low consequence for total system performance.

TSPA Disposition: None

6.8 REPOSITORY-PERTURBED THMC

This group of FEPs is excluded from the TSPA-LA calculation. These FEPs concern the effects of changes to the thermal/hydrological/mechanical/chemical (THMC) environment as a result of repository excavations, heat, and materials, and the effects of these changes on hydrological, geochemical, and geomechanical processes.

Table 6-11 gives the FEP numbers and names categorized under Repository Perturbed THMC.

Table 6-11. Excluded FEPs: Repository Perturbed THMC

Section Number	FEP Number	FEP Name
6.8.1	2.1.09.12.0A	Rind (chemically altered zone) forms in the near-field
6.8.2	2.2.01.01.0B	Chemical effects of excavation/construction in the near-field
6.8.3	2.2.01.02.0A	Thermally-induced stress changes in the near-field
6.8.4	2.2.01.03.0A	Changes in fluid saturations in the excavation disturbed zone
6.8.5	2.2.01.04.0A	Radionuclide solubility in the excavation disturbed zone
6.8.6	2.2.01.05.0A	Radionuclide transport in the excavation disturbed zone
6.8.7	2.2.08.03.0B	Geochemical interactions and evolution in the UZ
6.8.8	2.2.08.07.0B	Radionuclide solubility limits in the UZ
6.8.9	2.2.10.01.0A	Repository-induced thermal effects on flow in the UZ
6.8.10	2.2.10.04.0A	Thermo-mechanical stresses alter characteristics of fractures near repository
6.8.11	2.2.10.04.0B	Thermo-mechanical stresses alter characteristics of faults near repository
6.8.12	2.2.10.05.0A	Thermo-mechanical stresses alter characteristics of rocks above and below the repository
6.8.13	2.2.10.06.0A	Thermo-chemical alteration in the UZ (solubility, speciation, phase changes, precipitation/dissolution)
6.8.14	2.2.10.07.0A	Thermo-chemical alteration of the Calico Hills unit
6.8.15	2.2.10.09.0A	Thermo-chemical alteration of the Topopah Spring basal vitrophyre
6.8.16	2.2.10.14.0A	Mineralogic dehydration reactions

DTN: MO0307SEPFEPS4.000 [164527]

6.8.1 Rind (chemically altered zone) Forms in the Near-Field (2.1.09.12.0A)

FEP Description: Thermal-chemical processes involving precipitation, condensation, and re-dissolution alter the properties of the adjacent rock. These alterations may form a rind, or altered zone, in the rock, with hydrological, thermal, and mineralogical properties different from the initial conditions.

Descriptor Phrases: Time-dependent THC characteristics in near-field (precipitates, sorption), Chemical alteration of near-field fractures

Screening Decision: Excluded—Low Consequence

Screening Argument: The thermal-chemical interactions that will occur in the repository environment have been studied with respect to effects on the seepage water entering the waste emplacement drifts using the THC Seepage Model (BSC 2004 [167974]). This model, which explicitly captures the effects of changes in temperature, pH, Eh, ionic strength (and other compositional variables), time dependency, precipitation/dissolution effects, and effects of resaturation, was used to examine near-field and drift seepage flow and chemistry (BSC 2004 [167974], Section 6.2). Changes in fracture permeabilities were found to be on the order of the natural variation in these properties (BSC 2004 [167974], Section 6.6.2.3.1), with most of the substantial effects limited to regions above and to the side of the drift within about a drift diameter (BSC 2004 [167974], Figures 6.5-16, 6.6-4, 6.8-40b, 6.8-41b). The predicted mineral precipitation reduces permeability in the affected regions and leads to a reduction in flow around the drift. Likewise, any mineralogical changes are of very limited extent below the drift, resulting in negligible effects on radionuclide sorption. THC effects on fracture characteristics

have been evaluated with process models that explicitly account for fracture flow affected by THC parameter alterations (BSC 2004 [167970], Section 6.4.4.2). It was demonstrated that the effects of these potential alterations on near-field and drift seepage flow can be neglected in the TSPA-LA, because the expected changes would lead to less seepage (BSC 2004 [167970], Section 6.5.1.4). Consequently, neglect of this effect is likely to result in slightly conservative model predictions for both drift seepage and radionuclide transport phenomena. Therefore, this FEP is excluded on the basis of low consequence because it has no adverse effects on performance. See Section 6 in this Analysis Report for a discussion explaining why low consequence for specific elements of the UZ system leads to low consequence for total system performance.

Note that the THC effects (e.g., mineral precipitation) on fracture characteristics as they relate to near-field and drift seepage chemistry were also evaluated with the THC Seepage Model. A discussion is provided in Section 6.1.11 (FEP 2.2.03.02.0A).

TSPA Disposition: None.

6.8.2 Chemical Effects of Excavation/Construction in the Near-Field (2.2.01.01.0B)

FEP Description: Excavation may result in chemical changes to the incoming groundwater and to the rock in the excavation disturbed zone.

Descriptor Phrases: Chemical alteration of EDZ fractures, Chemical effects from rock reinforcement material on in-flowing water

Screening Decision: Excluded—Low Consequence

Screening Argument: This FEP concerns the changes in the host rock environment immediately surrounding the waste emplacement drifts. Changes are expected in the rock fracture properties due to excavation disturbance, stress relief around the opening, and ground support. However, these changes will not affect water chemistry. Excavation will introduce water (for dust control), but this should not have any significant affect on water chemistry. This is based on the limited volumes of water that are typically lost during underground excavation (e.g., for ESF construction the average was approximately $1 m^3/m^2$ of the projected horizontal area of an excavation (BSC 2002 [160689], Section 13.2.16)). Furthermore, any water that remains local to the emplacement drifts will be more strongly affected by the thermal dryout. Any construction water that penetrates the UZ deeply through fractures is not likely to have any significant interaction with released radionuclides. The ground support for the emplacement drifts can affect water flow patterns in the immediate vicinity of the drift and can affect the aqueous geochemistry in the drift environment and along flow pathways from the drift to the water table. However, detailed simulations were made using the predictive Seepage Model for PA (BSC 2003 [163226], Section 6.5) to study the effect of rock bolts in the drift crown on seepage into drifts. The effect of these features were found to have only a minor effect on seepage (less than 2% (BSC 2003 [163226], Table 6-4)), owing to the small area for water to enter the rock-bolt boreholes from the surrounding formation (BSC 2004 [167970], Section 6.4.2.5). From these results, the presence of rock bolts is not considered a relevant factor for seepage into drifts. Based on this finding, only a minor quantity of the total water intercepting a

drift is likely to move through rock-bolt pathways. Other ground-support materials will not affect flow patterns in the rock, because these materials are entirely within the emplacement drift.

Identified ground-support materials in the waste emplacement drifts are steel sets (ASTM A 572), pipe spacers used with steel sets (ASTM A 53), tie rods used with steel sets (ASTM A 397), and SS 316L stainless steel rock bolts, wire mesh, and sheets (ASTM A 276) (BSC 2003 [164101]). The principal ground support in the emplacement drifts is expected to be SS 316L rock bolts and steel sheets (BSC 2003 [164101], p. 1). A model of the effects of steel ground support on aqueous chemistry was recently generated (BSC 2004 [167461], Section 6.8). The model considered the interaction of "Bin 11" water with SS 316L ground support materials. Interaction with the abstracted "Bin 11" seepage water was chosen, because this is the most likely water to be present, occurring in almost 40% of the abstracted periods (BSC 2004 [167461], Table 6.6-4). In addition, this Bin 11 water is seen to occur during the relevant period for the corrosion of 316L stainless steel, in the range of ~500 to 5,000 years for four of the five seepage water compositions shown in BSC (2004 [167461], Tables 6.6-8 through 6.6-12). The effect of dissolving the abstracted SS316L steel species into Bin 11 water was found to be negligible. The Bin 11 water with and without the 5.52E–5 moles of SS316L added was found to only have two differences in the water chemistries at the 6th significant figure for ionic strength and C total molality (BSC 2004 [167461], Section 6.8.4.3). Use of "Bin 7" seepage water was selected as an uncertainty case and is described in BSC (2004 [167461], Section 6.12.4.1). There is effectively no change in the aqueous water chemistry caused by abstracted stainless steel corrosion and corrosion product formation in this case, as with the basecase Bin 11 seepage water (BSC 2004 [167461], Section 6.12.4.1.3).

Cementitious materials (shotcrete) are planned for use as part of the ground support for the turnouts of repository emplacement drifts (BSC 2003 [164052], p. 1). These materials can result in changes in water composition, particularly alkalinity and sulfate concentration (Hardin 1998 [100123], Section 6.3.4). However, the lateral offset between such materials and waste emplacement will ensure that these materials do not affect waste emplacement drifts. The potential effect of such materials on radionuclide transport is also greatly reduced because of the mainly vertical flow patterns in the host rock. Water is expected to move in a general vertical flow pattern through the waste emplacement horizon relative to the length scale of these drifts, with some flow diversion around the drifts resulting from the capillary barrier effect. This flow pattern is consistent with the drift-scale seepage model having no-flow lateral boundary conditions (BSC 2003 [163226], Section 6.3.1). Lateral flow beneath the repository (particularly at zeolitic interfaces) may lead to some interaction between radionuclide pathways and water affected by cementitious ground support materials. However, several factors, including buffering of the alkalinity by the rock mass, carbonation of the cement by CO_2, and the generally low levels of lateral dispersion between streamlines, indicate that this should have a negligible effect on radionuclide transport. The low levels of lateral dispersion are apparent in the simulations of chloride plumes (BSC 2004 [167975], Section 6.4.3.3.2, Figure 6.4-15) in which the plume variations between individual drifts and pillars between drifts are maintained from the repository to the water table. See Section 6 in this Analysis Report for a discussion explaining why low consequence for specific elements of the UZ system leads to low consequence for total system performance.

Therefore, this FEP is excluded on the basis of low consequence.

TSPA Disposition: None.

6.8.3 Thermally-Induced Stress Changes in the Near-Field (2.2.01.02.0A)

FEP Description: Changes in host rock properties result from thermal effects or other factors related to emplacement of the waste. Properties that may be affected include rock strength, fracture spacing and block size, and hydrologic properties such as permeability and sorption.

Descriptor Phrases: Thermal-mechanical effects on EDZ fractures, Thermal-mechanical effects on near-field fractures

Screening Decision: Excluded—Low Consequence

Screening Argument: The results of the coupled drift-scale THM model presented in BSC (2004 [167973], Sections 6.5 and 6.6) shows that the impact of time-dependent THM processes will last for well over 10,000 years, but these processes have a small or moderate impact on the drift scale TH behavior, including a negligible impact on the temperature evolution and small impact on the percolation flux (BSC 2004 [167973], Section 6.7). These model results were obtained for a conservative estimate of input THM properties (thermal expansion coefficient and stress versus permeability function), which is sufficient for bounding the possible impact of the THM processes on permeability and percolation flux.

The THM simulations discussed in BSC (2004 [167970], Section 6.4.4.1) suggest that temperature-induced stress changes give rise to changes in the vertical fracture permeability in the vicinity of waste emplacement drifts, in particular in the Tptpmn unit (BSC 2004 [167970], Section 6.5.1.4). However, these permeability changes do not result in significant changes in the flow fields BSC (2004 [167973], Sections 6.5.5 and 6.6.2). In particular, the seepage rates calculated for a permeability field including THM permeability changes were similar to, but slightly smaller than, those calculated for a permeability field representative of the initial post-excavation conditions. The simulation results from BSC (2004 [167973]) provide reasonably accurate (slightly conservative) estimates of the expected seepage rates at long-term conditions with coupled THM property changes (BSC 2004 [167970], Section 6.4.4.1). Therefore, the impact of THM property changes is neglected in the seepage abstraction.

The overall effect of THM coupled processes on drift-scale radionuclide transport may also be excluded, because the primary effect of THM processes leads to enhanced seepage diversion and reduced drift seepage, reduced water saturations beneath the drift, and therefore greater partitioning of radionuclide releases to the rock matrix. Therefore, this FEP is excluded based on low consequence because it has no adverse effects on performance. See Section 6 in this Analysis Report for a discussion explaining why low consequence for specific elements of the UZ system leads to low consequence for total system performance.

TSPA Disposition: None

6.8.4 Changes in Fluid Saturations in the Excavation Disturbed Zone (2.2.01.03.0A)

FEP Description: Fluid flow in the region near the repository will be affected by the presence of the excavation, waste, and EBS. Some dry-out will occur during excavation and operations.

Descriptor Phrases: Flow in the EDZ, Saturation decrease in the EDZ, Saturation increase in the EDZ, Pre-closure ventilation (fluid removal from EDZ)

Screening Decision: Excluded—Low Consequence

Screening Argument: Sensitivity studies in BSC (2001 [155950], Section 5.3.2.4.4) indicate that inclusion of preclosure dryout gives rise to slightly higher temperatures during the heating period compared to a model that ignores the influence of preclosure dryout. However, inclusion of preclosure dryout is not significant for thermal seepage (BSC 2003 [166512], Section 6.2.1.3.3). The overall effect of ventilation dryout on drift-scale radionuclide transport may also be excluded, because thermal dryout and rewetting will erase nearly any effect of the ventilation dryout. Therefore, this FEP may be excluded based on low consequence. See Section 6 in this Analysis Report for a discussion explaining why low consequence for specific elements of the UZ system leads to low consequence for total system performance.

Other aspects of this FEP are discussed elsewhere. For the effects of the excavation on fluid flow, see Section 6.1.26, FEP 2.2.07.20.0A; for the effects of waste heat on fluid flow see Sections 6.1.38, FEP 2.2.10.10.0A and 6.1.39, FEP 2.2.10.12.0A; for the effects of the EBS (rock bolt holes) on fluid flow see Section 6.2.2 FEP 1.1.01.01.0B.

TSPA Disposition: None.

6.8.5 Radionuclide Solubility in the Excavation Disturbed Zone (2.2.01.04.0A)

FEP Description: Radionuclide solubility limits in the excavation-disturbed zone may differ from those in the EBS.

Descriptor Phrases: Radionuclide solubility (concentration) limits in the EDZ, Radionuclide solubility in the EDZ

Screening Decision: Excluded—Low Consequence.

Screening Argument: If solubility limits are lower in the EDZ than in the emplacement drifts, then more radionuclides will precipitate as water flows out of the drifts. This corresponds to fewer dissolved radionuclides being available for transport into the geosphere, which is beneficial and results in no adverse effects on performance. See also Section 6.8.6 (FEP 2.2.01.05.0A) for additional information on this subject. If solubility limits are higher in the EDZ than in the emplacement drifts, then there is no effect on transport because all available radionuclides from the emplacement drift are already aqueous species.

Solubility limits could also affect the formation of certain kinds of true colloids, such as polymeric forms of plutonium oxide (BSC 2003 [166845], Figure 1b). However, these forms of

colloids have not been observed to form in experiments on waste form degradation (BSC 2003 [166845], Section 6.3.1). Furthermore, these colloids are expected to undergo formation of pseudocolloids in the near-field aquifer system (BSC 2003 [166845], Section 6.3.1) and are, therefore, excluded.

Therefore, the effects of different solubility limits in the EDZ are excluded from TSPA-LA on the basis of low consequence. See Section 6 in this Analysis Report for a discussion explaining why low consequence for specific elements of the UZ system leads to low consequence for total system performance.

TSPA Disposition: None

6.8.6 Radionuclide Transport in the Excavation Disturbed Zone (2.2.01.05.0A)

FEP Description: Radionuclide transport through the excavation disturbed zone may differ from transport in the EBS and the undisturbed host rock. Transport processes such as dissolution and precipitation, sorption, and colloid filtration should be considered.

Descriptor Phrases: Effects of the EDZ on transport, Effects of alteration of fractures on transport in the EDZ

Screening Decision: Excluded—Low Consequence

Screening Argument: This FEP refers to the effects of altered fracture properties in the disturbed zone immediately surrounding the waste emplacement drifts on radionuclide transport. The effects of changes in fracture aperture on radionuclide transport were investigated at the mountain scale (see Section 6.7.7; FEP 2.2.06.02.0B). The results of this analysis indicate that transport behavior is relatively insensitive to changes in fracture aperture by as much as a factor of 10. Drift-scale radionuclide transport analyses showed that the partitioning of radionuclides between fractures and matrix upon exiting the drift is also dependent upon the fracture water content (BSC 2004 [167959], Sections 6.4 and 6.4.2). This parameter is treated as uncertain in the drift-scale transport model (BSC 2004 [167959], Section 6.4.5). However, the uncertainty in fracture water content is dominated by the uncertainty in fracture residual saturation. The uncertainty for fracture residual saturation uses a broad range (0.001 to 0.1) based on experimental data for higher permeability capillary materials (BSC 2004 [167959], Section 6.4.5). However, due to limited information regarding functional dependencies, this is not treated as a function of fracture aperture. Therefore, the neglect of the EDZ is not significant in terms of uncertainty for the residual saturation. Investigations on the effects of stress relief on fracture permeability in the EDZ have found that the vertical permeability beneath the drift is affected over a very narrow zone, on the order of 1 to 2 meters for changes in permeability more than a factor of 2 (BSC 2004 [167973], Sections 6.5.1 and 6.6.1). Therefore, the limited extent of the EDZ compared with the overall transport path length in the UZ (approximately 300 m) also leads to the conclusion that the effects of the excavation disturbed zone is negligible for colloid and radionuclide transport. Therefore, the effects of altered fracture properties in the EDZ are excluded from TSPA-LA on the basis of low consequence. See Section 6 in this Analysis Report for a discussion explaining why low consequence for specific elements of the UZ system leads to low consequence for total system performance.

The effects of precipitation of aqueous radionuclides on transport in the excavation disturbed zone are also excluded (see Section 6.8.5; FEP 2.2.01.04.0A). Excluding precipitation for radionuclides that undergo simple decay is conservative because this can only enhance the radionuclide mass flux at the accessible environment. For radionuclides that undergo chain decay, excluding precipitation will be conservative because the radionuclide source is not significantly depleted within the 10,000-year regulatory time period. In the latest total-system performance assessment, dose rates for all radionuclides are predicted to increase over tens of thousands of years (CRWMS M&O 2000 [153246], Figures 4.1-5 and 4.1-7). This is a result of the spread of waste package failures over time (CRWMS M&O 2000 [153246], Figures 4.1-9) and the slow release of radionuclides from the waste emplacement drifts. Therefore, during the 10,000-year period, the highest concentration for any radionuclide at the receptor is expected to occur under conditions giving the greatest transport rates. Reduced solubilities for neptunium americium, plutonium, thorium, and uranium were investigated as a sensitivity in TSPA-SR (CRWMS M&O 2000 [153246], Sections 3.5.5, 4.1.3, and Figures 4.1-19a and 4.1-20). The dose rates for radionuclides affected by the lower solubilities (including decay products such as Ra226) were found to be lower in the reduced-solubility case. This leads to the conclusion that suppressing precipitation of radionuclides in the TSPA-LA is expected to result in higher dose rates. Therefore, precipitation of radionuclides can be excluded because it has no adverse effects on performance.

TSPA Disposition: None

6.8.7 Geochemical Interactions and Evolution in the UZ (2.2.08.03.0B)

FEP Description: Groundwater chemistry and other characteristics, including temperature, pH, Eh, ionic strength, and major ionic concentrations, may change through time, as a result of the evolution of the disposal system or from mixing with other waters. Geochemical interactions may lead to dissolution and precipitation of minerals along the groundwater flow path, affecting groundwater flow, rock properties and sorption of contaminants. Effects on hydrologic flow properties of the rock, radionuclide solubilities, sorption processes, and colloidal transport are relevant. Kinetics of chemical reactions should be considered in the context of the time scale of concern.

Descriptor Phrases: Time-dependent THC characteristics in the UZ (temperature, pH, Eh, water conc., gas conc., ionic strength), Time-dependent chemical effects on sorption in the UZ, Effects of precipitation/dissolution in the UZ, Effects of weathering in the UZ, Chemical alteration of near-field fractures, Chemical effects of infiltration in the UZ, Effects of resaturation of dry-out zone (UZ geochemistry)

Screening Decision: Excluded—Low Consequence

Screening Argument: The thermal-chemical interactions that will occur in the repository environment have been studied with respect to effects on the seepage water entering the waste emplacement drifts using the THC Seepage Model (BSC 2004 [167974]). This model, which explicitly captures the effects of changes in temperature, pH, Eh, ionic strength (and other compositional variables), time dependency, precipitation/dissolution effects, and effects of resaturation, was used to examine near-field and drift seepage flow and chemistry (BSC 2004

[167974], Section 6.2). Changes in fracture permeabilities were found to be on the order of the natural variation in these properties (BSC 2004 [167974], Section 6.6.2.3.1), with most of the substantial effects limited to regions above and to the side of the drift within about a drift diameter (BSC 2004 [167974], Figures 6.5-16, 6.6-4, 6.8-40b, 6.8-41b). The predicted mineral precipitation reduces the permeability in the affected regions, and leads to a reduction in flow around the drift. This is conservative for both flow and transport phenomena and, therefore, neglect of these types of permeability changes on near-field and drift seepage flow has no adverse effects on repository performance. Note that the effects of mineral precipitation on fracture permeability as it relates to near-field and drift seepage chemistry was also evaluated with the THC Seepage Model. A discussion is provided in Section 6.1.11, FEP 2.2.03.02A.

Two alternative conceptualizations of the modeled geochemical system were used for the model. The systems were denoted as "base case" and "extended case," and differ somewhat from one model variation to another (BSC 2004 [167974], Table 6.2-2). The extended case includes the major solid phases (minerals and glass) encountered in geological units at Yucca Mountain, together with a range of possible reaction product minerals, CO_2 gas, and the aqueous species necessary to include these solid phases and the pore-water composition within the THC model. The base case is a subset of the extended case excluding aluminum silicate minerals, which form or dissolve much less easily than minerals such as calcite or gypsum, and for which thermodynamic and kinetic data are not as well established as for the other minerals. As such, the base-case system conceptualizes a geochemical system in which aluminum silicate minerals are nonreactive. The base-case system also does not include Fe- and Mg-bearing phases and aqueous species.

Compositional changes were only calculated near the drift boundary for the drift-scale THC seepage model (BSC 2004 [167974]). Results from the extended and base case models show most compositional variations returning to unperturbed conditions in 10,000 years or less. Variations in pH (BSC 2004 [167974], Figures 6.5-9, 6.7-11, 6.8-13), a key compositional variable for sorption of some radionuclides (BSC 2003 [163228], Attachment I), roughly lie within the range of variability investigated for initial pore-water compositions (BSC 2004 [167974], Table 6.2-1). Bicarbonate is found to be depressed in concentration upon water resaturation at the drift wall, as expected based on the reduced pH values for the same time period.

Results were also investigated for the Tptpll (lower lithophysal unit) model considering a range of initial pore-water compositions. In this model, five different initial pore water compositions were investigated (BSC 2004 [167974], Table 6.2-1). Peak concentrations usually found at the time of rewetting in both models reflect mostly the small values of the first non-zero liquid-saturation output. In any case, elevated concentrations are predicted only for small liquid saturations that are not subject to significant fluid movement. The improved treatment of mineral precipitation at the boiling front used in the most recent THC model for the Tptpll also results in the prediction of lower, more realistic aqueous silica concentrations than in earlier models (BSC 2004 [167974], Figure 6.8-17). This model also predicts upon rewetting, more rapid return to near-ambient conditions for aqueous Ca, Na, and Cl.

The findings indicate that at the drift wall, most of the significant compositional variations resulting from thermal-chemical processes are limited to low-saturation conditions over time

periods that are short relative to the 10,000-year performance period. Similar magnitudes of variation in chloride and pH were found in the mountain-scale THC model results (BSC 2004 [167975], Section 6.4.3.3.2). The magnitudes of the variations are found to be smaller at greater distances from the drift wall. As for the drift-scale study, variations in chloride are driven mainly by evaporation and are found to return to near-ambient values upon rewetting (BSC 2004 [167975], Section 6.4.3.3.2). Variations in pH were found to lie roughly between 7 and 9, which is similar to the results for the drift-scale THC model (BSC 2004 [167974], Figures 6.5-9, 6.7-11, 6.8-13). The most persistent change in pH is a level of about 7 in the Calico Hills (BSC 2004 [167975], Section 6.4.3.3.2, Figure 6.4-17), but this lies within the range of pH investigated for radionuclide sorption (BSC 2003 [163228], Attachment I). Therefore, the effects of these changes are excluded from TSPA-LA on the basis of low consequence. See Section 6 in this Analysis Report for a discussion explaining why low consequence for specific elements of the UZ system leads to low consequence for total system performance.

TSPA Disposition: None.

6.8.8 Radionuclide Solubility Limits in the UZ (2.2.08.07.0B)

FEP Description: Solubility limits for radionuclides may be different in unsaturated zone groundwater than in the water in the waste and EBS.

Descriptor Phrase: Radionuclide solubility (concentration) limits in the UZ

Screening Decision: Excluded—Low Consequence

Screening Argument: If solubility limits are lower in the geosphere than in the emplacement drifts, then more radionuclides will precipitate there. This corresponds to fewer dissolved radionuclides being available for transport in the geosphere, which is beneficial and results in no adverse effects on performance. See also Section 6.8.6 (FEP 2.2.01.05.0A) for additional information on this subject. If solubility limits are higher in the geosphere than in the emplacement drifts, then there is no effect on transport because all available radionuclides from the emplacement drift are already aqueous species.

Solubility limits could also affect the formation of certain kinds of true colloids, such as polymeric forms of plutonium oxide (BSC 2003 [166845], Figure 1b). However, these forms of colloids have not been observed to form in experiments on waste form degradation (BSC 2003 [166845], Section 6.3.1). Furthermore, these colloids are expected to undergo formation of pseudocolloids in the near- or far-field aquifer system (BSC 2003 [166845], Section 6.3.1) and are, therefore, excluded.

Therefore, the effects of different solubility limits in the geosphere are excluded from TSPA-LA on the basis of low consequence. See Section 6 in this Analysis Report for a discussion explaining why low consequence for specific elements of the UZ system leads to low consequence for total system performance.

TSPA Disposition: None

6.8.9 Repository-Induced Thermal Effects on Flow in the UZ (2.2.10.01.0A)

FEP Description: Thermal effects in the geosphere could affect the long-term performance of the disposal system, including effects on groundwater flow (e.g., density-driven flow), mechanical properties, and chemical effects in the UZ.

Descriptor Phrases: Thermal effects on flow in the UZ, Time-dependent THC characteristics in the UZ (temperature, pH, density), Repository edge effects on flow in the UZ

Screening Decision: Excluded—Low Consequence

Screening Argument: Thermal-hydrological modeling at the mountain scale has been performed using 2-D cross-sectional and 3-D dual-permeability models (BSC 2004 [167975], Section 6.1.2). During the early part of the heating period, important TH processes occur near the emplacement drifts. The mountain-scale models are used to capture the TH behavior at later times, when the perturbation in temperature, and fracture and matrix liquid saturation, extends over a much larger space domain compared to the drift-scale effects. These mountain-scale TH processes include repository edge effects, large-scale enhanced water and gas flow, and potential alteration of perched-water bodies. Results from the modeling indicate that the induced flow from TH processes are much smaller than changes in flow resulting from climate change at 600 and 2,000 years (BSC 2004 [167975], Figures 6.2-10a and b, 6.3.1-18), which are included in the flow and transport models (Section 6.1.4, FEP 1.3.01.00.0A). Percolation flux maps at the top of the CHn for the ambient and thermally perturbed case (at 500 years of heating) show very similar flow patterns with the exception of reduced flow through a central portion of the waste emplacement area under the thermally perturbed case (BSC 2004 [167975], Figures 6.3.1-16a and b). For thermal effects on chemical processes, see Section 6.8.7, FEP 2.2.08.03.0B. For thermal effects on mechanical processes, see Section 6.8.10, FEP 2.2.10.04.0A.

Numerical simulations of flow at 100 years and 500 years after emplacement show reduced fracture saturation and diversion of percolating water around the dryout zone (BSC 2003 [166512], Section 6.2.2.1). Because of the flow diversion, the dryout is more extensive and longer lasting beneath the drift; this is called the “drift shadow” effect. Note that there is no water flux inside the dryout region, because fracture saturation is zero. After resaturation in 1,000 to 2,000 years, saturations below the drift remain smaller than above, because of the “shadow zone” created by the diversion of flow around the drift (BSC 2003 [166512], Section 6.2.2.1). In general, the TH dryout and associated coupled processes will lead to an environment where radionuclide transport in the vicinity of the drift is less likely (BSC 2003 [166512], Section 6.2.2.1.1; BSC 2004 [167974], Section 6.8.5.4).

The effects of repository heat and the associated dryout on shallow infiltration at the surface of Yucca Mountain were investigated in CRWMS M&O (1999 [105031]). The primary issue for thermal effects at the ground surface is the change in temperature and its associated effect on vegetation. Based on the detailed analysis of soil temperature changes documented in CRWMS M&O (1999 [103618]), the temperature rise will have a negligible effect on vegetation, and hence on surface infiltration.

Therefore, this FEP is excluded from TSPA-LA, based on low consequence. See Section 6 in this Analysis Report for a discussion explaining why low consequence for specific elements of the UZ system leads to low consequence for total system performance.

Note that the effects of thermal-hydrologic processes on drift seepage and seepage water chemistry are addressed in Sections 6.1.21, FEP 2.2.07.10.0A; 6.1.22, FEP 2.2.07.11.0A; 6.1.35, FEP 2.2.08.12.0A; 6.1.38, FEP 2.2.10.10.0A; and 6.1.39, FEP 2.2.10.12.0A.

TSPA Disposition: None

6.8.10 Thermo-Mechanical Stresses Alter Characteristics of Fractures near Repository (2.2.10.04.0A)

FEP Description: Heat from the waste causes thermal expansion of the surrounding rock, generating changes in the stress field that may change the fracture properties (both hydrologic and mechanical) of fractures in the rock. Cooling following the peak thermal period will also change the stress field, further affecting fracture properties near the repository.

Descriptor Phrases: Thermal-mechanical effects (fractures in the UZ), Thermal-mechanical effects (stress change)

Screening Decision: Excluded – Low Consequence

Screening Argument: The results of the coupled drift-scale Thermal-Hydrological-Mechanical (THM) model presented in BSC (2004 [167973], Sections 6.5 and 6.6) show that the impact of time-dependent, THM processes will last for well over 10,000 years, but these processes have a small or moderate impact on the drift scale TH behavior, including a negligible impact on the temperature evolution and small impact on the percolation flux (BSC 2004 [167973], Section 6.7). These model results were obtained for a conservative estimate of input THM properties (thermal expansion coefficient and stress versus permeability function), which is sufficient for bounding the possible impact of the THM processes on permeability and percolation flux.

The THM simulations discussed in BSC (2004 [167970], Section 6.4.4.1) suggest that temperature-induced stress changes give rise to changes in the vertical fracture permeability in the vicinity of waste emplacement drifts, particularly in the Tptpmn unit (BSC 2004 [167970], Section 6.5.1.4). However, these permeability changes do not result in significant changes in the flow fields BSC (2004 [167973], Sections 6.5.5 and 6.6.2). In particular, the seepage rates calculated for a permeability field including THM permeability changes were similar to, but slightly smaller than, those calculated for a permeability field representative of the initial post-excavation conditions. The simulation results from BSC (2004 [167973]) provide reasonably accurate (slightly conservative) estimates of the expected seepage rates at long-term conditions with coupled THM property changes (BSC 2004 [167970], Section 6.4.4.1). Therefore, the impact of THM property changes is neglected in the seepage abstraction.

The overall effect of THM coupled processes on drift-scale radionuclide transport may also be excluded because the primary effect of THM processes leads to enhanced seepage diversion and reduced drift seepage, reduced water saturations beneath the drift, and therefore, greater partitioning of radionuclide releases to the rock matrix. Therefore this FEP may be excluded

based on low consequence because it has no adverse effects on performance. See Section 6 in this Analysis Report for a discussion explaining why low consequence for specific elements of the UZ system leads to low consequence for total system performance.

TSPA Disposition: None.

6.8.11 Thermo-Mechanical Stresses Alter Characteristics of Faults near Repository (2.2.10.04.0B)

FEP Description: Heat from the waste causes thermal expansion of the surrounding rock, generating changes to the stress field that may change the fault properties (both hydrologic and mechanical) in and along faults. Cooling following the peak thermal period will also change the stress field, further affecting fault properties near the repository.

Descriptor Phrases: Thermal-mechanical effects (faults in the UZ), Thermal-mechanical effects (stress change)

Screening Decision: Excluded—Low Consequence

Screening Argument: The primary differences represented by faults, as compared with the general fractured rock mass, for flow, transport, drift seepage, and coupled processes, are the greater permeability and potential continuity of high-permeability pathways through the UZ. Thermal-mechanical effects on fault-fractures may be expected to be qualitatively similar to rock-mass fractures in the sense that THM processes will lead to reductions in vertical permeabilities but increased horizontal permeability above the drift. Faults may be viewed as a specific type of heterogeneity in the fractured rock mass. From this viewpoint, BSC (2004 [167973], Section 6.8.5) indicates that the main effect of THM processes is on the mean permeability, and that it is appropriate to apply the mean permeability changes to a seepage analysis that considers either the homogenous or heterogeneous permeability field. This is the approach is presented in Section 6.8.10, FEP 2.2.10.04.0A. Therefore, the screening arguments used in Section 6.8.10, FEP 2.2.10.04.0A also apply here, and consequently this FEP may be excluded on the basis of low consequence. See Section 6 in this Analysis Report for a discussion explaining why low consequence for specific elements of the UZ system leads to low consequence for total system performance.

TSPA Disposition: None.

6.8.12 Thermo-Mechanical Stresses Alter Characteristics of Rocks above and below the Repository (2.2.10.05.0A)

FEP Description: Thermal-mechanical compression at the repository produces tension-fracturing in the PTn and other units above the repository. These fractures alter unsaturated zone flow between the surface and the repository. Extreme fracturing may propagate to the surface, affecting infiltration. Thermal fracturing in rocks below the repository affects flow and radionuclide transport to the saturated zone.

Descriptor Phrases: Thermal-mechanical effects (rock properties in the UZ), Thermal-mechanical effects (stress change)

Screening Decision: Excluded – Low Consequence

Screening Argument: The Mountain-Scale THM Model developed in BSC (2004 [167975], Section 6.5) assesses the magnitude and distribution of changes in hydrological properties and analyzes the impact of such changes on the mountain-scale vertical percolation flux through the repository horizon. The result shows that a maximum THM-induced change in hydrological properties occurs at around 1,000 years after emplacement, when the average temperature in the mountain is maximal. Near the repository level, thermal-elastic stresses tend to tighten vertical fractures to smaller apertures, leading to reduced permeability and increased capillary. At the ground surface, in a zone extending about 100 m deep, compressive stresses are completely relieved from tension. In this zone, fractures will open elastically, and fracturing or shear-slip along pre-existing fractures is possible.

Using a conservative estimate of input THM properties, changes in permeability by elastic closure or opening of pre-existing fractures are within a factor of 0.3 to 5, whereas calculated changes in capillary pressure are within a factor of 0.7 to 1.2. In addition, a conservative three-order-of-magnitude increase in permeability and one-order-of-magnitude reduction in capillary strength were imposed for the zone of possible fracturing and shear slip near the ground surface. Despite these conservative estimates of potential changes in hydrological properties, the main conclusion from the results of BSC (2004 [167975], Sections 6.5.10 to 6.5.14) is that THM-induced changes in the mountain-scale hydrological properties have no significant impact on the vertical percolation flux through the repository horizon. Again, these results were obtained for conservative estimates of the input THM properties, which is sufficient for bounding the possible impact of the THM processes on permeability and percolation flux on the mountain scale.

The effects of mechanical disturbance of fractures along radionuclide transport pathways are discussed in Section 6.7.7, FEP 2.2.06.02.0B. The conclusion reached in that section is that the effects of changes to fracture aperture or spacing on radionuclide transport are expected to be negligible over a wide range of permeability variation. In this case, the disturbance is caused by thermal-mechanical effects rather than by a seismic event. However, the conclusions reached in Section 6.7.7, FEP 2.2.06.02.0B are also applicable here because the analysis supporting the conclusions in Section 6.7.7, FEP 2.2.06.02.0B are based on a general sensitivity study of how fracture properties affect radionuclide transport. Furthermore, the general effects of thermal stresses on fracture permeability due to repository heating are evaluated in BSC (2004 [167975], Section 6.5.12). This analysis indicates that in the zones near the repository and below the repository, the fracture permeability is either reduced or unaffected. Thus, it is conservative to not include thermal effects on fracture permeability because radionuclide transport is slower with reduced permeability (CRWMS M&O 2000 [151953], Section 6.2.2.4). Therefore, this FEP may be excluded based on low consequence because it has no adverse effects on performance. See Section 6 in this Analysis Report for a discussion explaining why low consequence for specific elements of the UZ system leads to low consequence for total system performance.

TSPA Disposition: None

6.8.13 Thermo-Chemical Alteration in the UZ (Solubility, Speciation, Phase Changes, Precipitation/Dissolution) (2.2.10.06.0A)

FEP Description: Thermal effects may affect radionuclide transport directly by causing changes in radionuclide speciation and solubility in the UZ or indirectly, by causing changes in the host rock mineralogy that affect the flow path. Relevant processes include volume effects associated with silica phase changes, precipitation and dissolution of fracture-filling minerals (including silica and calcite), and alteration of zeolites and other minerals to clays.

Descriptor Phrases: Thermal-chemical effects (precipitation/dissolution in the UZ), Thermal-chemical effects (alteration in the UZ), Thermal-chemical effects (solubility limits in the UZ)

Screening Decision: Excluded—Low Consequence

Screening Argument: This FEP raises some issues already addressed in Section 6.8.7, FEP 2.2.08.03.0B and Section 6.8.8, FEP 2.2.08.07.0B. If solubility limits decrease in the geosphere compared with the waste emplacement drifts, then more radionuclides will precipitate as water flows out of the drifts. This corresponds to fewer dissolved radionuclides being available for transport into the geosphere, which is beneficial and results in no adverse effects on performance. See also Section 6.8.6 (FEP 2.2.01.05.0A) for additional information on this subject. If solubility limits increase in the geosphere compared with the waste emplacement drift, there is no effect on transport because all available radionuclides from the source at the waste emplacement drift are already aqueous species. The effects of colloid formation are accounted for in the colloid source term. Colloids are formed from the degradation of the High-Level Waste (HLW) and Spent Nuclear Fuel (SNF) waste forms, EBS materials, and rock (BSC 2003 [166845], Section 6.3.1). Radionuclides associated with colloids are modeled as either irreversibly or reversibly attached to colloids to encompass the broadest range of potential radionuclide-colloid interactions (BSC 2004 [162730], Section 6.4.5). Elevated temperatures are expected to lead to fewer colloids due to the decrease in colloid stability. This is due to the greater energy of colloid motion at higher temperatures, which allows colloids to overcome the energy barrier associated with coagulation (BSC 2003 [166845], Section 6.3.2.1). Boiling results in evaporation and this tends to increase the ionic strengths of colloid suspensions. This also leads to colloid instability due to compression of the electric double layer surrounding colloids (BSC 2003 [166845], Section 6.3.2.1). Therefore, colloid entrainment as a result of boiling is not expected.

The effects of temperature on radionuclide sorption were evaluated in BSC (2004 [167972], Section 6.4). This evaluation focused on the radionuclides Cs, Sr, Ba (a proxy for Ra), Ce, Eu, U(VI), Np, Pu and Am (BSC 2004 [167972], Section 8.3). The effects of temperature on sorption were found to be negligible for these radionuclides, except for Sr, Np, and U(VI). For these three radionuclides the effects of increased temperature leads to increased sorption (BSC 2004 [167972], Section 8.3). Therefore, the effects of temperature on radionuclide transport can be excluded on the basis of low consequence because it has no adverse effects on performance.

The thermal-chemical interactions that will occur in the repository environment have been studied with respect to effects on the seepage water entering the waste emplacement drifts (BSC 2004 [167974]). This model explicitly captures the effects of changes in temperature, pH, Eh,

ionic strength (and other compositional variables), time dependency, precipitation/dissolution effects, and effects of re-saturation (BSC 2004 [167974], Section 6.2). Changes in fracture permeabilities were found to be on the order of the natural variation in these properties (BSC 2004 [167974], Section 6.6.2.3.1), with most of the substantial effects limited to regions above and to the side of the drift within about a drift diameter (BSC 2004 [167974], Figures 6.5-16, 6.6-4, 6.8-40b, 6.8-41b). The predicted mineral precipitation decreases permeability in the affected regions, and leads to a reduction in flow around the drift. This is conservative for both drift seepage and radionuclide transport phenomena and, therefore, neglect of these types of permeability changes has no adverse effects on repository performance.

Two alternative conceptualizations of the modeled geochemical system were used for the model. The systems were denoted as "base case" and "extended case," and differ somewhat from one model variation to another (BSC 2004 [167974], Table 6.2-2). The extended case includes the major solid phases (minerals and glass) encountered in geological units at Yucca Mountain, together with a range of possible reaction-product minerals, CO_2 gas, and the aqueous species necessary to include these solid phases and the pore-water composition within the THC model. The base case is a subset of the extended case excluding aluminum silicate minerals, which form or dissolve much less easily than minerals such as calcite or gypsum, and for which thermodynamic and kinetic data are not as well established as for the other minerals. As such, the base-case system conceptualizes a geochemical system in which aluminum silicate minerals are nonreactive. The base-case system also does not include Fe- and Mg-bearing phases and aqueous species.

Compositional changes were only calculated at the drift boundary for the drift-scale THC seepage model (BSC 2004 [167974]). Results from the extended and base case models show most compositional variations returning to unperturbed conditions in 10,000 years or less. Variations in pH (BSC 2004 [167974], Figures 6.5-9, 6.7-11, 6.8-13), a key compositional variable for sorption of some radionuclides (BSC 2003 [163228], Attachment I), roughly lie within the range of variability investigated for initial pore-water compositions (BSC 2004 [167974], Table 6.2-1). Bicarbonate is found to be depressed in concentration upon water resaturation at the drift wall, as expected based on the reduced pH values at the same time period.

Results were also investigated for the Tptpll (lower lithophysal unit) model considering a range of initial pore-water compositions. In this model, five different initial pore-water compositions were investigated (BSC 2004 [167974], Table 6.2-1). Peak concentrations found at the time of rewetting in both models reflect mostly the small values of the first, non-zero, liquid-saturation output. In any case, elevated concentrations are predicted only for small liquid saturations that are not subject to significant fluid movement. The improved treatment of mineral precipitation at the boiling front used in the most recent THC model for the Tptpll also results in the prediction of lower, more realistic aqueous silica concentrations than in earlier models (BSC 2004 [167974], Figure 6.8-17). This model also predicts, upon rewetting, more rapid return to near-ambient conditions for aqueous Ca, Na, and Cl.

The findings indicate that at the drift wall, most of the significant compositional variations resulting from thermal-chemical processes are limited to low-saturation conditions over time periods that are short relative to the 10,000-year performance period. Similar magnitudes of

variation in chloride and pH were found in the mountain-scale THC model results (BSC 2004 [167975], Section 6.4.3.3.2). The magnitudes of the variations are found to be smaller at greater distances from the drift wall. As for the drift-scale study, variations in chloride are driven mainly by evaporation and are found to return to near-ambient values upon rewetting (BSC 2004 [167975], Section 6.4.3.3.2). Variations in pH were found to lie roughly between 7 and 9, which is similar to the results for the drift-scale THC model (BSC 2004 [167974], Figures 6.5-9, 6.7-11, 6.8-13). The most persistent change in pH is a level of about 7 in the Calico Hills (BSC 2004 [167975], Section 6.4.3.3.2, Figure 6.4-17), but this lies within the range of pH investigated for radionuclide sorption (BSC 2003 [163228], Attachment I). Therefore, the effects of these changes are excluded from TSPA-LA on the basis of low consequence. See Section 6 in this Analysis Report for a discussion explaining why low consequence for specific elements of the UZ system leads to low consequence for total system performance.

TSPA Disposition: None.

6.8.14 Thermo-Chemical Alteration of the Calico Hills Unit (2.2.10.07.0A)

FEP Description: Fracture pathways in the Calico Hills are altered by the thermal and chemical properties of the water flowing out of the repository.

Descriptor Phrases: Thermal-chemical effects (precipitation/dissolution in the CH), Thermal-chemical effects (alteration in the CH)

Screening Decision: Excluded—Low Consequence

Screening Argument: Model results show that significant glass alteration is found in the CHn at locations where temperatures by thermal heating exceed approximately 50°C (BSC 2004 [167975], Section 6.4.3.3.3). Much of the reaction has taken place by 3000 years, with the alteration rate decreasing strongly as temperatures decline in the rocks below the repository. The extent of glass alteration is limited to the strongly heated regions directly below the repository drifts, with little effects elsewhere. The dominant phases formed by volcanic glass reactions with aqueous fluids are zeolites, potassium feldspar, and albite (BSC 2004 [167975], Section 6.4.3.3.3). Differences in radionuclide sorption between vitric and zeolitic rock are generally found to have either greater sorption on zeolitic rock (e.g. americium and uranium) or little difference in sorption (e.g. neptunium and plutonium) (BSC 2003 [163228], Attachment I). Therefore, the effects of mineral alteration from glass to zeolites on radionuclide sorption are expected to be either negligible or will have no adverse effect on repository performance.

The basal vitrophyre of the TSw and the underlying vitric units and glass-rich zeolitic units all contain abundant clinoptilolite, which (in the model simulations) breaks down at elevated temperatures (BSC 2004 [167975], Section 6.4.3.3.3, Figure 6.4-24) to form predominantly stellerite (BSC 2004 [167975], Section 6.4.3.3.3, Figure 6.4-21). Although stellerite is common in fractures in the devitrified tuffs in the TSw, it is not typical as an alteration product of glass in the vitric units. It is likely that the fixed composition of clinoptilolite used in the thermodynamic database limits its ability to form preferentially to stellerite under the changing calcium, sodium, and potassium concentrations in the aqueous fluid, thus reducing its relative stability to stellerite, potassium feldspar, and albite at elevated temperatures. At near-ambient temperatures,

clinoptilolite is stable in the simulation and actually precipitates preferentially in the glass-rich layers (BSC 2004 [167975], Section 6.4.3.3.3, Figure 6.4-24). This trend is consistent with the observed mineral assemblage, although the 1% reacted in 7000 years is probably greater than that actually formed in this short period of time (BSC 2004 [167975], Section 6.4.3.3.3).

Changes in porosity and hence permeability are related to the net effects of volume changes taking place via mineral dissolution/precipitation. Mineral precipitation takes place through several different mechanisms, and therefore the distribution in the changes in hydrological properties is related to the spatial distributions of the various processes. In the CHn there is a modest increase in porosity of about 1%, owing primarily to the reaction of clinoptilolite and glass to feldspars and stellerite (BSC 2004 [167975], Section 6.4.3.3.4). As a consequence of the small fracture porosity changes, the fracture permeability does not show a significant reduction (BSC 2004 [167975], Section 6.4.3.3.4, Figure 6.4-26). Permeability changes in the matrix of the CHn vitric and zeolitic units are minor because of the initially high porosity of these rocks (BSC 2004 [167975], Section 6.4.3.3.4, Figures 6.4-25 and 6.4-26). Therefore, the porosity and permeability values in the matrix are essentially the same as the initial values. Consequently, this FEP is excluded on the basis of low consequence. See Section 6 in this Analysis Report for a discussion explaining why low consequence for specific elements of the UZ system leads to low consequence for total system performance.

TSPA Disposition: None.

6.8.15 Thermo-Chemical Alteration of the Topopah Spring Basal Vitrophyre (2.2.10.09.0A)

FEP Description: Heating the Topopah Spring basal vitrophyre with water available causes alteration of the glasses to clays and zeolites. Possible effects include volume increases that plug fractures, changes in flow paths, creation of perched water zones, and an increase in the sorptive properties of the unit.

Descriptor Phrases: Thermal-chemical effects (precipitation/dissolution in the TSbv), Thermal-chemical effects (alteration in the TSbv)

Screening Decision: Excluded—Low Consequence

Screening Argument: Model results show that, due to repository heating of the rock matrix, after 1000 years over 5% of the volcanic glass in the basal vitrophyre of the TSw has reacted and by 7000 years it has dissolved up to nearly 20% by volume (BSC 2004 [167975], Section 6.4.3.3.3, Figure 6.4-20). The dominant phases formed by volcanic glass reactions with aqueous fluids are zeolites, potassium feldspar, and albite (BSC 2004 [167975], Section 6.4.3.3.3). At locations beneath waste emplacement drifts, the principle precipitate is zeolite (stellerite) (BSC 2004 [167975], Figures 6.4-20 through 6.4-24). Differences in radionuclide sorption between vitric and zeolitic rock are generally found to have either greater sorption on zeolitic rock (e.g. americium and uranium) or little difference in sorption (e.g. neptunium and plutonium) (BSC 2003 [163228], Attachment I). Therefore, the effects of mineral alteration from glass to zeolites on radionuclide sorption are expected either to be negligible or to have no adverse effects.

The basal vitrophyre of the TSw and the underlying vitric units and glass-rich zeolitic units all contain abundant clinoptilolite, which (in the model simulations) breaks down at elevated temperatures (BSC 2004 [167975], Section 6.4.3.3.3, Figure 6.4-24) to form predominantly stellerite (BSC 2004 [167975], Section 6.4.3.3.3, Figure 6.4-21). Although stellerite is common in fractures in the devitrified tuffs in the TSw, it is not typical as an alteration product of glass in the vitric units. It is likely that the fixed composition of clinoptilolite used in the thermodynamic database limits its ability to form preferentially to stellerite under the changing calcium, sodium, and potassium concentrations in the aqueous fluid, thus reducing its relative stability to stellerite, potassium feldspar, and albite at elevated temperatures. At near-ambient temperatures, clinoptilolite is stable in the simulation and actually precipitates preferentially in the glass-rich layers (BSC 2004 [167975], Section 6.4.3.3.3, Figure 6.4-24). This trend is consistent with the observed mineral assemblage, although the 1% reacted in 7000 years is probably greater than that actually formed in this short period of time (BSC 2004 [167975]).

Changes in porosity and hence permeability are related to the net effects of volume changes taking place via mineral dissolution/precipitation. Mineral precipitation takes place through several different mechanisms, and therefore the distribution in the changes in hydrological properties is related to the spatial distributions of the various processes. As in the CHn, there is a modest increase in porosity in the TSw basal vitrophyre owing primarily to the reaction of clinoptilolite and glass to feldspars and stellerite. As a consequence of the small fracture porosity changes, the fracture permeability does not show a significant reduction (BSC 2004 [167975], Section 6.4.3.3.4, Figure 6.4-26). Permeability changes in the matrix are minor because of the initially high porosity of the vitric TSw vitrophyre rocks (BSC 2004 [167975], Section 6.4.3.3.4, Figures 6.4-25 and 6.4-26). Therefore, the porosity and permeability values in the matrix are essentially the same as the initial values. Consequently, this FEP is excluded on the basis of low consequence. See Section 6 in this Analysis Report for a discussion explaining why low consequence for specific elements of the UZ system leads to low consequence for total system performance.

TSPA Disposition: None.

6.8.16 Mineralogic Dehydration Reactions (2.2.10.14.0A)

FEP Description: Mineralogic dehydration reactions release water affecting hydrologic conditions. Dehydration of zeolites below the repository may lead to large-scale volume changes affecting flow and/or drift stability.

Descriptor Phrase: Mineralogic dehydration reactions

Screening Decision: Excluded—Low Consequence

Screening Argument: The predominant zone of zeolite-bearing minerals is at the base of the TSw (tsw39) and in the Calico Hills nonwelded unit (ch1, ch2, ch3, ch4, ch5, and ch6) (BSC 2003 [160109], Section 5.2). Dehydration of zeolites below the repository could occur if temperatures in the zeolitic units exceed the estimated minimum alteration temperature of 85°C (Smyth 1982 [119483], p. 201). Results of the 2-D mountain-scale TH calculations suggest that temperatures at the base of the TSw will remain below 77°C (BSC 2004 [167975], Figure 6.2-6c). Note, however, that the highest temperatures occur in the southern portion of the repository

(BSC 2004 [167975], Figure 6.2-6c), where the percent of zeolitic alteration is low (BSC 2003 [160109], Figures 5 and 6). Peak temperatures in the northern portion of the repository remain below 74°C. Furthermore, peak temperatures in the 3-D mountain-scale TH calculations predict a peak temperature of less than 65°C at the TSw-CHn interface (BSC 2004 [167975], Section 6.3.1). Therefore, the temperature changes induced by the repository are not high enough to cause significant zeolite dehydration or volume changes in the zeolitic rock. Therefore, this FEP is excluded on the basis of low consequence. See Section 6 in this Analysis Report for a discussion explaining why low consequence for specific elements of the UZ system leads to low consequence for total system performance.

TSPA Disposition: None

INTENTIONALLY LEFT BLANK

7. CONCLUSIONS

This document presents the 94 FEPs associated with UZ flow and transport processes. The 44 FEPs identified in Section 6.1 are included in TSPA-LA. The remaining 50 FEPs are excluded from TSPA-LA, based on arguments presented in this document. The FEPs analysis results are given in Table 7-1.

The output DTN: LB0310FEPS0170.001 contains the sequence of calculations used to evaluate perched water as discussed in Appendix A. This DTN is intended only to provide information on the calculations carried out for this analysis report. This data is not intended to be used as a source of input for other analyses.

For included FEPs, uncertainty is captured in the treatment of the processes as implemented in TSPA-LA. Therefore, uncertainty from the standpoint of the FEPs evaluation is concerned only with uncertainty in the exclusion of FEPs. Because there is no mechanism to capture uncertainty in the FEPs analysis in TSPA-LA, uncertainty leads to conservatism in the FEPs exclusion analyses, i.e. exclusions are based on conservative arguments that are unlikely to change with more detailed or accurate input information. The only restrictions for subsequent use that result from this approach is that worst-case or conservative analyses may overemphasize the importance of FEPs included on that basis. This overemphasis should be weighted appropriately when prioritizing future work to reduce uncertainties.

Table 7-1. FEPs Analysis Results

Section Number	FEP Number	FEP Name	Screening Decision	Screening Basis for Excluded FEPs
6.2.1	1.1.01.01.0A	Open site investigation boreholes	Excluded	Low Consequence
6.2.2	1.1.01.01.0B	Influx through holes drilled in drift wall or crown	Excluded	Low Consequence
6.2.3	1.1.02.01.0A	Site flooding (during construction and operation)	Excluded	Low Consequence
6.1.1	1.1.02.02.0A	Pre-closure ventilation	Included	
6.2.4	1.1.04.01.0A	Incomplete closure	Excluded	Low Consequence and by Regulation
6.2.5	1.1.11.00.0A	Monitoring of repository	Excluded	Low Consequence
6.1.2	1.2.02.01.0A	Fractures	Included	
6.1.3	1.2.02.02.0A	Faults	Included	
6.7.1	1.2.04.02.0A	Igneous activity changes rock properties	Excluded	Low Consequence
6.7.2	1.2.06.00.0A	Hydrothermal activity	Excluded	Low Consequence
6.4.1	1.2.07.01.0A	Erosion/denudation	Excluded	Low Consequence
6.4.2	1.2.07.02.0A	Deposition	Excluded	Low Consequence
6.4.3	1.2.09.02.0A	Large-scale dissolution	Excluded	Low Consequence
6.7.3	1.2.10.01.0A	Hydrologic response to seismic activity	Excluded	Low Consequence and Low Probability
6.7.4	1.2.10.02.0A	Hydrologic response to igneous activity	Excluded	Low Consequence
6.1.4	1.3.01.00.0A	Climate change	Included	
6.3.1	1.3.04.00.0A	Periglacial effects	Excluded	Low Consequence and Low Probability

Table 7-1. FEPs Analysis Results (continued)

Section Number	FEP Number	FEP Name	Screening Decision	Screening Basis for Excluded FEPs
6.3.2	1.3.05.00.0A	Glacial and ice sheet effect	Excluded	Low Probability
6.3.3	1.3.07.01.0A	Water table decline	Excluded	Low Consequence
6.1.5	1.3.07.02.0B	Water table rise affects UZ	Included	
6.5.1	1.4.01.00.0A	Human influences on climate	Excluded	By Regulation
6.1.6	1.4.01.01.0A	Climate modification increases recharge	Included	
6.5.2	1.4.01.02.0A	Greenhouse gas effects	Excluded	By Regulation
6.5.3	1.4.01.03.0A	Acid rain	Excluded	By Regulation
6.5.4	1.4.01.04.0A	Ozone layer failure	Excluded	By Regulation
6.5.5	1.4.06.01.0A	Altered soil or surface water chemistry	Excluded	By Regulation
6.2.6	2.1.05.01.0A	Flow through seals (access ramps and ventilation shafts)	Excluded	Low Consequence
6.2.7	2.1.05.02.0A	Radionuclide transport through seals	Excluded	Low Consequence
6.2.8	2.1.05.03.0A	Degradation of seals	Excluded	Low Consequence
6.1.7	2.1.08.01.0A	Water influx at the repository	Included	
6.1.8	2.1.08.02.0A	Enhanced influx at the repository	Included	
6.8.1	2.1.09.12.0A	Rind (chemically altered zone) forms in the near-field	Excluded	Low Consequence
6.3.4	2.1.09.21.0C	Transport of particles larger than colloids in the UZ	Excluded	Low Consequence
6.1.9	2.2.01.01.0A	Mechanical effects of excavation/construction in the near field	Included	
6.8.2	2.2.01.01.0B	Chemical effects of excavation/construction in the near-field	Excluded	Low Consequence
6.8.3	2.2.01.02.0A	Thermally-induced stress changes in the near-field	Excluded	Low Consequence
6.8.4	2.2.01.03.0A	Changes in fluid saturations in the excavation disturbed zone	Excluded	Low Consequence
6.8.5	2.2.01.04.0A	Radionuclide solubility in the excavation disturbed zone	Excluded	Low Consequence
6.8.6	2.2.01.05.0A	Radionuclide transport in the excavation-disturbed zone	Excluded	Low Consequence
6.1.10	2.2.03.01.0A	Stratigraphy	Included	
6.1.11	2.2.03.02.0A	Rock properties of host rock and other units	Included	
6.7.5	2.2.06.01.0A	Seismic activity changes porosity and permeability of rock	Excluded	Low Consequence
6.7.6	2.2.06.02.0A	Seismic activity changes porosity and permeability of faults	Excluded	Low Consequence
6.7.7	2.2.06.02.0B	Seismic activity changes porosity and permeability of fractures	Excluded	Low Consequence
6.7.8	2.2.06.03.0A	Seismic activity alters perched water zones	Excluded	Low Consequence
6.4.4	2.2.06.04.0A	Effects of subsidence	Excluded	Low Consequence

Table 7-1. FEPs Analysis Results (continued)

Section Number	FEP Number	FEP Name	Screening Decision	Screening Basis for Excluded FEPs
6.1.12	2.2.07.01.0A	Locally saturated flow at bedrock/alluvium contact	Included	
6.1.13	2.2.07.02.0A	Unsaturated groundwater flow in the geosphere	Included	
6.1.14	2.2.07.03.0A	Capillary rise in the UZ	Included	
6.1.15	2.2.07.04.0A	Focusing of unsaturated flow (fingers, weeps)	Included	
6.3.5	2.2.07.05.0A	Flow in the UZ from episodic infiltration.	Excluded	Low Consequence
6.1.16	2.2.07.06.0A	Episodic / pulse release from repository	Included	
6.1.17	2.2.07.06.0B	Long-term release of radionuclides from the repository	Included	
6.1.18	2.2.07.07.0A	Perched water develops	Included	
6.1.19	2.2.07.08.0A	Fracture flow in the UZ	Included	
6.1.20	2.2.07.09.0A	Matrix imbibition in the UZ	Included	
6.1.21	2.2.07.10.0A	Condensation zone forms around drifts	Included	
6.1.22	2.2.07.11.0A	Resaturation of geosphere dry-out zone	Included	
6.1.23	2.2.07.15.0B	Advection and dispersion in the UZ	Included	
6.1.24	2.2.07.18.0A	Film flow into the repository	Included	
6.1.25	2.2.07.19.0A	Lateral flow from Solitario Canyon Fault enters drifts	Included	
6.1.26	2.2.07.20.0A	Flow diversion around repository drifts	Included	
6.1.27	2.2.07.21.0A	Drift shadow forms below repository	Included	
6.1.28	2.2.08.01.0B	Chemical characteristics of groundwater in the UZ	Included	
6.8.7	2.2.08.03.0B	Geochemical interactions and evolution in the UZ	Excluded	Low Consequence
6.1.29	2.2.08.04.0A	Redissolution of precipitates directs more corrosive fluids to containers	Included	
6.1.30	2.2.08.05.0A	Diffusion in the UZ	Included	
6.1.31	2.2.08.06.0B	Complexation in the UZ	Included	
6.8.8	2.2.08.07.0B	Radionuclide solubility limits in the UZ	Excluded	Low Consequence
6.1.32	2.2.08.08.0B	Matrix diffusion in the UZ	Included	
6.1.33	2.2.08.09.0B	Sorption in the UZ	Included	
6.1.34	2.2.08.10.0B	Colloidal transport in the UZ	Included	
6.1.35	2.2.08.12.0A	Chemistry of water flowing into the drift	Included	
6.1.36	2.2.09.01.0B	Microbial activity in the UZ	Included	
6.8.9	2.2.10.01.0A	Repository-induced thermal effects on flow in the UZ	Excluded	Low Consequence
6.1.37	2.2.10.03.0B	Natural geothermal effects on flow in the UZ	Included	
6.8.10	2.2.10.04.0A	Thermo-mechanical stresses alter characteristics of fractures near repository	Excluded	Low Consequence
6.8.11	2.2.10.04.0B	Thermo-mechanical stresses alter characteristics of faults near repository	Excluded	Low Consequence
6.8.12	2.2.10.05.0A	Thermo-mechanical stresses alter characteristics of rocks above and below the repository	Excluded	Low Consequence

Table 7-1. FEPs Analysis Results (continued)

Section Number	FEP Number	FEP Name	Screening Decision	Screening Basis for Excluded FEPs
6.8.13	2.2.10.06.0A	Thermo-chemical alteration in the UZ (solubility, speciation, phase changes, precipitation/dissolution)	Excluded	Low Consequence
6.8.14	2.2.10.07.0A	Thermo-chemical alteration of the Calico Hills unit	Excluded	Low Consequence
6.8.15	2.2.10.09.0A	Thermo-chemical alteration of the Topopah Spring basal vitrophyre	Excluded	Low Consequence
6.1.38	2.2.10.10.0A	Two-phase buoyant flow / heat pipes	Included	
6.6.1	2.2.10.11.0A	Natural air flow in the UZ	Excluded	Low Consequence
6.1.39	2.2.10.12.0A	Geosphere dry-out due to waste heat	Included	
6.8.16	2.2.10.14.0A	Mineralogic dehydration reactions	Excluded	Low Consequence
6.6.2	2.2.11.02.0A	Gas effects in the UZ	Excluded	Low Consequence
6.6.3	2.2.11.03.0A	Gas transport in geosphere	Excluded	Low Consequence
6.7.9	2.2.12.00.0A	Undetected features in the UZ	Excluded	Low Consequence
6.1.40	2.3.01.00.0A	Topography and morphology	Included	
6.1.41	2.3.11.01.0A	Precipitation	Included	
6.1.42	2.3.11.02.0A	Surface runoff and flooding	Included	
6.1.43	2.3.11.03.0A	Infiltration and recharge	Included	
6.1.44	3.1.01.01.0A	Radioactive decay and ingrowth	Included	

8. REFERENCES AND INPUTS

The following is a list of the references cited in this document. Column 1 represents the unique six digit numerical identifier (the Document Input Reference System [DIRS] number), which is placed in the text following the reference callout (e.g., BSC 2004 [167969]). The purpose of these numbers is to assist the reader in locating a specific reference. Within the reference list, multiple sources by the same author (e.g., BSC 2004) are sorted alphabetically by title.

8.1 DOCUMENTS CITED

156269 Bear, J. 1972. *Dynamics of Fluids in Porous Media*. Environmental Science Series. Biswas, A.K., ed. New York, New York: Elsevier. TIC: 217356.

118920 Bruhn, R.L. 1994. "Fracturing in Normal Fault Zones: Implications for Fluid Transport and Fault Stability." *The Mechanical Involvement of Fluids in Faulting, Proceedings of Workshop LXIII, 6-10 June 1993, Fish Camp, California*. Hickman, S.; Sibson, R.; and Bruhn, R., eds. Open-File Report 94-228. Pages 231-246. Menlo Park, California: U.S. Geological Survey. TIC: 248510.

154826 BSC (Bechtel SAIC Company) 2001. *Features, Events, and Processes in UZ Flow and Transport*. ANL-NBS-MD-000001 REV 01. Las Vegas, Nevada: Bechtel SAIC Company. ACC: MOL.20010423.0321.

155950 BSC (Bechtel SAIC Company) 2001. *FY 01 Supplemental Science and Performance Analyses, Volume 1: Scientific Bases and Analyses*. TDR-MGR-MD-000007 REV 00 ICN 01. Las Vegas, Nevada: Bechtel SAIC Company. ACC: MOL.20010801.0404; MOL.20010712.0062; MOL.20010815.0001.

154365 BSC (Bechtel SAIC Company) 2001. *The Development of Information Catalogued in REV00 of the YMP FEP Database*. TDR-WIS-MD-000003 REV 00 ICN 01. Las Vegas, Nevada: Bechtel SAIC Company. ACC: MOL.20010301.0237.

158726 BSC (Bechtel SAIC Company) 2001. *UZ Flow Models and Submodels*. MDL-NBS-HS-000006 REV 00 ICN 01. Las Vegas, Nevada: Bechtel SAIC Company. ACC: MOL.20020417.0382.

160247 BSC (Bechtel SAIC Company) 2002. *Analysis of Geochemical Data for the Unsaturated Zone*. ANL-NBS-HS-000017 REV 00 ICN 02. Las Vegas, Nevada: Bechtel SAIC Company. ACC: MOL.20020314.0051.

160689 BSC (Bechtel SAIC Company) 2002. *Determination of Importance Evaluation for the Subsurface Exploratory Studies Facility*. BAB000000-01717-2200-00005 REV 07 ICN 04. Las Vegas, Nevada: Bechtel SAIC Company. ACC: MOL.20021028.0126.

160857 BSC (Bechtel SAIC Company) 2002. *Subsurface Tunneling System Description Document*. 800-3YD-TU00-00100-000-000. Las Vegas, Nevada: Bechtel SAIC Company. ACC: MOL.20021223.0171.

158966 BSC (Bechtel SAIC Company) 2002. *The Enhanced Plan for Features, Events, and Processes (FEPs) at Yucca Mountain*. TDR-WIS-PA-000005 REV 00. Las Vegas, Nevada: Bechtel SAIC Company. ACC: MOL.20020417.0385.

161773 BSC (Bechtel SAIC Company) 2003. *Analysis of Hydrologic Properties Data*. MDL-NBS-HS-000014 REV 00. Las Vegas, Nevada: Bechtel SAIC Company. ACC: DOC.20030404.0004.

165991 BSC (Bechtel SAIC Company) 2003. *Analysis of Infiltration Uncertainty*. ANL-NBS-HS-000027 REV 01. Las Vegas, Nevada: Bechtel SAIC Company. ACC: DOC.20031030.0003.

166407 BSC (Bechtel SAIC Company) 2003. *Characterize Eruptive Processes at Yucca Mountain, Nevada*. ANL-MGR-GS-000002 REV 01. Las Vegas, Nevada: Bechtel SAIC Company. ACC: DOC.20031218.0003.

163769 BSC (Bechtel SAIC Company) 2003. *Characterize Framework for Igneous Activity at Yucca Mountain, Nevada*. ANL-MGR-GS-000001 REV 01. Las Vegas, Nevada: Bechtel SAIC Company. ACC: DOC.20040106.0003.

166104 BSC (Bechtel SAIC Company) 2003. *Chlorine-36 Validation Studies at Yucca Mountain, Nevada*. TDR-NBS-HS-000017 REV 00A-Draft. Las Vegas, Nevada: Bechtel SAIC Company. ACC: MOL.20031105.0082.

160109 BSC (Bechtel SAIC Company) 2003. *Development of Numerical Grids for UZ Flow and Transport Modeling*. ANL-NBS-HS-000015 REV 01. Las Vegas, Nevada: Bechtel SAIC Company. ACC: DOC.20030404.0005.

165923 BSC (Bechtel SAIC Company) 2003. *Dike/Drift Interactions*. MDL-MGR-GS-000005 REV 00. Las Vegas, Nevada: Bechtel SAIC Company. ACC: DOC.20031022.0001.

162711 BSC (Bechtel SAIC Company) 2003. *Drift Degradation Analysis*. ANL-EBS-MD-000027 REV 02. Las Vegas, Nevada: Bechtel SAIC Company. ACC: DOC.20030709.0003.

166512 BSC (Bechtel SAIC Company) 2003. *Drift-Scale Coupled Processes (DST and TH Seepage) Models*. MDL-NBS-HS-000015 REV 00C. Las Vegas, Nevada: Bechtel SAIC Company. ACC: MOL.20030910.0160. TBV-5666.

166509 BSC (Bechtel SAIC Company) 2003. *Errata for Calibrated Properties Model*. MDL-NBS-HS-000003 REV 01. Las Vegas, Nevada: Bechtel SAIC Company. ACC: DOC.20030219.0001; DOC.20031014.0011.

165843 BSC (Bechtel SAIC Company) 2003. *Evaluation of Features, Events, and Processes (FEP) for the Biosphere Model*. ANL-MGR-MD-000011 REV 03. Las Vegas, Nevada: Bechtel SAIC Company. ACC: DOC.20031014.0008.

163128 BSC (Bechtel SAIC Company) 2003. *Features, Events, and Processes in SZ Flow and Transport*. ANL-NBS-MD-000002 REV 02A. Las Vegas, Nevada: Bechtel SAIC Company. ACC: MOL.20030823.0129.

163574 BSC (Bechtel SAIC Company) 2003. *Features, Events, and Processes: System-Level.* ANL-WIS-MD-000019 REV 01D. Las Vegas, Nevada: Bechtel SAIC Company. ACC: MOL.20030827.0081.

163999 BSC (Bechtel SAIC Company) 2003. *MGR External Events Hazards Screening Analysis*. ANL-MGR-SE-000004 REV 001. Las Vegas, Nevada: Bechtel SAIC Company. ACC: DOC.20030728.0005.

163925 BSC (Bechtel SAIC Company) 2003. *Miscellaneous Waste-Form FEPs*. ANL-WIS-MD-000009 REV 01A. Las Vegas, Nevada: Bechtel SAIC Company. ACC: MOL.20030617.0220.

165179 BSC (Bechtel SAIC Company) 2003. *Q-List*. TDR-MGR-RL-000005 REV 00. Las Vegas, Nevada: Bechtel SAIC Company. ACC: DOC.20030930.0002.

163228 BSC (Bechtel SAIC Company) 2003. *Radionuclide Transport Models Under Ambient Conditions*. MDL-NBS-HS-000008 REV 01. Las Vegas, Nevada: Bechtel SAIC Company. ACC: DOC.20031201.0002.

164101 BSC (Bechtel SAIC Company) 2003. *Repository Design Project, Repository/PA IED Emplacement Drift Committed Materials (2)*. 800-IED-WIS0-00302-000-00A. Las Vegas, Nevada: Bechtel SAIC Company. ACC: ENG.20030627.0004.

164052 BSC (Bechtel SAIC Company) 2003. *Repository Design Project, Repository/PA IED Emplacement Drift Committed Materials 1 of 2*. 800-IED-WIS0-00301-000-00A. Las Vegas, Nevada: Bechtel SAIC Company. ACC: ENG.20030627.0003.

161727 BSC (Bechtel SAIC Company) 2003. *Repository Design, Repository/PA IED Subsurface Facilities*. 800-IED-EBS0-00402-000-00B. Las Vegas, Nevada: Bechtel SAIC Company. ACC: MOL.20030109.0146.

163226 BSC (Bechtel SAIC Company) 2003. *Seepage Model for PA Including Drift Collapse*. MDL-NBS-HS-000002 REV 02. Las Vegas, Nevada: Bechtel SAIC Company. ACC: DOC.20030709.0001.

166262 BSC (Bechtel SAIC Company) 2003. *Site-Scale Saturated Zone Flow Model*. MDL-NBS-HS-000011 REV 01. Las Vegas, Nevada: Bechtel SAIC Company. ACC: DOC.20040126.0004.

164870 BSC (Bechtel SAIC Company) 2003. *SZ Flow and Transport Model Abstraction*. MDL-NBS-HS-000021 REV 00. Las Vegas, Nevada: Bechtel SAIC Company. ACC: DOC.20030818.0007.

166296 BSC (Bechtel SAIC Company) 2003. *Total System Performance Assessment-License Application Methods and Approach*. TDR-WIS-PA-000006 REV 00 ICN 01. Las Vegas, Nevada: Bechtel SAIC Company. ACC: DOC.20031215.0001.

165572 BSC (Bechtel SAIC Company) 2003. *Underground Layout Configuration*. 800-P0C-MGR0-00100-000-00E. Las Vegas, Nevada: Bechtel SAIC Company. ACC: ENG.20031002.0007.

161317 BSC (Bechtel SAIC Company) 2003. *WAPDEG Analysis of Waste Package and Drip Shield Degradation.* ANL-EBS-PA-000001 REV 01. Las Vegas, Nevada: Bechtel SAIC Company. ACC: DOC.20031208.0004.

166845 BSC (Bechtel SAIC Company) 2003. *Waste Form and In-Drift Colloids-Associated Radionuclide Concentrations: Abstraction and Summary*. MDL-EBS-PA-000004 REV 00 ICN 01. Las Vegas, Nevada: Bechtel SAIC Company. ACC: DOC.20031222.0012.

167040 BSC (Bechtel SAIC Company) 2004. *D&E / PA/C IED Emplacement Drift Configuration*. 800-IED-MGR0-00201-000-00A. Las Vegas, Nevada: Bechtel SAIC Company. ACC: ENG.20040113.0011.

164519 BSC (Bechtel SAIC Company) 2004. *D&E / PA/C IED Subsurface Facilities*. 800-IED-WIS0-00101-000-00A. Las Vegas, Nevada: Bechtel SAIC Company. ACC: ENG.20040309.0026.

168370 BSC (Bechtel SAIC Company) 2004. *D&E/PA/C IED Subsurface Facilities (Sheet 3)*. 800-IED-WIS0-00103-000-00A. Las Vegas, Nevada: Bechtel SAIC Company. ACC: ENG.20040309.0028.

168180 BSC (Bechtel SAIC Company) 2004. *D&E/ PA/C IED SUBSURFACE FACILITIES (SHEET 4)*. 800-IED-WIS0-00104-000-00A. Las Vegas, Nevada: Bechtel SAIC Company. ACC: ENG.20040309.0029.

167253 BSC (Bechtel SAIC Company) 2004. *Engineered Barrier System Features, Events, and Processes*. ANL-WIS-PA-000002 REV 02E. Las Vegas, Nevada: Bechtel SAIC Company. ACC: MOL.20040119.0129.

167461 BSC (Bechtel SAIC Company) 2004. *Engineered Barrier System: Physical and Chemical Environment Model*. ANL-EBS-MD-000033 REV 02. Las Vegas, Nevada: Bechtel SAIC Company. ACC: DOC.20040212.0004.

167970 BSC (Bechtel SAIC Company) 2004. *Errata 001 for Abstraction of Drift Seepage*. MDL-NBS-HS-000019 REV 00 ICN 01. Las Vegas, Nevada: Bechtel SAIC Company. ACC: DOC.20031112.0002; DOC.20040223.0001.

167972 BSC (Bechtel SAIC Company) 2004. *Errata 001 for Abstraction of Drift-Scale Coupled Processes*. MDL-NBS-HS-000018 REV 00. Las Vegas, Nevada: Bechtel SAIC Company. ACC: DOC.20031223.0004; DOC.20040223.0003.

167973 BSC (Bechtel SAIC Company) 2004. *Errata 001 for Drift Scale THM Model*. MDL-NBS-HS-000017 REV 00 ICN 01. Las Vegas, Nevada: Bechtel SAIC Company. ACC: DOC.20031014.0009; DOC.20040223.0002.

167974 BSC (Bechtel SAIC Company) 2004. *Errata 001 for Drift-Scale Coupled Processes (DST and THC Seepage) Models*. MDL-NBS-HS-000001 REV 02. Las Vegas, Nevada: Bechtel SAIC Company. ACC: DOC.20030804.0004; DOC.20040219.0002.

167975 BSC (Bechtel SAIC Company) 2004. *Errata 001 for Mountain-Scale Coupled Processes (TH/THC/THM)*. MDL-NBS-HS-000007 REV 01. Las Vegas, Nevada: Bechtel SAIC Company. ACC: DOC.20031216.0003; DOC.20040211.0006.

167976 BSC (Bechtel SAIC Company) 2004. *Errata 002 for Seepage Calibration Model and Seepage Testing Data*. MDL-NBS-HS-000004 REV 02. Las Vegas, Nevada: Bechtel SAIC Company. ACC: DOC.20030408.0004; DOC.20040202.0003; DOC.20040219.0003.

167959 BSC (Bechtel SAIC Company) 2004. *Errata for Drift-Scale Radionuclide Transport*. MDL-NBS-HS-000016 REV 00. Las Vegas, Nevada: Bechtel SAIC Company. ACC: DOC.20030902.0009; DOC.20040219.0001.

167720 BSC (Bechtel SAIC Company) 2004. *Errata for Features, Events, and Processes: Disruptive Events*. ANL-WIS-MD-000005 REV 001. Las Vegas, Nevada: Bechtel SAIC Company. ACC: DOC.20031212.0005; DOC.20040209.0001.

167969 BSC (Bechtel SAIC Company) 2004. *Errata for Technical Work Plan for: Performance Assessment Unsaturated Zone*. TWP-NBS-HS-000003 REV 02. Las Vegas, Nevada: Bechtel SAIC Company. ACC: MOL.20030102.0108; DOC.20040121.0001.

167657 BSC (Bechtel SAIC Company) 2004. *Errata for Ventilation Model and Analysis Report*. ANL-EBS-MD-000030 REV 03 ICN 03. Las Vegas, Nevada: Bechtel SAIC Company. ACC: DOC.20031216.0002; DOC.20040202.0004.

163056 BSC (Bechtel SAIC Company) 2004. *Multiscale Thermohydrologic Model*. ANL-EBS-MD-000049 REV 01. Las Vegas, Nevada: Bechtel SAIC Company. ACC: DOC.20040301.0004.

162730 SC (Bechtel SAIC Company) 2004. *Particle Tracking Model and Abstraction of Transport Processes*. MDL-NBS-HS-000020 REV 00. Las Vegas, Nevada: Bechtel SAIC Company. ACC: DOC.20040120.0001.

166883 BSC (Bechtel SAIC Company) 2004. *UZ Flow Models and Submodels*. MDL-NBS-HS-000006 REV 01 ICN 01A. Las Vegas, Nevada: Bechtel SAIC Company. ACC: MOL.20040126.0082. TBV-5677.

166275 Canori, G.F. and Leitner, M.M. 2003. *Project Requirements Document*. TER-MGR-MD-000001 REV 02. Las Vegas, Nevada: Bechtel SAIC Company. ACC: DOC.20031222.0006.

100967 Carrigan, C.R.; King, G.C.P.; Barr, G.E.; and Bixler, N.E. 1991. "Potential for Water-Table Excursions Induced by Seismic Events at Yucca Mountain, Nevada." *Geology, 19*, (12), 1157-1160. Boulder, Colorado: Geological Society of America. TIC: 242407. TBV-5743.

160928 Carter Krogh, K.E. and Valentine, G.A. 1996. *Structural Control on Basaltic Dike and Sill Emplacement, Paiute Ridge Mafic Intrusion Complex, Southern Nevada*. LA-13157-MS. Los Alamos, New Mexico: Los Alamos National Laboratories. ACC: MOL.20030828.0138.

129957 CRWMS M&O (Civilian Radioactive Waste Management System Management and Operating Contractor) 1996. *Forensic Evaluation of Geophysical Log Data for Borehole USW SD-7 in Support of the Yucca Mountain Site Characterization Project*. BAAA00000-01717-0200-00007 REV 00. Las Vegas, Nevada: CRWMS M&O. ACC: MOL.19971023.0133.

114799 CRWMS M&O 1996. *Forensic Evaluation of Geophysical Log Data for Borehole USW SD-9 in Support of the Yucca Mountain Site Characterization Project*. BAAA00000-01717-0200-00005 REV 00. Las Vegas, Nevada: CRWMS M&O. ACC: MOL.19970606.0345.

130425 CRWMS M&O 1996. *Forensic Evaluation of Geophysical Log Data for Borehole USW SZ-7a in Support of the Yucca Mountain Site Characterization Project*. BAAA00000-01717-0200-00004 REV 00. Las Vegas, Nevada: CRWMS M&O. ACC: MOL.19960517.0080.

130429 CRWMS M&O 1996. *Forensic Evaluation of Geophysical Log Data for Borehole USW UZ-14 in Support of the Yucca Mountain Site Characterization Project*.

BAAA00000-01717-0200-00012 REV 00. Las Vegas, Nevada: CRWMS M&O. ACC: MOL.19960522.0169.

124052 CRWMS M&O 1997. *The Site-Scale Unsaturated Zone Transport Model of Yucca Mountain*. Milestone SP25BM3, Rev. 1. Las Vegas, Nevada: CRWMS M&O. ACC: MOL.19980224.0314.

100356 CRWMS M&O 1998. "Unsaturated Zone Hydrology Model." Chapter 2 of *Total System Performance Assessment-Viability Assessment (TSPA-VA) Analyses Technical Basis Document*. B00000000-01717-4301-00002 REV 01. Las Vegas, Nevada: CRWMS M&O. ACC: MOL.19981008.0002. TBV-5744.

105347 CRWMS M&O 1998. *Synthesis of Volcanism Studies for the Yucca Mountain Site Characterization Project*. Deliverable 3781MR1. Las Vegas, Nevada: CRWMS M&O. ACC: MOL.19990511.0400.

105031 CRWMS M&O 1999. *Final Report: Plant and Soil Related Processes Along a Natural Thermal Gradient at Yucca Mountain, Nevada*. B00000000-01717-5705-00109 REV 00. Las Vegas, Nevada: CRWMS M&O. ACC: MOL.19990513.0037.

103618 CRWMS M&O 1999. *Impact of Radioactive Waste Heat on Soil Temperatures*. BA0000000-01717-5700-00030 REV 0. Las Vegas, Nevada: CRWMS M&O. ACC: MOL.19990309.0403. TBV-5745.

151953 CRWMS M&O 2000. *Fault Displacement Effects on Transport in the Unsaturated Zone*. ANL-NBS-HS-000020 REV 01. Las Vegas, Nevada: CRWMS M&O. ACC: MOL.20001002.0154.

153246 CRWMS M&O 2000. *Total System Performance Assessment for the Site Recommendation*. TDR-WIS-PA-000001 REV 00 ICN 01. Las Vegas, Nevada: CRWMS M&O. ACC: MOL.20001220.0045.

151945 CRWMS M&O 2000. *Yucca Mountain Site Description*. TDR-CRW-GS-000001 REV 01 ICN 01. Las Vegas, Nevada: CRWMS M&O. ACC: MOL.20001003.0111.

153935 CRWMS M&O 2001. *Features, Events, and Processes in Thermal Hydrology and Coupled Processes*. ANL-NBS-MD-000004 REV 00 ICN 01. Las Vegas, Nevada: CRWMS M&O. ACC: MOL.20010220.0007.

103180 Davies, J.B. and Archambeau, C.B. 1997. "Geohydrological Models and Earthquake Effects at Yucca Mountain, Nevada." *Environmental Geology, 32*, (1), 23-35. New York, New York: Springer-Verlag. TIC: 237118.

100282 DOE (U.S. Department of Energy) 1988. *Site Characterization Plan Yucca Mountain Site, Nevada Research and Development Area, Nevada*. DOE/RW-0199. Nine

volumes. Washington, D.C.: U.S. Department of Energy, Office of Civilian Radioactive Waste Management. ACC: HQO.19881201.0002. TBV-5746.

100548 DOE (U.S. Department of Energy) 1998. *Introduction and Site Characteristics.* Volume 1 of *Viability Assessment of a Repository at Yucca Mountain*. DOE/RW-0508. Washington, D.C.: U.S. Department of Energy, Office of Civilian Radioactive Waste Management. ACC: MOL.19981007.0028.

155970 DOE (U.S. Department of Energy) 2002. *Final Environmental Impact Statement for a Geologic Repository for the Disposal of Spent Nuclear Fuel and High-Level Radioactive Waste at Yucca Mountain, Nye County, Nevada*. DOE/EIS-0250. Washington, D.C.: U.S. Department of Energy, Office of Civilian Radioactive Waste Management. ACC: MOL.20020524.0314; through; MOL.20020524.0320. TBV-5747.

126415 Fenix & Scisson. 1987. *NNWSI Hole Histories, USW H-1, USW H-3, USW H-4, USW H-5, USW H-6*. DOE/NV/10322-18. Washington, D.C.: U.S. Department of Energy, Office of Civilian Radioactive Waste Management. ACC: NNA.19871006.0069.

165939 Fenix & Scisson. 1987. *NNWSI Hole Histories, USW UZ-1, UE-25 UZ #4, UE-25 UZ #5, USW UZ-6, USW UZ-6s, USW UZ-7, USW UZ-8, USW UZ-13*. DOE/NV/10322-20. Washington, D.C.: U.S. Department of Energy, Office of Civilian Radioactive Waste Management. ACC: HQS.19880517.1193.

101238 Fenix & Scisson. 1986. *NNWSI Hole Histories, UE-25 WT #3, UE-25 WT #4, UE-25 WT #5, UE-25 WT #6, UE-25 WT #12, UE-25 WT #13, UE-25 WT #14, UE-25 WT #15, UE-25 WT #16, UE-25 WT #17, UE-25 WT #18, USW WT-1, USW WT-2, USW WT-7, USW WT-10, USW WT-11*. DOE/NV/10322-10. Mercury, Nevada: Fenix & Scisson. ACC: NNA.19870317.0155.

103102 Fenix & Scisson. 1987. *NNWSI Hole Histories, USW G-1, USW G-2, USW G-3, USW G-4, USW GA-1, USW GU-3*. DOE/NV/10322-19. Mercury, Nevada: Fenix & Scisson. ACC: HQS.19880517.1194.

109425 Forester, R.M.; Bradbury, J.P.; Carter, C.; Elvidge-Tuma, A.B.; Hemphill, M.L.; Lundstrom, S.C.; Mahan, S.A.; Marshall, B.D.; Neymark, L.A.; Paces, J.B.; Sharpe, S.E.; Whelan, J.F.; and Wigand, P.E. 1999. *The Climatic and Hydrologic History of Southern Nevada During the Late Quaternary*. Open-File Report 98-635. Denver, Colorado: U.S. Geological Survey. TIC: 245717.

165394 Freeze, G. 2003. *KTI Letter Report, Response to Additional Information Needs on TSPAI 2.05 and TSPAI 2.06*. REG-WIS-PA-000003 REV 00 ICN 04. Las Vegas, Nevada: Bechtel SAIC Company. ACC: DOC.20030825.0003.

100123 Hardin, E.L. 1998. *Near-Field/Altered-Zone Models Report*. UCRL-ID-129179. Livermore, California: Lawrence Livermore National Laboratory. ACC: MOL.19980630.0560.

146831 Keller, E.A. 1992. *Environmental Geology*. Sixth Edition. New York, New York: Macmillan Publishing. TIC: 247330.

165898 Mineart, P. 2003. *Hydrologic Engineering Studies for the North Portal Pad and Vicinity*. 000-00C-CD04-00100-000-00A. Las Vegas, Nevada: Bechtel SAIC Company. ACC: MOL.20031021.0299. TBV-5492.

161362 Minwalla, H.J. 2003. *Project Design Criteria Document*. 000-3DR-MGR0-00100-000-001. Las Vegas, Nevada: Bechtel SAIC Company. ACC: ENG.20030402.0001.

158449 NRC (U.S. Nuclear Regulatory Commission) 2002. *Yucca Mountain Review Plan, Draft Report for Comment*. NUREG-1804, Rev. 2. Washington, D.C.: U.S. Nuclear Regulatory Commission, Office of Nuclear Material Safety and Safeguards. TIC: 252488.

163274 NRC (U.S. Nuclear Regulatory Commission) 2003. *Yucca Mountain Review Plan, Final Report*. NUREG-1804, Rev. 2. Washington, D.C.: U.S. Nuclear Regulatory Commission, Office of Nuclear Material Safety and Safeguards. TIC: 254568.

104946 Perry, R.H. and Chilton, C.H., eds. 1973. *Chemical Engineers' Handbook*. 5th Edition. New York, New York: McGraw-Hill. TIC: 242591.

119693 Reamer, C.W. 1999. "Issue Resolution Status Report (Key Technical Issue: Igneous Activity, Revision 2)." Letter from C.W. Reamer (NRC) to Dr. S. Brocoum (DOE/YMSCO), July 16, 1999, with enclosure. ACC: MOL.19990810.0639.

163008 Reimus, P.W.; Ware, S.D.; Benedict, F.C.; Warren, R.G.; Humphrey, A.; Adams, A.; Wilson, B.; and Gonzales, D. 2002. *Diffusive and Advective Transport of {superscript 3}H, {superscript 14}C, and {superscript 99}Tc in Saturated, Fractured Volcanic Rocks from Pahute Mesa, Nevada*. LA-13891-MS. Los Alamos, New Mexico: Los Alamos National Laboratory. TIC: 253905.

104252 Richards, L.A. 1931. "Capillary Conduction of Liquids Through Porous Mediums." *Physics, 1*, 318-333. [New York, New York: American Physical Society]. TIC: 225383.

100075 Sawyer, D.A.; Fleck, R.J.; Lanphere, M.A.; Warren, R.G.; Broxton, D.E.; and Hudson, M.R. 1994. "Episodic Caldera Volcanism in the Miocene Southwestern Nevada Volcanic Field: Revised Stratigraphic Framework, {superscript 40}Ar/{superscript 39}Ar Geochronology, and Implications for Magmatism and

Extension." *Geological Society of America Bulletin, 106*, (10), 1304-1318. Boulder, Colorado: Geological Society of America. TIC: 222523.

161591 Sharpe, S. 2003. *Future Climate Analysis—10,000 Years to 1,000,000 Years After Present*. MOD-01-001 REV 01. [Reno, Nevada: Desert Research Institute]. ACC: MOL.20030407.0055. TBV-5749.

166960 Simmons, A.M. 2004. *Yucca Mountain Site Description*. TDR-CRW-GS-000001 REV 02. Two volumes. Las Vegas, Nevada: Bechtel SAIC Company. ACC: DOC.20040120.0004.

119483 Smyth, J.R. 1982. "Zeolite Stability Constraints on Radioactive Waste Isolation in Zeolite-Bearing Volcanic Rocks." *Journal of Geology, 90*, (2), 195-201. Chicago, Illinois: University of Chicago Press. TIC: 221104. TBV-5750.

166219 Snell, R.D.; Beesley, J.F.; Blink, J.A.; Duguid, J.O.; Jenni, K.E.; Lin, W.; Monib, A.M.; Nieman, T.L.; and Hommel, S. 2003. *Performance Confirmation Plan*. TDR-PCS-SE-000001 REV 02 ICN 02. Las Vegas, Nevada: Bechtel SAIC Company. ACC: DOC.20031124.0003.

101022 Stock, J.M. and Healy, J.H. 1988. "Stress Field at Yucca Mountain, Nevada." Chapter 6 of *Geologic and Hydrologic Investigations of a Potential Nuclear Waste Disposal Site at Yucca Mountain, Southern Nevada*. Carr, M.D. and Yount, J.C., eds. Bulletin 1790. Denver, Colorado: U.S. Geological Survey. TIC: 203085. TBV-5752.

101027 Stock, J.M.; Healy, J.H.; Hickman, S.H.; and Zoback, M.D. 1985. "Hydraulic Fracturing Stress Measurements at Yucca Mountain, Nevada, and Relationship to the Regional Stress Field." *Journal of Geophysical Research, 90*, (B10), 8691-8706. Washington, D.C.: American Geophysical Union. TIC: 219009. TBV-5751.

106963 Szymanski, J.S. 1989. *Conceptual Considerations of the Yucca Mountain Groundwater System with Special Emphasis on the Adequacy of This System to Accommodate a High-Level Nuclear Waste Repository*. Three volumes. Las Vegas, Nevada: U.S. Department of Energy, Nevada Operations Office. ACC: NNA.19890831.0152.

100422 Triay, I.R.; Meijer, A.; Conca, J.L.; Kung, K.S.; Rundberg, R.S.; Strietelmeier, B.A.; and Tait, C.D. 1997. *Summary and Synthesis Report on Radionuclide Retardation for the Yucca Mountain Site Characterization Project*. Eckhardt, R.C., ed. LA-13262-MS. Los Alamos, New Mexico: Los Alamos National Laboratory. ACC: MOL.19971210.0177.

167961 USGS (U.S. Geological Survey) 2003. *Errata for Future Climate Analysis*. ANL-NBS-GS-000008 REV 00 ICN 01. Denver, Colorado: U.S. Geological Survey. ACC: MOL.20011107.0004; DOC.20031015.0003.

166518 USGS (U.S. Geological Survey) 2003. *Simulation of Net Infiltration for Modern and Potential Future Climates, with Errata*. ANL-NBS-HS-000032 REV 00 ICN 02. Denver, Colorado: U.S. Geological Survey. ACC: MOL.20011119.0334; DOC.20031014.0004; DOC.20031015.0001.

100354 USGS (U.S. Geological Survey) 1998. *Probabilistic Seismic Hazard Analyses for Fault Displacement and Vibratory Ground Motion at Yucca Mountain, Nevada*. Milestone SP32IM3, June 15, 1998. Three volumes. Oakland, California: U.S. Geological Survey. ACC: MOL.19980619.0640. TBV-5753.

165176 USGS (U.S. Geological Survey) 2003. *Errata, Hydrogeologic Framework Model for the Saturated-Zone Site-Scale Flow and Transport Model*. ANL-NBS-HS-000033 REV 00 ICN 02. Denver, Colorado: U.S. Geological Survey. ACC: DOC.20030319.0002; MOL.20011112.0070.

119132 Valentine, G.A.; WoldeGabriel, G.; Rosenberg, N.D.; Carter Krogh, K.E.; Crowe, B.M.; Stauffer, P.; Auer, L.H.; Gable, C.W.; Goff, F.; Warren, R.; and Perry, F.V. 1998. "Physical Processes of Magmatism and Effects on the Potential Repository: Synthesis of Technical Work Through Fiscal Year 1995." Chapter 5 of *Volcanism Studies: Final Report for the Yucca Mountain Project*. Perry, F.V.; Crowe, B.M.; Valentine, G.A.; and Bowker, L.M., eds. LA-13478. Los Alamos, New Mexico: Los Alamos National Laboratory. TIC: 247225. TBV-5754.

164901 Vanoni, V.A., ed. 1977. "Sediment Transportation Mechanics." *Sedimentation Engineering*. Pages 17-315. New York, New York: American Society of Civil Engineers. TIC: 255225.

163589 Wilson, N.S.F.; Cline, J.S.; and Amelin, Y.V. 2003. "Origin, Timing, and Temperature of Secondary Calcite–Silica Mineral Formation at Yucca Mountain, Nevada." *Geochimica et Cosmochimica Acta, 67*, (6), 1145-1176. [New York, New York]: Pergamon. TIC: 254369. TBV-5755.

154918 Wu, Y-S.; Zhang, W.; Pan, L.; Hinds, J.; and Bodvarsson, G.S. 2000. *Capillary Barriers in Unsaturated Fractured Rocks of Yucca Mountain, Nevada*. LBNL-46876. Berkeley, California: Lawrence Berkeley National Laboratory. TIC: 249912. TBV-5756.

100520 YMP (Yucca Mountain Site Characterization Project) 1993. *Evaluation of the Potentially Adverse Condition "Evidence of Extreme Erosion During the Quaternary Period" at Yucca Mountain, Nevada*. Topical Report YMP/92-41-TPR. Las Vegas, Nevada: Yucca Mountain Site Characterization Office. ACC: NNA.19930316.0208. TBV-5757.

102215 YMP (Yucca Mountain Site Characterization Project) 1995. *Technical Basis Report for Surface Characteristics, Preclosure Hydrology, and Erosion*. YMP/TBR-001,

Rev. 0. Las Vegas, Nevada: Yucca Mountain Site Characterization Office. ACC: MOL.19951201.0049. TBV-5758.

166080 YMP (Yucca Mountain Site Characterization Project) 1999. *Borehole USW SD-6*. Field Work Package FWP-SB-97-002, Rev. 2. Las Vegas, Nevada: Yucca Mountain Site Characterization Office. ACC: MOL.19990414.0267.

154386 YMP (Yucca Mountain Site Characterization Project) 2001. *Reclamation Implementation Plan*. YMP/91-14, Rev. 2. Las Vegas, Nevada: Yucca Mountain Site Characterization Office. ACC: MOL.20010301.0238. TBV-5759.

162133 Zhou, Q.; Liu, H-H.; Bodvarsson, G.S.; and Oldenburg, C.M. 2003. "Flow and Transport in Unsaturated Fractured Rock: Effects of Multiscale Heterogeneity of Hydrogeologic Properties." *Journal of Contaminant Hydrology, 60*, ([1-2]), 1-30. New York, New York: Elsevier. TIC: 253978. TBV-5760.

8.2 CODES, STANDARDS, REGULATIONS, AND PROCEDURES

156605 10 CFR 63. Energy: Disposal of High-Level Radioactive Wastes in a Geologic Repository at Yucca Mountain, Nevada. Readily available.

156671 66 FR 55732. Disposal of High-Level Radioactive Wastes in a Proposed Geologic Repository at Yucca Mountain, NV, Final Rule. 10 CFR Parts 2, 19, 20, 21, 30, 40, 51, 60, 61, 63, 70, 72, 73, and 75. Readily available.

162317 67 FR 62628. Specification of a Probability for Unlikely Features, Events and Processes. Readily available.

AP-2.22Q, Rev. 1. *Classification Analyses and Maintenance of the Q-List*. Washington, D.C.: U.S. Department of Energy, Office of Civilian Radioactive Waste Management. ACC: DOC.20030807.0002.

AP-SI.1Q, Rev. 5, ICN 2. *Software Management.* Washington, D.C.: U.S. Department of Energy, Office of Civilian Radioactive Waste Management. ACC: DOC.20030902.0003.

AP-SIII.9Q, Rev. 1, ICN 3. *Scientific Analyses*. Washington, D.C.: U.S. Department of Energy, Office of Civilian Radioactive Waste Management. ACC: DOC.20040301.0002.

8.3 SOURCE DATA, LISTED BY DATA TRACKING NUMBER

147613 GS000308311221.005. Net Infiltration Modeling Results for 3 Climate Scenarios for FY99. Submittal date: 03/01/2000.

153485 LA0009SL831151.001. Fracture Mineralogy of the ESF Single Heater Test Block, Alcove 5. Submittal date: 09/28/2000.

162575 LA0302AM831341.002. Unsaturated Zone Distribution Coefficients (K_ds) for U, Np, Pu, Am, Pa, Cs, Sr, Ra, and Th. Submittal date: 02/04/2003.

163558 LA0303HV831352.002. Colloid Retardation Factors for the Saturated Zone Fractured Volcanics. Submittal date: 03/31/2003.

163789 LA0305AM831341.001. 1977 to 1987 Sorption Measurements of AM, BA, CS, NP, PU, PA, SR, TH, and U with Yucca Mountain Tuff Samples. Submittal date: 05/21/2003.

165523 LA0309AM831341.002. Batch Sorption Coefficient Data for Barium on Yucca Mountain Tuffs in Representative Water Compositions. Submittal date: 09/25/2003.

165524 LA0309AM831341.003. Batch Sorption Coefficient Data for Cesium on Yucca Mountain Tuffs in Representative Water Compositions. Submittal date: 09/25/2003.

165525 LA0309AM831341.004. Batch Sorption Coefficient Data for Neptunium on Yucca Mountain Tuffs in Representative Water Compositions. Submittal date: 09/25/2003.

165526 LA0309AM831341.005. Batch Sorption Coefficient Data for Plutonium on Yucca Mountain Tuffs in Representative Water Compositions. Submittal date: 09/25/2003.

165527 LA0309AM831341.006. Batch Sorption Coefficient Data for Strontium on Yucca Mountain Tuffs in Representative Water Compositions. Submittal date: 09/25/2003.

165528 LA0309AM831341.007. Batch Sorption Coefficient Data for Uranium on Yucca Mountain Tuffs in Representative Water Compositions. Submittal date: 09/25/2003.

165865 LA0310AM831341.001. Sorption/Desorption Measurements of Cesium on Yucca Mountain Tuff. Submittal date: 10/21/2003.

167015 LA0311AM831341.001. Correlation Matrix for Sampling of Sorption Coefficient Probability Distributions. Submittal date: 11/06/2003.

166924 LA0311BR831229.001. UZ Transport Abstraction Model, Transfer Function Calculation Files. Submittal date: 11/17/2003.

166515 LA0311BR831371.003. UZ Transport Abstraction Model, Transport Parameters and Base Case Simulation Results. Submittal date: 11/25/2003.

113495 LA9908JC831321.001. Mineralogic Model "MM3.0" Version 3.0. Submittal date: 08/16/1999.

146447 LA9912SL831151.001. Fracture Mineralogy of Drill Core ESF-HD-TEMP-2. Submittal date: 01/05/2000.

146449 LA9912SL831151.002. Percent Coverage by Fracture-Coating Minerals in Core ESF-HD-TEMP-2. Submittal date: 01/05/2000.

163906 LB0104AMRU0185.012. Section 6.4.2 Focusing and Discrete Flow Paths in the TSW - Data Summary. Submittal date: 05/15/2001.

159525 LB0205REVUZPRP.001. Fracture Properties for UZ Model Layers Developed from Field Data. Submittal date: 05/14/2002.

159526 LB0207REVUZPRP.001. Revised UZ Fault Zone Fracture Properties. Submittal date: 07/03/2002.

159672 LB0207REVUZPRP.002. Matrix Properties for UZ Model Layers Developed from Field and Laboratory Data. Submittal date: 07/15/2002.

161243 LB0208UZDSCPMI.002. Drift-Scale Calibrated Property Sets: Mean Infiltration Data Summary. Submittal date: 08/26/2002.

161433 LB02091DSSCP3I.002. 1-D Site Scale Calibrated Properties: Data Summary. Submittal date: 09/18/2002.

162128 LB02092DSSCFPR.002. 2-D Site Scale Calibrated Fault Properties: Data Summary. Submittal date: 09/18/2002.

160799 LB0210THRMLPRP.001. Thermal Properties of UZ Model Layers: Data Summary. Submittal date: 10/25/2002.

163689 LB0301DSCPTHSM.002. Drift-Scale Coupled Process Model for Thermohydrologic Seepage: Data Summary. Submittal date: 01/29/2003. TBV-5390.

163044 LB03023DSSCP9I.001. 3-D Site Scale UZ Flow Field Simulations for 9 Infiltration Scenarios. Submittal date: 02/28/2003.

161976 LB0302DSCPTHCS.002. Drift-Scale Coupled Processes (THC Seepage) Model: Data Summary. Submittal date: 02/11/2003.

162277 LB0302PTNTSW9I.001. PTn/TSw Interface Percolation Flux Maps for 9 Infiltration Scenarios. Submittal date: 02/28/2003.

162273 LB0302SCMREV02.002. Seepage-Related Model Parameters K and 1/A: Data Summary. Submittal date: 02/28/2003.

163687 LB0304SMDCREV2.002. Seepage Modeling for Performance Assessment, Including Drift Collapse: Summary Plot Files and Tables. Submittal date: 04/11/2003.

163690 LB0305PTNTSW9I.001. PTn/TSw Interface Percolation Flux Maps for 9 Alternative Infiltration Scenarios. Submittal date: 05/12/2003.

165625 LB0305TSPA18FF.001. Eighteen 3-D Site Scale UZ Flow Fields Converted from TOUGH2 to T2FEHM Format. Submittal date: 05/09/2003.

165541 LB0307DSTTHCR2.002. Drift-Scale Coupled Processes (DST Seepage) Model: Data Summary. Submittal date: 07/24/2003.

164337 LB0307SEEPDRCL.002. Seepage Into Collapsed Drift: Data Summary. Submittal date: 07/21/2003.

166714 LB0311ABSTHCR2.001. Drift Scale Coupled Process Abstraction Model (for Intact-Drift Case). Submittal date: 11/07/2003.

166713 LB0311ABSTHCR2.003. THC Simulations Considering Drift Degradation: Summary/Abstraction Data Files. Submittal date: 11/07/2003.

166671 LB0312TSPA06FF.001. Six Flow Fields with Raised Water Tables. Submittal date: 12/23/2003.

111475 LB990501233129.004. 3-D UZ Model Calibration Grids for AMR U0000, "Development of Numerical Grids of UZ Flow and Transport Modeling". Submittal date: 09/24/1999.

111480 LB991091233129.006. Thermal Properties and Tortuosity Factor for the UZ Model Layers for AMR U0090, "Analysis of Hydrologic Properties Data". Submittal date: 10/15/1999.

142973 LL000122051021.116. Summary of Analyses of Glass Dissolution Filtrates. Submittal date: 01/27/2000.

152554 MO0004QGFMPICK.000. Lithostratigraphic Contacts from MO9811MWDGFM03.000 to be Qualified Under the Data Qualification Plan, TDP-NBS-GS-000001. Submittal date: 04/04/2000.

155959 MO0010CPORGLOG.003. Calculated Porosity Values at Depth Derived from Qualified Geophysical Log Data from Modern Boreholes. Submittal date: 10/16/2000.

153777 MO0012MWDGFM02.002. Geologic Framework Model (GFM2000). Submittal date: 12/18/2000.

154177 MO0101COV00396.000. Coverage: Bores3. Submittal date: 01/05/2001.

164527 MO0307SEPFEPS4.000. LA FEP List. Submittal date: 07/31/2003. TBV-5422.

164898 MO9805YMP98040.000. Flood Prone Areas and Maximum Potential Flood in the Vicinity of the Conceptual Controlled Area. Submittal date: 05/05/1998. TBV-5748.

109059 MO9906GPS98410.000. Yucca Mountain Project (YMP) Borehole Locations. Submittal date: 06/23/1999.

165922 MO9912GSC99492.000. Surveyed USW SD-6 As-Built Location. Submittal date: 12/21/1999.

164132 SN0306T0504103.005. Revised Groundwater Colloid Mass Concentration Parameters for TSPA (Total System Performance Assessment). Submittal date: 06/30/2003.

164131 SN0306T0504103.006. Revised Sorption Partition Coefficients (K_d Values) for Selected Radionuclides Modeled in the TSPA (Total System Performance Assessment). Submittal date: 06/30/2003.

165640 SN0308T0503100.008. Revised Frequency Distributions for Net Infiltrations and Weighting Factors Applied to Lower, Mean, and Upper Climates. Submittal date: 08/28/2003.

107372 SNF40060298001.001. Unsaturated Zone Lithostratigraphic Contacts in Borehole USW SD-6. Submittal date: 10/15/1998.

105627 TM000000SD12RS.012. USW SD-12 Composite Borehole Log (0.0'-1435.3') and Weight Logs (1,438.8-2,151.7'). Submittal date: 09/08/1995.

166424 TMUSWNRG7A0096.002. Geophysical Logs for Borehole USW NRG-7/7A. Submittal date: 11/27/1996.

8.4 SOFTWARE CODES

155323 BSC (Bechtel SAIC Company) 2001. *Software Code: PHREEQC*. V2.3. PC, LINUX , Windows 95/98/NT, Redhat 6.2. 10068-2.3-00.

165741 LANL (Los Alamos National Laboratory) 2003. *Software Code: FEHM*. V2.21. SUN, SunOS 5.8; PC, Windows 2000 and Linux 7.1. 10086-2.21-00.

161256 LBNL (Lawrence Berkeley National Laboratory) 2002. *Software Code: TOUGHREACT*. V3.0. DEC ALPHA/OSF1 V5.1, DEC ALPHA/OSF1 V5.0, Sun UltraSparc/Sun OS 5.5.1, PC/Linux Redhat 7.2. 10396-3.0-00.

163453 LBNL (Lawrence Berkeley National Laboratory) 2003. *Software Code: WTRISE*. V2.0. PC/WINDOWS 2000/98; DEC ALPHA/OSF1 V5.1. 10537-2.0-00.

147608 SNL (Sandia National Laboratories) 2001. *Software Code: INFIL*. VA_2.a1. DEC Alpha, OpenVMS V7.2-1. 10253-A_2.a1-00.

139422 USGS (U.S. Geological Survey) 2001. *Software Code: INFIL*. V2.0. PC, Windows NT 4.0. 10307-2.0-00.

8.5 OUTPUT DATA, LISTED BY DATA TRACKING NUMBER

LB0310FEPS0170.001. Computations of Perched Water Volume in Repository Footprint and Flux through Repository. Submittal date: 10/31/2003.

INTENTIONALLY LEFT BLANK

APPENDIX A

PERCHED WATER VOLUME

INTENTIONALLY LEFT BLANK

Computing Perched Water Volume in Repository Footprint and Flux through Repository

Perched water volumes and flux through the repository are evaluated here to support arguments concerning the potential effects of boreholes on drainage of perched water as discussed in Section 6.2.1 and seismic effects on perched water in Section 6.7.8. Perched water volumes and flux through the repository are extracted from the UZ flow model output data set contained in DTN: LB03023DSSCP9I.001 [163044]. To assess the flux through the proposed repository horizon, the flux represented in the first 241,914 connections in the flux output are searched for flux through repository cells. The first 237,338 connections in the TOUGH2 output file are the vertical connections for the interior cells (not including the boundary cells), as can be seen in the mesh file. However, the additional 4,576 (horizontal) connections do not involve any of the 469 repository cells and therefore do not contribute to the calculations of vertical flux through the proposed repository.

The cells are first checked against the list of 469 repository cells. The first 62,000 connections are copied as text from the flow field output file (a text file created in MS Word) to Excel. The text in the Excel file is converted to column data using the "Text to Columns" function. The spreadsheet is then sorted in ascending order on Column 1. This sorts the fracture and matrix cells and also sorts the header information, which is deleted. The matrix cells are cut and pasted onto the second worksheet in the file. Columns F, G, H, and I are redundant and deleted. The 469 repository cell names are pasted into Column L. The following formulas are used to check which cells in Columns A and B are in the repository:

Frn = MATCH(Arn,L$1:L$469,0)

Grn = MATCH(Brn,L$1:L$469,0)

These are used for both the fracture and matrix worksheets. These expressions return the index number of Column L if the cell names match and return the error message #N/A if the cell names do not match. Similar manipulations are used for the flux output from TOUGH2, connections 62001 – 124000, 124001 – 186000, and 186001 – 241914. Once the cell identifications have been made for the glacial transition upper case, the same results for columns F and G are copied onto the files generated for the other infiltration and climate scenarios. The manipulations are carried out for each of the nine flow fields. These files are saved as:

gt upper flux 1-62000.xls
gt upper flux 62001-124000.xls
gt upper flux 124001-186000.xls
gt upper flux 186001-241914.xls

gt mean flux 1-62000.xls
gt mean flux 62001-124000.xls
gt mean flux 124001-186000.xls
gt mean flux 186001-241914.xls

gt lower flux 1-62000.xls
gt lower flux 62001-124000.xls
gt lower flux 124001-186000.xls
gt lower flux 186001-241914.xls

ms upper flux 1-62000.xls
ms upper flux 62001-124000.xls
ms upper flux 124001-186000.xls
ms upper flux 186001-241914.xls

ms mean flux 1-62000.xls
ms mean flux 62001-124000.xls
ms mean flux 124001-186000.xls
ms mean flux 186001-241914.xls

ms lower flux 1-62000.xls
ms lower flux 62001-124000.xls
ms lower flux 124001-186000.xls
ms lower flux 186001-241914.xls

pd upper flux 1-62000.xls
pd upper flux 62001-124000.xls
pd upper flux 124001-186000.xls
pd upper flux 186001-241914.xls

pd mean flux 1-62000.xls
pd mean flux 62001-124000.xls
pd mean flux 124001-186000.xls
pd mean flux 186001-241914.xls

pd lower flux 1-62000.xls
pd lower flux 62001-124000.xls
pd lower flux 124001-186000.xls
pd lower flux 186001-241914.xls

For each case (1-62000, 620001-124000, 124001-186000, and 186001-241914), Columns A through G for the repository cells are copied and pasted into a summary file for the given climate scenario. The same operations are performed for the fractures and matrix on separate worksheets in the summary file. The data are then sorted by Columns G and F, respectively, in ascending order. Each cell has two vertical fluxes representing inflow and outflow. The second set of values ordered through Column G are cut and pasted into Columns I through O. Columns B, G, H, and M are not needed and deleted. “Duplicate” cells are identified in 24 instances due to the cells having the same name except for the case of one of the letters (i.e., upper case vs. lower case), which are not distinguished by the MATCH command. The “duplicate” cells are identified manually in Column L by marking them with a “1”. The other cells are marked with a

"0" in Column L. The summary files with marked duplicates are stored in the following files (for each of the nine flow fields):

Repository cells with vertical flux and marked duplicates gt upper.xls
Repository cells with vertical flux and marked duplicates gt mean.xls
Repository cells with vertical flux and marked duplicates gt lower.xls
Repository cells with vertical flux and marked duplicates ms upper.xls
Repository cells with vertical flux and marked duplicates ms mean.xls
Repository cells with vertical flux and marked duplicates ms lower.xls
Repository cells with vertical flux and marked duplicates pd upper.xls
Repository cells with vertical flux and marked duplicates pd mean.xls
Repository cells with vertical flux and marked duplicates pd lower.xls

The worksheet is then sorted on Column L in descending order and the 24 "duplicates" are deleted. Column L is deleted, and Column A is copied into Column M. The largest of the two vertical fluxes is found through the following formula:

Orn = IF(Crn>Irn,Crn,Irn)

The total flux for each continuum is summed in Cell O470, and then the fracture and matrix flux are summed on the fracture worksheet in Cell O471. The total flux in kg/s is converted to kg/yr in Cell O473, using the following formula on the fracture worksheet:

O472 = O471*3600*24*365.25

This flux is converted to m^3/yr by dividing by the density (997 kg/m^3) in Cell O473 on the fracture worksheet. These results are saved in the following files:

Repository cells with vertical flux - gt upper.xls
Repository cells with vertical flux - gt mean.xls
Repository cells with vertical flux - gt lower.xls

Repository cells with vertical flux - ms upper.xls
Repository cells with vertical flux - ms mean.xls
Repository cells with vertical flux - ms lower.xls

Repository cells with vertical flux - pd upper.xls
Repository cells with vertical flux - pd mean.xls
Repository cells with vertical flux - pd lower.xls

Perched water volumes are extracted from the summary files described below in "Extracting Output from UZ Flow Model for Saturation and Relative Permeability". These summary files contain the capillary pressure, saturation, and volume information needed to determine perched water volumes. Only perched water within the fractures of the repository footprint is considered. For each climate/infiltration scenario, the segments 61000-122000, 122001-184000, and 184001-

245506. The segment 1-61000 is not needed because it doesn't contain any repository elements. For each case, Columns A through AN are sorted on Column T in descending order. This brings all of the repository footprint cells to the top of the list. The cells not in the footprint are deleted. The data in Columns A through AN are then sorted on the fracture capillary pressure in Column E in descending order. Cells with fracture capillary pressure less than 0 are deleted. The matrix data and layer properties are also deleted. The fracture bulk volume is given in Column L and fracture porosity in Column R. The product of the bulk volume times the porosity gives the volume of water in the fracture cells (since the cell is saturated). This is computed as follows:

Vrn = Lrn*Rrn

The data are sorted in descending order, based on the permeability in Column S. The total fracture volume is computed as follows:

AC1 = SUM(V:V)

The total fracture volume in high-permeability fractures (permeability greater than 10^{-15} m^2) is found by first assigning the volumes of high-permeability fractures as follows:

Wrn = IF(Srn>10^-15,Vrn,0)

Then the volumes are summed:

AC2 = SUM(W:W)

These calculations are given in the following files:

gt upper perched 61001-122000.xls
gt upper perched 122001-184000.xls
gt upper perched 184001-245506.xls

gt mean perched 61001-122000.xls
gt mean perched 122001-184000.xls
gt mean perched 184001-245506.xls

gt lower perched 61001-122000.xls
gt lower perched 122001-184000.xls
gt lower perched 184001-245506.xls

ms upper perched 61001-122000.xls
ms upper perched 122001-184000.xls
ms upper perched 184001-245506.xls

ms mean perched 61001-122000.xls
ms mean perched 122001-184000.xls

ms mean perched 184001-245506.xls

pd lower perched 61001-122000.xls
pd lower perched 122001-184000.xls
pd lower perched 184001-245506.xls

pd upper perched 61001-122000.xls
pd upper perched 122001-184000.xls
pd upper perched 184001-245506.xls

pd mean perched 61001-122000.xls
pd mean perched 122001-184000.xls
pd mean perched 184001-245506.xls

pd lower perched 61001-122000.xls
pd lower perched 122001-184000.xls
pd lower perched 184001-245506.xls

The results of these extractions are summarized here:

	Total Volume of Perched Water in High-Permeability Fractures (m^3)	Total Flow through Repository Footprint (m^3/yr)	Flux Years
Present day, Lower Infiltration Scenario	4.66E+02	2.00E+03	2.33E-01
Present day, Mean Infiltration Scenario	4.66E+02	2.07E+04	2.25E-02
Present day, Upper Infiltration Scenario	6.50E+02	6.03E+04	1.08E-02
Monsoon, Lower Infiltration Scenario	6.50E+02	2.31E+04	2.81E-02
Monsoon, Mean Infiltration Scenario	6.50E+02	6.18E+04	1.05E-02
Monsoon, Upper Infiltration Scenario	6.50E+02	1.58E+05	4.12E-03
Glacial transition, Lower Infiltration Scenario	6.50E+02	1.04E+04	6.25E-02
Glacial transition, Mean Infiltration Scenario	6.50E+02	9.75E+04	6.67E-03
Glacial transition, Upper Infiltration Scenario	1.19E+03	1.92E+05	6.22E-03

DTN: LB0310FEPS0170.001 [Output]

Extracting Output from UZ Flow Model for Saturation and Relative Permeability

Each of 9 flow fields contains data for saturation and relative permeability. The flow field output is given in DTN: LB03023DSSCP9I.001 [163044]. For each flow field, the output for cells 1-61000, 61001-122000, 122001-184000, and 184001-245506 were copied as text from text files downloaded from the DTN and pasted into MS Excel as text. The text was then converted to columns (A through H) in the spreadsheet using the Excel function "text to columns". The spreadsheet was then sorted by cell name in ascending order and the header information was deleted. Columns A-G of the mesh files for the same range of cells were copied into columns J-P and column H (with the repository footprint designation) was copied into column T. The

assignment of the footprint designation is discussed below under the heading "Extraction of repository footprint from mesh file". Then all of the matrix elements were cut from the bottom of the file and pasted into columns V through AN such that the fracture cells in column A match the matrix cells in Column V. Data for the porosity and permeability by rock type was extracted from a file in DTN: LB03023DSSCP9I.001 [163044] (e.g. glaq_uA.dat). This information was copied into columns AP through AR, with the rock type designation in column AP, the porosity of the rock type in column AQ, and the permeability of the rock type in column AR. The porosity and permeability for the fractures and matrix were then assigned to each grid. First, the rock type of the fractures in column K and the rock type of the matrix in column AF were compared with the rock types in column AP:

Qrn = MATCH(Krn,AP1:AP98,0) for the fractures
ALrn = MATCH(AFrn,AP1:AP98,0) for the rock matrix

The MATCH function returns the array index of the first value in column AP that matches the value in columns K or AF. This index is then used to extract the porosity and permeability as follows:

Rrn = INDEX(AQ$1:AQ$98,$Qrn) for fracture porosity
Srn = INDEX(AR$1:AR$98,$Qrn) for fracture permeability
AMrn = INDEX(AQ$1:AQ$98,$ALrn) for matrix porosity
ANrn = INDEX(AR$1:AR$98,$ALrn) for matrix permeability

The resulting output files are:

gt upper 1-61000.xls
gt upper 61001-122000.xls
gt upper 122001-184000.xls
gt upper 184001-245506.xls

gt mean 1-61000.xls
gt mean 61001-122000.xls
gt mean 122001-184000.xls
gt mean 184001-245506.xls

gt lower 1-61000.xls
gt lower 61001-122000.xls
gt lower 122001-184000.xls
gt lower 184001-245506.xls

ms upper 1-61000.xls
ms upper 61001-122000.xls
ms upper 122001-184000.xls
ms upper 184001-245506.xls

ms mean 1-61000.xls
ms mean 61001-122000.xls
ms mean 122001-184000.xls
ms mean 184001-245506.xls

ms lower 1-61000.xls
ms lower 61001-122000.xls
ms lower 122001-184000.xls
ms lower 184001-245506.xls

pd upper 1-61000.xls
pd upper 61001-122000.xls
pd upper 122001-184000.xls
pd upper 184001-245506.xls

pd mean 1-61000.xls
pd mean 61001-122000.xls
pd mean 122001-184000.xls
pd mean 184001-245506.xls

pd lower 1-61000.xls
pd lower 61001-122000.xls
pd lower 122001-184000.xls
pd lower 184001-245506.xls

Extraction of repository footprint from mesh file.

Extract from the file mesh_2kb.dkm (from DTN: LB03023DSSCP9I.001 [163044]) under the ELEM label the mesh in three, 64000-row groups and one 53,506-row group. This comprises the entire listing of cells for the 3-D UZ site-scale flow model. Store these in files called the following:

1-64000 1st file.xls
64001-128000 1st file.xls
128001-192000 1st file.xls
192001-245506 1st file.xls

The structure of the grid leads to many cells having the same x-y coordinates. The ELEM file is also structured such that these cells are listed in adjacent rows. The "raw" cell information is trimmed to contain only the cell name and the x and y coordinates (columns E and F in the "1st files"). These are given in columns A, B, and C. Columns D and E contain a repeat of the contents of B and C. In column F, the following formula is applied:

Frn = IF(Drn=Drn-1,IF(Ern=Ern-1,Frn-1+1,1))

where Drn = the element of column D in the same row as in column F. The exception is in row 1, where F1=1. This generates a count of the number of consecutive rows with the same x-y coordinates. A "reverse count" is done in column G by initiating the count from the last row using the following formula:

Grn = IF(Drn+1=Drn,IF(Ern+1=Ern,1+Grn+1,1),1)

Column F is used to identify the first (top) grid with the given x-y coordinate using the following formula in Column H:

Hrn = IF(Frn=1,1,0)

Column I is used to identify the total number of consecutive rows having the same x-y coordinate using the following formula:

Irn = IF(Hrn=1,Grn,0)

The results of these calculations are stored in the following files:

1-64001 sorting for independent x-y 2nd file.xls
64001-128000 sorting for independent x-y 2nd file.xls
128001-192000 sorting for independent x-y 2nd file.xls
192001-245506 sorting for independent x-y 2nd file.xls

The results are sorted by column H, which contains 1 or 0 depending on whether or not the cell is at the top of a column of cells or not. Only cells with a 1 in column H are retained. 531 independent columns are identified. Note that the values in column I give the number of cells in the column having the same x-y values. Repository cells are identified in file rep.xls in Output-DTN: LB0310FEPS0170.001. Plots confirm that these cells lie within the proposed repository footprint. The list of repository cells in the UZ grid and the cell coordinates are given in:

repository cells.xls

The drift end-point coordinates in meters (Nevada State Plane (NSP) coordinates) for the repository design are given in BSC 2003 [161727].

Plots given here show the correspondence between the UZ grid coordinates for the repository cells and the design coordinates for the end points of the waste emplacement drifts:

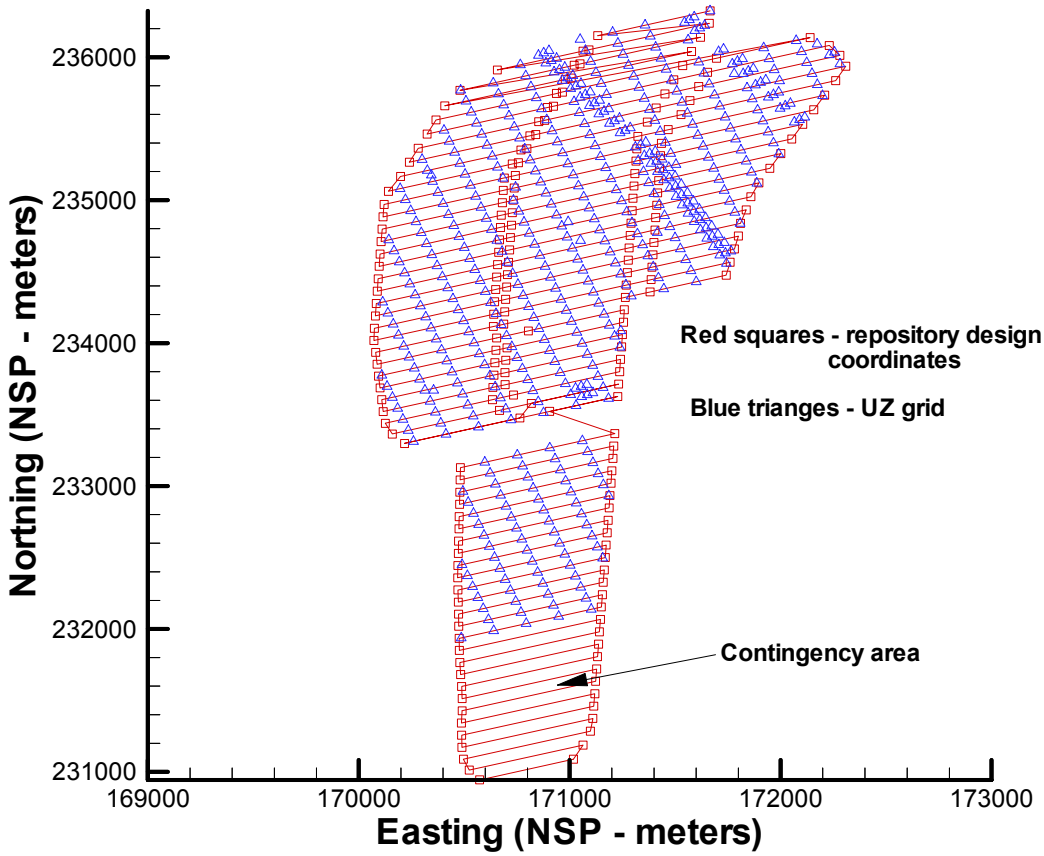

DTN: LB0310FEPS0170.001 [OUTPUT]
DTN: LB03023DSSCP9I.001 [163044]

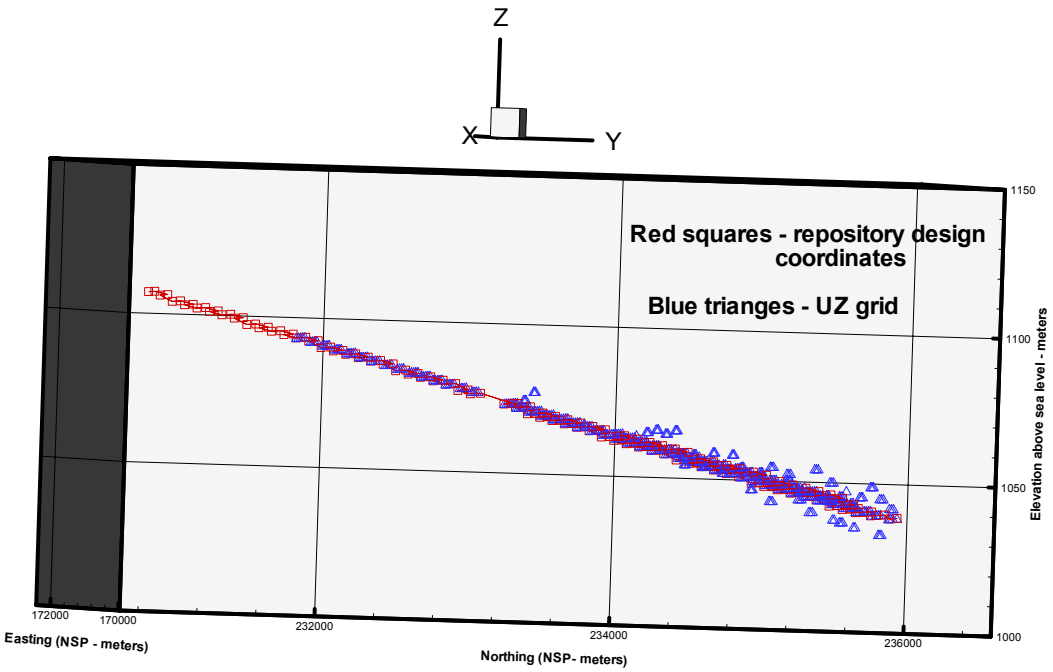

DTN: LB0310FEPS0170.001 [OUTPUT]
DTN: LB03023DSSCP9I.001 [163044]

The remaining results described here are for processing the cells 64001 to 128000. The same procedure is applied to the other cell groupings (128001 to 192000 and 192001 to 245506) but the specific number of cells involved changes. The x-y coordinates for the UZ grid in the repository are compared against the x-y coordinates of the grid columns identified for "top" cells. Repository easting coordinates are put in row 1 in columns K through IK and in row and repository northing coordinates are put in row 2, columns K through IK. This accounts for 235 repository x-y coordinates. The remaining 234 coordinates are put in rows 534 and 535 following the last identified "top" cell, columns K through IJ. Then, the x-y coordinate for the grid columns in columns B and C, rows 3 thorugh 533, are compared with the repository x-y coordinates using the following formula:

clrn = IF(ABS(cl$1-$Brn)<10,1,0)*IF(ABS(cl$2-$Crn)<10,1,0)

Here, cl$1 designates a value from row 1 with a variable column letter (cl). This is notation analogous to the use of rn for a variable row number. This formula identifies if the grid column and the repository cell lie within 10 m of each other in both the northing and easting directions. If so, a value of 1 is returned and the column lies within the repository footprint. If not, a value of 0 is returned and the cell lies outside the repository footprint. For the repository cells coordinates in rows 534 and 535, an analogous formula is used:

cl(rn+533) = IF(ABS(cl$534-$Brn)<10,1,0)*IF(ABS(cl$535-$Crn)<10,1,0)

Column J is used to sum the values across the spreadsheet columns to find if a UZ grid column lies within the footprint:

Jrn = SUM(Krn:IKrn)

For rn = 3 to 533
and

Jrn = SUM(Krn:IJrn)

For rn = 536 to 1066.

These files are saved as

1-64000 comparison with repository x-y 3rd file.xls
64001-128000 comparison with repository x-y 3rd file.xls
128001-192000 comparison with repository x-y 3rd file.xls
192001-245506 comparison with repository x-y 3rd file.xls

Due to the large number of "top" cells in the first 64000 cells, the x-y 3rd file is split into two parts, part 1 one for the first 235 repository cell comparison and part 2 for the second 234 repository cell comparison. Note that no cells were found within the footprint for cells 1-64000. Therefore, further processing for this group is not needed. The results in column J from rows 536 to 1066 are combined with the results for column J from rows 3 to 533, such that if a "1" is returned from either list, the value of column J is "1" and "0" otherwise. The data from these files are then sorted by column J to reduce the to spreadsheet entries to the footprint columns in the UZ grid. Then column A contains the node name for the top of each footprint column in the UZ grid, columns B and C contain the x-y coordinates and column D contains the number of elements in each UZ grid column. This results in 352 columns in the repository footprint. The top cell names and the number of elements in each grid are transposed into rows 3 and 4, respectively from columns F through IS (248 cells) and in rows 251 and 252, columns F through DE (104 cells). These spreadsheets are saved as

64001-128000 repository footprint top cells 4th file.xls
128001-192000 repository footprint top cells 4th file.xls
192001-245506 repository footprint top cells 4th file.xls

The files containing the ELEM information are then reopened (see "1st files discussed above). Rows 1 and 2, columns F through IS are copied to rows 1 and 2 of the corresponding 1st file in columns I through IV from the 4th files. The repository footprint top cells for each column are compared with the cells in Column A of the spreadsheet using the formula:

clrn = IF(cl$1=$Arn,cl$2,0)

Thus, if the cell name from the ELEM information in column A equals the top cell of a grid column inside the footprint, the value of the number of cells in that grid column returned. If not, a value of 0 is returned. Once all columns have been checked, the values for each row are summed using the following formula:

=SUM(Irn:IVrn)

for rows 3 through the last element in each spreadsheet.

The results are stored in

64001-128000 construct footprint tag for cells part 1 5th file.xls
128001-192000 construct footprint tag for cells part 1 5th file.xls
192001-245506 construct footprint tag for cells part 1 5th file.xls

The same search operation is conducted on the "1st file" using the repository top cell names and # of elements from rows 251 and 252, columns F through DE of the "4th file". The results are stored in

64001-128000 construct footprint tag for cells part 2 5th file.xls
128001-192000 construct footprint tag for cells part 2 5th file.xls
192001-245506 construct footprint tag for cells part 2 5th file.xls

The "1st file" is again reopened and the results from columns H in part 1 and part 2 of the 5th files are copied into columns H and I respectively for the 1st file. The combination of columns H and I give the total number of cells in each column of the footprint and are computed in column J using the formula

Jrn = Hrn+Irn

The cells are identified in column K as to whether or not the corresponding cell lies in the footprint through the following formula:

Krn = IF(K(rn-1)>1,K(rn-1)-1,2*J2)

This formula initiates a count at the top cell if the previous cell in column K is 0 or 1 and if J in the given row is greater than 0. The count is initiated as 2*Jrn because there are fracture and matrix cells in each column. Then each cell is given a designation as being in the repository footprint in column L using the following formula:

Lrn = IF(Krn>0,"RF",0)

The results are saved in the following files:

1-64000 cells with footprint tag 6th file.xls
64001-128000 cells with footprint tag 6th file.xls

128001-192000 cells with footprint tag 6th file.xls
192001-245506 cells with footprint tag 6th file.xls

The file is then consolidated to columns A-G and columns H – K are deleted leaving column G containing either a 0 (outside footprint) or and "RF" denoting inside the footprint. These are saved as:

1-64000 cells with footprint tag summary 7th file.xls
64001-128000 cells with footprint tag summary 7th file.xls
128001-192000 cells with footprint tag summary 7th file.xls
192001-245506 cells with footprint tag summary 7th file.xls

Note that files for steps 4, 5, and 6 for the cells 1-64000 were not created because there are no repository footprint cells in these first 64000 cells.

For subsequent uses, these four sets of files were broken down into the following:

1-61000 cells with footprint tag.xls
61001-122000 cells with footprint tag.xls
122001-184000 cells with footprint tag.xls
184001-245506 cells with footprint tag.xls

In addition, these groupings were ordered (in ascending order) by the cell names in column A, which segregates the fracture and matrix cells.

File information including all file names, file dates and times, and file sizes are documented in DTN: LB03023DSSCP9I.001 [163044] and Output-DTN: LB0310FEPS0170.001

INTENTIONALLY LEFT BLANK

APPENDIX B

PTn LOCATIONS RELATIVE TO WASTE EMPLACEMENT

INTENTIONALLY LEFT BLANK

Figure II-1 shows the PTn coverage over the UZ Flow Model and waste emplacement areas. The PTn is present over all waste emplacement locations. The coordinates for the PTn are given in the mesh_3dn.dkm file of DTN: LB03023DSSCP9I.001 [163044]. The repository coordinates are in file rep.xls in Output-DTN: LB0310FEPS0170.001.

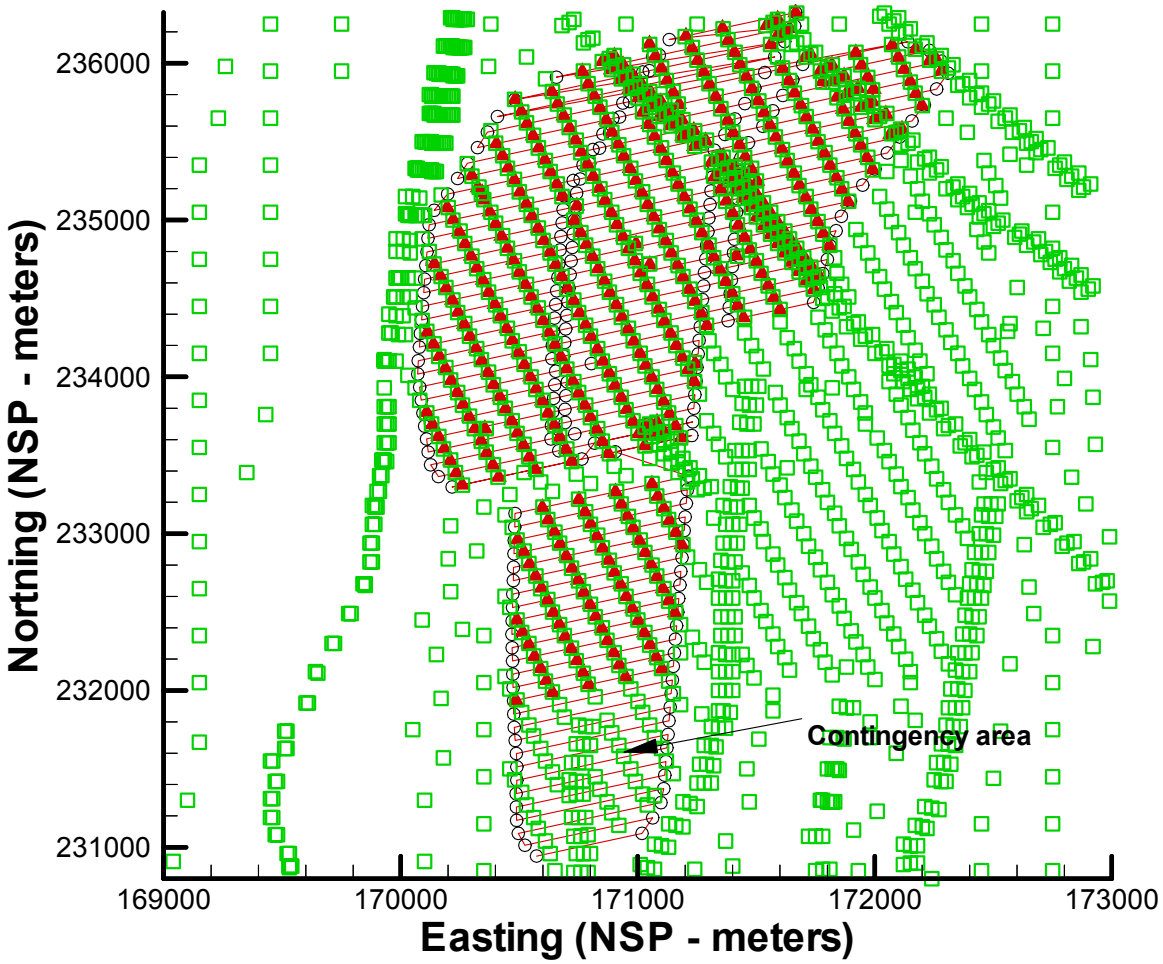

Figure II-1. PTn Coverage over the UZ Flow Model and Waste Emplacement Areas. Green squares – UZ model grid locations with PTn cover; Red triangles – UZ model repository grid locations; Black circles – waste emplacement drift endpoints

File information including all file names, file dates and times, and file sizes are documented in DTN: LB03023DSSCP9I.001 [163044] and Output-DTN: LB0310FEPS0170.001

INTENTIONALLY LEFT BLANK